Biochemical and structural studies of aminoglycoside acetyltransferases

by

Wenjing Chen

A dissertation submitted in partial fulfillment
of the requirements for the degree of
Doctor of Philosophy
(Chemical Biology)
in The University of Michigan
2012

Doctoral Committee:

Assistant Professor Sylvie Garneau-Tsodikova, Chair
Professor David H. Sherman
Associate Professor Jason E. Gestwicki
Associate Professor Bruce A. Palfey

2012

To my parents

谨以此文献给我最亲爱的父母，感谢他们把我带到这个世界上，做我永远的守护者，教导我人生的道理，并给予我他们一生的爱。

Acknowledgments

Foremost, I want to thank my advisor Professor Sylvie Garneau-Tsodikova. It has been an honor to be her first Ph.D. student. I would like to express my sincere gratitude for her continuous support of my Ph.D. study and research. I appreciate all her contributions of time, ideas, and funding to make my Ph.D. study a productive and joyful experience. The patience, motivation, enthusiasm, and knowledge she has for her research were motivational for me, even during tough times in my Ph.D. pursuit. I am grateful that she understood and helped me to overcome the obstacles I had either in research or life as a foreign student. I am also thankful for the excellent example she has provided as a successful woman scientist and mentor.

My sincere thanks also go to my committee members: Professors Jason E. Gestwicki, Bruce A. Palfey and David H. Sherman, for their encouragement, insightful comments, and critical questions during every data meeting.

The members, both former and present, of the Garneau-Tsodikova group have contributed immensely to my professional time here at the University of Michigan. The group has been a great source of friendships as well as good advice and collaboration. It is my pleasure to work with a group of such smart, fun, hard-working scientists. I want to thank Dr. Keith D. Green, who collaborated with me for the past four years, for his help, his great insights and innovational advice on every project I have done. I would like to thank Jacob L. Houghton for teaching me organic synthesis and NMR analysis. I also appreciate the help of our lab technician Dr. Olga E. Zolova, for preparing our experiment reagents and instrumentation. To the rest of the group members, I am grateful for your time, patience and intelligent discussion during every group meeting and practice talk.

The crystal structures discussed in this dissertation would not have been possible without Dr. Tapan Biswas and Professor Oleg V. Tsodikov. I appreciate their ingenious ideas and original suggestions on the Eis project. I would also thank our collaborator Professor Micha Fridman (Tel Aviv University, Israel) for his creative input on the aminoglycoside-modifying enzyme project. I want to thank Tom McQuade, Steve van de Roest, and those from the Center for Chemical Genomics (University of Michigan) who helped with the high-throughput screening project. I also want to thank Professors Tomasz Cierpicki, Mi Hee Lim and John J. Tesmer (University of Michigan) for letting me use their lab instrumentations to collect valuable data for my research projects. I appreciate the help of Dr. Brian K. Janes (from Professor Philip C. Hanna's laboratory, University of Michigan) on the *Bacillus anthracis* eis analog gene knockout project. I thank Professors Véronique Dubois (Université de Bordeaux, France), Timor Baasov (Technion, Israel Institute of Technology, Israel), John S. Blanchard (Albert Einstein College of Medicine, USA), and Juan L. Asensio (Instituto de Química Bio-orgánica General (CSIC), Spain) for their generous gift of the plasmids harboring genes encoding the enzymes I used in my research. I owe sincere thankfulness to Professor Neil R. Thomas (University of Nottingham), for helping me with the graduate school application.

I thank all the funding source that have supported me through the past five years: the Life Sciences Institute and the College of Pharmacy at the University of Michigan start-up fund (S.G.T), the Center for Chemical Genomics (CCG) Pilot Grant at the University of Michigan, the United States-Israel Binational Science Foundation (BSF, grant 2008017, S.G.T. and M.F.), the Rackham Graduate School (University of Michigan) summer research grant, the Firland Foundation, and National Institutes of Health (NIH) Grant AI090048.

I would like to thank the Chemical Biology Doctoral Program for offering me the opportunity to pursue my Ph.D. degree here at the University of Michigan. I am thankful to all the friends and colleagues in my program, for the social and academic fun and diversions they provided. My special thanks to the former and present program managers

Justine Altman, Amy McGovern, and Laura Howe, for their continuous support and help in both my personal and academic life.

My time in Ann Arbor was made enjoyable due to the many friends I made during the past five years that became a part of my life. I am grateful for the time spent with my roommate Dr. Xiao Liu, from whom I learnt perseverance and patience. I thank Dr. Chia-yin Chang for bringing great laughs and inspiration into my life. I also appreciate the friendship of Dr. Suman Atwal and Elaina Zverina for the past five years, for being great company and helping me adjust to a foreign culture here in the United States. I would also like to thank all my friends in Ann Arbor for bringing great fun and memorable moments to my life here in this little town. My thanks also go to my dearest friends in my hometown: Lin Gui, Shiyi Li, Jia Jia, and all my old friends back home, for their long time encouragement and support. I owe my gratitude to my high school teachers Jing Luo, Hong He, Yunxia Tang and Xichen Zhang, for teaching me critical thinking and bringing me to the world of science.

Finally and most importantly, none of this would have been possible without the love and support of my family. My parents to whom this dissertation is dedicated to have been a constant source of love, guidance, support, concern, energy, strength and encouragement through every stage of my life. They brought me to this world in the first place, protected me, educated me, and gave me all their love. Their faith and confidence in me is what has shaped me to be the person I am today. I would also like to express my heartfelt gratitude to my grandparents, for their never-ending love and patience. I am truly indebted and thankful to my auntie Yanxia who has aided and encouraged me throughout this endeavor. I warmly appreciate the generosity and understanding of all my family members.

Preface

This dissertation contains eight chapters covering my Ph.D. studies on aminoglycoside-modifying enzymes. Chapter one, which is partially adapted from a review article (Houghton, J. L.; Green, K. D.; **Chen, W.**; Garneau-Tsodikova, S. *ChemBioChem* **2010**, *11*, 880), is the introduction which discusses the antimicrobial properties of aminoglycosides and problems associated with their use. Chapter two investigates the possibility of using a chemoenzymatic methodology to generate novel *N*-acylated aminoglycosides (Green, K. D.; **Chen, W.**; Houghton, J. L.; Fridman, M.; Garneau-Tsodikova, S. *ChemBioChem* **2010**, *11*, 119). In chapter three, we demonstrate that aminoglycoside-modifying enzymes can sequentially modify aminoglycosides (Green, K. D.; **Chen, W.**; Garneau-Tsodikova, S. *Antimicrobial agents and chemotherapy* **2011**, *55*, 3207). Chapter four focuses on the biochemical and structural studies on Eis from *Mycobacterium tuberculosis* which was found to be an aminoglycoside acetyltransferase with unprecedented multi-acetylation properties (**Chen, W.**; Biswas, T.; Porter, V. R.; Tsodikov, O. V.; Garneau-Tsodikova, S. *PNAS* **2011**, *108*, 9804). We identified and characterized several inhibitors of Eis via high-thoughput screening and the results from the studies are presented in chapter five (Green, K. D.; **Chen, W.**; Garneau-Tsodikova, S. *ChemMedChem* **2012**, *7*, 73). Chapter six summarizes the cosubstrate profile of Eis. In chapter seven, an Eis homolog from *Mycobacterium smegmatis* is studied. Chapter eight discusses the on-going work and future directions of the Eis projects.

Table of Contents

List of Figures

Chapter 1

Chapter 2

Chapter 3

Chapter 4

Chapter 5

Chapter 6

Chapter 7

Chapter 8

List of Tables

Chapter 2

Chapter 3

Chapter 4

Chapter 5

Chapter 6

Chapter 7

Chapter 8

List of Abbreviations

AG	Aminoglycoside
A	Adenine
AAC	Aminoglycoside acetyltransferase
Abs	Absorbance
Ac	Acetyl
AcCoA	Acetyl coenzyme A
AHB	1-*N*-(S)-α-hydroxy-γ-amino-*n*-butyryl
AIDS	Acquired immune deficiency syndrome
Ala or A	Alanine
AME	Aminoglycoside-modifying enzyme
AMK	Amikacin
AMP	Adenosine monophosphate
AMPPCP	β,γ-Methyleneadenosine 5'-triphosphate
ANT	Aminoglycoside nucleotidyltransferase
APH	Aminoglycoside phosphotransferase
APR	Apramycin
Arg or R	Arginine
Asn or N	Asparagine
Asp or D	Aspartic acid

ATP	Adenosine triphosphate
B. anthracis	*Bacillus anthracis*
B. subtilis	*Bacillus subtilis*
C	Cytosine
CAN	Cerium ammonium nitrate
CAP	Capreomycin
CoA	Coenzyme A
COSY	Correlation spectroscopy
CroCoA	Crotonyl coenzyme A
Cys or C	Cysteine
D	Dimension
DEPT	Distortionless enhancement by polarization
DMSO	Dimethyl sulfoxide
DNA	Deoxyribonucleic acid
DOS	Deoxystreptamine
DTDP	4,4'-dithiodipyridine
DTNB	5,5'-dithiobis-(2-nitrobenzoic acid)
DTT	Dithiothreitol
E. coli	*Escherichia coli*
EDTA	Ethylenediaminetetraacetic acid
Eis	Enhanced intracellular survival
EMB	Ethambutol
eq	Equivalent

EtOAc	Ethyl acetate
FPLC	Fast protein liquid chromatography
G	Guanine
GCN5	General control non-derepressible 5
GEN	Gentamicin
Glu or E	Glutamic acid
Gly or G	Glycine
GNAT	GCN5-related *N*-acetyltransferase
GTP	Guanosine triphosphate
HCl	Hydrogen chloride
HEPES	4-(2-hydroxyethyl)-1-piperazineethanesulfonic acid
HETCOR	Heteronuclear correlation experiment
His or H	Histidine
HIV	Human immunodeficiency virus
HRMS	High resolution mass spectrometry
HYG	Hygromycin
IC_{50}	Half maximal inhibitory concentration
Ile or I	Isoleucine
INH	Isoniazid
IPTG	Isopropryl-β-thiogalactopyranoside
KAN	Kanamycin A
KCl	Potassium chloride
KOH	Potassium hydroxide

LB	Luria-Bertani
LCMS	Liquid chromatography mass spectrometry
Leu or L	Leucine
Lys or K	Lysine
MalCoA	Malonyl coenzyme A
MBC	Minimum bactericidal concentration
Mbo	*Mycobacterium bovis* BCG
MDR	Multidrug-resistant
Me	Methyl
MeOH	Methanol
MES	2-(*N*-morpholino)ethanesulfonic acid
Met or M	Methionine
MIC	Minimum inhibitory concentration
mRNA	Messenger RNA
Msm	*Mycobacterium smegmatis*
Mtb	*Mycobacterium tuberculosis*
MWCO	Molecular weight cut-off
NaCl	Sodium chloride
NADH	β-nicotinamide adenine dinucleotide reduced
NEA	Neamine
NEO	Neomycin B
NET	Netilmicin
NH_4OH	Ammonium hydroxide

Ni-NTA	Nickel-nitrilotriacetic acid
NMR	Nuclear magnetic resonance spectroscopy
O/N	Overnight
OD	Optical density
PAR	Paromomycin
PCR	Polymerase chain reaction
pdb	Protein data bank
Phe or F	Phenylalanine
Ppant	Phosphopantetheinyl
ppm	parts-per-million
Pro or P	Proline
ProCoA	*n*-propionyl coenzyme A
PZA	Pyrazinamide
R_f	Retention factor
RIB	Ribostamycin
RMP	Rifampicin
RNA	Ribonucleic acid
rt	Room temperature
S. aureus	*Staphylococcus aureus*
SDS-PAGE	Sodium dodecyl sulfate-polyacrylamide gel electrophoresis
SeMet	Selenomethionine
Ser or S	Serine
SIS	Sisomicin

SOE	Splicing by overlapping extension
spp.	Species
SPT	Spectinomycin
STR	Streptomycin
T	Thymine
TB	Tuberculosis
Thr or T	Threonine
TLC	Thin layer chromatography
TOB	Tobramycin
TOCSY	Total correlation spectroscopy
Tris-HCl	Tris(hydroxymethyl)aminomethane-hydrochloride
tRNA	Transfer RNA
Trp or W	Tryptophan
Tyr or Y	Tyrosine
U	Uracil
Val or V	Valine
WHO	World health organization
XDR	Extensively drug-resistant

Abstract

Aminoglycosides are broad-spectrum antibiotics widely used as chemotherapeutic agents for the treatment of serious bacterial infections. Aminoglycosides were first established as antibiotics in the 1940s with the discovery of the first treatment for tuberculosis, streptomycin. Aminoglycosides target the prokaryotic ribosome by binding the decoding A-site of the 16S rRNA, inhibiting protein translation and ultimately leading to cell death. One of the major problems with this class of drugs is that decades of intensive clinical use has selected for bacterial resistance. The most common mechanism of bacterial resistance arises from their structural modifications by aminoglycoside-modifying enzymes (AMEs). This dissertation focuses on the aminoglycoside acetyltransferase (AAC) family of AMEs which uses AcCoA to regio-specifically acetylate amino groups on aminoglycosides.

We reported the development of a chemoenzymatic methodology that utilizes AACs for the generation of *N*-acylated aminoglycoside analogs. The studied AACs showed diverse substrate promiscuity towards a variety of aminoglycosides as well as acyl-CoA derivatives. Some acylated aminoglycosides retained antibacterial properties against *Bacillus subtilus.* Our chemoenzymatic approach offers access to regioselectively *N*-acylated aminoglycosides in quantities that allow testing of antibacterial potential, making it possible to identify molecules worth synthesizing on a larger scale. This is a demonstration of utilizing the cosubstrate promiscuity of enzymes to re-purpose their use for scaffold diversification towards the development of new drugs. We also demonstrated that aminoglycosides can be doubly modified by the sequential actions of AMEs in some cases. These observations will help anticipate the effect of a modification on the subsequent activity of AMEs and guide the design of novel aminoglycoside antibiotics.

Next, we focused on studying the the unusually regioversatile acetyltransferase, Eis, which is responsible for resistance to kanamycin in a significant fraction of kanamycin-resistant *Mycobacterium tuberculosis* clinical isolates. We found that mycobacterial Eis has an unprecedented ability to acetylate multiple amines of many aminoglycosides. We also found that Eis, in contrast to its broad substrate profile, has limited cosubstrate promiscuity. In addition, several inhibitors of the Eis enzyme were identified and characterized. We hope that understanding the mechanism of this resistance conferring enzyme, will enable us to design better drugs/regimens to fight *Mycobacterium tuberculosis* infection.

Chapter 1

Introduction: potentials and problems of aminoglycoside antibiotics

1.1. Introduction

Since the 1928 discovery of the first major antibiotic, penicillin, a multitude of antibiotics including aminoglycosides (AG), β-lactams and fluoroquinolones, etc. have been discovered and applied towards the treatment of bacterial infection, including multi-drug resistant (MDR) strains of bacteria. AGs (Fig. 1.1) in particular are being extensively examined in order to find new compounds that overcome the existing resistance or slow the development of new resistant pathogens.

The AG antibiotics are a group of broad-spectrum bactericidal antibiotics of important clinical use. The typical AG may have up to five rings in its structure and exhibit considerable conformational flexibility at the glycosidic bonds. Most of the AG families contain a central core aminocyclitol 2-deoxystreptamine ring (2-DOS) decorated with various amino-sugar substituents. According to the current nomenclature, the 2-DOS ring is numbered as ring II, the central ring. The sugar ring bound at postion 4 of the central ring is numbered ring I, and the ring bound to either the 5- or 6-position is ring III.[1] These 4,5- and 4,6-disubstituted derivatives are the two most important classes of clinically useful AG antibiotics. For example, neomycin B is used typically in the form of creams for the treatment of bacterial infections occurring from skin burns and paromomycin is used therapeutically against intestinal parasites.

AGs were first established as antibiotics in the 1940s with the discovery of streptomycin (STR) and are still widely used worldwide as chemotherapeutic agents in the treatments of many types of bacterial infections, including those associated with both Gram-positive and Gram-negative pathogens.[2] STR, the first drug that was effective in the treatment of

tuberculosis (TB), together with kanamycin A (KAN) and amikacin (AMK) which are used as second-line anti-TB drugs, are important compounds in the treatment of drug-resistant TB. Current and potential applications of AGs include antibacterials, antivirals, anti-AIDS, and treatment of genetic disorders associated with premature termination codons (PTCs). Due to their heavy use in treating bacterial infections, many strains of bacteria have become resistant to normal doses of AGs, through production and use of AG-modifying enzymes (AMEs) and other methods. To side step the issue of antibiotic resistance, many scientists have taken on the task of synthesizing AG derivatives, including AG dimers and conjugates with other biomolecules.[3,4] Efforts aiming to create better AGs have utilized several new strategies including chemoenzymatic modification, and coupling of antibiotics, both AGs as well as other classes of drugs, by synthetic or semi-synthetic methods.

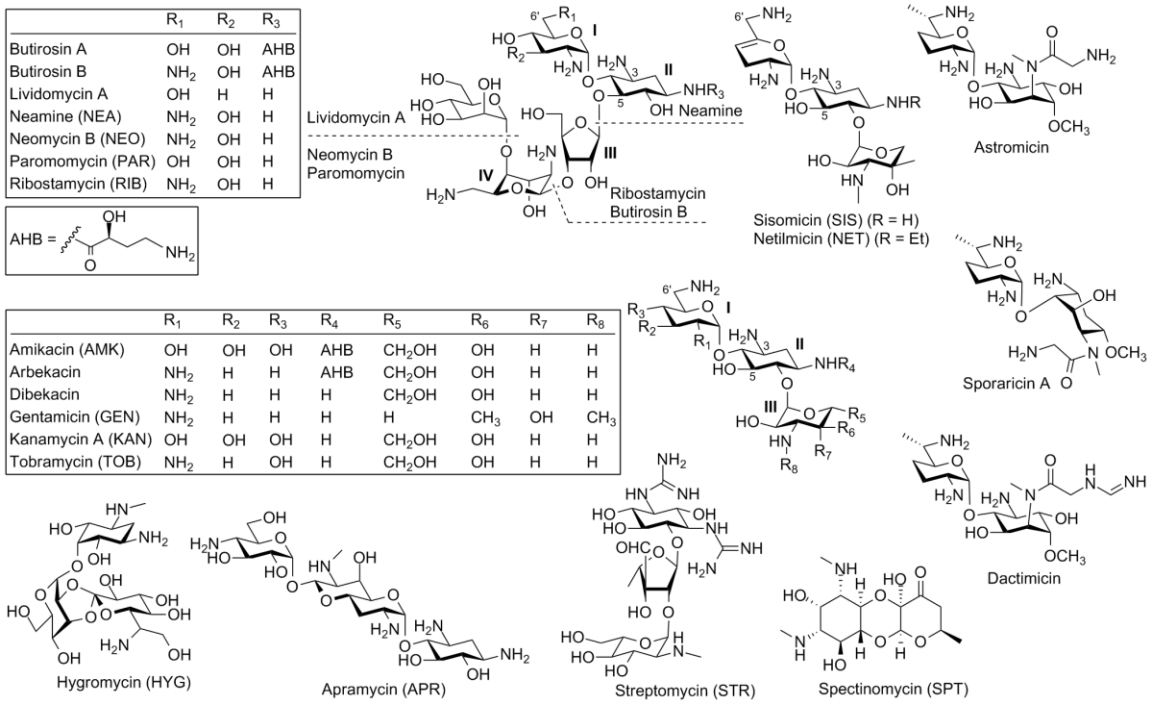

	R_1	R_2	R_3
Butirosin A	OH	OH	AHB
Butirosin B	NH_2	OH	AHB
Lividomycin A	OH	H	H
Neamine (NEA)	NH_2	OH	H
Neomycin B (NEO)	NH_2	OH	H
Paromomycin (PAR)	OH	OH	H
Ribostamycin (RIB)	NH_2	OH	H

AHB =

	R_1	R_2	R_3	R_4	R_5	R_6	R_7	R_8
Amikacin (AMK)	OH	OH	OH	AHB	CH_2OH	OH	H	H
Arbekacin	NH_2	H	H	AHB	CH_2OH	OH	H	H
Dibekacin	NH_2	H	H	H	CH_2OH	OH	H	H
Gentamicin (GEN)	NH_2	H	H	H	H	CH_3	OH	CH_3
Kanamycin A (KAN)	OH	OH	OH	H	CH_2OH	OH	H	H
Tobramycin (TOB)	NH_2	H	OH	H	CH_2OH	OH	H	H

Fig.1.1. Chemical structures of natural and synthetic AGs.

1.2. AGs' mechanism of action

The antibacterial mechanism of action of AGs has been well characterized and it was discovered in the late 1980s that the AGs' molecular target is the 16S rRNA subunit of the 30S bacterial ribosome.[5] While alternative modes of binding have been observed with various AG derivatives,[6] the general interactions of AGs with three unpaired adenine

residues in the decoding loop displaces non-complementary adenines and locks them into a so-called 'flipped-out' orientation similar to that observed during mRNA decoding.[7-10] Structural examples of these interactions from crystallographic or modelling studies are shown in Fig. 1.2, which depicts tobramycin (TOB), geneticin, amikacin (AMK), and paromomycin (PAR) in complex with A-site oligonucleotides.[11-14] During the decoding process of protein translation, the formation of a mini helix between the codon of mRNA and the anti-codon of tRNA determines the correct selection. In this process, the conformation of the A-site is changed from an "off" state, where the two conserved adenines A1492 and A1493 are folded back within the helix, to an "on" state, where these two adenines are flipped out from the A-site and interact with the mini helix. This conformational change is a molecular switch that irreversibly determines on the continuation of protein translation. The interaction between AG and A-site reduces the fidelity of normal translational processes by reducing the ability of the ribosome to discriminate between the proper mRNA-tRNA complexes, leading to the accumulation of truncated or non-functional proteins in the bacterial cells, eventually leading to cell death.[15]

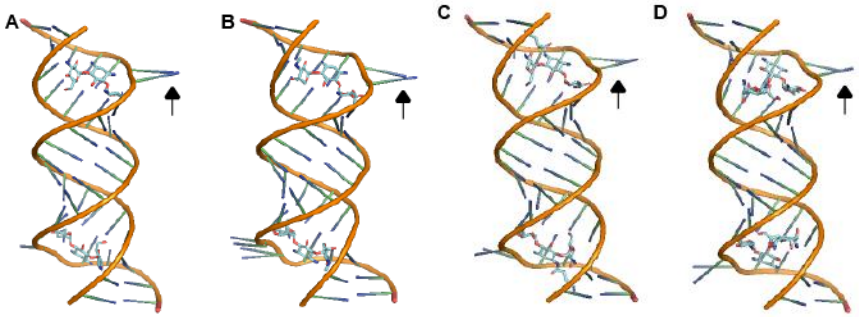

Fig. 1.2. Structures of 16S oligonucleotides mimicking the bacterial decoding A-site with **A.** TOB, **B.** geneticin, and **C.** AMK bound. Also shown is **D.** the crystal structure of PAR docked into a bacterial A-site oligonucleotide. These images illustrate the 'flipped-out' (indicated by black arrows) conformation of the residues displaced upon binding of AGs to the decoding A-site, which is the basis of the compounds' antibacterial activity.

Another contribution to the antibacterial activity of AGs, exemplified by PAR, comes from their ability to interfere with translocation via stabilization of the 70S subunit. In 2008, Kaji and co-workers showed that PAR inhibits the anti-association activity of translation initiation factor 3 (IF3), which is involved in the disassembly reaction of ribosomal complexes, post-termination.[16] It does so by strengthening the interactions

between the 50S and 30S subunits, thus stabilizing the 70S complex, which leads to a loss of internal mobility and ability to properly translocate tRNAs. Recent studies have shown that this activity may arise from the AGs' ability to interact with specific sites of the 16S rRNA.[17]

It has been shown that there are two primary types of interactions that facilitate the recognition and binding of AGs to their targets. The most significant contribution comes from electrostatic interactions occurring between the positively-charged amino groups of the AG and the negatively-charged phosphate backbones of the RNA target.[18] The other contribution comes from hydrogen bonds formed between the multiple amino and hydroxyl groups of both the RNA bases and AGs.[15,19-21] The intricate network of electrostatic contacts and hydrogen bonds between the RNA and AGs produces a very tightly bound complex prone to decreased translational fidelity.

For example the 2-DOS ring (ring II) of PAR has hydrogens binding to U1406, U1495, and G1494 of the 16S bacterial RNA. Ring I, depending on the substitution pattern of the particular AG, has been shown to bind to a number of ribosomal nucleobases including A1408, A1493, A1492, and G1491.[20,21] Crystal structures of KAN, NEA, GEN C1A, RIB, lividomycin, NEO, and TOB with oligonucleotides including the decoding A-site of bacterial ribosomes revealed that not only are rings I and II essential for the recognition of the above AGs, but they are also conserved and sequence-specific.[15]

The selectivity of AGs towards the bacterial ribosomal subunit over the analogous human subunit is due to fundamental differences in the respective nucleotide sequences, which leads to lower affinity of the AGs for the human ribosome.[22] Permeability of the cells is also a critical factor in the selectivity of AGs towards bacterial cells. The poly-cationic nature of the AGs prevents the efficient uptake of the compounds in most eukaryotic cells but enhances the agents' uptake in many bacterial cells due to the presence of energy-dependent transport pathways that utilize the membrane-bound electron transporters.[23,24]

An increasing number of biochemical and structural studies have correlated the incorporation of the γ-aminohydroxybutyric acid (AHB) at the N1-position of the 2-DOS ring, common in many AGs, with an improved antibacterial profile.[13,25] Interestingly, the acyl moiety lowers the pK_a of the N1 nitrogen atom, and this alteration of the N1 nitrogen of compounds such as AMK, butirosin B, and others, significantly enhances the binding of ring II to RNA. Additionally, the ammonium on the terminus of the AHB group provides another favourable interaction with a backbone phosphate.[26] As a result of these observations, current strategies for increasing the antibacterial activity of AGs involve the incorporation of AHB or analogous functionalities to the scaffold of known AGs as well as synthetic and semi-synthetic analogs, a strategy that has produced results and shown enormous promise.

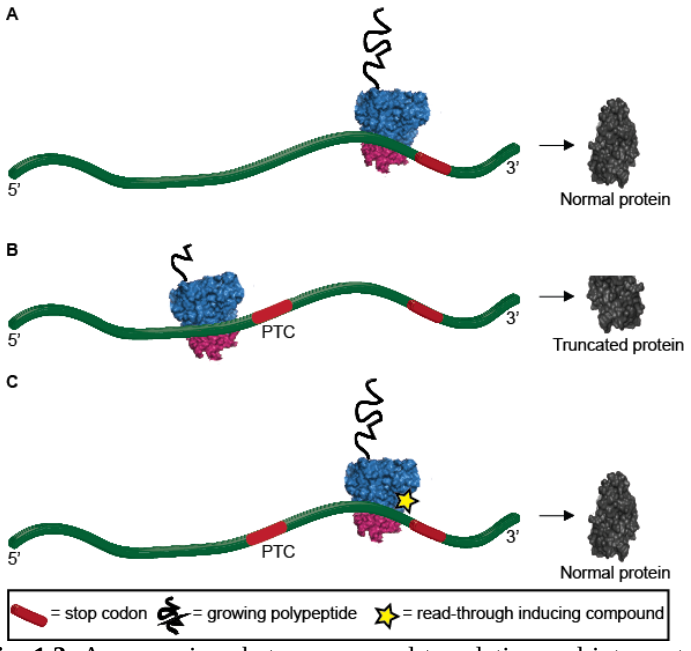

Fig. 1.3. A comparison between normal translation and interrupted translation by a premature termination codon (PTC) **A.** normal translation process leading to functional protein, **B.** translation which is interrupted by a PTC leading to a truncated non-functional protein, and **C.** translation process which was restored by a read-through inducing compound such as an AG.

1.3 AGs' antiviral and anti-AIDS activity

An exciting area of AG research is the application of AG-based compounds in the treatment of HIV, as over the past few decades their efficacy against HIV-1 has become more widely realized. It has been shown that AGs and derivatives/conjugates are capable of targeting many steps in the HIV life cycle, and the development of compounds that show specificity towards a particular target has become the goal of many research efforts in recent years.[27-35] Another exciting application for AGs that has recently come to light is their ability to induce the production of retrocyclins, which shows promise towards the development of AG-based compounds for HIV prevention.[36]

1.4. AGs in the treatment of genetic diseases

Nearly 20 years after the discovery of STR, it was discovered that AGs are able to suppress premature termination codons (PTCs), restoring full-length protein production in *E. coli*.[37] PTCs, often the result of base pair insertion, deletion, or substitutions, generally lead to the production of incorrectly truncated, non-functional proteins (Fig. 1.3). In humans, PTCs have been linked to over 1800 genetic disorders.[38] The potential of PTC suppression in mammalian cells was first demonstrated by the ability of GEN to suppress PTCs resulting from common mutations in the cystic fibrosis transmembrane conductance regulator (CFTR).[39,40] Subsequent studies of AGs such as GEN, TOB, AMK and a novel AG derivative (NB54) showed a dose-dependent increase in the levels of full-length proteins relative to the truncated proteins produced by PTCs, suggesting that AGs could prove effective in suppressing PTCs implicated in other genetic disorders.[41-44]

1.5. Problems associated with AGs

Three major problems associated with the use of AGs are bacterial resistance, toxicity, and the complexity associated with their chemical syntheses. The toxicity experienced upon administration of AGs is usually nephrotoxicity or ototoxicity, and rarely neuromuscular blockage or hypersensitivity reactions. Bacterial resistance to AGs, resulting from intensive clinical use, is becoming increasingly prevalent worldwide and this phenomenon in particular presents a significant threat to public health.

1.5.1. Toxicity

One of the primary obstacles preventing more widespread use of AGs as long-term treatment for genetic, viral, or microbial issues is the inherent toxicity associated with non-specific binding of RNA. Some of the most important risk factors for AG-induced toxicity include: the duration, dosage, and frequency of therapy, the patient's age, the patient's liver and kidney health, and drug-drug interactions with other potential nephrotoxic agents.[45,46] Toxicity and selectivity are two intertwining issues associated with targeting the ribosome due to its presence and importance in all forms of life.[10,21,47-51] In general, AGs with fewer amino groups on the scaffold will show less toxicity, and

the same is true of AGs with lower relative basicity of their existing amino groups, notably the 2'-amine.[52,53]

1.5.1.1. Nephrotoxicity

Nephrotoxicity, arising from toxins or drug compounds damaging the kidneys. If untreated, an eventual concurrent rise in electrolytes in the blood may lead to permanent kidney damage or even failure.[54] Although hydration treatment often alleviates the symptoms of AG-induced nephrotoxicity, it is not always fully reversible and recovery may take many months.

1.5.1.2. Ototoxicity

Another major hurdle in AG therapy is ototoxicity, which, in contrast to nephrotoxicity, is mostly irreversible. There are two types of ototoxicity: vestibular toxicity and cochlear toxicity. AGs toxicity may lead to a temporary vestibular hypofunction or permanent high-frequency hearing loss.[55] Vestibulotoxicity occurs in up to 15% of patients after AG administration, whereas cochleotoxicity in 2% to 25% of patients due to different regimens of AG administration.[56] The permanence of AGs ototoxicity is a result of degeneration of hair cells and neurons in the cochlea, which do not regenerate once damaged.[54,55,57-65]

1.5.2. Problems associated with AGs' total syntheses

While chemical synthesis is a great tool for generating large quantities of AGs, producing a large library of compounds is often an overwhelming task.[66-69] The steps required to manipulate saccharide rings into the correct protection states quickly grow quite numerous, often providing only enough material to test for MIC and toxicity from grams of starting material. Combinatorial methods have taken a step closer to generating a larger number of compounds using a single reaction. However, the starting materials in these reactions still require the appropriate protection chemistry.[70,71] Chemoenzymatic methods hold great promise in generating large libraries of compounds. Although generating large amounts of material chemoenzymatically may be challenging, enough

material can be produced to discover promising compounds to further pursue synthetically. [72]

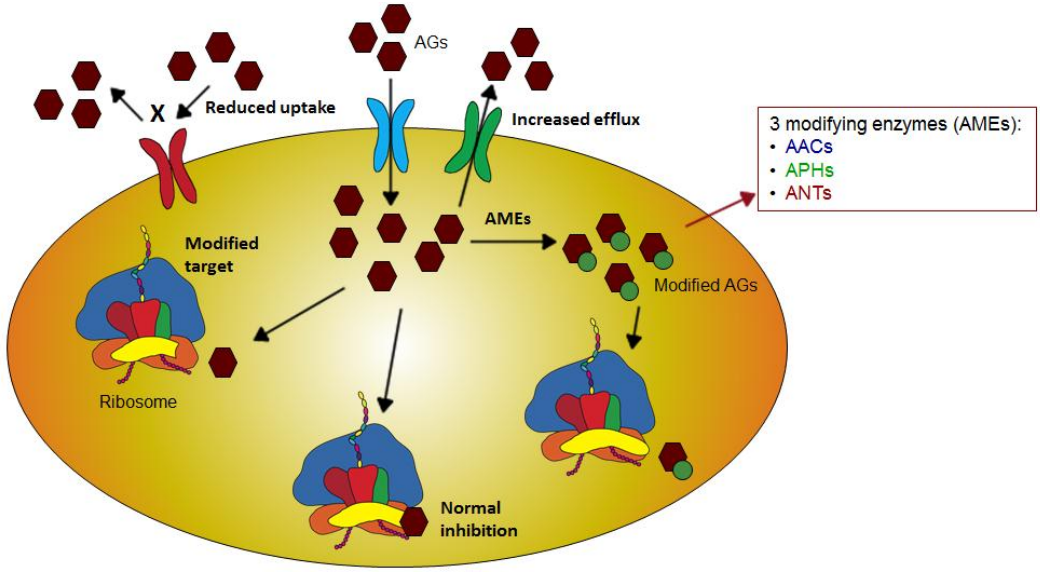

Fig. 1.4. Depiction of the various mechanisms of bacterial resistance.

1.5.3. Resistance

There are three mechanisms of bacterial resistance to AGs: (1) the reduction of the intracellular concentration of AGs due to alteration of the bacterial outer membrane, decreasing drug transport into the cell and/or increasing the activity of active efflux systems, (2) the alteration of the 16S RNA of bacterial 30S ribosomal subunit by mutation or methylation of the AG binding site, and (3) the deactivation of AGs by *N*-acetylation, *O*-nucleotidylation, or *O*-phosphorylation (Fig. 1.4). More than one of the above mechanisms may be simultaneously active, leading to complex resistance mechanisms.

1.5.3.1. Reduced uptake and increased efflux

Although the exact mechanism of AG uptake remains unclear, it is thought that three steps are involved. The first step is the adsorption of the poly-cationic AG to the surface of bacteria by electrostatic interactions with the negatively charged portions of biomolecules found on the outer cell membranes of bacteria.[73-76] In the case of *Pseudomonas aeruginosa*, changes in membrane components involved in interactions with AGs are associated with increased levels of resistance.[74-83] MdfA from *E. coli* was

the first discovered putative major facilitator superfamily MFS protein that contributes to AG resistance.[84] The two subsequent steps are oxygen dependent, making anaerobic bacteria intrinsically resistant to AGs.[85] It was also found that in *E. coli*, *Staphylococcus aureus*, and *P. aeruginosa*, mutations in ATP synthases cause decreased susceptibility to AGs.[86]

1.5.3.2. Modification of the target RNA

Another resistance mechanism that bacterial cells use is alteration of the AGs' target, the 16S RNA of the bacterial ribosome. Many AG-producing organisms, including *Streptomyces* spp. and *Micromonospora* spp., are capable of expressing rRNA methylases, which are able to methylate the 16S rRNA.[87,88] One example, RmtA, was identified as a 16S rRNA methylase capable of conferring high-level AG resistance in *P. aeruginosa*,[89] while another example, RmtB, was found to be responsible for AG resistance in *Serratia marcescens*.[87] Recently, another putative 16S rRNA methylase, ArmA, conferring high-level resistance to AGs, was found in a *Klebsiella pneumoniae* clinical isolate.[90] Resistance to AGs resulting from a mutation of the ribosomal target has also been found in clinical isolates of *Mycobacterium tuberculosis* (*Mtb*).[91] In general, the modifications carried out by these enzymes occur in two highly conserved regions, resulting in decreased affinity of the AG for its oligonucleotide partner such that the compounds are no longer effective.[10]

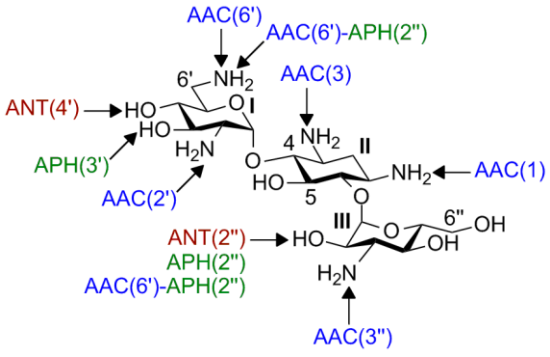

Fig. 1.5. AMEs' modification sites on kanamycin B.

1.5.3.3. Modification of the AGs

Even though the target site for AGs is often the 16S rRNA, the most common cause of AG resistance is not conferred by alteration of this target, owing to the highly preserved function of the rRNA across genera. Rather, the most common mechanism for bacterial resistance arises from the structural modification of the AGs by specific enzymes expressed by resistant strains. The AG resistance genes are derived from bacterial genes that once encoded for

enzymes involved in normal cellular metabolism. The selective pressure of AG usage altered the expression patterns of these genes, ultimately leading to the production of enzymes capable of regio-specifically modifying AGs, effectively rendering them inert. Most modifications take place at the 1-, 3-, 2'-, and 6'-amino groups and the 3'-, 4'-, and 2''-hydroxyl groups (Fig. 1.5).[92] AGs with alternate structures may have variable amounts of modifiable sites, with the majority of these positions being located on rings I and II.

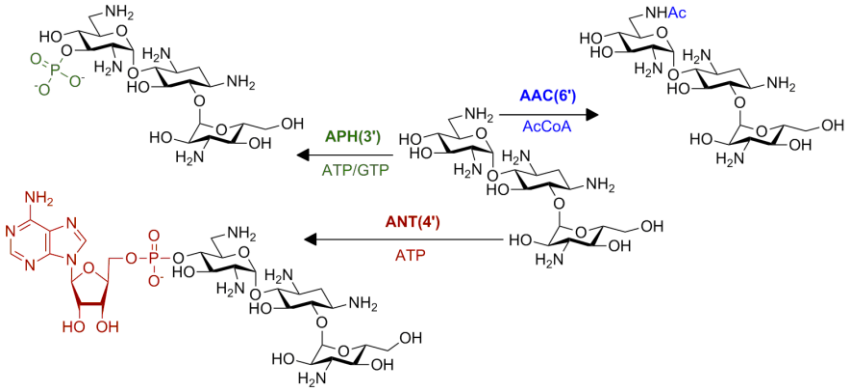

Fig. 1.6. Three AMEs and their modified kanamycin B products.

There are three classes of AMEs: ATP-dependent AG nucleotidyltransferases (ANTs), ATP (and/or GTP)-dependent AG phosphotransferases (APHs), and AcCoA-dependent AG acetyltransferases (AACs) (Fig. 1.6). Within each class, enzymes are grouped according to their different regio-specificities for AG modifications. There are four nucleotidyltransferases (ANT(6), ANT(4'), ANT(3''), and ANT(2'')), seven phosphotransferases (APH(3'), APH(2''), APH(3''), APH(6), APH(9), APH(4), and APH(7'')), and four acetyltransferases (AAC(2'), AAC(3), AAC(6'), AAC(1)). The enhanced intracellular survival (Eis) protein, an AAC that confers resistance in *Mtb*, has also recently been reported.[93] There is also a bifunctional enzyme AAC(6')-APH(2'')[92,94,95] that can catalyze both acetylation and phosphorylation of its substrates. Recently, three additional genes encoding bifunctional enzymes, designated ANT(3'')-Ii/AAC(6')-IId,[96] AAC(3)-Ib/AAC(6')-Ib',[97] and AAC(6')-30/AAC(6')-Ib',[98] have been isolated from *S. marcescens*[96,99] and *P. aeruginosa*.[97,98] The various sites of modification demonstrated with kanamycin B are shown in Fig. 1.5.

1.5.3.3.1. AG acetyltransferases (AACs)

Over 50 members of the AAC family have been identified. These enzymes catalyze the AcCoA-dependent *N*-acetylation of AGs. They modify the 1- and 3-amino groups of the

central 2-DOS ring (ring II, Fig. 1.5) and the 2'- and 6'-amino groups of the 6-deoxy-6-aminoglucose ring (ring I, Fig. 1.5). Two AAC(1) enzymes have been found in *E. coli* and *actinomycetes* strains, but their clinical importance is minor due to the fact that neither have been reported in dangerous pathogenic bacterial strains.[100,101]

The AACs that acetylate at the 2'-amino group are all chromosomally encoded and AAC(2')-Ia was the first to be identified from *Providencia stuartii* in 2001.[102,103] Interestingly, mutations in the *aac*(2')-Ia gene may cause increased levels of peptidoglycan *O*-acetylation, suggesting that peptidoglycan acetylation may be the original physiological function of the enzyme. The chromosomally encoded *Mtb* AAC(2')-Ic was shown, in contrast to some other AACs, to be active against AMK and KAN, both of which contain 2'-hydroxyl group, suggesting that this enzyme may also catalyze *O*-acetylation.[104] The structures of the apo form of AAC(2')-Ic with CoA and TOB, KAN, or RIB are reported (Fig. 1.7A).[105-107]

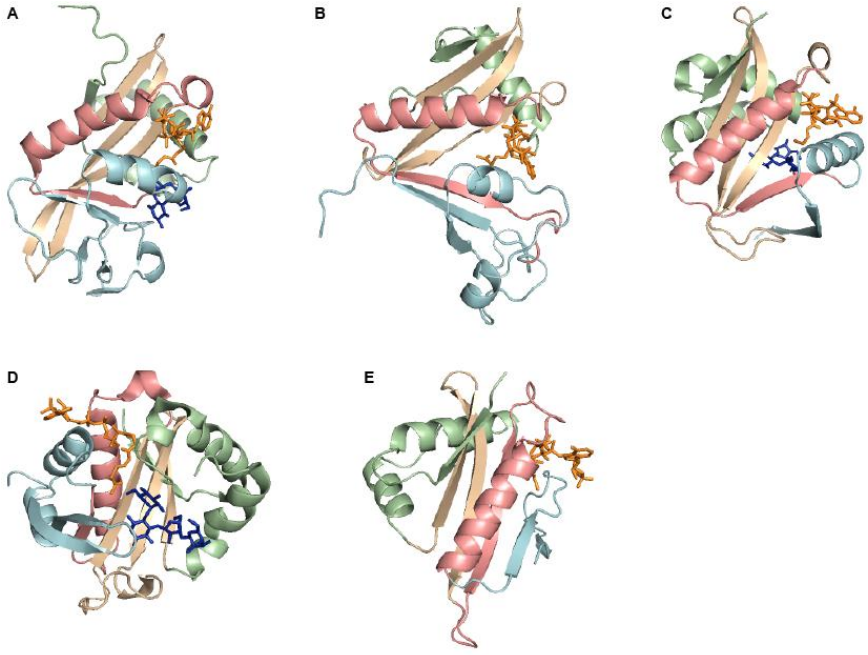

Fig. 1.7. Crystal structures of various AACs. **A.** AAC(2')-Ic (PDB 1M4G) in complex with CoA and RIB, **B.** AAC(6')-Ii (PDB 1B87) in complex with AcCoA, **C.** AAC(6')-Iy (PDB 1S3Z) in complex with CoA and RIB, **D.** AAC(6')-Ib (PDB 2VQY) in complex with AcCoA and PAR, **E.** AAC(3)-Ia (PDB 1BO4) in complex with CoA. CoAs and AGs are shown. The overall structural folds place those AACs in the GCN5 acetyltransferase superfamily. There are four key structural modules per structure.

The 6'-amino group plays an important role in rRNA binding as probed by the structural analysis of bound AGs to the 30S ribosomal subunit.[108,109] Thus, the 6'-position is, not surprisingly, the target of one of the major classes of AMEs, the AAC(6') sub-family, which

consists of more than 25 members identified from various microorganisms. Type-I AAC(6') causes resistance to the majority of useful AGs. Three enzymes have been extensively studied, including two chromosomally encoded AAC(6')-Ii's[106] from *Enterococcus faecium* (Fig. 1.7B), AAC(6')-Iy[110-112] from *Salmonella enterica* (Fig. 1.7C), and a plasmid-encoded bifunctional enzyme AAC(6')-Ie/APH(2'')-Ia found in enterococci and staphylococci.[113] Two of the other AAC(6') members, AAC(6')-Ii and AAC(6')-Ib (Fig. 1.7D), have also been well studied.[114-118]

A recently discovered variant of AAC(6'), the AAC(6')-Ib-cr, has been shown to be able to modify AGs as well as fluoroquinolones.[119] It seems likely that the steady increase in the clinical use of ciprofloxacin during the 1990s has generated selective pressure for this variant.[120]

The bifunctional enzyme AAC(6')-Ie/APH(2'')-Ia, which confers broad spectrum AG resistance differs from the other AAC(6')s in its genetic localization and catalytic capabilities.[113] This enzyme has been proposed to arise by gene fusion and to confer a wider range of AG resistance, illustrating the ability of bacteria to adapt to changes in AG use and selective pressure.[121,122]

The AAC(3) sub-family is one of the largest AME families of enzymes and includes four major types, I-IV, based on the AG resistance profile. The AAC(3)-I from *S. marcescens* was the first AAC whose 3D structure was determined (Fig. 1.7E).[107,123] The enzyme-CoA complex determined at 2.3 Å allowed for identification of the interactions between the enzyme and the product. Unfortunately, there is no structure of AAC(3) with bound AG substrate available at this time.

Although the primary amino acid sequence identity among these AAC enzymes is negligible, the overall structural fold places AACs in the GCN5-related *N*-acetyltransferase (GNAT) superfamily. Structural and mechanistic studies have aided our understanding of the interactions between the enzyme and the AG, and in the future will aid in the design of new drugs that avoid deactivation by AACs.

1.5.3.3.2. AG phosphotransferases (APHs)

APHs catalyze the regio-specific transfer of the γ-phosphoryl group of ATP (or other nucleotides) to a hydroxyl group on an AG (Fig. 1.5 and Fig. 1.6). The genes encoding these enzymes are often found on multi-drug resistance R plasmids, transposons, and integrons, and thus are hurdles in the treatment of some *Enterococcal* and *Staphylococcal* species with AGs. Phosphorylation of AGs results in a dramatic decrease in their ability to bind to their target on the A-site of the ribosome. One useful application of APHs is the resistance maker, the *Kan*^{R} gene, which codes for an APH(3') that leads to the phosphorylation of KAN at the 3'-position. As a result, cells carrying this gene are able to survive treatment with KAN.[124,125]

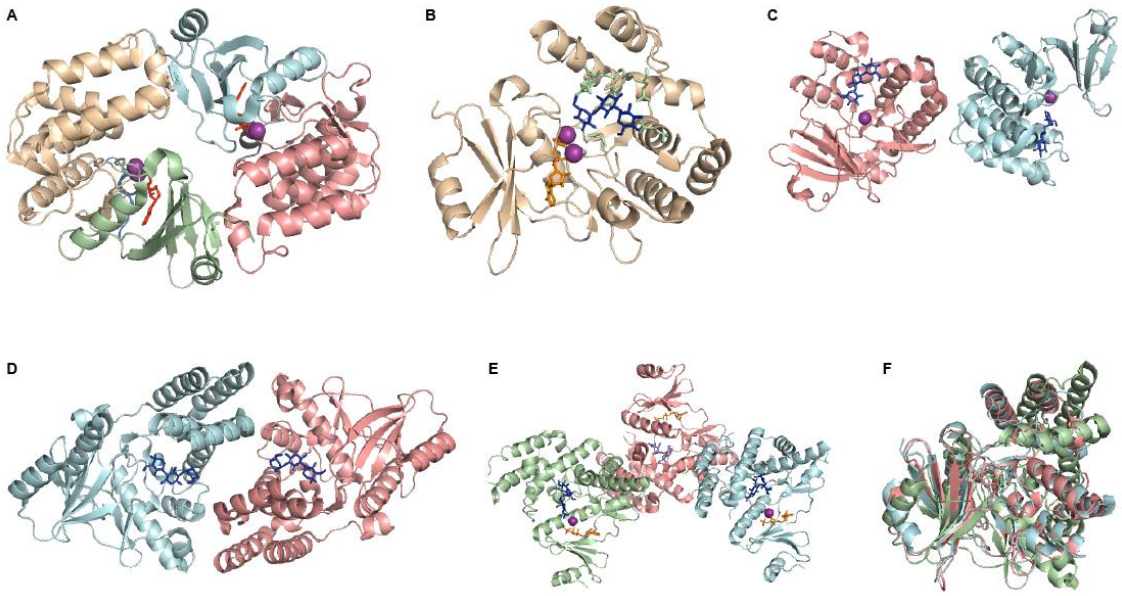

Fig. 1.8. Crystal structures of various APHs. **A.** APH(3')-IIIa (PDB 1J7L) in complex with ADP. The enzyme exists as a doubly disulfide-bonded dimer. Each monomer consists of a C-terminal lobe and a smaller N-terminal lobe connected by a 12-residue linker region, **B.** APH(3')-IIIa (PDB 1L8T) in complex with ADP and KAN. The C-terminal residues that make contacts with the AG are highlighted in pale gray, **C.** APH(3')-IIa (PDB 1ND4) in complex with KAN. The two monomers are displayed, **D.** APH(2")-IIa (PDB 3HAM) in complex with KAN. The two monomers are displayed, **E.** APH(3')-IIa (PDB 1ND4) in complex with STR and ATP. Three monomers are shown, **F.** Superimposition of APH(3')-IIIa (PDB 1L8T), APH(3')-IIa (PDB 1ND4), and APH(2")-IIa (PDB 3HAM). ATP/ADP and AGs are displayed as sticks. The spheres represent Mg^{2+} ions.

The largest and most well studied sub-families of APHs are the APH(3')s, and the best studied enzyme of this class is the plasmid encoded APH(3')-IIIa from *Enterococcus faecalis*.[126,127] Interestingly, TOB, which lacks the 3'-hydroxyl group, is not a substrate but rather a potent inhibitor of APH(3')-IIIa.[127] It was also found that for AGs lacking a

3'-hydroxyl group, such as lividomycin A, phosphorylation may occur at the 5''-hydroxyl group of the ribose ring.[128] In the case of butirosin and NEO, both of which have 3'- and 5''-hydroxyl groups, phosphorylation was found to occur at either position. Those 4,5-disubstituted AGs were shown to be rapidly mono-phosphorylated, and subsequently di-phosphorylated.[129,130]

The crystal structure of the APH(3')-IIIa•ADP complex was solved in 1997 (Fig. 1.8A,B).[131] Despite a complete lack of sequence homology to eukaryotic protein kinases, APH(3')-IIIa displays a striking similarity to several kinases, with nearly half of the APH(3')-IIIa sequence adopting a conformation identical to that seen in eukaryotic kinases. Recently, Fong and Berghuis demonstrated that further derivatization of the AHB group is a promising strategy for producing AGs with the potential to elude inactivation by APH enzymes.[132] Another common APH found in a variety of Gram-negative bacteria (*Avibacterium paragallinarum* and *E. coli*) is APH(3')-Ia, which displays additional ATPase activity in the absence of an AG.[133-135] The X-ray crystal structure of APH(3')-IIa in complex with KAN became available in 2002 (Fig. 1.8C).[136]

Another member of this family for which there is structural information is APH(2'')-IIa (Fig. 1.8D).[137] The structures of two complexes, the binary GEN complex as well as a ternary complex containing ATP and STR, were reported (Fig. 1.8E).[137] Analysis of the two complexes gives insights as to why APH(2'')-IIa favors 4,6-disubstituted AGs as substrates rather than the 4,5-disubstituted antibiotics. In GEN, the molecule is easily able to adopt an extended conformation with a large spacing between the primed and doubly primed rings, whereas in STR, such motion is constrained to adopt a sterically unfavorable conformation.

1.5.3.3.3. AG nucleotidyltransferases (ANTs)

Although they are the smallest family of AMEs, ANTs, with only 10 enzymes identified to date, have a major impact on clinical resistance, as both GEN and TOB are substrates of ANT(2''). The genes encoding ANTs are widely found in pathogenic bacteria. The *ant*(4'), *ant*(6), and *ant*(9) genes are found on plasmids or transposons in Gram-positive

bacteria whilst the *ant*(2") and *ant*(3") are often found on mobile genetic elements in Gram-negative strains. These enzymes are able to catalyze *O*-adenylation reaction between ATP and AG in the presence of Mg^{2+} ions.

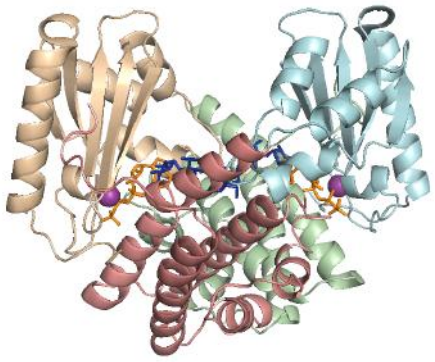

Fig. 1.9. Crystal structure of ANT(4') (PDB 1KNY) in complex with AMPPCP and KAN. The enzyme functions as a dimer and each monomer is divided into two structural domains (N-terminal and C-terminal domains) of approximately equal size. The spheres represent Mg^{2+} ions.

Enzymes that are able to regio-selectively adenylate the 6- and 3"-positions of STR and the 9- and 3"-positions of spectinomycin (SPT) have been identified. The reactions catalyzed by ANT(2") and ANT(4') are most significant and have been the most studied mechanistically. The enzyme exhibits activity with a broad array of 4,6-disubstituted substrates.[138]

Structural data for only one ANT has been reported, which is an ANT(4') from *S. aureus*.[139] The crystal structure was reported as enzyme complexed with both the non-hydrolyzable nucleotide analog AMPPCP and KAN (Fig. 1.9). The AMPPCP molecule is locked into position by extensive hydrogen bonding, but there were few interactions found between adenine ring and protein, explaining why ANT(4') accepts other nucleotides such as GTP. More recently, Mobashery and co-workers investigated the bifunctional ANT(3")-Ii/AAC(6')-IId from *S. marcescens*.[96] The structure assignment of the enzymatic products indicated that acetylation takes place on the 6'-amine of KAN and the adenylation on the 3"- and 9-hydroxyl groups of STR and SPT, respectively.

1.6. Tuberculosis (TB): current development and treatment

TB, a disease caused by infection of *Mtb* bacilli, is highly contagious and life-threatening. According to the world health organization (WHO), more than two billion people, which is about one third of the world's population, are infected with the bacteria.[140] Most infections in humans result in an asymptomatic infection.[141] The immune system protects the TB bacilli by a thick waxy coat, causing it to lie dormant for years. When the immune system is weakened, the chances of getting the active TB become greater. TB is the

leading killer among people living with HIV, who have weakened immune systems.[142-146] About one in ten of those people with latent infections will eventually progress to active disease in his or her lifetime. If left untreated, each person with active TB can infect on average 10 to 15 people a year. If it does become active, it most commonly involves infection in the lungs and only pulmonary TB is infectious. TB is a worldwide pandemic but also a disease related to poverty, more people in the developing world contract TB because their immune systems are more likely to be compromised due to higher rates of HIV infection and they have reduced access to anti-TB drugs. Therefore, the distribution of TB is not even across the globe.[147] About 80% of the population in many Asian and African countries shows positive result in tuberculin tests, while only 5-10% of the U.S. population is positive. Although TB is an airborne and in many cases lethal, disease it is preventable and curable. The WHO is working together with many organizations and countries to dramatically reduce the burden of TB. In 2010, the number of people who fell ill with TB dropped to 8.8 million, including 1.1 million cases among people with HIV. This number has been falling since 2005. The TB mortality rate has fallen by 40% since 1990 and the percentage of people successfully treated peaked at 87% in 2009.[140,148] Although slowly falling from the peak in 2002, the estimated global incidence rate was still higher than 0.1%, with 128 cases per 100,000 population in 2010. And 1.4 million people died from TB in 2010, equal to approximately 3800 deaths a day.[149]

1.6.1. TB resistance

One of the biggest obstacles in TB treatment is the drug resistance problem. *Mtb* is naturally resistant to several classes of antibiotics such as β-lactams because of the presence of periplasmic β-lactamases, as well as a highly hydrophobic cell wall that acts as a barrier for the treatment.[150-152] The prevalence of resistance to anti-TB drugs is mainly due to the improper use of chemotherapy. It is a combination of a number of actions, including inappropriate administration of treatment regimens by the doctors and failure to complete the whole course of treatment by patients.[153] Drug resistance largely arises in areas with poor TB control programs. The drug resistance in TB treatment is almost as old as the introduction of the first anti-TB drug. As the TB monotherapy induces the selection of drug-resistant bacteria, a combined therapy is necessary since the

probability of a bacteria strain to develop resistance to multiple drugs at the same time is lower. However, multi-drug resistant (MDR) TB, which is defined as tuberculosis that is resistant at least to isoniazid (INH) and rifampicin (RMP), soon emerged.[154,155] In 2010, there was an estimated prevalence of 650,000 cases of MDR-TB.[156] Each year, about 150,000 persons with MDR-TB die.[156] In 2006, the first reports of extensively drug-resistant (XDR) TB, an even more severe form of MDR-TB, began to appear.[156-158] XDR-TB is defined as TB with resistance to at least INH, RMP, any fluoroquinolone, and one of the three second-line injectable drugs including KAN, AMK and capreomycin (CAP).[157,159] There are an estimated 25,000 cases of XDR-TB emerging every year. Sixty-nine countries have reported at least one case of XDR-TB by the end of 2010.[156,160] Recently, the terms extremely drug resistant (XXDR-TB) and totally drug-resistant TB (TDR-TB) were given by authors reporting these cases in India.[161,162] These terms have not been recognized by the WHO yet because of the limitations of *in vitro* drug susceptibility testing (DST), the relevance of DST results to clinical response, and the ongoing development of anti-TB drugs.[160]

1.6.2. TB drugs and treatment

Anti-TB drugs cure the disease through three major actions including bactericidal action, sterilizing action, and prevention of the emergence of bacillary resistance to drugs.[163-165] First commenced in the 70s, short-course chemotherapy regimen for treating drug-susceptible TB takes advantage of four first-line drugs INH, RMP, ethambutol (EMB) and pyrazinamide (PZA).[166] Currently, the standard short-course chemotherapy, as recommended by the WHO, comprises a six-month regimen, with all four first-line drug for two months, followed by INH and RMP for another four months.[166,167] The treatment regimen for MDR-TB typically include a prolonged duration, generally more than 18 months, of 5 to 6 drugs that are effective based on the result of DST and/or previous treatment history. Second-line drugs such as AG, CAP, fluoroquinolone, ethionamide or prothionamide are often included in the regimen. Options to treat XDR-TB are available but are not routinely recommended.[168,169] These may include the use of high-dose INH, linezolid, clofazimine, amoxicillin, thioacetazone, clarithromycin, etc.[154,170] While the present chemotherapy for TB is highly efficacious if used properly, it has the

disadvantages of being lengthy and complex, and has not met the expectation of the WHO-recommended Stop TB Strategy. New anti-TB drugs, especially compounds to combat MDR and XDR-TB, are urgently needed.[170-173] Several important properties should be considered. First of all, drugs that have long lasting anti-mycobacterial activity and better potency *in vivo*, especially against MDR- and XDR-TB, are desirable. They can be administered with long intervals, shortened regimen time, and consequently enhance patient compliance and reduce treatment cost. Secondly, drugs with low toxicity and little adverse effects are preferred. Moreover, new classes of anti-TB drugs that is capable of treating the dormant form of TB, especially drug-resistance latent TB, is very promising for prevention of TB incidence since it will remarkably reduce the incidence of active TB. In addition, effective treatment of TB in HIV-positive individuals is desperately in need.

1.6.3. AGs as anti-TB drugs

Streptomycin (STR), the first drug that was effective in the treatment of TB, was an antibiotic derived from *Streptomyces griseus* in the 1940s.[174-176] Because STR has been used early in TB treatment as a monotherapy drug, nowadays the resistant rate of STR in TB clinical isolate is the highest among anti-TB drugs.[177,178] Similar to STR, KAN, which is isolated from *Streptomyces kanamyceticus*, as well as AMK, which is a semi-synthetic derivative of KAN, are aminocyclitol glycosides (*i.e.* AGs) used as second-line anti-TB drugs.[56,179,180]

In *Mtb* clinical isolates, resistance to STR, KAN, and AMK results from mutations of drug target the 16s rRNA and S12 protein, as well as inactivation by AME.[93,175,181-183] Missense mutations in the *rpsL* gene, which encode the S12 protein, have been shown to be associated with STR resistance.[174,184] An A to G mutation at codon 43 of the *rpsL* gene, which causes an Arg to Lys substitution, is the most frequent mutation found in the *rpsL* gene.[185,186] Two other mutations with much less frequency result in the substitution of Arg43 by Thr and Lys88 by Arg in the S12 protein.[185] The second resistance mechanism results from mutations of the *rrs* gene which encodes the 16s rRNA.[187] These recessive mutations occur quite frequently in TB because unlike most other bacteria, TB only has a

single copy of the *rrs* operon.[188] The changes in 16S rRNA cause possible cross-resistance between STR, KAN, and AMK. However, this cross-resistance is not always complete or reciprocal.[174,179,180,189,190] Mutations at the well conserved C904 (to A or G) and A905 (to G) of *rrs* gene have been found in STR resistant isolates of *Mtb*.[5,175,191] Also in the 530 loop region, which includes C491, C512, A513, C515 and C516, when one or more of the aforementioned bases are substituted, high level of STR resistance occur.[185,188,191,192] The two main mutations in the *rrs* gene that confer KAN/AMK resistance in *Mtb* are mapped to A1400 (to G) and C1401 (to T).[193,194]

The most common form of AG resistance in other bacteria is through the chemical inactivation of the drug by AMEs. This mechanism had not been encountered before in *Mtb*, which has no known resistance plasmid or transposons.[195,196] Recently, a chromosomal encoded protein Eis (enhanced intracellular survival protein) was found responsible for KAN resistance in *Mtb*.[93] The *eis* gene was found in the genomic DNA of various *Mtb* strains and of *Mycobacterium bovis* BCG but not in that of several other non-pathogenic mycobacterial species.[197] This enzyme was initially found to play a role in intracellular survival of *Mycobacterium smegmatis* within the human macrophage-like cell line U-937.[197-199] Phase separation assay suggested that Eis appears primarily in the cytoplasm and in modest amounts in the cell envelope and in the culture supernatant.[199] Further studies suggested that it inhibits T-cell proliferation *in vitro*, and subsequent production of tumor necrosis factor-α and interleukin-4.[200,201] It was suggested that Eis is a mycobacterial effector that is released into the host cell to modulate inflammatory responses, possibly via transcriptional or post-translational means.[201] The putative -10 and -35 regions of the *eis* promoter were found essential for Eis expression.[202] The protein plays key roles in regulating macrophage autophagy, inflammatory responses, and cell death via a reactive oxygen species dependent pathway.[203] Up-regulation of the *eis* gene due to mutations in the promoter region leads to increased expression of Eis, causing resistance to KAN in H37Rv, an AG-sensitive strain of *Mtb*.[93] Based on the biochemical and structural studies in our laboratory, we have demonstrated that Eis belongs to the AAC family and has an unprecedented ability to acetylate multiple amines of many AGs using AcCoA as the acetyl group donor.[204] Structural and mutagenesis

studies of Eis indicate that its acetylation mechanism is enabled by a complex tripartite fold that includes two GCN5-related *N*-acetyltransferase regions.[204] A recent study done by Ganaie *et al* found that only the hexameric form of Eis has a thermostable AAC activity.[205]

This dissertation consists of eight chapters which summarize the research that I did under the supervision of Professor Garneau-Tsodikova. Chapter one is the introduction to AGs, AMEs, and TB, whilst chapter eight discusses the future directions of the projects. In chapter two, we report the development of a chemoenzymatic methodology which took advantage of the AACs' cosubstrate promiscuity for the generation of *N*-acylated AG analogs. In chapter two, we show that AGs can be doubly modified by the sequential actions of AMEs. Chapters three to six focus on the Eis protein from *Mtb* which is an AAC that is capable of acetylating multiple amines on AGs. The crystal structure of the protein, along with the mutagenesis studies and biochemical assays, helped us proposed a reaction mechanism. We also find that unlike other AACs, this enzyme displays limited cosubstrate promiscuity. Several inhibitors of this enzyme are identified and characterized via high-throughput screening assay. In chapter seven, studies on the Eis homolog from *Mycobacterium smegmatis* are presented.

1.7. References

(1) Walter, F.; Vicens, Q.; Westhof, E. *Current opinion in chemical biology* **1999**, *3*, 694.
(2) Davies, J.; Wright, G. D. *Trends Microbiol* **1997**, *5*, 234.
(3) H, W.; Y, T. *Bioorganic & medicinal chemistry letters* **1997**, *7*, 1951.
(4) Kumar, S.; Xue, L.; Arya, D. P. *Journal of the American Chemical Society* **2011**, *133*, 7361.
(5) Moazed, D.; Noller, H. F. *Nature* **1987**, *327*, 389.
(6) Kondo, J.; Pachamuthu, K.; Francois, B.; Szychowski, J.; Hanessian, S.; Westhof, E. *ChemMedChem* **2007**, *2*, 1631.
(7) Ogle, J. M.; Ramakrishnan, V. *Annu Rev Biochem* **2005**, *74*, 129.
(8) Shandrick, S.; Zhao, Q.; Han, Q.; Ayida, B. K.; Takahashi, M.; Winters, G. C.; Simonsen, K. B.; Vourloumis, D.; Hermann, T. *Angew Chem Int Ed Engl* **2004**, *43*, 3177.
(9) Vicens, Q.; Westhof, E. *Biopolymers* **2003**, *70*, 42.
(10) Pfister, P.; Hobbie, S.; Vicens, Q.; Bottger, E. C.; Westhof, E. *Chembiochem : a European journal of chemical biology* **2003**, *4*, 1078.
(11) Vicens, Q.; Westhof, E. *Chemistry & biology* **2002**, *9*, 747.
(12) Vicens, Q.; Westhof, E. *Journal of molecular biology* **2003**, *326*, 1175.
(13) Kondo, J.; Francois, B.; Russell, R. J.; Murray, J. B.; Westhof, E. *Biochimie* **2006**, *88*, 1027.
(14) Vicens, Q.; Westhof, E. *Structure* **2001**, *9*, 647.
(15) Francois, B.; Russell, R. J.; Murray, J. B.; Aboul-ela, F.; Masquida, B.; Vicens, Q.; Westhof, E. *Nucleic Acids Res* **2005**, *33*, 5677.
(16) Hirokawa, G.; Kaji, H.; Kaji, A. *Antimicrobial agents and chemotherapy* **2007**, *51*, 175.
(17) Dlugosz, M.; Trylska, J. *J Phys Chem B* **2009**, *113*, 7322.
(18) Wang, H.; Tor, Y. *Journal of the American Chemical Society* **1997**, *119*, 8734.
(19) Jiang, L.; Patel, D. J. *Nature structural biology* **1998**, *5*, 769.
(20) Hobbie, S. N.; Pfister, P.; Bruell, C.; Sander, P.; Francois, B.; Westhof, E.; Bottger, E. C. *Antimicrobial agents and chemotherapy* **2006**, *50*, 1489.
(21) Hobbie, S. N.; Pfister, P.; Brull, C.; Westhof, E.; Bottger, E. C. *Antimicrobial agents and chemotherapy* **2005**, *49*, 5112.
(22) Kondo, J.; Hainrichson, M.; Nudelman, I.; Shallom-Shezifi, D.; Barbieri, C. M.; Pilch, D. S.; Westhof, E.; Baasov, T. *Chembiochem : a European journal of chemical biology* **2007**, *8*, 1700.
(23) Vakulenko, S. B.; Mobashery, S. *Clin Microbiol Rev* **2003**, *16*, 430.
(24) Hermann, T. *Current opinion in structural biology* **2005**, *15*, 355.
(25) Russell, R. J.; Murray, J. B.; Lentzen, G.; Haddad, J.; Mobashery, S. *Journal of the American Chemical Society* **2003**, *125*, 3410.
(26) Cashman, D. J.; Rife, J. P.; Kellogg, G. E. *Bioorganic & medicinal chemistry letters* **2001**, *11*, 119.
(27) Lapidot, A.; Berchanski, A.; Borkow, G. *The FEBS journal* **2008**, *275*, 5236.
(28) Hegde, R.; Borkow, G.; Berchanski, A.; Lapidot, A. *The FEBS journal* **2007**, *274*, 6523.
(29) Blount, K. F.; Tor, Y. *Chembiochem : a European journal of chemical biology* **2006**, *7*, 1612.
(30) Blount, K. F.; Zhao, F.; Hermann, T.; Tor, Y. *Journal of the American Chemical Society* **2005**, *127*, 9818.
(31) Ennifar, E.; Paillart, J. C.; Bernacchi, S.; Walter, P.; Pale, P.; Decout, J. L.; Marquet, R.; Dumas, P. *Biochimie* **2007**, *89*, 1195.
(32) Tok, J. B.; Dunn, L. J.; Des Jean, R. C. *Bioorganic & medicinal chemistry letters* **2001**, *11*, 1127.
(33) Tok, J. B.; Fenker, J. *Bioorganic & medicinal chemistry letters* **2001**, *11*, 2987.
(34) Riguet, E.; Desire, J.; Boden, O.; Ludwig, V.; Gobel, M.; Bailly, C.; Decout, J. L. *Bioorganic & medicinal chemistry letters* **2005**, *15*, 4651.

(35) Belousoff, M. J.; Graham, B.; Spiccia, L.; Tor, Y. *Organic & biomolecular chemistry* **2009**, *7*, 30.
(36) Venkataraman, N.; Cole, A. L.; Ruchala, P.; Waring, A. J.; Lehrer, R. I.; Stuchlik, O.; Pohl, J.; Cole, A. M. *PLoS Biol* **2009**, *7*, e95.
(37) Gorini, L.; Kataja, E. *Proceedings of the National Academy of Sciences of the United States of America* **1964**, *51*, 487.
(38) Kellermayer, R. *Eur J Med Genet* **2006**, *49*, 445.
(39) Howard, M.; Frizzell, R. A.; Bedwell, D. M. *Nature medicine* **1996**, *2*, 467.
(40) Bedwell, D. M.; Kaenjak, A.; Benos, D. J.; Bebok, Z.; Bubien, J. K.; Hong, J.; Tousson, A.; Clancy, J. P.; Sorscher, E. J. *Nature medicine* **1997**, *3*, 1280.
(41) Rowe, S. M.; Clancy, J. P. *BioDrugs* **2009**, *23*, 165.
(42) Howard, M. T.; Anderson, C. B.; Fass, U.; Khatri, S.; Gesteland, R. F.; Atkins, J. F.; Flanigan, K. M. *Ann Neurol* **2004**, *55*, 422.
(43) Nudelman, I.; Rebibo-Sabbah, A.; Cherniavsky, M.; Belakhov, V.; Hainrichson, M.; Chen, F.; Schacht, J.; Pilch, D. S.; Ben-Yosef, T.; Baasov, T. *Journal of medicinal chemistry* **2009**, *52*, 2836.
(44) Welch, E. M.; Barton, E. R.; Zhuo, J.; Tomizawa, Y.; Friesen, W. J.; Trifillis, P.; Paushkin, S.; Patel, M.; Trotta, C. R.; Hwang, S.; Wilde, R. G.; Karp, G.; Takasugi, J.; Chen, G.; Jones, S.; Ren, H.; Moon, Y. C.; Corson, D.; Turpoff, A. A.; Campbell, J. A.; Conn, M. M.; Khan, A.; Almstead, N. G.; Hedrick, J.; Mollin, A.; Risher, N.; Weetall, M.; Yeh, S.; Branstrom, A. A.; Colacino, J. M.; Babiak, J.; Ju, W. D.; Hirawat, S.; Northcutt, V. J.; Miller, L. L.; Spatrick, P.; He, F.; Kawana, M.; Feng, H.; Jacobson, A.; Peltz, S. W.; Sweeney, H. L. *Nature* **2007**, *447*, 87.
(45) Desai, T. K.; Tsang, T. K. *The American journal of medicine* **1988**, *85*, 47.
(46) Corcoran, G. B.; Salazar, D. E.; Schentag, J. J. *The American journal of medicine* **1988**, *85*, 279.
(47) Sander, P.; Prammananan, T.; Bottger, E. C. *Molecular microbiology* **1996**, *22*, 841.
(48) Springer, B.; Kidan, Y. G.; Prammananan, T.; Ellrott, K.; Bottger, E. C.; Sander, P. *Antimicrobial agents and chemotherapy* **2001**, *45*, 2877.
(49) Pfister, P.; Risch, M.; Brodersen, D. E.; Bottger, E. C. *Antimicrobial agents and chemotherapy* **2003**, *47*, 1496.
(50) Pfister, P.; Hobbie, S.; Brull, C.; Corti, N.; Vasella, A.; Westhof, E.; Bottger, E. C. *Journal of molecular biology* **2005**, *346*, 467.
(51) Prammananan, T.; Sander, P.; Brown, B. A.; Frischkorn, K.; Onyi, G. O.; Zhang, Y.; Bottger, E. C.; Wallace, R. J., Jr. *J Infect Dis* **1998**, *177*, 1573.
(52) Hainrichson, M.; Nudelman, I.; Baasov, T. *Organic & biomolecular chemistry* **2008**, *6*, 227.
(53) Chen, L.; Hainrichson, M.; Bourdetsky, D.; Mor, A.; Yaron, S.; Baasov, T. *Bioorganic & medicinal chemistry* **2008**, *16*, 8940.
(54) Janknegt, R. *Pharm Weekbl Sci* **1990**, *12*, 81.
(55) Guthrie, O. W. *Toxicology* **2008**, *249*, 91.
(56) MA, A.; C, V. M.; HR, S.; FA., M. *J Bras Pneumol.* **2010**, *36*, 641.
(57) Tange, R. A. *Ziekenhuisfarmacie* **1987**, *3*, 15.
(58) Huth, M. E.; Ricci, A. J.; Cheng, A. G. *International journal of otolaryngology* **2011**, *2011*.
(59) Guan, M. X. *Mitochondrion* **2011**, *11*, 237.
(60) Rybak, L. P.; Ramkumar, V. *Kidney international* **2007**, *72*, 931.
(61) Bindu, L. H.; Reddy, P. P. *Int J Audiol* **2008**, *47*, 702.
(62) Harvey, S. C.; Skolnick, P. *J Pharmacol Exp Ther* **1999**, *291*, 285.
(63) Hong, S. H.; Park, S. K.; Cho, Y. S.; Lee, H. S.; Kim, K. R.; Kim, M. G.; Chung, W. H. *Hear Res* **2006**, *211*, 46.

(64) Hobbie, S. N.; Akshay, S.; Kalapala, S. K.; Bruell, C. M.; Shcherbakov, D.; Bottger, E. C. *Proceedings of the National Academy of Sciences of the United States of America* **2008**, *105*, 20888.
(65) Kondo, J.; Westhof, E. *Nucleic Acids Res* **2008**, *36*, 2654.
(66) Hanessian, S.; Butterworth, R. F.; Nakagawa, T. *Carbohydrate research* **1973**, *26*, 261.
(67) Hanessian, S.; Masse, R.; Capmeau, M. L. *J Antibiot (Tokyo)* **1977**, *30*, 893.
(68) Hanessian, S.; Takamoto, T.; Masse, R. *J Antibiot (Tokyo)* **1975**, *28*, 835.
(69) Hanessian, S.; Vatele, J. M. *J Antibiot (Tokyo)* **1980**, *33*, 675.
(70) Westermann, B.; Dorner, S. *Chem Commun (Camb)* **2005**, 2116.
(71) Park, W. K. C.; Auer, M.; Jaksche, H.; Wong, C.-H. *J. Am. Chem. Soc.* **1996**, *118*, 10150.
(72) Green, K. D.; Chen, W.; Houghton, J. L.; Fridman, M.; Garneau-Tsodikova, S. *Chembiochem : a European journal of chemical biology* **2010**, *11*, 119.
(73) Hancock, R. E.; Farmer, S. W.; Li, Z. S.; Poole, K. *Antimicrobial agents and chemotherapy* **1991**, *35*, 1309.
(74) Taber, H. W.; Mueller, J. P.; Miller, P. F.; Arrow, A. S. *Microbiological reviews* **1987**, *51*, 439.
(75) Hancock, R. E. *Annu Rev Microbiol* **1984**, *38*, 237.
(76) Magnet, S.; Blanchard, J. S. *Chemical reviews* **2005**, *105*, 477.
(77) Putman, M.; van Veen, H. W.; Konings, W. N. *Microbiol Mol Biol Rev* **2000**, *64*, 672.
(78) Shakil, S.; Khan, R.; Zarrilli, R.; Khan, A. U. *Journal of biomedical science* **2008**, *15*, 5.
(79) Aires, J. R.; Kohler, T.; Nikaido, H.; Plesiat, P. *Antimicrobial agents and chemotherapy* **1999**, *43*, 2624.
(80) Westbrock-Wadman, S.; Sherman, D. R.; Hickey, M. J.; Coulter, S. N.; Zhu, Y. Q.; Warrener, P.; Nguyen, L. Y.; Shawar, R. M.; Folger, K. R.; Stover, C. K. *Antimicrobial agents and chemotherapy* **1999**, *43*, 2975.
(81) Masuda, N.; Sakagawa, E.; Ohya, S.; Gotoh, N.; Tsujimoto, H.; Nishino, T. *Antimicrobial agents and chemotherapy* **2000**, *44*, 3322.
(82) Murakami, S.; Nakashima, R.; Yamashita, E.; Yamaguchi, A. *Nature* **2002**, *419*, 587.
(83) Yu, E. W.; Aires, J. R.; Nikaido, H. *Journal of bacteriology* **2003**, *185*, 5657.
(84) Edgar, R.; Bibi, E. *Journal of bacteriology* **1997**, *179*, 2274.
(85) Bryan, L. E.; Kowand, S. K.; Van Den Elzen, H. M. *Antimicrobial agents and chemotherapy* **1979**, *15*, 7.
(86) Miller, M. H.; Edberg, S. C.; Mandel, L. J.; Behar, C. F.; Steigbigel, N. H. *Antimicrobial agents and chemotherapy* **1980**, *18*, 722.
(87) Doi, Y.; Yokoyama, K.; Yamane, K.; Wachino, J.; Shibata, N.; Yagi, T.; Shibayama, K.; Kato, H.; Arakawa, Y. *Antimicrobial agents and chemotherapy* **2004**, *48*, 491.
(88) Chow, J. W. *Clinical infectious diseases : an official publication of the Infectious Diseases Society of America* **2000**, *31*, 586.
(89) Galimand, M.; Sabtcheva, S.; Courvalin, P.; Lambert, T. *Antimicrobial agents and chemotherapy* **2005**, *49*, 2949.
(90) Yan, J. J.; Wu, J. J.; Ko, W. C.; Tsai, S. H.; Chuang, C. L.; Wu, H. M.; Lu, Y. J.; Li, J. D. *The Journal of antimicrobial chemotherapy* **2004**, *54*, 1007.
(91) Powers, T.; Noller, H. F. *EMBO J* **1991**, *10*, 2203.
(92) Kotra, L. P.; Haddad, J.; Mobashery, S. *Antimicrobial agents and chemotherapy* **2000**, *44*, 3249.
(93) Zaunbrecher, M. A.; Sikes, R. D., Jr.; Metchock, B.; Shinnick, T. M.; Posey, J. E. *Proceedings of the National Academy of Sciences of the United States of America* **2009**, *106*, 20004.
(94) Wright, G. D.; Berghuis, A. M.; Mobashery, S. *Advances in experimental medicine and biology* **1998**, *456*, 27.

(95) Mingeot-Leclercq, M. P.; Glupczynski, Y.; Tulkens, P. M. *Antimicrobial agents and chemotherapy* **1999**, *43*, 727.
(96) Kim, C.; Hesek, D.; Zajicek, J.; Vakulenko, S. B.; Mobashery, S. *Biochemistry* **2006**, *45*, 8368.
(97) Dubois, V.; Poirel, L.; Marie, C.; Arpin, C.; Nordmann, P.; Quentin, C. *Antimicrob Agents Chemother* **2002**, *46*, 638.
(98) Mendes, R. E.; Toleman, M. A.; Ribeiro, J.; Sader, H. S.; Jones, R. N.; Walsh, T. R. *Antimicrobial agents and chemotherapy* **2004**, *48*, 4693.
(99) Centron, D.; Roy, P. H. *Antimicrobial agents and chemotherapy* **2002**, *46*, 1402.
(100) Lovering, A. M.; White, L. O.; Reeves, D. S. *The Journal of antimicrobial chemotherapy* **1987**, *20*, 803.
(101)Sunada, A.; Nakajima, M.; Ikeda, Y.; Kondo, S.; Hotta, K. *J Antibiot (Tokyo)* **1999**, *52*, 809.
(102) Franklin, K.; Clarke, A. J. *Antimicrobial agents and chemotherapy* **2001**, *45*, 2238.
(103) Rather, P. N.; Orosz, E.; Shaw, K. J.; Hare, R.; Miller, G. *Journal of bacteriology* **1993**, *175*, 6492.
(104) Hegde, S. S.; Javid-Majd, F.; Blanchard, J. S. *The Journal of biological chemistry* **2001**, *276*, 45876.
(105) Vetting, M. W.; Hegde, S. S.; Javid-Majd, F.; Blanchard, J. S.; Roderick, S. L. *Nature structural biology* **2002**, *9*, 653.
(106) Wybenga-Groot, L. E.; Draker, K.; Wright, G. D.; Berghuis, A. M. *Structure* **1999**, *7*, 497.
(107) Wolf, E.; Vassilev, A.; Makino, Y.; Sali, A.; Nakatani, Y.; Burley, S. K. *Cell* **1998**, *94*, 439.
(108) Wimberly, B. T.; Brodersen, D. E.; Clemons, W. M., Jr.; Morgan-Warren, R. J.; Carter, A. P.; Vonrhein, C.; Hartsch, T.; Ramakrishnan, V. *Nature* **2000**, *407*, 327.
(109) Carter, A. P.; Clemons, W. M.; Brodersen, D. E.; Morgan-Warren, R. J.; Wimberly, B. T.; Ramakrishnan, V. *Nature* **2000**, *407*, 340.
(110) Vetting, M. W.; Magnet, S.; Nieves, E.; Roderick, S. L.; Blanchard, J. S. *Chemistry & biology* **2004**, *11*, 565.
(111) Magalhaes, M. L.; Vetting, M. W.; Gao, F.; Freiburger, L.; Auclair, K.; Blanchard, J. S. *Biochemistry* **2008**, *47*, 579.
(112) Magnet, S.; Lambert, T.; Courvalin, P.; Blanchard, J. S. *Biochemistry* **2001**, *40*, 3700.
(113) Daigle, D. M.; Hughes, D. W.; Wright, G. D. *Chemistry & biology* **1999**, *6*, 99.
(114) Radika, K.; Northrop, D. B. *The Journal of biological chemistry* **1984**, *259*, 12543.
(115) Burk, D. L.; Ghuman, N.; Wybenga-Groot, L. E.; Berghuis, A. M. *Protein science : a publication of the Protein Society* **2003**, *12*, 426.
(116) Burk, D. L.; Xiong, B.; Breitbach, C.; Berghuis, A. M. *Acta Crystallogr D Biol Crystallogr* **2005**, *61*, 1273.
(117) Draker, K. A.; Northrop, D. B.; Wright, G. D. *Biochemistry* **2003**, *42*, 6565.
(118) Vetting, M. W.; Park, C. H.; Hegde, S. S.; Jacoby, G. A.; Hooper, D. C.; Blanchard, J. S. *Biochemistry* **2008**, *47*, 9825.
(119) Robicsek, A.; Strahilevitz, J.; Jacoby, G. A.; Macielag, M.; Abbanat, D.; Park, C. H.; Bush, K.; Hooper, D. C. *Nature medicine* **2006**, *12*, 83.
(120) Neuhauser, M. M.; Weinstein, R. A.; Rydman, R.; Danziger, L. H.; Karam, G.; Quinn, J. P. *JAMA* **2003**, *289*, 885.
(121) Boehr, D. D.; Jenkins, S. I.; Wright, G. D. *The Journal of biological chemistry* **2003**, *278*, 12873.
(122) Fujimura, S.; Tokue, Y.; Takahashi, H.; Kobayashi, T.; Gomi, K.; Abe, T.; Nukiwa, T.; Watanabe, A. *FEMS microbiology letters* **2000**, *190*, 299.
(123) Javier Teran, F.; Alvarez, M.; Suarez, J. E.; Mendoza, M. C. *The Journal of antimicrobial chemotherapy* **1991**, *28*, 333.
(124) Reece, K. S.; Phillips, G. J. *Gene* **1995**, *165*, 141.

(125) Goldstein, D. A.; Tinland, B.; Gilbertson, L. A.; Staub, J. M.; Bannon, G. A.; Goodman, R. E.; McCoy, R. L.; Silvanovich, A. *Journal of applied microbiology* **2005**, *99*, 7.
(126) McKay, G. A.; Robinson, R. A.; Lane, W. S.; Wright, G. D. *Biochemistry* **1994**, *33*, 14115.
(127) McKay, G. A.; Thompson, P. R.; Wright, G. D. *Biochemistry* **1994**, *33*, 6936.
(128) Kondo, S.; Yamamoto, H.; Naganawa, H.; Umezawa, H. *J Antibiot (Tokyo)* **1972**, *25*, 483.
(129) Thompson, P. R.; Hughes, D. W.; Wright, G. D. *Biochemistry* **1996**, *35*, 8686.
(130) Cox, J. R.; McKay, G. A.; Wright, G. D.; Serpersu, E. H. *J Am Chem Soc* **1996**, *118*, 1295.
(131) Hon, W. C.; McKay, G. A.; Thompson, P. R.; Sweet, R. M.; Yang, D. S.; Wright, G. D.; Berghuis, A. M. *Cell* **1997**, *89*, 887.
(132) Fong, D. H.; Berghuis, A. M. *Antimicrobial agents and chemotherapy* **2009**, *53*, 3049.
(133) Siregar, J. J.; Lerner, S. A.; Mobashery, S. *Antimicrobial agents and chemotherapy* **1994**, *38*, 641.
(134) Radika, K.; Northrop, D. *Analytical biochemistry* **1984**, *141*, 413.
(135) Siregar, J. J.; Miroshnikov, K.; Mobashery, S. *Biochemistry* **1995**, *34*, 12681.
(136) Nurizzo, D.; Shewry, S. C.; Perlin, M. H.; Brown, S. A.; Dholakia, J. N.; Fuchs, R. L.; Deva, T.; Baker, E. N.; Smith, C. A. *Journal of molecular biology* **2003**, *327*, 491.
(137) Young, P. G.; Walanj, R.; Lakshmi, V.; Byrnes, L. J.; Metcalf, P.; Baker, E. N.; Vakulenko, S. B.; Smith, C. A. *Journal of bacteriology* **2009**, *191*, 4133.
(138) Williams, J. W.; Northrop, D. B. *The Journal of biological chemistry* **1978**, *253*, 5908.
(139) Pedersen, L. C.; Benning, M. M.; Holden, H. M. *Biochemistry* **1995**, *34*, 13305.
(140) WHO *Tuberculosis fact sheet 2011-2012* **2012**.
(141) Jasmer, R. M.; Nahid, P.; Hopewell, P. C. *The New England journal of medicine* **2002**, *347*, 1860.
(142) Sepkowitz, K. A.; Raffalli, J.; Riley, L.; Kiehn, T. E.; Armstrong, D. *Clin Microbiol Rev* **1995**, *8*, 180.
(143) Sepkowitz, K. A. *Clinical infectious diseases : an official publication of the Infectious Diseases Society of America* **1995**, *20*, 232.
(144) WHO *Accelerating the implementation of collaborative TB HIV activities in the WHO european region, Vienna, Austri* **2010**.
(145) Sculier, D. *Priority research questions for TB HIV in HIV prevalent and resource limited settings, WHO* **2010**.
(146) Lawn, S. D.; Zumla, A. I. *lancet* **2011**, *378*, 57.
(147) WHO *Global tuberculosis control: epidemiology, strategy, financing* **2009**, 6.
(148) Yew, W. W.; Lange, C.; Leung, C. C. *The European respiratory journal : official journal of the European Society for Clinical Respiratory Physiology* **2011**, *37*, 441.
(149) Dolin, P. J.; Raviglione, M. C.; Kochi, A. *Bulletin of the World Health Organization* **1994**, *72*, 213.
(150) Dudley, M. *Pharmacotherapy* **1995**, *15*, 9S.
(151) Dutka-Malen, S.; Evers, S.; Courvalin, P. *Journal of clinical microbiology* **1995**, *33*, 1434.
(152) Doern, G. V.; Brueggemann, A.; Holley, H. P., Jr.; Rauch, A. M. *Antimicrobial agents and chemotherapy* **1996**, *40*, 1208.
(153) Neu, H. C. *Science* **1992**, *257*, 1064.
(154) Caminero, J. A. *Int J Tuberc Lung Dis* **2006**, *10*, 829.
(155) Chan, E. D.; Laurel, V.; Strand, M. J.; Chan, J. F.; Huynh, M. L.; Goble, M.; Iseman, M. D. *American journal of respiratory and critical care medicine* **2004**, *169*, 1103.
(156) WHO *Tuberculosis MDR XDR 2011 progress report* **2011**.
(157) WHO *Report of the meeting of the WHO Global Task Force on XDR-TB, Geneva, Switzerland* **2006**.
(158) Banerjee, R.; Schecter, G. F.; Flood, J.; Porco, T. C. *Expert Rev Anti-Infe* **2008**, *6*, 713.
(159) *MMWR. Morbidity and mortality weekly report* **2006**, *55*, 301.

(160) Velayati, A. A.; Masjedi, M. R.; Farnia, P.; Tabarsi, P.; Ghanavi, J.; Ziazarifi, A. H.; Hoffner, S. E. *Chest* **2009**, *136*, 420.
(161) Udwadia, Z. F.; Amale, R. A.; Ajbani, K. K.; Rodrigues, C. *Clinical infectious diseases : an official publication of the Infectious Diseases Society of America* **2012**, *54*, 579.
(162) Rowland, K. *Nature* **2012**.
(163) Nuermberger, E. L.; Spigelman, M. K.; Yew, W. W. *Respirology* **2010**, *15*, 764.
(164) EK, S.; N, d. S.; DS, S.; JS, B.; LA., B. *Curr Pharm Biotechnol* **2002**, *3*, 197.
(165) Janin, Y. L. *Bioorganic & medicinal chemistry* **2007**, *15*, 2479.
(166) Mitchison, D. A. *American journal of respiratory and critical care medicine* **2005**, *171*, 699.
(167) Huebner, R. E.; Castro, K. G. *Annual review of medicine* **1995**, *46*, 47.
(168) Leimane, V.; Riekstina, V.; Holtz, T. H.; Zarovska, E.; Skripconoka, V.; Thorpe, L. E.; Laserson, K. F.; Wells, C. D. *lancet* **2005**, *365*, 318.
(169) Mitnick, C.; Bayona, J.; Palacios, E.; Shin, S.; Furin, J.; Alcantara, F.; Sanchez, E.; Sarria, M.; Becerra, M.; Fawzi, M. C.; Kapiga, S.; Neuberg, D.; Maguire, J. H.; Kim, J. Y.; Farmer, P. *The New England journal of medicine* **2003**, *348*, 119.
(170) Caminero, J. A.; Sotgiu, G.; Zumla, A.; Migliori, G. B. *Lancet Infect Dis* **2010**, *10*, 621.
(171) Z, M.; C, L.; H, M.; AJ, N.; X., W. *lancet* **2010**, *375*, 2100.
(172) E, L.; WN, R. *Expert Rev. Anti Infect. Ther.* **2010**, *8*, 801.
(173) Ginsberg, A. M. *Tuberculosis (Edinb)* **2010**, *90*, 162.
(174) *Tuberculosis* **2008**, *88*, 162.
(175) B, H.; ST., C. *International journal of antimicrobial agents* **1997**, *8*, 61.
(176) *British medical journal* **1948**, *2*, 769.
(177) Mitchison, D. A. *British medical bulletin* **1954**, *10*, 115.
(178) Canetti, G.; Rist, N.; Grosset, J. *The American review of respiratory disease* **1964**, *90*, 792.
(179) *Tuberculosis* **2008**, *88*, 117.
(180) *Tuberculosis* **2008**, *88*, 87.
(181)Maus, C. E.; Plikaytis, B. B.; Shinnick, T. M. *Antimicrobial agents and chemotherapy* **2005**, *49*, 3192.
(182) Zhang, Y. *Annual review of pharmacology and toxicology* **2005**, *45*, 529.
(183) Ramaswamy, S.; Musser, J. M. *Tubercle and lung disease : the official journal of the International Union against Tuberculosis and Lung Disease* **1998**, *79*, 3.
(184) Chan, E. In *Pyrazinamide, ethambutol, ethionamide, and aminoglycosides.*; WN, R., SM, G., Eds.; Lippincott Williams & Wilkins: Philadelphia, 2003, p 773.
(185) Meier, A.; Kirschner, P.; Bange, F. C.; Vogel, U.; Bottger, E. C. *Antimicrobial agents and chemotherapy* **1994**, *38*, 228.
(186) Cooksey, R. C.; Morlock, G. P.; McQueen, A.; Glickman, S. E.; Crawford, J. T. *Antimicrobial agents and chemotherapy* **1996**, *40*, 1186.
(187) Kempsell, K. E.; Ji, Y. E.; Estrada, I. C.; Colston, M. J.; Cox, R. A. *Journal of general microbiology* **1992**, *138 Pt 8*, 1717.
(188) Bottger, E. C. *Trends Microbiol* **1994**, *2*, 416.
(189) Di Perri, G.; Bonora, S. *The Journal of antimicrobial chemotherapy* **2004**, *54*, 593.
(190) Ho, Y. I.; Chan, C. Y.; Cheng, A. F. *The Journal of antimicrobial chemotherapy* **1997**, *40*, 27.
(191) Honore, N.; Cole, S. T. *Antimicrobial agents and chemotherapy* **1994**, *38*, 238.
(192) Finken, M.; Kirschner, P.; Meier, A.; Wrede, A.; Bottger, E. C. *Molecular microbiology* **1993**, *9*, 1239.
(193)Suzuki, Y.; Katsukawa, C.; Tamaru, A.; Abe, C.; Makino, M.; Mizuguchi, Y.; Taniguchi, H. *Journal of clinical microbiology* **1998**, *36*, 1220.
(194) Alangaden, G. J.; Kreiswirth, B. N.; Aouad, A.; Khetarpal, M.; Igno, F. R.; Moghazeh, S. L.; Manavathu, E. K.; Lerner, S. A. *Antimicrobial agents and chemotherapy* **1998**, *42*, 1295.

(195) Crawford, J. T.; Bates, J. H. *Infect Immun* **1979**, *24*, 979.
(196) Martin, C.; Timm, J.; Rauzier, J.; Gomez-Lus, R.; Davies, J.; Gicquel, B. *Nature* **1990**, *345*, 739.
(197) J, W.; JL, D.; JW, M.; EA, R.; P, O. G.; DB, Y.; RL., F. *Journal of bacteriology* **2000**, *182*, 377.
(198) Wei, J.; Dahl, J. L.; Moulder, J. W.; Roberts, E. A.; O'Gaora, P.; Young, D. B.; Friedman, R. L. *Journal of bacteriology* **2000**, *182*, 377.
(199) Dahl, J. L.; Wei, J.; Moulder, J. W.; Laal, S.; Friedman, R. L. *Infect Immun* **2001**, *69*, 4295.
(200) Lella, R. K.; Sharma, C. *The Journal of biological chemistry* **2007**, *282*, 18671.
(201) Samuel, L. P.; Song, C. H.; Wei, J.; Roberts, E. A.; Dahl, J. L.; Barry, C. E., 3rd; Jo, E. K.; Friedman, R. L. *Microbiology* **2007**, *153*, 529.
(202) Roberts, E. A.; Clark, A.; McBeth, S.; Friedman, R. L. *Journal of bacteriology* **2004**, *186*, 5410.
(203) Shin, D. M.; Jeon, B. Y.; Lee, H. M.; Jin, H. S.; Yuk, J. M.; Song, C. H.; Lee, S. H.; Lee, Z. W.; Cho, S. N.; Kim, J. M.; Friedman, R. L.; Jo, E. K. *PLoS Pathog* **2010**, *6*, e1001230.
(204) Chen, W.; Biswas, T.; Porter, V. R.; Tsodikov, O. V.; Garneau-Tsodikova, S. *Proceedings of the National Academy of Sciences of the United States of America* **2011**, *108*, 9804.
(205) Ganaie, A. A.; Lella, R. K.; Solanki, R.; Sharma, C. *PloS one* **2011**, *6*, e27590.

Note:

This chapter is partially adapted from a published review article: Houghton, J. L.; Green, K. D.; **Chen, W.**; Garneau-Tsodikova, S. *ChemBioChem* **2010**, *11*, 880.

Chapter 2

Exploring the substrate promiscuity of drug-modifying enzymes for the chemoenzymatic generation of *N*-acylated aminoglycosides

2.1. Abstract

Aminoglycosides (AGs) are broad-spectrum antibiotics commonly used for the treatment of serious bacterial infections. Decades of clinical use have led to the widespread emergence of bacterial resistance to this family of drugs limiting their efficacy in the clinic. Here, we report the development of a methodology that utilizes AG acetyltransferases (AACs) and unnatural acyl coenzyme A analogs for the chemoenzymatic generation of *N*-acylated AG analogs. Generation of *N*-acylated AGs is followed by a simple qualitative test to assess their potency as potential antibacterials. The studied AACs AAC(6')/APH(2'') and AAC(3)-IV show diverse substrate promiscuity towards a variety of AGs as well as acyl coenzyme A derivatives. The enzymes were also used for the sequential generation of homo- and hetero-di-*N*-acylated AGs. Following the clinical success of the *N*-acylated amikacin (AMK) and arbekacin, our chemoenzymatic approach offers access to regioselectively *N*-acylated AGs in quantities that allow testing of the antibacterial potential of the synthetic analogs making it possible to decide which molecules will be worth synthesizing on a larger scale.

2.2. Introduction

AGs are broad-spectrum antibiotics commonly used for the treatment of serious bacterial infections.[1-3] These antibacterial agents target the prokaryotic ribosome by binding the decoding A-site of the 16S ribosomal RNA and cause interference with protein translation, which ultimately leads to cell death.[1,4-6] Decades of intensive clinical use of AGs has led to evolutionarily driven bacterial resistance that compromises their clinical use.[7] A common mode of bacterial resistance evolved through the acquisition of enzymes

that chemically modify the AG including AACs, AG nucleotidyltransferases (ANTs), and AG phsophotransferases (APHs).[2,4] Other modes of resistance include decreasing cell membrane permeability towards AG uptake and structural alteration in the ribosomal target of the drug, as well as extrusion of the AGs from the cell by efflux pumps.[8]

While *N*-acetylation by the AAC family of AG-modifying enzymes (AMEs) evolved in bacteria to deactivate the AGs, some natural and effective AGs contain an *N*-acylated amine (Fig. 2.1). In most cases, these natural *N*-acylated AGs show broad-spectrum activity against strains that are resistant to non-*N*-acylated AGs. One such example is butirosin, which is produced by *Bacillus circulans* and has been identified as 1-*N*-(S)-α-hydroxy-γ-amino-*n*-butyryl (AHB) ribostamycin (RIB). Butirosin was found to be active against some RIB-resistant bacteria thus demonstrating the efficacy of the AHB *N*-acylation effect.[9-11]

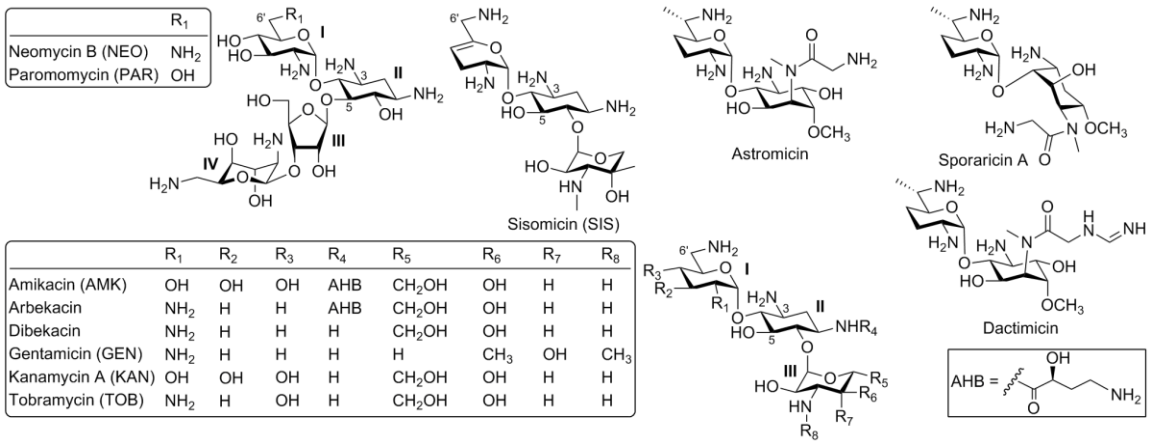

	R_1	R_2	R_3	R_4	R_5	R_6	R_7	R_8
Amikacin (AMK)	OH	OH	OH	AHB	CH_2OH	OH	H	H
Arbekacin	NH_2	H	H	AHB	CH_2OH	OH	H	H
Dibekacin	NH_2	H	H	H	CH_2OH	OH	H	H
Gentamicin (GEN)	NH_2	H	H	H	H	CH_3	OH	CH_3
Kanamycin A (KAN)	OH	OH	OH	H	CH_2OH	OH	H	H
Tobramycin (TOB)	NH_2	H	OH	H	CH_2OH	OH	H	H

Fig. 2.1. Chemical structures of natural and synthetic 2-deoxystreptamine-derived (ring II) AGs used in this study.

These observations led to the development of the semi-synthetic arbekacin, a marketed chemotherapeutic agent, and AMK,[12] both of which have an AHB group at the 1-*N*-position (Scheme 1).[13] Mobashery and co-workers applied AHB substitution at position *N*-1 of neamine (NEA) with the rational that AHB substitution in AMK is responsible for the protection against a number of AMEs.[14] Some of the structures showed considerably enhanced activity against different pathogenic and resistant strains, and their activities were comparable to that of AMK. Baasov and colleagues also took advantage of the

AHB moiety at the *N*-1 position of paromamine to generate the novel AG NB54. NB54 exhibits significant read-through activity that offers a potential solution to overcome genetic disorders that result from stop codon mutations.[15] While the majority of the known *N*-acylated AGs have an AHB group at position *N*-1, other examples of different acyl groups with different positioning around the rings of the AG exist. Sporaricin A and astromicin, which is also known as fortimicin A, are pseudodisaccharide AGs containing an *N*-methyl-*N*-glycinyl group and exhibit antibacterial activity against a variety of bacterial strains.[16,17] Dactimicin, with an *N*-methyl-*N*-formimidoylglycyl moiety, exhibits antibacterial activity superior to that of AMK against resistant strains.[18] These characteristics demonstrate the medicinal potential of *N*-acylated AGs and the need to explore the antibacterial potential of novel analogs containing a variety of *N*-acyl groups at different positions on the AG.

The synthesis of *N*-acylated AG derivatives poses the challenge of approaching a specific amine position on an AG. The multiple amines about the AG skeleton (ranging between four on kanamycin A (KAN) to six on neomycin B (NEO)) share similar chemical reactivity and make it difficult to selectively *N*-acylate amines on the AGs. The existing derivatives, such as AMK and dibekacin, rely on regioselective activation of the amine by metal chelation and protecting group manipulations for their synthesis.[13] Selecting an amine position other than the *N*-1, which was chosen in the case of AMK and arbekacin, sets a new synthesis challenge. We therefore reasoned that we could exploit the regioselectivity offered by AACs for the *in vitro* chemoenzymatic generation of novel regioselectively *N*-acylated AGs to circumvent the need for multi-step syntheses. In this study we report the use of a family of enzymes that evolved in bacteria to confer resistance to AGs, the AACs, as a tool for the development of *N*-acylated antibiotic analogs. Even though limited amounts of products are generated chemoenzymatically, the method is extremely valuable as it allows for an initial activity screen that can guide further decisions as to which compounds justify large scale and multi-step syntheses.

In a previous publication we demonstrated that synthetic acyl coenzyme A (CoA) analogs are accepted by the CouN1 and CouN7 proteins involved in transfer of the pyrrolyl

moiety during the late stage of coumermycin A1 biosynthesis. By using a chemoenzymatic approach, we demonstrated that novel novobiocin analogs can be produced in milligram quantities by the action of the pair of enzymes CouN1 and CouN7.[19] Recently, we also demonstrated the substrate and cosubstrate promiscuity of choline acetyltransferase (ChAT) for the production of acetylcholine analogs.[20] These studies clearly demonstrate how the promiscuity of an acyltransferase system can be used for the chemoenzymatic generation of novel molecules that would otherwise require multi-step syntheses.

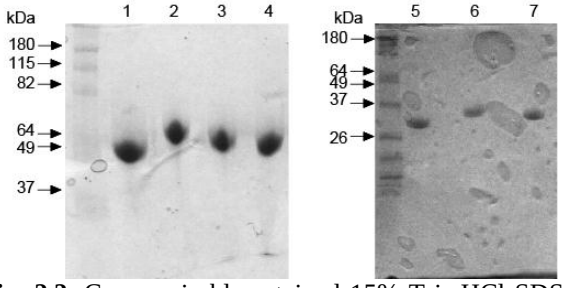

Fig. 2.2. Coomassie blue-stained 15% Tris-HCl SDS-PAGE gel showing the purified AAC(6')/APH(2")(no tag) (Int-pET19b-pps) (56992 Da, lane 1), AAC(6')/APH(2")(NHis) (Int-pET19b-pps) (60897 Da, lane 2), AAC(6')/APH(2")(NHis) (pET28a) (59155 Da, lane 3), AAC(6')/APH(2")(CHis) (pET22b) (57678 Da, lane 4), AAC(3)-IV(no tag) (Int-pET19b-pps) (27906 Da, lane 5), AAC(3)-IV(NHis) (Int-pET19b-pps) (31882 Da, lane 6), and AAC(3)-IV(NHis) (pET28a) (30069 Da, lane 7). 6 μg of each protein were loaded on the gel.

2.3. Results and discussion

The promiscuity of AACs towards a variety of AGs is well established. However, the promiscuity of these AACs towards acyl-CoA cosubstrates has had limited exploration. Due to the challenges and multiple protecting group manipulations required for the generation of a single *N*-acylated AG analog, we aimed to develop a methodology that will rapidly allow access to the desired compound and will enable an initial screen to assess the antibacterial potential of the desired *N*-acylated AG analogs. Two AACs, AAC(3)-IV and AAC(6')/APH(2") were chosen for overexpression, purification, and testing for substrate and cosubstrate promiscuity (Fig. 2.2 and Table 2.1). It has previously been reported that incorporation of an N-terminal histidine tag to AAC(6')/APH(2") affects the kinetic parameters of both AcCoA and KAN.[21] We therefore tested N-terminal hexahistidine tagged ($NHis_6$), N-terminal decahistidine tagged ($NHis_{10}$), C-terminal hexahistidine ($CHis_6$) tagged, and a N-terminal tag cleaved AAC(6')/APH(2") to compare kinetic parameters. In our hands all forms of AAC(6')/APH(2") display a K_m of the same magnitude for AcCoA (2.0 ± 0.8 to 9.9 ± 1.9 μM), however, the catalytic turnovers were drastically different (Table 2.2). The $NHis_6$-tagged enzyme has a turnover (k_{cat}) of 0.012

± 0.003 s^{-1}, the $NHis_{10}$-tagged enzyme has a k_{cat} of 0.163 ± 0.019 s^{-1}, the $CHis_6$-tagged enzyme has a k_{cat} of 0.300 ± 0.075 s^{-1}, and the tag-cleaved (untagged) enzyme had an observed k_{cat} of 0.559 ± 0.155 s^{-1}. As the $CHis_6$-tagged and untagged enzymes have nearly identical catalytic efficiencies with AcCoA, we chose to test the remaining AG and CoA derivative pairs with the $CHis_6$-tagged enzyme due to the ease of purification and its improved catalytic activity compared to the NHis-tagged forms.

Table 2.1. Substrates accepted by AAC(6')/APH(2") and AAC(3)-IV† from pET28a using various AGs at pH 6.6 and pH 5.7 (for NEO, SIS, and GEN with AAC(3)-IV).

		AMK‡	GEN		KAN‡	NEO		PAR†	SIS		TOB	
Substrate	Structure	6'	6'	3	6'	6'	3	3	6'	3	6'	3
Acetoacetyl-CoA		×	--	√	×	--	×	×	×	×	×	×
AcCoA		√	--	√	√	√	√	√	√	√	√	√
Benzoyl-CoA	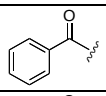	--	--	√	--	--	×	×	--	×	--	×
Butyryl-CoA	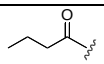	--	--	×	√	--	×	×	--	×	--	×
Crotonyl-CoA	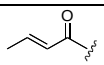	×	--	×	×	--	×	×	×	×	--	×
Glutaryl-CoA	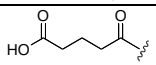	√	--	×	√	--	×	×	--	×	--	--
Glycinyl-CoA	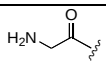	√	√	--	√	√	×	--	√	×	√	--
D,L-β-OH-Butyryl-CoA	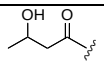	--	--	×	--	--	×	×	--	×	--	×
Isovaleryl-CoA	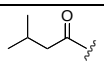	--	--	×	--	--	×	×	--	×	--	×
Malonyl-CoA	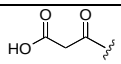	√	√	--	×	√	×	×	--	×	--	--
Methylmalonyl-CoA	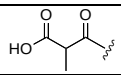	--	--	×	--	√	×	×	--	×	--	×
Palmitoyl-CoA		×	×	×	×	×	×	×	×	×	×	×
ProCoA		√	√	√	√	√	--	√	√	√	√	√

√ Compound accepted as a substrate for the enzyme. × Compound not accepted as a substrate for the enzyme.
-- Compound that is a poor substrate for the enzyme.
† PAR was not tested with AAC(6')/APH(2") as there is no NH_2 at position 6'.
‡ AMK and KAN were not tested with AAC(3)-IV due to their previously reported precipitously K_m with AcCoA.

Based on the results from AAC(6')/APH(2") we thought that the $CHis_6$-tagged AAC(3)-IV would be the construct of choice. However, examination of AAC(3) X-ray crystal structures similar to AAC(3)-IV revealed that dimerization takes place near the C-terminal residues of the protein.[22] Therefore, the proximity of the $CHis_6$-tag to the dimer

Table 2.2. Kinetic parameters for AAC(6')/APH(2") and AAC(3)-IV.

CoA analogs kinetic parameters

Enzyme (vector used)	pH	AG	CoA analogs	K_m (μM)	k_{cat} (s^{-1})	k_{cat}/K_m ($\mu M^{-1}s^{-1}$)
AAC(6')/APH(2")(NHis) (pET28a)	6.6	KAN	AcCoA	2.0 ±0.8	0.012 ±0.003	0.024
			ProCoA	4.8 ±1.5	0.017 ±0.001	0.003
AAC(6')/APH(2")(NHis) (Int-pET19b-pps)	6.6	KAN	AcCoA	3.3 ±0.2	0.163 ±0.019	0.050
			ProCoA	9.1 ±0.9	0.044 ±0.001	0.005
AAC(6')/APH(2")(no tag) (Int-pET19b-pps)	6.6	KAN	AcCoA	9.9 ±1.9	0.559 ±0.155	0.056
			ProCoA	13.5 ±1.5	0.144 ±0.005	0.011
AAC(6')/APH(2")(CHis) (pET22b)	6.6	KAN	AcCoA	5.5 ±0.4	0.300 ±0.075	0.055
			AcCoA*	2.8 ±0.1	0.075 ±0.008	0.027
			ProCoA	11.1 ±2.4	0.134 ±0.032	0.012
	6.6	AMK	AcCoA	0.96 ±0.17	0.126 ±0.028	0.131
			ProCoA	2.1 ±0.6	0.124 ±0.017	0.060
			Malonyl-CoA	71.6 ±14.6	0.146 ±0.008	0.002
	6.6	GEN	AcCoA	4.6 ±0.4	0.182 ±0.052	0.040
			ProCoA	2.9 ±0.6	0.123 ±0.015	0.043
			Malonyl-CoA	18.9 ±5.0	0.041 ±0.004	0.002
	6.6	NEO	AcCoA	14.8 ±6.3	0.188 ±0.063	0.013
			ProCoA	3.1 ±0.9	0.076 ±0.015	0.024
	6.6	SIS	AcCoA	1.5 ±0.5	0.173 ±0.028	0.112
			ProCoA	0.57 ±0.16	0.121 ±0.007	0.211
	6.6	TOB	AcCoA	2.7 ±0.5	0.179 ±0.026	0.066
			ProCoA	5.4 ±1.1	0.089 ±0.004	0.016
AAC(3)-IV(NHis) (pET28a)	5.7	GEN	AcCoA	0.803 ±0.001	0.043 ±0.004	0.053
			ProCoA	94.6 ±16.8	0.037 ±0.008	0.0004
AAC(3)-IV(NHis) (Int-pET19b-pps)	5.7	GEN	AcCoA	0.68 ±0.09	0.104 ±0.069	0.152
			Acetoacetyl-CoA	91.8 ±8.0	0.088 ±0.003	0.001
			Benzoyl-CoA	23.1 ±2.1	0.020 ±0.001	0.001
			ProCoA	78.8 ±12.1	0.025 ±0.002	0.0003
	5.7	NEO	AcCoA	9.17 ±1.90	0.350 ±0.083	0.039
			ProCoA	24.9 ±1.1	0.045 ±0.002	0.0018
	6.6	PAR	AcCoA	3.7 ±0.9	0.130 ±0.018	0.035
			ProCoA	46.9 ±1.7	0.075 ±0.003	0.0016
	5.7	SIS	AcCoA	2.05 ±0.74	0.057 ±0.007	0.028
			ProCoA	15.1 ±0.9	0.032 ±0.003	0.002
	6.6	TOB	AcCoA	3.76 ±1.17	0.045 ±0.002	0.012
			ProCoA	43.0 ±1.1	0.69 ±0.11	0.016
			Malonyl-CoA	46.5 ±12.4	0.189 ±0.049	0.004

AGs kinetic parameters

Enzyme (vector used)	pH	AG	CoA analogs	K_m (μM)	k_{cat} (s^{-1})	k_{cat}/K_m ($\mu M^{-1}s^{-1}$)
AAC(6')/APH(2")(CHis) (pET22b)	6.6	KAN	AcCoA	0.40 ±0.13	0.034 ±0.005	0.087
	6.6	SIS	AcCoA	5.9 ±1.8	0.382 ±0.104	0.065
AAC(3)-IV(NHis) (Int-pET19b-pps)	5.7	GEN	AcCoA	0.89 ±0.12	0.036 ±0.004	0.040
	5.7	NEO	AcCoA	0.56 ±0.26	0.045 ±0.030	0.082
	6.6	PAR	AcCoA	1.26 ±0.19	0.290 ±0.004	0.023
	5.7	SIS	AcCoA	0.35 ±0.02	0.026 ±0.003	0.074
	6.6	TOB	AcCoA	1.87 ±0.51	0.12 ±0.02	0.066

* = The reaction was performed with the ThioGlo-1 fluorescent detection method.

interface might affect the ability of AAC(3)-IV to bind well to the Ni(II)-NTA column, explaining the difficulties associated with purification of the AAC(3)-IV $CHis_6$-tagged

construct that we encountered. The NHis-tagged AAC(3)-IV was, therefore, the construct of choice for our study. Kinetic analysis showed that the $NHis_6$-tagged AAC(3)-IV gave a K_m of 0.803 ± 0.001 μM and catalytic turnover of k_{cat} = 0.043 ± 0.004 s^{-1} for AcCoA to give a catalytic efficiency of 0.053 $\mu M^{-1}s^{-1}$. The $NHis_{10}$-tagged AAC(3)-IV gave similar results for the K_m (0.68 ± 0.09 μM), but an increased catalytic turnover (0.104 ± 0.069 s^{-1}) for AcCoA resulting in an increased efficiency (0.152 $\mu M^{-1}s^{-1}$). From these experiments we decided to use the $NHis_{10}$-tagged AAC(3)-IV enzyme to determine the kinetic values for the remaining substrate/cosubstrate pairs.

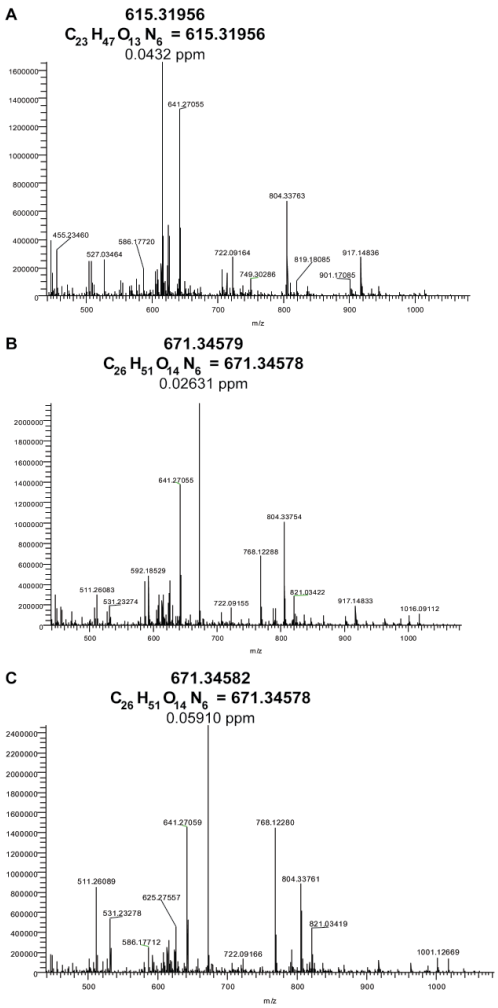

Fig. 2.3. Mass spectra for: **A.** NEO, **B.** 6'-*N*-*n*-propionyl-NEO, and **C.** 3-*N*-*n*-propionyl-NEO.

We first tested the chosen AACs using ProCoA in an initial attempt to assess the substrate specificity of the catalytic site towards larger groups compared with the methyl group of AcCoA. AAC(6')/APH(2") and AAC(3)-IV readily transferred ProCoA to the *N*-6' and *N*-3 of a wide variety of AGs, respectively (Table 2.2). The formation of 6'-*N*-n-propionyl-NEO and 3-*N*-*n*-propionyl-NEO were confirmed by HRMS (Fig. 2.3B, C).

The formation of the products can also be easily and clearly detected by a simple TLC test as demonstrated in Fig. 2.4. With the initial results demonstrating the tolerance of the chosen AACs towards more sterically demanding acyl groups, we tested a selection of both commercially available and synthetic acyl-CoAs (Table 2.1). All of the synthetic acyl-CoA analogs used in this study were prepared according to our previously reported methodology.[19]

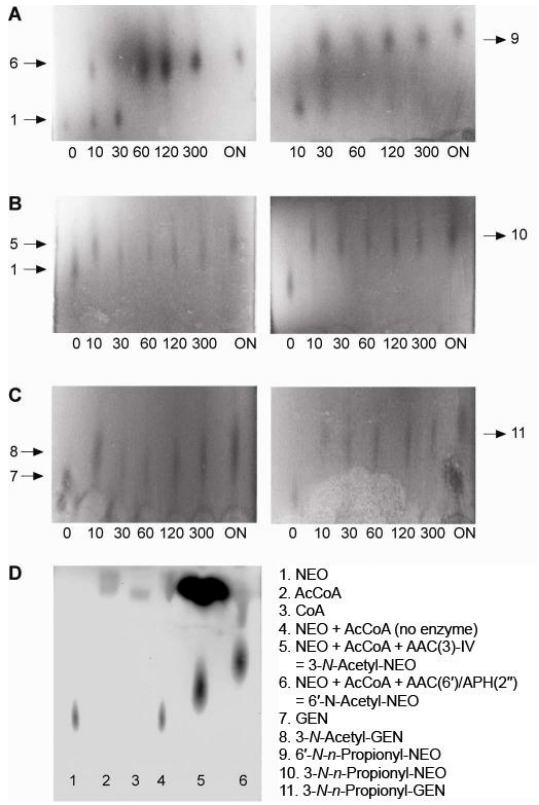

Fig 2.4. TLC time courses using AcCoA or ProCoA of the **A.** AAC(6')/APH(2") reactions with NEO showing the formation of 6'-*N*-acetyl-NEO and 6'-*N*-*n*-propionyl-NEO, **B.** AAC(3)-IV reaction with NEO showing the formation of 3-*N*-acetyl-NEO and 3-*N*-*n*-propionyl-NEO, and **C.** AAC(3)-IV reaction with GEN showing the formation of 3-*N*-acetyl-GEN and 3-*N*-*n*-propionyl-GEN. **D.** Control TLC showing that without an AAC enzyme the substrate remains unchanged, whereas with AACs the substrate gets acylated.

2.3.1. 6'-*N*-Acylation of AGs by AAC(6')/APH(2") bifunctional enzyme

AAC(6')/APH(2") exhibited relaxed substrate specificity by readily transferring a diverse set of acyl-CoAs to a diverse set of AG scaffolds. Out of the 96 combinations tested, 29 exhibited good transfer activity and demonstrated appreciable product increases when compared to AcCoA after incubation for 30 min. Reactions were monitored at 324 nm for the reaction of DTDP (4,4'-dithiodipyridine) with the CoA released upon product formation.[23]

Interestingly, methylmalonyl-CoA was successfully transferred to NEO while it was a poor substrate for KAN and AMK. This can be rationalized by the common pseudotrisaccharide structural features of KAN and AMK compared with the pseudopentasaccharide structure of NEO. Interestingly, the opposite case occurred with glutaryl-CoA. The relative relaxed acyl-CoA specificity of the enzyme towards *N*-1 acylated AMK demonstrates the potential of the AAC(6')/APH(2") for the preparation of doubly and hetero-*N*-acylated AGs. The potential of *N*-glycinylated AGs has been established by the active astromicin and sporaricin A. The successful transfer of the glycyl moiety to the 6'- position of all AGs tested demonstrates the power of our chemoenzymatic methodology for the generation of potentially novel active *N*-glycinylated AGs (Table 2.1).

2.3.2. 3-*N*-Acylation of AGs by AAC(3)-IV

AAC(3)-IV exhibited tolerance towards a variety of combinations of AGs and acyl-CoA analogs: out of the 80 combinations tested, 25 had successful transfers. Interestingly, combinations that involved gentamicin (GEN) exhibited the highest percentage of success with acyl-CoAs ranging from the natural and small acetyl group to the functionalized and sterically demanding acetoacetyl and 6-fluoropicolinyl groups. Given the vast use of GEN in the clinic as a last resort treatment for some severe respiratory system infections and the emergence of GEN-resistant strains, the generation of *N*-acylated analogs of this drug by using AAC(3)-IV will enable a more diverse exploration of potentially potent derivatives of GEN.

2.3.3. Sequential double acylation by AAC(3)-IV and AAC(6')/APH(2") yields double hetero- as well as homo-*N*-acylated AGs

Based on the observed relaxed substrate specificity of a variety of acyl-CoAs and the *N*-1 acylated AMK, we tested the possibility of dual acylation of AGs using a sequential transfer of acyl groups by the two enzymes. In order to further extend our methodology, NEO was acylated at both the 6'- and 3-positions by using AAC(6')/APH(2") and AAC(3)-IV sequentially. An increase in absorbance was observed after adding AAC(6')/APH(2") to a mixture of AcCoA (or ProCoA) and NEO. After 30 min incubation, an additional portion of AcCoA (or ProCoA) was added followed by the addition of AAC(3)-IV. An increase in the absorbance indicated the acylation at 3-position of 6'-acylated NEO to form 3,6'-di-acylated NEO (Fig. 2.5). The formation of 6'-*N*-acetyl-NEO by AAC(6')/APH(2") followed by the formation of 3,6'-*N'*,*N*-di-acetyl-NEO by AAC(3)-IV could be visualized by TLC (Fig. 2.5C). When SIS was used with a combination of AcCoA and ProCoA, respectively, 6'-*N*-acetyl-3-*N*-*n*-propionyl-SIS was obtained. These examples demonstrate the utility of our chemoenzymatic method for the generation of AG derivatives with more than one *N*-acylated position. AGs that were initially acylated by AAC(3)-IV failed to go through the second acylation by AAC(6')/APH(2"). However, if the same AGs were initially acylated by AAC(6')/APH(2"), the 6'-*N*-acylated AG was readily accepted as a substrate of AAC(3)-IV (Fig. 2.5) as proved to be the case for NEO. When the 3-position of NEO was acylated

by AAC(3)-IV, AAC(6')/APH(2") was unable to perform acylation on the 3-acylated NEO. On the other hand, initial acylation by AAC(6')/APH(2") resulted in the 6'-acylated NEO, which was readily acylated by AAC(3)-IV to yield the 3,6'-di-acylated NEO. This proved to be the case for SIS as well. We suggest that the amino group at the 3-position of these antibacterials is crucial for the binding to the active site of AAC(6')/APH(2") and therefore the desired di-acylation must commence with a transfer by AAC(6')/APH(2") followed by the second transfer by AAC(3)-IV.

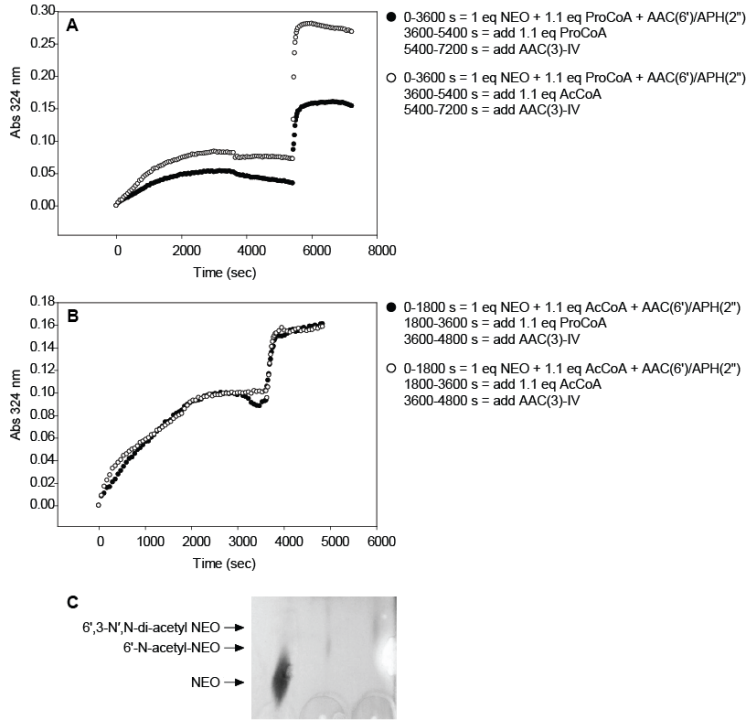

Fig. 2.5. Spectrophotometric assay plots. **A.** The formation of 6'-*N*-*n*-propionyl-NEO by using AAC(6')/APH(2") followed by the formation of 6',3-*N'*,*N*-di-*n*-propionyl-NEO by addition of AAC(3)-IV (•) and the formation of 6'-*N*-*n*-propionyl-NEO by using AAC(6')/APH(2") followed by the formation of 6'-*N*-*n*-propionyl-3-acetyl-NEO by addition of AAC(3)-IV (○). •: 0–3600 s = 1 eq NEO + 1.1 eq ProCoA + AAC(6')/APH(2"); 3600–5400 s = add 1.1 eq ProCoA; 5400–7200 s = add AAC(3)-IV; ○: 0–3600 s = 1 eq NEO + 1.1 eq ProCoA + AAC(6')/APH(2"); 3600–5400 s = add 1.1 eq AcCoA; 5400–7200 s = add AAC(3)-IV. **B.** The formation of 6'-*N*-acetyl-NEO by using AAC(6')/APH(2") followed by the formation of 6'-*N*-acetyl-3-*N*-*n*-propionyl-NEO by addition of AAC(3)-IV (•) and the formation of 6'-*N*-acetyl-NEO by using AAC(6')/APH(2") followed by the formation of 6',3-*N'*,*N*-di-acetyl NEO by addition of AAC(3)-IV (○). •: 0–1800 s = 1 eq NEO + 1.1 eq AcCoA + AAC(6')/APH(2"); 1800–3600 s = add 1.1 eq ProCoA; 3600–4800 s = add AAC(3)-IV; ○: 0–1800 s = 1 eq NEO + 1.1 eq AcCoA + AAC(6')/APH(2"); 1800–3600 s = add 1.1 eq AcCoA; 3600-4800 s = add AAC(3)-IV. **C.** TLC showing the formation of 6'-acetyl-NEO and 6',3-*N'*,*N*-di-acetyl-NEO.

2.3.4. BioTLC-based antibacterial activity screen

With the relaxed substrate and cosubstrate specificity of both AACs established, a suitable assay to assess the antibacterial activity of small quantities of the *N*-acylated AGs was needed. As the synthesis and purification of milligram scales of each analog would require a large amount of the acyl-CoAs and time, we needed a way to perform an initial qualitative antibacterial test on a pre-purified analog. We successfully accomplished both the pre-purification and qualitative antibacterial

test using a bioTLC protocol.[24] The bioTLCs revealed that NEO that was acetylated or *n*-propionylated at the 6'-amine showed a clear inhibition of the growth of *B. subtilis* (Fig. 2.6A). GEN acylated at the 3-position with AcCoA and ProCoA also exhibited a clear zone of growth inhibition (Fig. 2.6C). The minimum inhibitory concentrations (MICs) of NEO and GEN against *B. subtilus* are 0.1525 and 0.0549 μg/mL, respectively.[25] Our novel *N*-acylated AGs could be either more or less active than their parent drugs. However, because NEO and GEN are highly active against *B. subtilis*, the bioTLC does not allow detecting a small reduction or increase in activity. On the other hand, NEO acylated at the 3-position showed no inhibition compared to NEO (Fig. 2.6B). The bioTLC procedure successfully combines a short and simple TLC isolation of the active compound followed by a qualitative antibacterial assay that can indicate the antibacterial potential of the tested analog. The minimal quantity of compounds required for the bioTLC procedure allows the production of a large number of analogs with reasonable quantities of the acyl-CoAs.

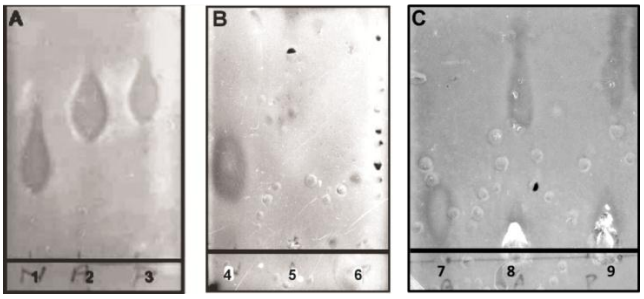

Fig. 2.6. BioTLC showing: **A.** Inhibition of *B. subtilis* growth by NEO (lanes 1 and 4), 6'-*N*-acetyl-NEO (lane 2), and 6'-*N*-*n*-propionyl-NEO (lane 3). **B.** There is no inhibition of *B. subtilis* growth by 3-*N*-acetyl-NEO (lane 5) and 3-*N*-*n*-propionyl-NEO (lane 6). **C.** Inhibition of *B. subtilis* growth by GEN (lane 7), 3-*N*-acetyl-GEN (lane 8), and 3-*N*-*n*-propionyl-GEN (lane 9).

2.4. Conclusions

AAC(6')/APH(2") and AAC(3)-IV were found to exhibit tolerance towards a variety of AGs as well as a diverse set of acyl-CoAs. The relaxed substrate specificity of both enzymes proved to be a useful tool for the preparation of a variety of regioselectively *N*-acylated AGs. The chemoenzymatic methodology proposed herein could be used for the generation of sufficient amounts of compound for a qualitative screen for antibacterial activity. The enzymes proved efficient not only for catalyzing single *N*-acylation but could also be used for sequential dual acylations. In view of the success of *N*-acylated AGs in exhibiting superior antimicrobial activity and reduced toxicity, our methodology sets the ground for the rapid generation and exploration of novel members of this family of compounds.

2.5. Experimental section

2.5.1. Bacterial strains, plasmids, materials, and instrumentation

Chemically competent *E. coli* TOP10 and BL21 (DE3) were bought from Invitrogen. Restriction endonucleases, T4 DNA ligase, and Phusion DNA polymerase were purchased from NEB. DNA primers for PCR were purchased from Integrated DNA Technologies. The pET28a and pET22b vectors were purchased from Novagen. The Int-pET19b-pps containing a decahistidine tag separated from the gene by PreScission protease was generously provided by Dr. Tapan Biswas (Univeristy of Michigan, MI, USA).[26] Precision protease was purchased from GE Healthcare (Piscataway, NJ, USA). DNA sequencing was performed at the University of Michigan DNA sequencing Core. DTDP, commercially available CoA derivatives (acetoacetyl-CoA, acetyl-CoA, benzoyl-CoA, butyryl-CoA, crotonyl-CoA, glutaryl-CoA, $_{D,L}$-β-hydroxybutyryl-CoA, isovaleryl-CoA, malonyl-CoA, methylmalonyl-CoA, palmitoyl-CoA, *n*-propionyl-CoA,) and AGs (AMK, GEN, KAN, NEO, PAR, SIS, and TOB) were purchased from Sigma-Aldrich and used without any further purification. ThioGlo-1 was bought from Calbiochem. Determination of kinetic parameters by UV-Vis assays was done on a multimode SpectraMax M5 plate reader using 96-well plates (Fisher Scientific). FPLC was performed as the last protein purification step on a Bio-Rad BioLogic DuoFlow using a HighPrep^{TM} 26/60 Sephacryl^{TM} S-200 High Resolution column. All buffer pH were adjusted at rt.

2.5.2. Preparation of pAAC(6')/APH(2")-pET28a, pAAC(6')/APH(2")-pET22b, pAAC(6')/APH(2")-Int-pET19b-pps, pAAC(3)-IV-pET28a, and pAAC(3)-IV-Int-pET19b-pps overexpression constructs

The gene encoding AAC(6')/APH(2") was PCR-amplified using the vector pSF815 in which the gene was stored as a template (provided by Prof. Timor Baasov, Israel Institute of Technology) and Phusion High-Fidelity DNA polymerase. The gene encoding AAC(3)-IV was PCR-amplified using plasmid DNA pAAC(3)-IV-pET23a (a gift from Dr. John S. Blanchard, Albert Einstein College of Medicine, NY). The primers used for the amplification of each gene are listed in Table 2.3.

The amplified genes were inserted into the linearized pET28a, pET22b, and Int-pET19b-pps vectors via the corresponding *Nde*I/*Xho*I pAAC(6')/APH(2")-pET28a(NHis), pAAC(6')/APH(2")-pET22b(CHis), and pAAC(6')/APH(2")-Int-pET19b-pps(NHis)), *Nde*I/*Hind*III (pAAC(3)-IV-pET28a(NHis)), and *Nde*I/*Bam*HI (pAAC(3)-IV-Int-pET19b-pps(NHis)) restriction sites, to afford constructs that encode for NHis-tagged and CHis-tagged proteins. The Int-pET19b-pps vector was utilized to produce proteins with an easily cleavable NHis-tag by use of precision protease. Expression of AAC(6')/APH(2")-pET28a(NHis), AAC(6')/APH(2")-pET22b(CHis), AAC(6')/APH(2")-Int-pET19b-pps(NHis), AAC(3)-IV-pET28a(NHis), and AAC(3)-IV-Int-pET19b-pps(NHis) was done following transformation into *E. coli* TOP10 competent cells. The plasmids were sequenced (The University of Michigan DNA Sequencing Core) and showed perfect alignment with the reported sequences (PubMed accession number NC_002774 for AAC(6')/APH(2") and PubMed accession number DQ241380 for AAC(3)-IV).

Table 2.3. Primers used for the PCR amplification of the AAC(6')/APH(2") gene from *S. aureus* and the AAC(3)-IV gene from *E. coli*.

gene (vector used for cloning)	5' primer	3' primer
aac(3)-IV(NHis) (pET28a)	ACATATGCAATACGAATGGCGAAAA GCC	GTGGGCAAGCTTTCAGCCAATCGACT GGCGAGCGG
aac(3)-IV(NHis) (Int-pET19b-pps)	ACATATGCAATACGAATGGCGAAAA GCC	GTGGGCGGATCCTCAGCCAATCGAC TGGCGAGCGG
AAC(6')/APH(2")(NHis) (pET28a and Int-pET19b-pps)	GATAAACATATGAATATAGTTGAAA ATGAAATATG	TATATTCTCGAGTCAATCTTTATAAG TCCTTTTATAAATTTC
AAC(6')/APH(2")(CHis) (pET22b)	GATAAACATATGAATATAGTTGAAA ATGAAATATG	ATTATACTCGAGATCTTTATAAGTCC TTTTATAAATTTC

The introduced restriction sites are underlined for each primer. The 5' primers all introduced an *Nde*I restriction site. The 3' primer for aac(3)-IV(NHis) (pET28a), aac(3)-IV(NHis) (Int-pET19b-pps), and all AAC(6')/APH(2") introduced *Hind*III, *Bam*HI, and *Xho*I restriction sites, respectively.
The tags added to the proteins are:
NHis (pET28a/*Nde*I) = MGSSHHHHHHSSGLVPRGSH
NHis (Int-pET19b-pps/*Nde*I) = MGHHHHHHHHHHSSGHINNNNKHTSLEVLFQGPH
No tag (after cleavage using precision protease and Int-pET19b-pps/*Nde*I) = GPH
CHis (pET22b/*Xho*I) = LEHHHHHH
CHis (pET22b/*Hind*III) = KLAALEHHHHHH

2.5.3. Overproduction and purification of AAC(6')/APH(2")(NHis), AAC(6')/APH(2")(CHis), and AAC(3)-IV(NHis)

Purified plasmids AAC(6')/APH(2")-pET28a(NHis), AAC(6')/APH(2")-pET22b(CHis), AAC(6')/APH(2")-Int-pET19b-pps(NHis), AAC(3)-IV-pET28a(NHis), and AAC(3)-IV-Int-pET19b-pps(NHis) were transformed into *E. coli* BL21 (DE3) competent cells for protein expression and purification. 1 L of Luria-Bertani (LB) medium supplemented with kanamycin (50 μg/mL) (for pET28a constructs) or ampicillin (100 μg/mL) (for pET22b and Int-pET19b-pps constructs) were inoculated with 10 mL of an overnight

culture of the transformants harboring the AAC(6')/APH(2")-pET28a, AAC(6')/APH(2")-pET22b, AAC(6')/APH(2")-Int-pET19b-pps, AAC(3)-IV-pET28a, and AAC(3)-IV-Int-pET19b-pps constructs and incubated at 37 ℃. The cultures were grown to an OD_{600} of ~0.6, induced with 1 mL of a 1 M stock of IPTG (final concentration of 1.0 mM) and shaken for an additional 4 h at 37 ℃. Cells were harvested by centrifugation (6,000 rpm, 10 min, 4 ℃, Beckman Coulter Aventi JE centrifuge, F10 rotor) and resuspended in buffer A (300 mM NaCl and 50 mM Na_2HPO_4 pH 8.0, (containing 10% glycerol for the AAC(3)-IV proteins)). Resuspended cells were lysed (1 pass at 10,000-15,000 psi, Avestin EmulsiFlex-C3 high-pressure homogenizer), and the cell debris was removed by centrifugation (16,000 rpm, 45 min, 4 ℃, Beckman Beckman Coulter Aventi JE centrifuge, JA-17 rotor). Imidazole (final concentration of 2 mM) was added to the supernatant, which was then incubated with 2 mL of Ni-NTA agarose resin (Qiagen) at 4 ℃ for 2 h with gentle rocking. The resin was loaded onto a column and washed with 10 mL of buffer A containing 5 mM imidazole and with 10 mL of buffer A containing 20 mM imidazole. The desired protein was eluted from the column in a stepwise imidazole gradient (10 mL fraction of 20 mM (1x), 5 mL fractions of 20 mM (3x), 40 mM (3x), and 250 mM imidazole (3x)). Fractions containing the pure desired proteins (as determined by SDS-PAGE) were combined and dialyzed at 4 ℃ against 1 L of buffer B (50 mM HEPES pH 7.5) for 3 h. The dialyzed proteins were either further purified on FPLC (1.5 mL/min using buffer C (50 mM HEPES pH 7.5)) or treated with precision protease to cleave the NHis tag from the proteins produced using the Int-pET19b-pps vector (see protocol in the next section) (Figs. 2.2, 2.7, and 2.8). Pure proteins were concentrated using Amicon Ultra PL-10. Protein concentrations were determined using a Nanodrop spectrometer (Thermo Scientific). Protein yields were 1.3-5.1 mg/L of culture for all AAC(6')/APH(2") and 3-22 mg/L of culture of all AAC(3)-IV. All AAC(6')/APH(2") proteins were stored at 4 ℃ while all AAC(3)-IV proteins were flash-frozen (with 10% glycerol added to the protein) using liquid nitrogen and stored at -80 ℃.

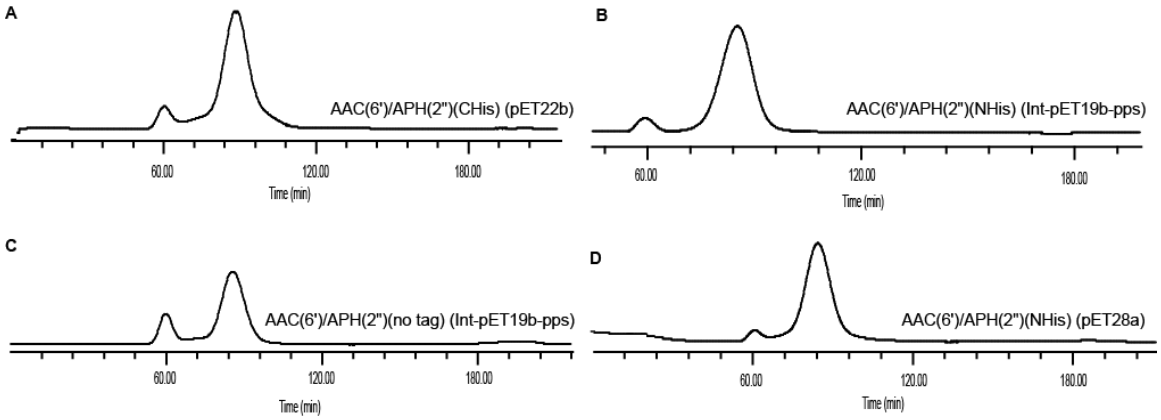

Fig. 2.7. FPLC traces observed at 280 nm for **A.** AAC(6')/APH(2")(CHis) (pET22b), **B.** AAC(6')/APH(2")(NHis) (Int-pET19b-pps), **C.** AAC(6')/APH(2")(no tag) (Int-pET19b-pps), and **D.** AAC(6')/APH(2")(NHis) (pET28a).

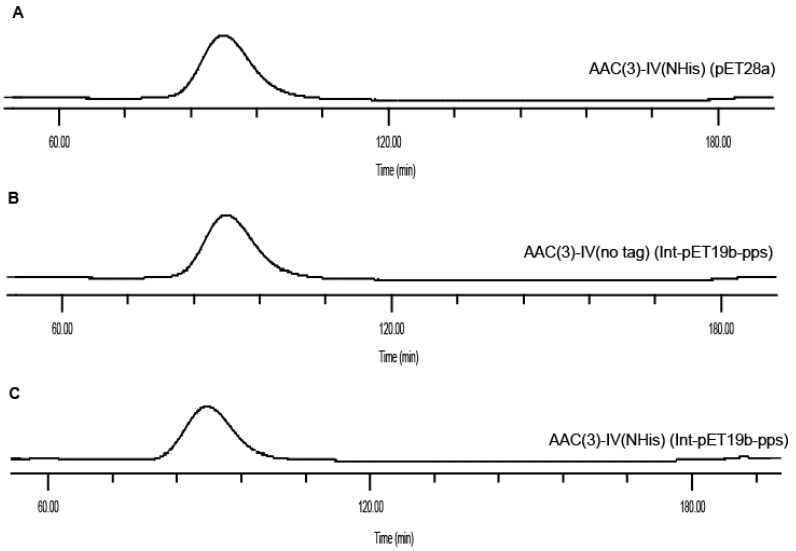

Fig. 2.8. FPLC traces observed at 280 nm for **A.** AAC(3)-IV(NHis) (pET28a), **B.** AAC(3)-IV(no tag) (Int-pET19b-pps), and **C.** AAC(3)-IV(NHis) (Int-pET19b-pps).

2.5.4. Cleavage of NHis tag from AAC(6')/APH(2") produced from the Int-pET19b-pps construct

The NHis tag was cleaved overnight at 4 ℃ with rocking using 30 μg of PreScission protease in 50 mM HEPES pH 7.5. The protein was loaded on 15% SDS-PAGE gel to verify that the tag was completely removed. If cleavage was incomplete, an additional 30 μg of precision protease was added and rocked at rt for an additional 3-6 h. The cleavage progress was checked again by SDS-PAGE gel and if incomplete, the remaining tagged

protein was separated from the untagged by binding to Ni-NTA agarose beads. The flow-through was collected and purified by FPLC (1.5 mL/min using buffer C).

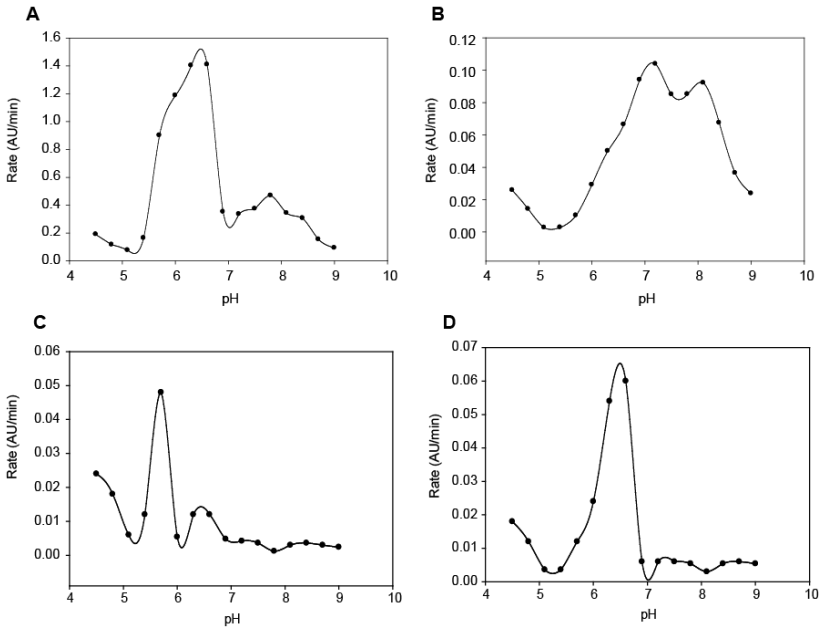

Fig. 2.9. Representative pH profiles for **A.** KAN with AAC(6')/APH(2")(NHis) (pET28a), **B.** SIS with AAC(6')/APH(2")(NHis) (pET28a), **C.** SIS with AAC(3)-IV(NHis) (pET28a), and **D.** PAR with AAC(3)-IV(NHis) (pET28a).

2.5.5. pH Profile of AAC(6')/APH(2")(NHis) and AAC(3)-IV(NHis) purified from pET28a

The pH profile of AAC(6')/APH(2")(NHis) and AAC(3)-IV(NHis) purified from pET28a were determined for each AG substrate (200 μL reaction volume) by monitoring CoA, released due to acylation, reacting with DTDP which gives an increase in absorbance at 324 nm (ε_{324} = 19,800 $M^{-1}cm^{-1}$)[27] due to the formation of 4-thiopyridone, using AcCoA (40 μM), DTDP (2 mM), and AG (20 μM) in the various buffers (50 mM). A pH range from 4.5 to 9.0 using 0.3 increments was used to determine the optimum pH of the AACs activity with individual sugars. Citrate-phosphate buffer (50 mM) was used for pHs 4.5 to 5.4, MES (50 mM) was used for pHs 5.7 to 6.6, HEPES (50 mM) for pHs 6.9 to 7.8, and Tris (50 mM) for pHs 8.1 to 9.0. Data were recorded every 30 sec for 15 to 30 min. The rate of each reaction was determined using the initial slope (in the first 2.5 min), and plotted versus the pH (Fig. 2.9). Plots generally indicated one optimum pH or a small range of pHs.

2.5.6. Determination of CoA derivatives substrate specificity for AAC(6')/APH(2")(NHis) and AAC(3)-IV(NHis) from pET28a

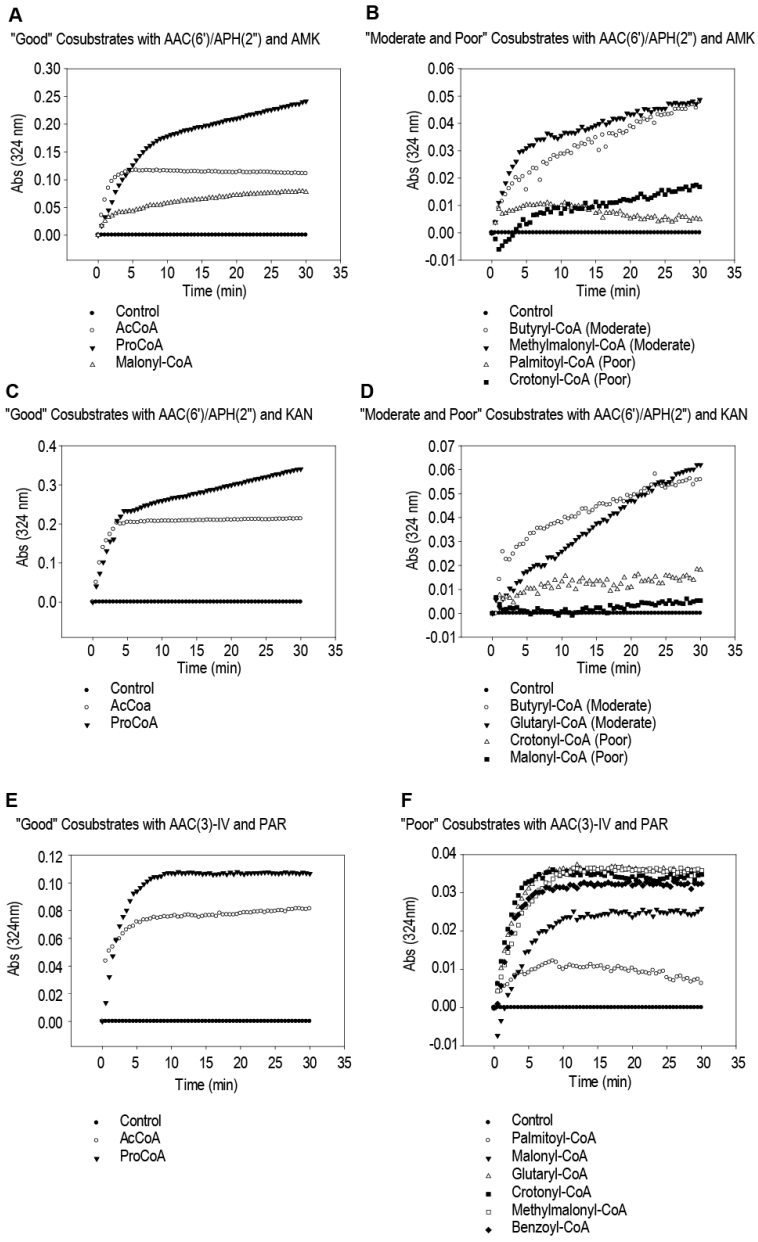

Fig. 2.10. Representative spectrophotometric assay plots of **A.** "good" substrates with AMK and AAC(6')/APH(2")(NHis) (pET28a), **B.** "moderate and poor" substrates with AMK and AAC(6')/APH(2")(NHis) (pET28a), **C.** "good" substrates with KAN and AAC(6')/APH(2")(NHis) (pET28a), **D.** "moderate and poor" substrates with KAN and AAC(6')/APH(2")(NHis) (pET28a), **E.** "good" substrates with PAR and AAC(3)-IV(NHis) (pET28a), and **F.** "poor" substrates with PAR and AAC(3)-IV(NHis) (pET28a).

To determine which CoA derivatives are substrates for AAC(6')/APH(2")(NHis) and AAC(3)-IV(NHis) from pET28a, the acylation of the AGs were monitored using the same spectrophotometric assay as above. Reaction volumes of 200 μL contained buffer (50 mM) (MES pH 6.6 for the AAC(6')/APH(2") enzyme for all AGs, MES pH 6.6 for the AAC(3)-IV enzyme for PAR and TOB, and MES pH 5.7 for AAC(3)-IV enzymes for GEN, SIS, and NEO), DTDP (2 mM), CoA derivatives (40 μM), and AG (20 μM). The reactions were initiated using 5.9 μg of protein. Solutions were pre-incubated at 37 ℃ for 5 min prior to addition of enzyme. The enzymatic reactions were monitored by taking readings every 30 sec for 30 min (Figs. 2.10-2.14).

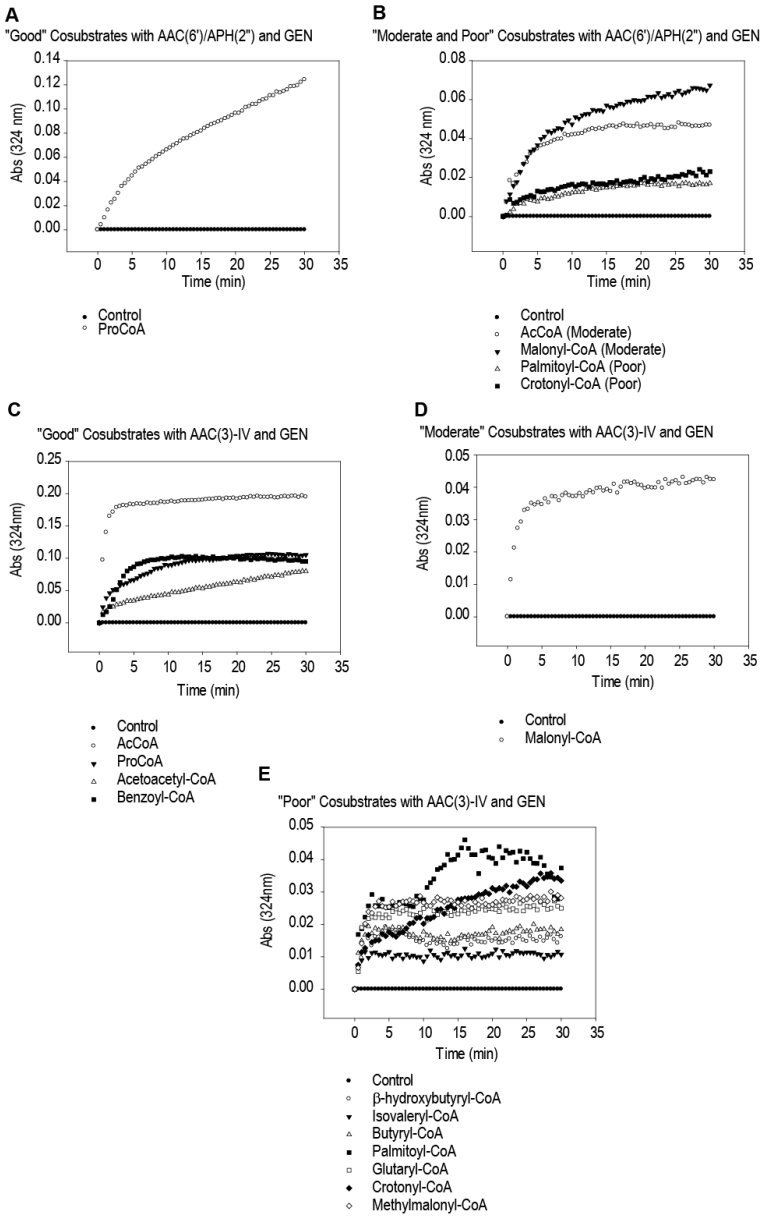

Fig. 2.11. Representative spectrophotometric assay plots of **A.** "good" substrates with GEN and AAC(6')/APH(2")(NHis) (pET28a), **B.** "moderate and poor" substrates with GEN and AAC(6')/APH(2")(NHis) (pET28a), **C.** "good" substrates with GEN and AAC(3)-IV(NHis) (pET28a), **D.** "poor" substrates with GEN and AAC(3)-IV(NHis) (pET28a), and **E.** "poor" substrates with GEN and AAC(3)-IV(NHis) (pET28a).

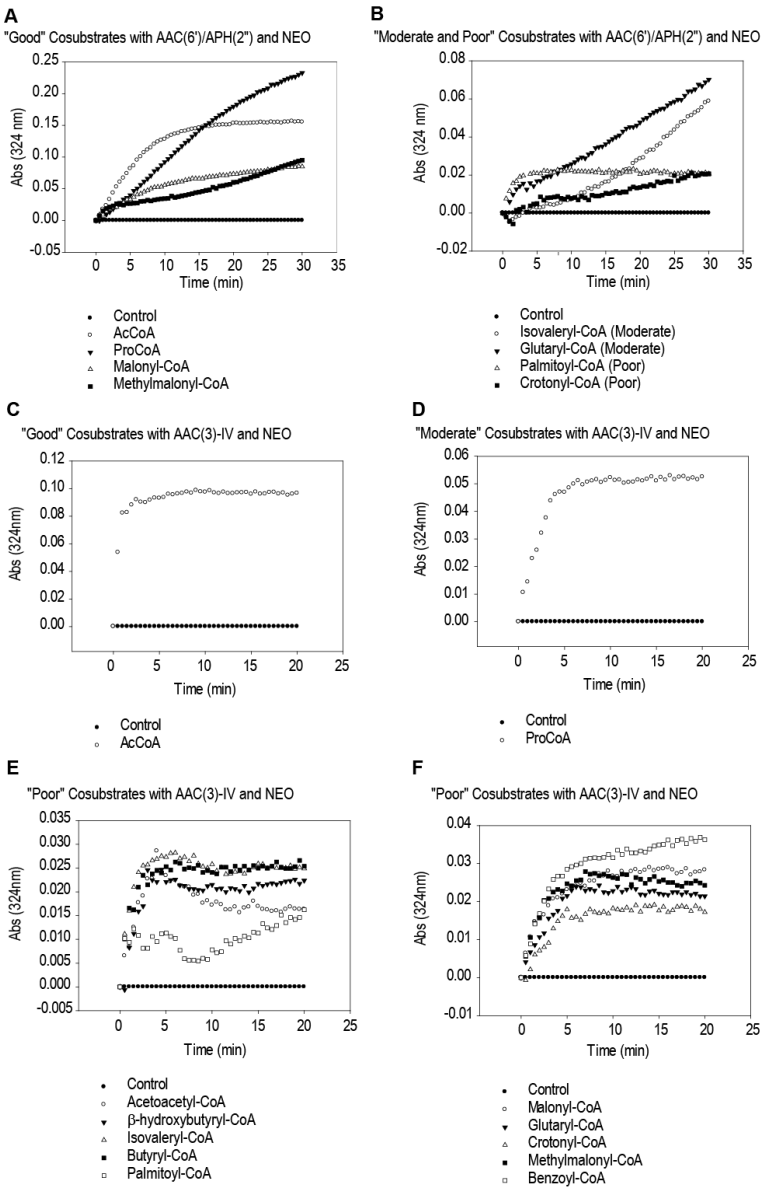

Fig. 2.12. Representative spectrophotometric assay plots of **A.** "good" substrates with NEO and AAC(6')/APH(2")(NHis) (pET28a), **B.** "moderate and poor" substrates with NEO and AAC(6')/APH(2")(NHis) (pET28a), **C.** "good" substrates with NEO and AAC(3)-IV(NHis) (pET28a), **D.** "moderate" substrates with NEO and AAC(3)-IV(NHis) (pET28a), **E.** "poor" substrates with NEO and AAC(3)-IV(NHis) (pET28a), and **F.** "poor" substrates with NEO and AAC(3)-IV(NHis) (pET28a).

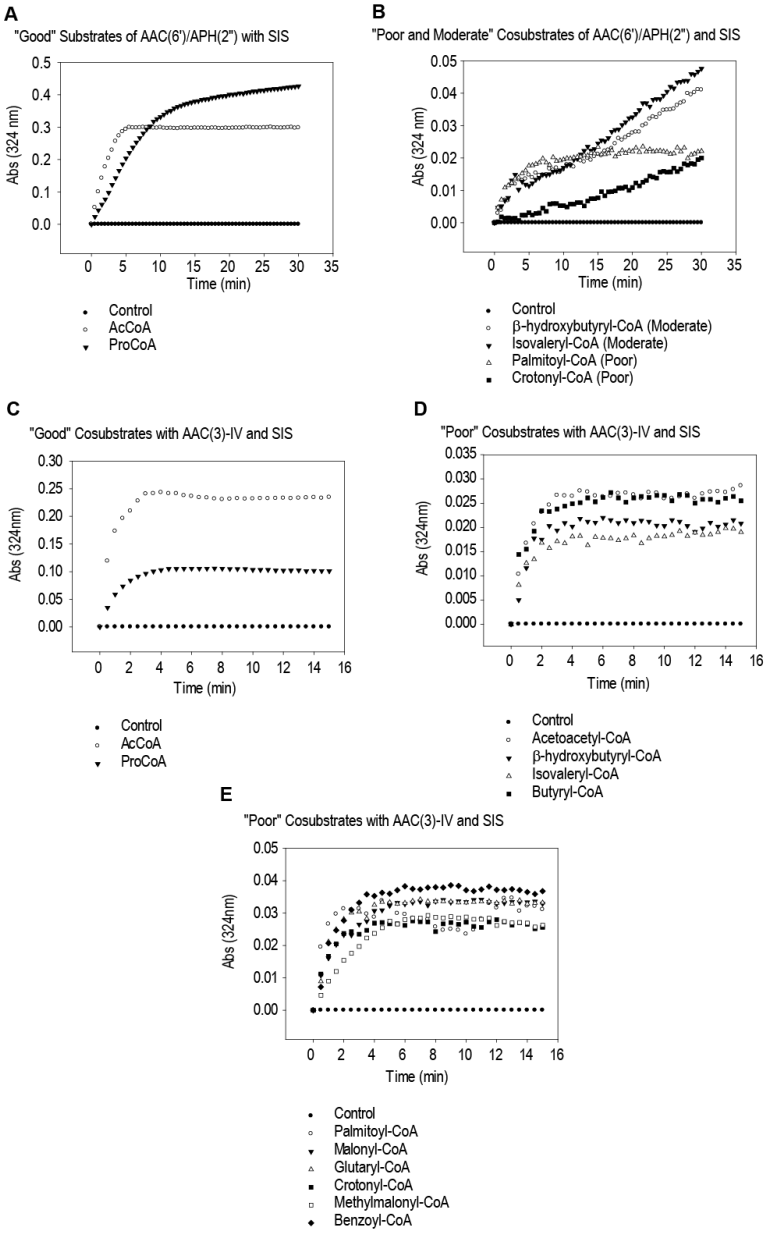

Fig. 2.13. Representative spectrophotometric assay plots of **A.** "good" substrates with SIS and AAC(6')/APH(2")(NHis) (pET28a), **B.** "moderate and poor" substrates with SIS and AAC(6')/APH(2")(NHis) (pET28a), **C.** "good" substrates with SIS and AAC(3)-IV(NHis) (pET28a), **D.** "poor" substrates with SIS and AAC(3)-IV(NHis) (pET28a), and **E.** "poor" substrates with SIS and AAC(3)-IV(NHis) (pET28a).

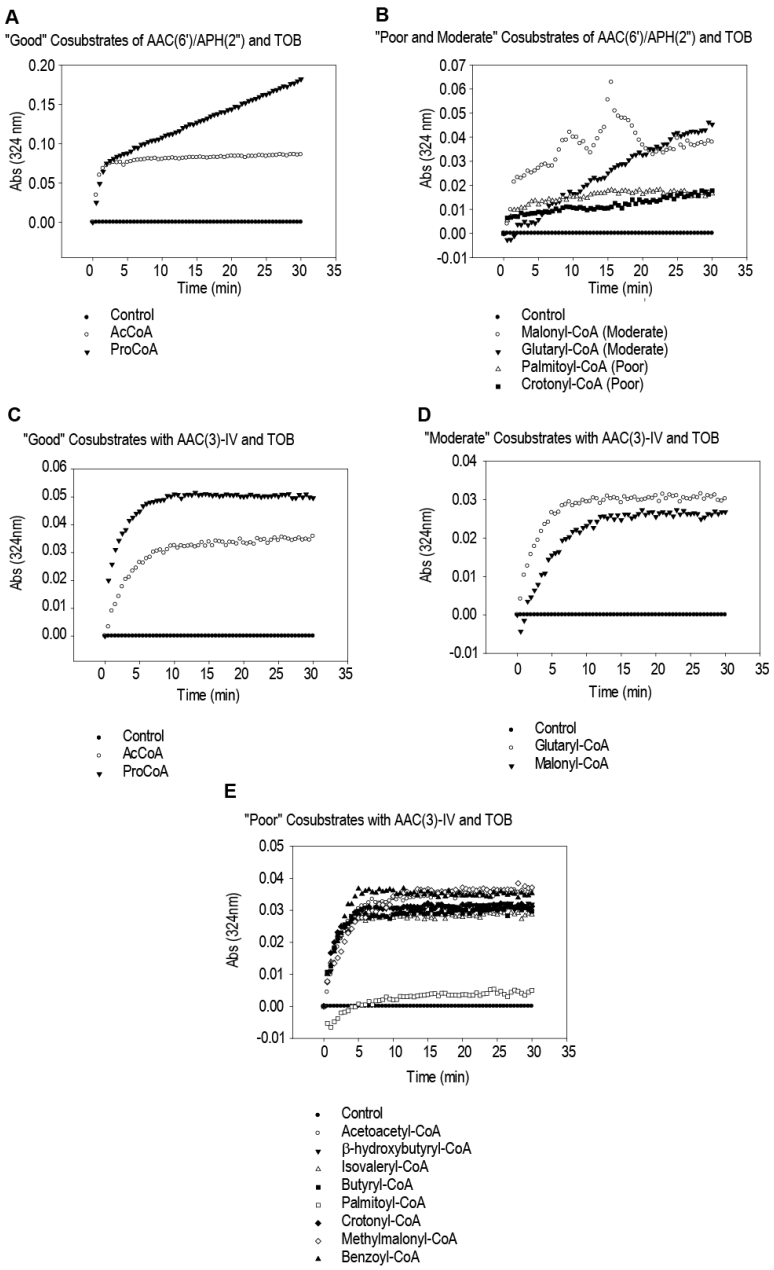

Fig. 2.14. Representative spectrophotometric assay plots of **A.** "good" substrates with TOB and AAC(6')/APH(2")(NHis) (pET28a), **B.** "moderate and poor" substrates with TOB and AAC(6')/APH(2")(NHis) (pET28a), **C.** "good" substrates with TOB and AAC(3)-IV(NHis) (pET28a), **D.** "poor" substrates with TOB and AAC(3)-IV(NHis) (pET28a), and **E.** "poor" substrates with TOB and AAC(3)-IV(NHis) (pET28a).

2.5.7. Determination of kinetic parameters

The kinetic parameters for each enzyme were determined in reactions (200 μL) containing 0-80 μM of CoA derivatives (0, 1, 2, 3, 4, 5, 6, 10, 20, 30, 40, 80 μM) (higher concentrations, up to 1 mM, were used in cases that revealed a K_m higher than 80 μM), AG (100 μM), DTDP (2 mM), and enzyme (0.25 μM) at the optimum pH for individual AGs as determined by the pH profile (*i.e.* the pH giving the fastest rate). Reactions were initiated by the addition of the CoA derivatives and were carried out in triplicate. The kinetic parameters, K_m and k_{cat} were determined using Lineweaver-Burk plots (Figs. 2.15-2.17). The determination of kinetic parameters using ThioGlo-1 was done identically, only using ThioGlo-1 (100 μM) in place of DTDP.

2.5.8. TLC time course

Reactions (100 μL) were carried out at 37 ℃ AAC(6')/APH(2")) or at rt (AAC(3)-IV) in MES (50 mM, pH 6.6) (NEO) or at rt in MES (50 mM, pH 5.7) (GEN) in the presence of CoA derivative (200 μM), AG (150 μM), and AAC (5-6 μM). Aliquots (~5 μL) were loaded on a TLC plate (EMD, Silica gel F254 250 μm tickness) after 0, 10, 30, 60, 120, 300 min, and overnight incubation. The eluent systems utilized were 3:2/MeOH:NH_4OH (NEO) and 6:1/MeOH:NH_4OH (GEN). Visualization was achieved using a cerium-molybdate stain (5 g CAN, 120 g ammonium molybdate, 80 mL H_2SO_4, 720 mL H_2O). The R_f values observed were 0.23 for NEO; 0.43 for 6'-*N*-acetyl-NEO; 0.47 for 6'-*N*-*n*-propionyl-NEO; 0.31 for 3-*N*-acetyl-NEO; 0.42 for 3-*N*-*n*-propionyl-NEO; 0.10 for GEN; 0.20 for 3-*N*-acetyl-GEN; 0.27 for 3-*N*-*n*-propionyl-GEN. Starting materials and by-product were visualized by TLC to determine their R_f values using the appropriate eluent systems (Fig. 2.18).

2.5.9. TLC time course for double acetylation of NEO

Reactions (100 μL) were carried out at 37 ℃ (for AAC(6')/APH(2") or at rt (for AAC(3)-IV) in MES (50 mM, pH 5.7) in the presence of AcCoA (600 μM), AG (150 μM), and AAC (6 μM) for 1 h. The second AAC was added to the mixture and the reaction was incubated for an additional 1 h. Aliquots (5 μL) of each reaction were loaded onto a TLC plate. The eluent systems utilized were 3:2/MeOH:NH_4OH and visualization was achieved using a cerium-molybdate. The R_f values observed were 0.46 for 6',3-*N*-di-acetyl-NEO.

2.5.10. BioTLC

Reactions (10-20 μL) were inspired by the work of Ostash *et al.*[24] and were carried out in MES (50 mM, pH 6.6) for AAC(6')/APH(2") (0.7 nmol) or MES (50 mM, pH 5.7) for AAC(3)-IV (0.5 nmol) in the presence of CoA derivative (40-80 nmol), AG (NEO, GEN) (30-60 nmol). After completion of the reaction (monitored by TLC), an equal volume of MeOH was added to precipitate the protein. The solutions were centrifuged (14,000 rpm, 10 min, rt) to pellet the protein. The entire reaction mixture was loaded onto a TLC plate and ran in the aforementioned eluent systems. A small amount of the reaction was stained

with a cerium-molybdate stain prior to loading on the BioTLC to check for reaction completion. *B. subtilis* was grown in LB (no antibiotic) at 30 ℃ for a 24 h period. The bacterial culture (100 μL) was added to soft agar (0.75%) LB (10 mL) at 37 ℃ and poured over the TLC plate in a sterile petri dish. The *B. subtilis* overlay was grown until clear zones of inhibited growth were observed (10 h to overnight) at 30 ℃. The R_f values of the starting materials and products on the stained TLCs corresponded to the R_f values of the zones of inhibition on the overlay.

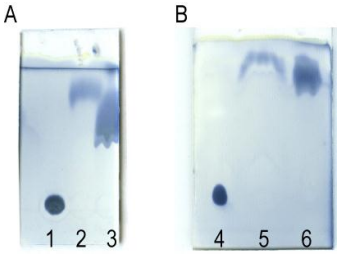

Fig. 2.18. TLC visualization of AAC reaction starting materials and byproduct **A.** NEO (R_f = 0.23) (lane 1), AcCoA (R_f = 0.91) (lane 2), and CoASH (R_f = 0.71) (lane 3) using a solvent system of 3:2/MeOH:NH_4OH, and **B.** GEN (R_f = 0.28) (lane 4), AcCoA (R_f = 0.95) (lane 5), and CoA (R_f = 0.85) (lane 6) using 6:1/MeOH:NH_4OH as the solvent system.

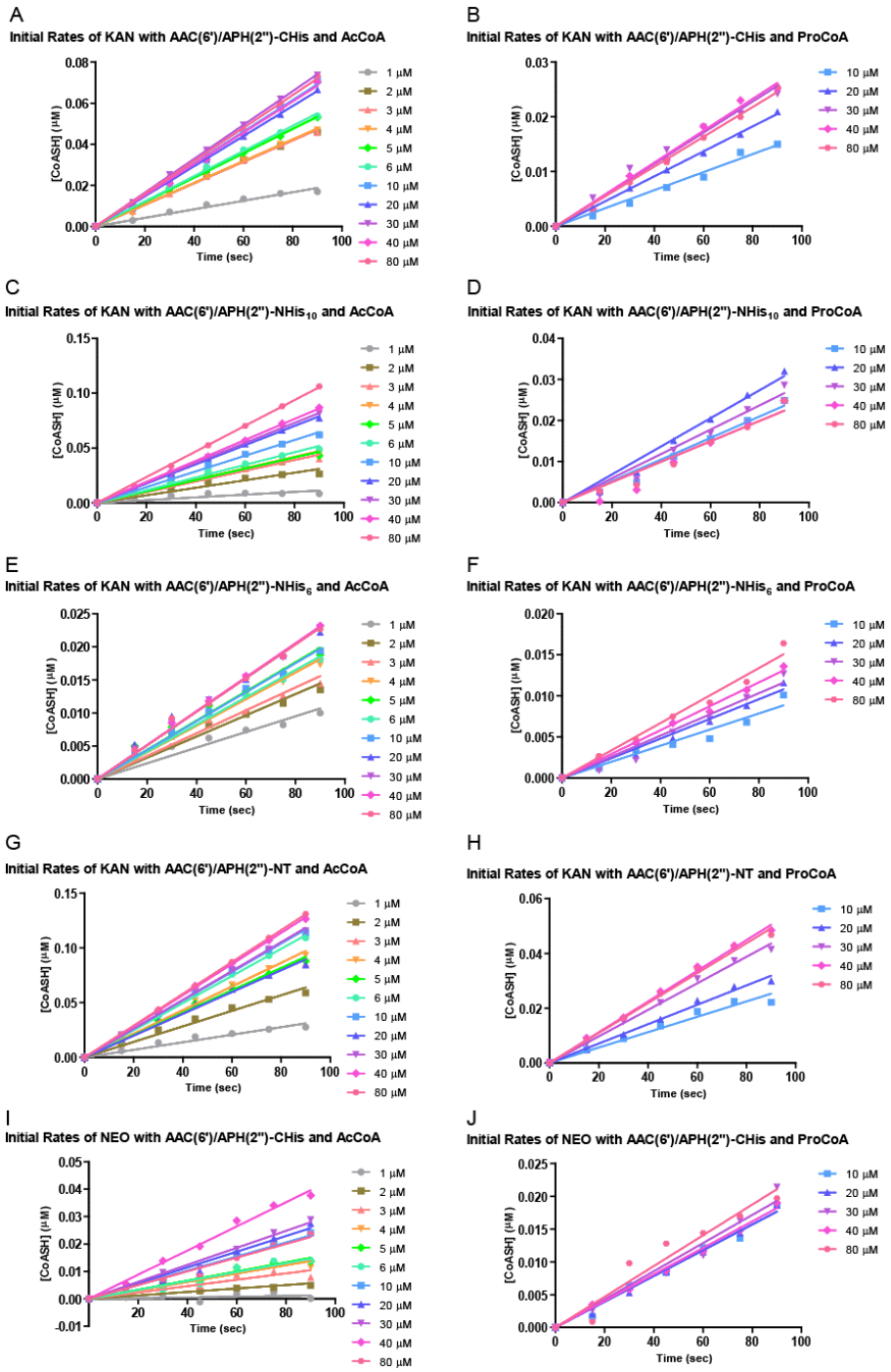

Fig. 2.15. Example kinetic initial rates of **A.** KAN with AAC(6')/APH(2")(CHis) (pET22b) and AcCoA, **B.** KAN with AAC(6')/APH(2")(CHis) (pET22b) and ProCoA, **C.** KAN with AAC(6')/APH(2")(NHis) (Int-pET19b-pps) and AcCoA, **D.** KAN with AAC(6')/APH(2")(NHis) (Int-pET19b-pps) and ProCoA, **E.** KAN with AAC(6')/APH(2")(NHis) (pET28a) and AcCoA, **F.** KAN with AAC(6')/APH(2")(NHis) (pET28a) and ProCoA, **G.** KAN with AAC(6')/APH(2")(no tag) (Int-pET19b-pps) and AcCoA, **H.** KAN with AAC(6')/APH(2")(no tag) (Int-pET19b-pps) and ProCoA, **I.** NEO with AAC(6')/APH(2")(CHis) (pET22b) and AcCoA, and **J.** NEO with AAC(6')/APH(2")(CHis) (pET22b) and ProCoA.

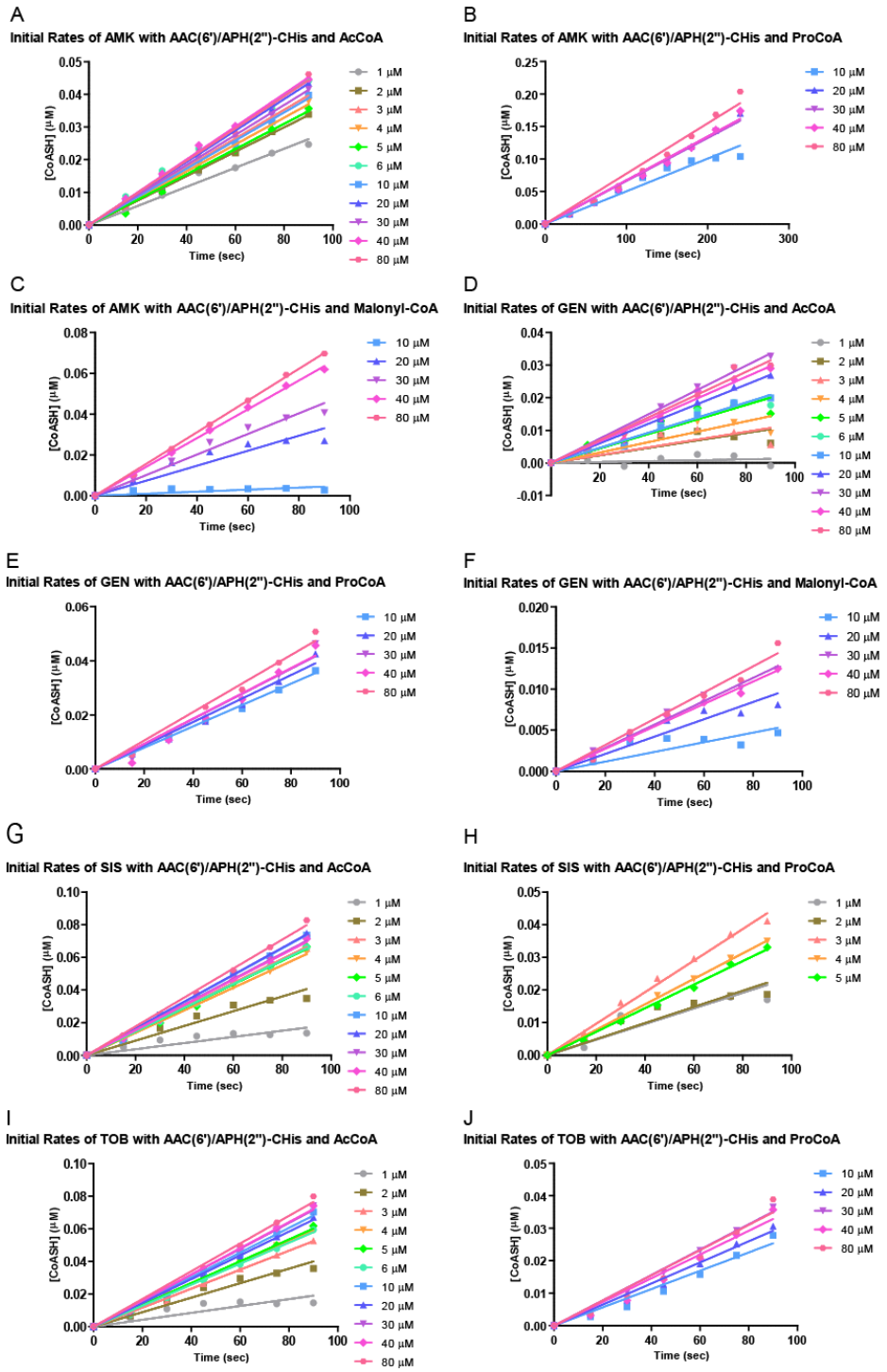

Fig. 2.16. Example kinetic initial rates of **A.** AMK with AAC(6')/APH(2")(CHis) (pET22b) and AcCoA, **B.** AMK with AAC(6')/APH(2")(CHis) (pET22b) and ProCoA, **C.** AMK with AAC(6')/APH(2")(CHis) (pET22b) and malonyl-CoA, **D.** GEN with AAC(6')/APH(2")(CHis) (pET22b) and AcCoA, **E.** GEN with AAC(6')/APH(2")(CHis) (pET22b) and ProCoA, **F.** GEN with AAC(6')/APH(2")(CHis) (pET22b) and malonyl-CoA, **G.** SIS with AAC(6')/APH(2")(CHis) (pET22b) and AcCoA, **H.** SIS with AAC(6')/APH(2")(CHis) (pET22b) and ProCoA, **I.** TOB with AAC(6')/APH(2")(CHis) (pET22b) and AcCoA, and **J.** TOB with AAC(6')/APH(2")(CHis) (pET22b) and ProCoA.

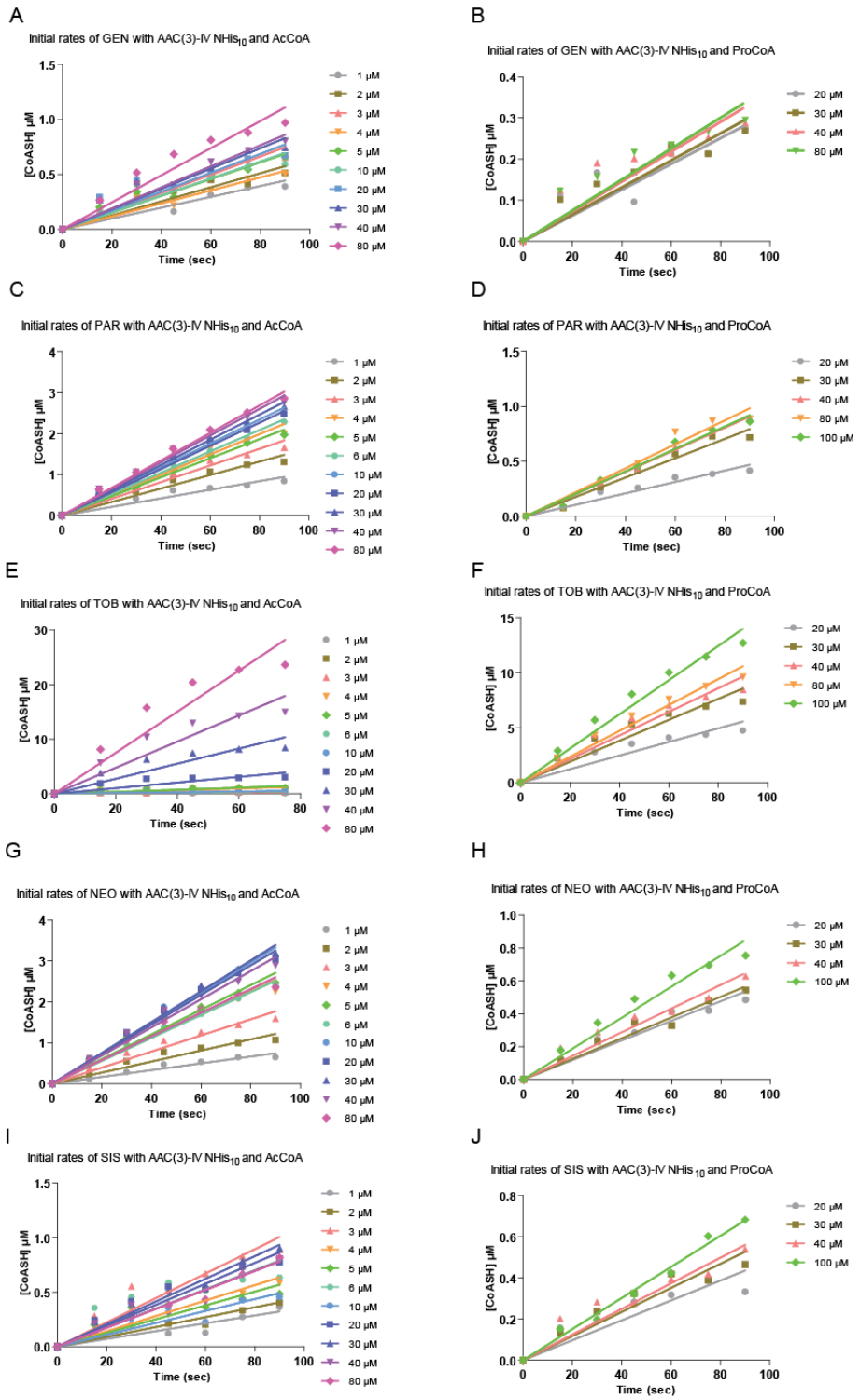

Fig. 2.17. Example kinetic initial rates of **A.** GEN with AAC(3)-IV(NHis) (Int-pET19b-pps) and AcCoA, **B.** GEN with AAC(3)-IV(NHis) (Int-pET19b-pps) and ProCoA, **C.** PAR with AAC(3)-IV(NHis) (Int-pET19b-pps) and AcCoA, **D.** PAR with AAC(3)-IV(NHis) (Int-pET19b-pps) and ProCoA, **E.** TOB with AAC(3)-IV(NHis) (Int-pET19b-pps) and AcCoA, **F.** TOB with AAC(3)-IV(NHis) (Int-pET19b-pps) and ProCoA, **G.** NEO with AAC(3)-IV(NHis) (Int-pET19b-pps) and AcCoA, **H.** NEO with AAC(3)-IV(NHis) (Int-pET19b-pps) and ProCoA, **I.** SIS with AAC(3)-IV(NHis) (Int-pET19b-pps) and AcCoA, and **J.** SIS with AAC(3)-IV(NHis) (Int-pET19b-pps) and ProCoA.

2.6. References

(1) Davis, B. D. *Microbiological reviews* **1987**, *51*, 341.
(2) Jana, S.; Deb, J. K. *Applied microbiology and biotechnology* **2006**, *70*, 140.
(3) Hainrichson, M.; Nudelman, I.; Baasov, T. *Organic & biomolecular chemistry* **2008**, *6*, 227.
(4) Magnet, S.; Blanchard, J. S. *Chemical reviews* **2005**, *105*, 477.
(5) Ogle, J. M.; Brodersen, D. E.; Clemons, W. M., Jr.; Tarry, M. J.; Carter, A. P.; Ramakrishnan, V. *Science* **2001**, *292*, 897.
(6) Q, V.; E., W. *Biopolymers.* **2003**, *70*, 42.
(7) Wright, G. D.; Berghuis, A. M.; Mobashery, S. *Advances in experimental medicine and biology* **1998**, *456*, 27.
(8) Kumar, A.; Schweizer, H. P. *Advanced drug delivery reviews* **2005**, *57*, 1486.
(9) Woo, P. W. K. *Tetrahedron Lett* **1971**, *12*, 2621.
(10) Woo, P. W. K.; Dion, H. W.; Bartz, Q. R. *Tetrahedron Lett* **1971**, *12*, 2617.
(11) Woo, P. W. K.; Dion, H. W.; Bartz, Q. R. *Tetrahedron Lett* **1971**, *12*, 2625.
(12) S, K.; K., H. *J Infect Chemother.* **1999**, *5*, 1.
(13) Kawaguchi, H.; Naito, T.; Nakagawa, S.; Fujisawa, K. I. *J Antibiot (Tokyo)* **1972**, *25*, 695.
(14) Haddad, J.; Kotra, L. P.; Llano-Sotelo, B.; Kim, C.; Azucena, E. F., Jr.; Liu, M.; Vakulenko, S. B.; Chow, C. S.; Mobashery, S. *Journal of the American Chemical Society* **2002**, *124*, 3229.
(15) Nudelman, I.; Rebibo-Sabbah, A.; Cherniavsky, M.; Belakhov, V.; Hainrichson, M.; Chen, F.; Schacht, J.; Pilch, D. S.; Ben-Yosef, T.; Baasov, T. *Journal of medicinal chemistry* **2009**, *52*, 2836.
(16) Hotta, K.; Ogata, T.; Ishikawa, J.; Okanishi, M.; Mizuno, S.; Morioka, M.; Naganawa, H.; Okami, Y. *J Antibiot (Tokyo)* **1996**, *49*, 682.
(17) Kobayashi, F.; Saino, Y.; Koshi, T.; Hattori, Y. *Antimicrobial agents and chemotherapy* **1980**, *17*, 337.
(18) Matsuhashi, Y.; Yoshida, T.; Hara, T.; Kazuno, Y.; Inouye, S. *Antimicrobial agents and chemotherapy* **1985**, *27*, 589.
(19) Fridman, M.; Balibar, C. J.; Lupoli, T.; Kahne, D.; Walsh, C. T.; Garneau-Tsodikova, S. *Biochemistry* **2007**, *46*, 8462.
(20) Green, K. D.; Fridman, M.; Garneau-Tsodikova, S. *Chembiochem : a European journal of chemical biology* **2009**, *10*, 2191.
(21) Boehr, D. D.; Lane, W. S.; Wright, G. D. *Chemistry & biology* **2001**, *8*, 791.
(22) E, W.; A, V.; Y, M.; A, S.; Y, N.; SK., B. *Cell* **1998**, *94*, 439.
(23) Magalhaes, M. L.; Blanchard, J. S. *Biochemistry* **2005**, *44*, 16275.
(24) Ostash, B.; Saghatelian, A.; Walker, S. *Chemistry & biology* **2007**, *14*, 257.
(25) Shahid, M. A.; Siddique, M.; Rehman, S.-U.; Hameed, S.; Hussain, A. *Am J Food Technol* **2007**, *2*, 457.
(26) Biswas, T.; Tsodikov, O. V. *The FEBS journal* **2008**, *275*, 3064.
(27) Hegde, S. S.; Javid-Majd, F.; Blanchard, J. S. *The Journal of biological chemistry* **2001**, *276*, 45876.

Note:

This chapter is adapted from a published manuscript: Green, K. D.; **Chen, W.**; Houghton, J. L.; Fridman, M.; Garneau-Tsodikova, S. *Chembiochem : a European journal of chemical biology* **2010**, *11*,119. **Wenjing Chen** did all the AAC(3)-IV related experiments.

Chapter 3

Effects of altering aminoglycoside structures on bacterial resistance enzyme activities

3.1. Abstract

Aminoglycoside-modifying enzymes (AMEs) constitute the most prevalent mechanism of resistance to AGs by bacteria. We show that AGs can be doubly modified by the sequential actions of AMEs, with the activity of the second AME in most cases unaffected, decreased, or completely abolished. We demonstrate that the bifunctional enzyme AAC(3)-Ib/AAC(6')-Ib' can di-acetylate GEN. Since single acetylation does not always inactivate the parent drugs completely, two modifications likely provide more robust inactivation *in vivo*.

3.2. Introduction

The extensive use of AGs in the treatment of serious bacterial infections has resulted in the emergence of bacterial strains resistant to these broad-spectrum antibiotics.[1] The most prevalent mechanism of resistance to AGs is the enzymatic modification of the AGs by three types of AMEs: AG acetyltransferases (AACs), AG phosphotransferases (APHs), and AG nucleotidyltransferases (ANTs) (Fig. 3.1). The inactive AG is unable to bind to its target, the bacterial ribosome. Due to their constant quest for survival, bacteria have further evolved bifunctional AMEs, including AAC(3)-Ib/AAC(6')-Ib',[2,3] AAC(6')/APH(2")-Ia,[4] ANT(3")-Ii/AAC(6')-IId,[5,6] and AAC(6')-30/AAC(6')-Ib.[7] One biological reason for these bifunctional AMEs could be the broadening of the resistance profile through the ability to inactivate a greater variety of AGs, with each enzymatic module targeting its own set of AG substrates (as observed with ANT(3")-Ii/AAC(6')-IId).[6] Another reason could be the inability of a single modification by either subunit to fully inactivate the parent AG, in which case the second modification could be required

to abolish the residual activity of the modified AG. We previously reported a methodology for the chemoenzymatic synthesis of 3- and 6'-*N*-acylated AGs and showed that 6'-*N*-acetyl-NEO and 6'-*N*-*n*-propionyl-NEO retain antibacterial activity against *B. subtilis*.[8] Here, by using synthetic 6'-*N*-acetylated AGs, we first confirm that acetylation does not always result in complete inactivation of AGs. It is well known that acylation of AGs can decrease the binding of the AG to the enzyme, as exemplified by the 20-fold and 5-fold increases in the K_m for KAN compared to AMK with AAC(6')/APH(2")-Ia[9] and AAC(3)-IV,[10] respectively. We have recently demonstrated that 6'-*N*-glycinyl-TOB and 6"'-*N*-glycinyl-PAR show reduced reaction rates with AAC(3)-IV.[11] The combination of these results warrants the investigation of the role that AGs modified at a variety of positions play in AME reactivity.

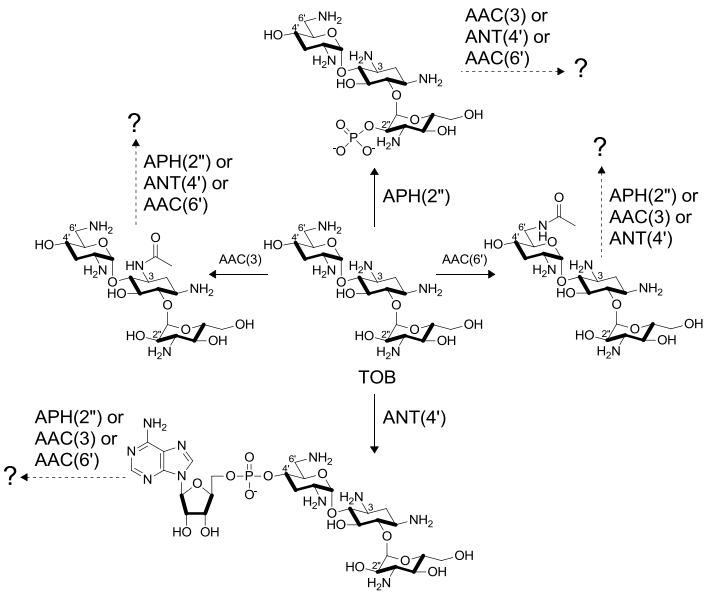

Fig. 3.1. Schematic representation of the sequential modifications performed by the AMEs APH(2"), AAC(3), ANT(4'), and AAC(6'), used in this study, with TOB as a representative AG.

To gain insight into the potential of *N*-acylated AGs to overcome resistance by AMEs and the potential of bifunctional AMEs to doubly modify AGs, one needs to understand if and how one chemical modification on an AG scaffold affects another, at a different position. Here we report the investigation of such effects by subjecting a variety of AGs (AMK, KAN, NEO, PAR, RIB, SIS, and TOB) to sequential alterations by the AMEs AAC(6')/APH(2") (used only for its AAC(6') activity), AAC(3)-IV, ANT(4'), and APH(2") from the bifunctional enzyme AAC(6')/APH(2") (Fig. 3.2). We also discuss the study of AAC(3)-Ib/AAC(6')-Ib' and its individually expressed components, and we demonstrate, for the first time, the ability of a bifunctional AME to di-acetylate an AG, GEN.

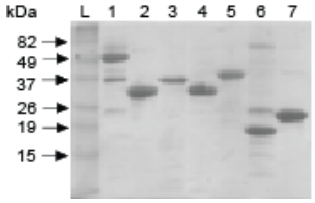

Fig. 3.2. Coomassie blue-stained 15% Tris-HCl SDS-PAGE gel showing the purified AMEs AAC(6')/APH(2'')-Ia (56,992 Da) (lane 1), AAC(3)-IV (31,882 Da) (lane 2), APH(2'') (34,791 Da) (lane 3), ANT(4') (33,299 Da) (lane 4), AAC(3)-Ib/AAC(6')-Ib' (37,582 Da) (lane 5), AAC(3)-Ib (19,707 Da) (lane 6), and AAC(6')-Ib' (21,344 Da) (lane 7). Lane L, BenchMark prestained protein ladder (Invitrogen). 6 μg of each protein was loaded onto the gel.

3.3. Results

3.3.1. Antimicrobial studies

To evaluate the effect of acetylation on antibacterial activity of AGs, the parent AGs KAN and TOB, as well as their synthetic 6'-*N*-acetylated counterparts were tested using the double-dilution method against *E. coli* BL21 (DE3) (strain A) and *B. subtilis* 168 (strain B). MIC values of 1.0 μg/mL (strain A) and 2.0 μg/mL (strain B) were determined for KAN, while MICs of 64 μg/mL (strain A) and 125 μg/mL (strain B) were established for 6'-*N*-acetyl-KAN. Even though an approximately 60-fold MIC increase is observed in both cases, 6'-*N*-acetyl-KAN still displays antibacterial activity. Similar observations were made with TOB and 6'-*N*-acetyl-TOB where MICs of 0.5 μg/mL (strain A) and 3.9 μg/mL (strain B) were determined for the parent AG, and MICs of 16 μg/mL (strain A) and 62.5 μg/mL (strain B) were observed for the 6'-*N*-acetylated drug, representing a 32-fold and 16-fold decrease in antibacterial activity, respectively. The 6'-*N*-acetylated AGs may retain activity through many factors including alteration of cellular uptake or cellular metabolism. Modified AGs are compared to their parent compounds for reference not considering the listed possible alterations. These results strongly suggest that *N*-acetylation alone may not be sufficient to completely inactivate AGs. Using bioTLCs, we demonstrated that these 6'-*N*-acetylated compounds can be completely inactivated by addition of another acetyl moiety by AAC(3)-IV (Fig. 3.3).

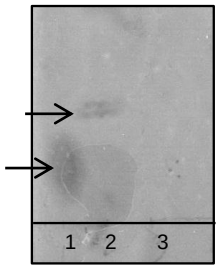

Fig. 3.3. BioTLC showing: Inhibition of *B. subtilis* growth by GEN (lanes 1), 6'-*N*-acetyl-GEN (lane 2), and there is no inhibition of *B. subtilis* growth by 6',3-*N*',*N*-di-acetyl-GEN (lane 3).

3.3.2. Alteration of enzymatic activities

In order to establish the effects of one modification on the second one, all enzymes were cloned and purified as previously reported,[3,4,8,11,12] except for AAC(3)-Ib/AAC(6')-Ib' where cloning into pET28a instead of pET22b resulted in production of N-terminally

His_6-tagged proteins instead of the previously reported untagged proteins (Fig. 3.2). The AGs were tested at concentrations of 100 and 50 μM for the first and second AME reactions, respectively. The initial rates of the reactions of the unmodified compounds were then compared to the initial rate of the enzymatic modification of the singly modified AGs (Fig. 3.4).

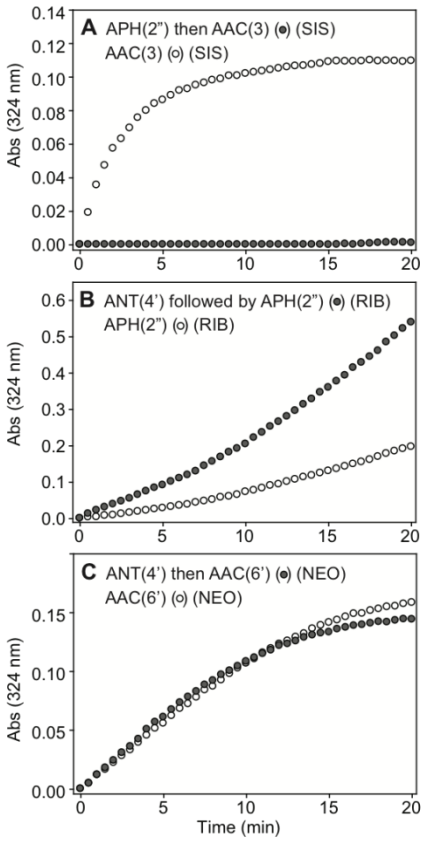

Fig. 3.4. Representative graphs comparing the activities of AMEs on an unmodified parent AG (○) with the activities of the same AMEs following AG modification (•). The graphs show examples of **A.** complete abolition in the case of SIS. **B.** An increase in the case of RIB. **C.** No change in the case of NEO, in the activity of the second AME following the action of the first AME.

We found that the rates of 3-acetylation of 6'-*N*-acetylated 4,6-disubstituted deoxystreptamine (DOS) AGs were significantly lower than those observed for the unmodified drugs (Table 3.1). No difference in the rates of 3-acetylation was observed for 6'-*N*-acetylated 4,5-DOS AGs and their unmodified counterparts (Table 3.2). It is important to note that acetylation at the 6'-position does not occur after acetylation at the 3-position consistent with our previous report.[8] This suggests that biologically active 3-*N*-acylated AGs could overcome resistance caused by AAC(6') enzymes. When tested using bioTLC, 3-*N*-acetyl-GEN and 3-*N*-*n*-propionyl-GEN both displayed antibacterial activity against *B. subtilis* (Fig. 3.5). Based on the available structural information of GEN bound to the bacterial ribosome small subunit target,[13,14] the ring I of GEN inserts into the RNA helix and causes the universally conserved 16S rRNA residues A1492 and A1493 to flip out, resulting in the increase of the tRNA binding affinity, ultimately leading to high error rates of translation (Fig. 3.6). When compared to the 6-amino moiety, the 3-amino group of GEN is positioned further away from A1492 and A1493 and the addition of the small acetyl and *n*-propionyl groups at this position is less likely to interfere with the binding of

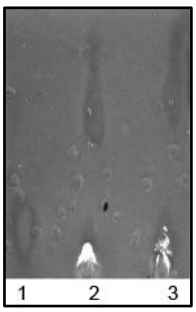

Fig. 3.5. BioTLC showing antibacterial activity against *B. subtilis.* of GEN (lane 1), 3-*N*-acetyl-GEN (lane 2), and 3-*N*-*n*-propionyl-GEN (lane 3),

the AG to the target. Therefore *N*-3 modified GEN may still be an active antibacterial compound as indicated by our bioTLC, and a second modification needed to abolish the activity is a highly plausible scenario. With regard to the sequential activities of AACs and APH(2"), we did not observe 2"-phosphorylation of 6'-*N*-acetylated or 3-*N*-acetylated 4,5-DOS AGs. It has been previously reported that the 4,5-DOS AGs are phosphorylated at the 3'- and 3"'-positions in the presence of cofactor and APH(2") enzymes.[9] This suggests that phosphorylation at the 3'- and 3"'-positions of 4,5-DOS AGs is not possible when the AGs are first acetylated at their 6'- or 3-position. We found that the rates of 3-acetylation were significantly reduced by prior 2"-phosphorylation for all AGs tested. Subsequent to 2"-phosphorylation, the rates of 6'-acetylation were unchanged for KAN and NEO, while reduced for the remaining AGs. Adenylation lowered the rates of 6'- and 3-acetylation as well as the rates of 2"-phosphorylation of 4,5-DOS AGs. Interestingly, in the case of the sequential 3-acetylation followed by 2"-phosphorylation of 4,6-DOS AGs, a unique increase in initial rate was observed. Finally, we observed that ANT(4') was in almost all cases inactive on AGs first modified by AACs and APH(2") with only 6'-*N*-acetyl-AMK, 6'-*N*-acetyl-SIS, and 6'-*N*-acetyl-TOB acting as substrates of ANT(4') by mass analysis. To confirm the production of the doubly modified AGs by sequential action of AMEs, mass spectrometric analyses were performed (Table 3.3). Mass analyses were in perfect agreement with spectrophotometric data.

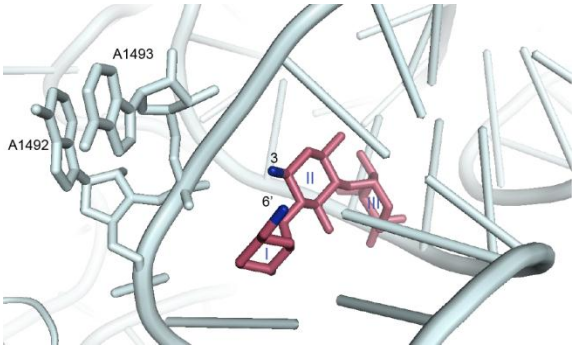

Fig. 3.6. Structure of GEN bound to the 30S ribosomal RNA (PDB: 2QB9).[13] The 6'- and 3-amine moieties of GEN (pink) are highlighted in blue.

Table 3.1. Analysis of sequential modifications of the 4,6-disubstituted DOS AGs (AMK, KAN, SIS, and TOB)

1st AME	2nd AME		
	APH(2")	AAC(3)-IV	AAC(6')
APH(2")	--	↓	↓
AAC(3)-IV	↑	--	×
ANT(4')	mix	↓	↓, =
AAC(6')	mix	↓	--

Note: × indicates that the second modification was not observed at all, ↓ indicates a decreased activity of the second enzyme, ↑ indicates an increased activity of the second enzyme, = indicates that the activity of the second enzyme remains the same, -- indicates that the reaction was not tested, and mix indicates that in some cases the activity of the second enzyme increases whereas in others cases it decreases.

Table 3.2. Analysis of sequential modifications of the 4,5-disubstituted DOS AGs (NEO, PAR, and RIB)

1st AME	2nd AME		
	APH(2")	AAC(3)-IV	AAC(6')
APH(2")	--	↓	↓, =
AAC(3)-IV	×	--	×
ANT(4')	↓	↓	↓
AAC(6')	×	=	--

Note: × indicates that the second modification was not observed at all, ↓ indicates a decreased activity of the second enzyme, ↑ indicates an increased activity of the second enzyme, = indicates that the activity of the second enzyme remains the same, -- indicates that the reaction was not tested, and mix indicates that in some cases the activity of the second enzyme increases whereas in others cases it decreases.

Table 3.3. Mass analysis of aminoglycosides (AGs) chemically modified (mono- or di-) by the AMEs AAC(6')/APH(2"),[a] AAC(3)-IV, ANT(4'), and APH(2").

AG[b]	Calcd	Observed $[M + H]^+$	AG	Calcd	Observed $[M + H]^+$	AG	Calcd	Observed $[M + H]^+$
2"-p-AMK[c]	665.25	666.30	3-Ac-TOB	509.27	510.30	2"-p-6'-Ac-NEO	736.29	737.25
4'-AMP-AMK[d]	914.34	915.30	4'-AMP-TOB	796.31	797.30	2"-p-6'-Ac-RIB	576.20	577.25
6'-Ac-AMK[e]	627.30	628.35	6'-Ac-TOB	509.27	510.30	2"-p-6'-Ac-SIS	569.25	570.30
2"-p-KAN	564.20	565.28	6',3-DiAc-AMK	669.31	670.35	2"-p-6'-Ac-TOB	589.24	590.30
4'-AMP-KAN	813.29	814.32	6',3-DiAc-KAN	568.26	569.30	4'-AMP-2"-p-AMK	994.30	995.35
6'-Ac-KAN	526.25	527.26	6',3-DiAc-NEO	698.33	699.30	4'-AMP-2"-p-KAN	893.26	894.30
2"-p-NEO	694.28	695.30	6',3-DiAc-RIB	538.25	539.30	4'-AMP-2"-p-NEO	1023.33	1046.35(+Na)
3-Ac-NEO	656.32	657.35	6',3-DiAc-SIS	531.29	532.30	4'-AMP-2"-p-PAR	1024.32	1025.35
4'-AMP-NEO	943.36	944.40	6',3-DiAc-TOB	551.28	552.30	4'-AMP-2"-p-RIB	864.25	865.35
6'-Ac-NEO	656.32	657.30	3-Ac-2"-p-SIS	569.25	570.30	4'-AMP-2"-p-SIS	856.29	857.30
2"-p-PAR	695.26	696.30	3-Ac-2"-p-TOB	589.24	590.30	4'-AMP-2"-p-TOB	876.28	877.30
3-Ac-PAR	657.31	658.30	6'-Ac-2"-p-AMK	707.26	708.30	4'-AMP-3-Ac-NEO	985.38	986.30
4'-AMP-PAR	944.35	945.30	6'-Ac-2"-p-KAN	606.22	607.20	4'-AMP-3-Ac-RIB	826.30	827.35
2"-p-RIB	534.19	535.25	6'-Ac-2"-p-SIS	569.25	570.30	4'-AMP-3-Ac-SIS	818.33	819.33
3-Ac-RIB	496.24	497.30	6'-Ac-2"-p-TOB	589.24	590.22	4'-AMP-3-Ac-TOB	838.32	839.33
4'-AMP-RIB	784.29	785.30	2"-p-3-Ac-NEO	736.29	737.35	4'-AMP-6'-Ac-AMK	956.35	957.40
6'-Ac-RIB	496.24	497.30	2"-p-3-Ac-PAR	737.27	738.35	4'-AMP-6'-Ac-KAN	855.30	856.35
2"-p-SIS	527.24	528.30	2"-p-3-Ac-RIB	576.20	577.30	4'-AMP-6'-Ac-NEO	985.38	986.35
3-Ac-SIS	489.29	490.25	2"-p-3-Ac-SIS	569.25	570.30	4'-AMP-6'-Ac-RIB	826.30	827.35
4'-AMP-SIS	776.32	777.35	2"-p-3-Ac-TOB	589.24	590.30	4'-AMP-6'-Ac-SIS	818.33	819.35
6'-Ac-SIS	489.29	490.30	2"-p-6'-Ac-AMK	707.26	708.35	4'-AMP-6'-Ac-TOB	838.32	839.35
2"-p-TOB	547.23	548.30	2"-p-6'-Ac-KAN	606.22	607.30			

[a]The bifunctional AAC(6')/APH(2") was used for its AAC(6') activity. [b]The order of modifications is indicated by the order presented in the name of the AG. [c]p = phospho. [d]AMP = adenosyl monophosphate. [e]Ac = acetyl.

3.4. Discussion

In order to rationalize the observed relative effects of modifications at various locations of AG scaffolds on the binding of these singly-modified AGs to subsequent resistance enzymes, we closely examined the structures of a variety of AMEs. Nearly a dozen crystal structures of AMEs have been reported, including five AACs, six APHs, and one ANT, have been reported.[15-30] Unfortunately, the structures of the exact AMEs tested on singly-modified AGs in this work have not be determined, limiting our rationale to analogous AMEs performing acetylation and phosphorylation of AGs at the 2"-, 3-, and

6'-positions studied. For 4,5- and 4,6-DOS AGs, we observed that 3-acetylation prevented 6'-acetylation by AAC(6')/APH(2''). In the structures of a similar enzyme, AAC(6')-Ib (PDB: 2QIR,[20] 2VQY[23]), the 3-amino group of KAN (or PAR) is in close proximity to the catalytic residues in the enzyme active site. Therefore, the addition of an acetyl group at the 3-position could disrupt the proper orientation of the AGs in enzyme active site, resulting in its inability to acetylate the 6'-position of the singly-modified AGs. For all AGs tested, we observed that the addition of a 4'-AMP group or a 2''-phospho group resulted in either a decrease or no change in the 6'-acetylating activity of AAC(6')/APH(2''). The AAC(6')-Ib structures show that the AG 4'-hydroxyl moiety is positioned away from the active site and that the 2''-hydroxyl is environmentally exposed. It is therefore expected that modifications on either the 2''- or 4'-position should not have detrimental effects on the acetylation activity of AAC(6')/APH(2''), which is in good agreement with our data.

For 4,6-DOS AGs, we observed that the rate of phosphorylation at the 2''-position increased as a result of 3- or 6'-acetylation. In the structure of APH(2'')-IIa (PDB: 3HAM[30]), the 6'-amine of GEN is positioned away from the active site. However, the 3-position is in close proximity of acidic residues (Asp or Glu) that are proposed to play a role in binding of the AG substrates. The addition of an acetyl group at the 3-position could bring the GEN closer to the catalytic Asp200 (corresponding to Asp192 in APH(2'')-IIa based on amino acid sequence alignment) and closer to the proposed location of the γ-phosphate at ATP leading to an increase in the observed 2''-phosphorylation rate. The 6'-*N*-acetlyation of GEN has the potential to disrupt the non-polar stacking interaction with the aromatic ring of Tyr274 (Trp265 in APH(2'')-IIa is found in place of Tyr274 in the APH(2'') used in this study) potentially bringing ring III of GEN bearing the 2''-hydroxyl to be phosphorylated closer to the catalytic residues, thereby facilitating the observed increased rate. As for AAC(3) activity on singly-modified AGs, a lack of available structure of AAC(3) in complex with AG substrates prevented a direct rationale of the results obtained with this enzyme.

With the ability of AMEs to doubly modify AGs by sequential action of isolated enzymes established, we set out to determine if the bifunctional AAC(3)-Ib/AAC(6')-Ib' could di-acetylate AGs. By comparing of the activity of the individual components of AAC(3)-Ib/AAC(6')-Ib' to that of the full-length bifunctional enzyme, we showed that AAC(3)-Ib/AAC(6')-Ib' can indeed yield 3,6'-*N*,*N'*-di-acetyl-GEN by MS (Fig. 3.7D). Double modification was previously reported for the bifunctional AAC(6')/APH(2") enzyme with KAN[31] as well as for the APH(3')-IIIa enzyme with butirosin, NEO, and RIB[32]. The GEN mixture that we used is composed of GEN C_1, C_2, and C_{1a} (Fig. 3.7C). Di-acetylation of all GEN compounds was observed by MS when using either the bifunctional enzyme (Fig. 3.7B) or through the sequential action of the individual AAC(3)-Ib and AAC(6')-Ib' enzymes (Fig. 3.7A). Interestingly, di-acetylation of GEN by AAC(3)-Ib/AAC(6')-Ib' was pH dependent: di-acetylation was observed at pH 7.5 or 8.0 whereas mono-acetylation was observed at pH < 7.0.

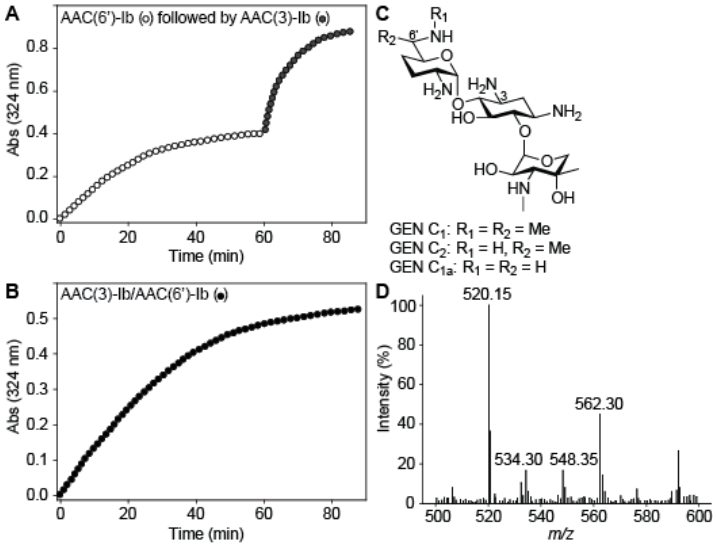

Fig. 3.7. A. A spectrophotometric assay demonstrating the di-acetylation of GEN via sequential reactions using the individual components AAC(6')-Ib' (white circles) followed by AAC(3)-Ib (dark gray circles) from the bifunctional AAC(3)-Ib/AAC(6')-Ib'. **B.** A spectrophotometric assay demonstrating the di-acetylation of GEN using the bifunctional AAC(3)-Ib/AAC(6')-Ib' (black circles). **C.** Structures of GEN C1, C2, and C1a. **D.** Mass spectra of the reaction of GEN with AcCoA using the bifunctional AAC(3)-Ib/AAC(6')-Ib' showing production of *N*-acetyl-GEN C1 (520.15), *N*,*N'*-di-acetyl-GEN C1a (534.30), *N*,*N'*-di-acetyl-GEN C2 (548.35), and *N*,*N'*-di-acetyl-GEN C1 (562.30). The same masses were observed when using AAC(6')-Ib' and AAC(3)-Ib sequentially.

To corroborate the *in vitro* di-acetylation data experiments, we analyzed the spent media and cell lysate of *E. coli* BL21 (DE3) harboring the *aac(3)-Ib/aac(6')-Ib'* gene grown in the presence of GEN (10 μM). Spent media from the aforementioned bacteria was analyzed by LCMS. Masses corresponding to di-acetylated GEN C_2 (548.40) and di-acetylated GEN C_1 (562.25) were found along with GEN C_1 (478.35), GEN C_2 (464.40), GEN C_{1a}

(450.10), and a small peak of phosphorylated GEN C_1 (558.50) from the APH(3") resistance enzyme contained in the pET28a vector utilized. These data confirm the ability of bifunctional AMEs to doubly modify AGs *in vivo* to infer resistance.

In summary, we have demonstrated that by their sequential actions, AMEs can doubly modify AGs. In many cases, we have observed that after a modification of one position, the ability of AMEs to perform a second modification is unchanged, decreased, or completely abolished. Not only are these observations useful as they will help anticipate the effect of a modification on the subsequent activity of AMEs and guide the design of novel AG antibiotics, they are also promising as they indicate the potential of biologically active *N*-acylated AGs to combat important factors responsible for the ever-growing resistance problem. We have showed that a single acetylation is not always powerful enough to completely inactive AGs. Even though the reasons for selection of fused genes over retention of the individual counterparts remain to be defined, we have demonstrated *in vitro* and *in vivo*, for the first time, the ability of a bifunctional AME to di-acetylate the same AG scaffold at two positions, complementing the previously reported di-modification (acetylation and phosphorylation) of KAN *in vitro*[31]. Guided by these results, efforts towards the development of novel AG antibiotics are currently underway in our group.

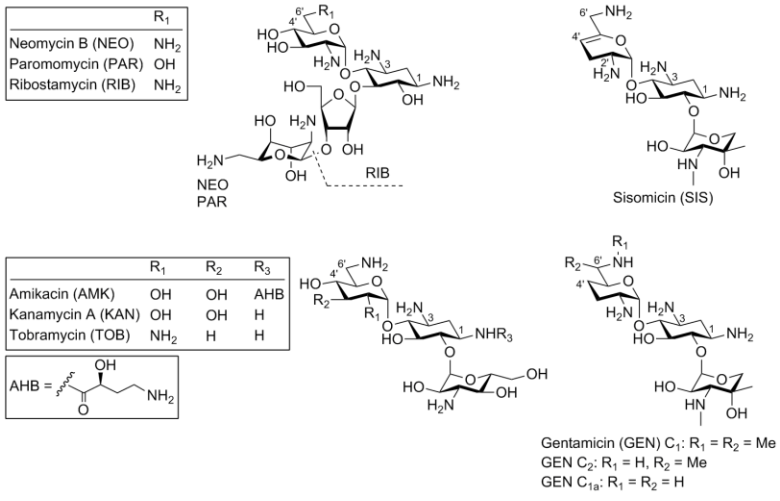

Fig. 3.8. Structures of aminoglycosides used in this chapter.

3.5. Materials and method

3.5.1. Bacterial strains, plasmids, materials, and instrumentation

B. subtilis 168 was obtained from the *Bacillus* Genetic Stock Center (Columbus, OH). The C-terminally His tagged enzyme AAC(6')/APH(2")(CHis),[8] the N-terminally His tagged enzyme AAC(3)-

IV(NHis) (from the Int-pET19b-pps vector),[8] ANT(4')(NHis),[12] and APH(2")(CHis) (amino acids 175 to 479 of the bifunctional AME AAC(6')/APH(2"))[11] were purified as described previously. The chemically competent bacteria *E. coli* TOP10 and *E. coli* BL21 (DE3) were obtained from Invitrogen (Carlsbad, CA). The DNA primers for PCR amplification were obtained from Integrated DNA Technologies (Coralville, IA). The pET28a and pET22b vectors were purchased from Novagen (Gibbstown, NJ). DNA sequencing was done at the University of Michigan DNA Sequencing Core. Reagents for cloning (restriction endonucleases, T4 DNA ligase, and Phusion DNA polymerase) were purchased from New England Biolabs (Ipswich, MA). DTDP (4,4'-dithiodipyridine), acetyl coenzyme A (AcCoA), ATP, GTP, a pyruvate kinase-lactic dehydrogenase mixture (catalog no. P0294), NADH, phosphoenolpyruvate (catalog no. P0564), and AGs (AMK, GEN, KAN, NEO, PAR, RIB, SIS, and TOB) (Fig. 3.8) were obtained from Sigma-Aldrich and were used without further purification. The UV-visible (UV-Vis) spectrophotometric assays were monitored on a multimode SpectraMax M5 plate reader using flat-bottom 96-well plates (Fisher Scientific). LCMS analyses were performed on the Shimadzu LCMS-2019EV mass spectrometer equipped with an LC-20AD liquid chromatograph and an SPD-20AV UV-Vis detector. All buffer pH were adjusted at rt.

3.5.2. Preparation of the pAAC(3)-Ib/AAC(6')-Ib'-pET28a, pAAC(3)-Ib-pET28a, and pAAC(6')-Ib'-pET28a overexpression constructs

The genes encoding AAC(3)-Ib/AAC(6')-Ib', AAC(3)-Ib, and AAC(6')-Ib' were PCR amplified from the pA3A6 plasmid[2] (kindly provided by Véronique Dubois, Université de Bordeaux) containing the fused AAC(3)-Ib/AAC(6')-Ib' gene in the pGEM-T vector. PCRs were carried out using Phusion high-fidelity DNA polymerase with primers identical to those reported previously.[3] The amplified genes were inserted into linearized pET28a via the corresponding *Nde*I- and *Eco*RI-cut sites. All proteins were expressed following transformation into competent *E. coli* TOP10 cells. The plasmids were sequenced (University of Michigan DNA Sequencing Core) and showed perfect alignment with the reported sequence (GenBank accession number AF355189.1).

3.5.3. Overproduction and purification of AAC(3)-Ib/AAC(6')-Ib'(NHis), AAC(3)-Ib(NHis), and AAC(6')-Ib'(NHis)

The purified plasmids pAAC(3)-Ib/AAC(6')-Ib'-pET28a(NHis), pAAC(3)-Ib-pET28a(NHis), and pAAC(6')-Ib'-pET28a(NHis) were transformed into chemically competent *E. coli* BL21 (DE3) cells for protein expression and purification. LB medium (1 L) supplemented with KAN (50 μg/mL) was inoculated with an overnight culture (10 mL) of the transformants harboring the pAAC(3)-Ib/AAC(6')-Ib'-pET28a, pAAC(3)-Ib-pET28a, and pAAC(6')-Ib'-pET28a overexpression constructs. The cultures were grown (37 ℃, 200 rpm) to an absorbance of ~0.6 at 600 nm, induced with IPTG (final concentration, 1.0 mM; 1 mL of a 1 M stock), and then grown (200 rpm) for an additional 16 h at 20 ℃. Cells were then harvested by centrifugation (6,000 rpm, 5 min, 4 ℃, Beckman Coulter Avanti JE centrifuge with an F10 rotor) and were resuspended in buffer A (10% glycerol, 200 mM NaCl, and 25 mM Tris-HCl pH 8.0). The resuspended cells were lysed (1 pass at 10,000 to 15,000 lb/in^2, Avestin EmulsiFlex-C3 high-pressure homogenizer), and the cell debris was removed by centrifugation (16,000 rpm, 45 min, 4 ℃, Beckman Coulter Avanti JE centrifuge with a JA-17 rotor). Imidazole (final concentration, 2 mM) was added to the supernatant prior to incubation (4 ℃, 2 h with gentle rocking) with Ni-NTA agarose resin (1.5 mL; Qiagen). The resin was loaded onto a column and was washed with buffer A (10 mL) containing 5 mM imidazole followed by buffer A (10 mL) containing 20 mM imidazole. The desired protein was eluted from the column in a stepwise imidazole gradient (a 10 mL fraction of 20 mM imidazole (1x) and 5 mL fractions of 20 mM (2x), 40 mM (3x), and 250 mM (3x) imidazole). Fractions containing the pure desired proteins, as determined by SDS-PAGE, were combined and dialyzed at 4 ℃ for 3 to 12 h against a total of 6 L of buffer B (10% glycerol, 300 mM NaCl, and 25 mM Tris-HCl pH 8.0). All proteins were concentrated using an Amicon Ultra PL-10 centrifugal filter device. Protein concentrations were determined using a NanoDrop spectrometer (Thermo Scientific). Protein yields were 2.4 (AAC(3)-Ib/AAC(6')-Ib'), 0.8 (AAC(3)-Ib), and 1.8 (AAC(6')-Ib') mg/L of culture. All proteins were flash-frozen using liquid nitrogen and were stored at -80 ℃.

3.5.4. Determination of MIC values

MIC values were determined using the double-dilution method against *E. coli* BL21 (DE3) (strain A) and *B. subtilis* 168 (strain B), using a starting concentration of 125 μg/mL as reported previously.[23] The negative and positive controls consisted of omission of the AG or of bacteria, respectively. All experiments were performed in triplicate.

3.5.5. BioTLC assays

To establish the activity, or lack thereof, of *N*-acylated AGs, the following bioTLC protocols were followed.

3.5.5.1. BioTLC assay for acylation of GEN

Enzymatic reactions (10 to 20 μL reaction mixture) were carried out in MES (50 mM, pH 5.7) using AAC(3)-IV (0.5 μM) in the presence of GEN (60 nmol) and acyl-CoA (AcCoA or ProCoA) (80 nmol). The progress of the reactions was monitored by thin-layer chromatography (TLC), and upon completion, reactions were quenched using MeOH (10 to 20 μL), and reaction mixtures were kept at -20 ℃ for at least 20 min. After removal of the precipitated protein by centrifugation (14,000 rpm, 10 min at rt), the reaction mixture was loaded onto a TLC and was run in MeOH-NH_4OH (ratio, 6:1; ~30% in H_2O). *B. subtilis* was grown overnight at 30 ℃ in LB medium (with no antibiotic). The culture was diluted (100 μL in 10 mL of soft agar (0.75%)-LB medium at 37 ℃), and the diluted culture was poured over the TLC plate in a sterile petri dish. The plate was then incubated at 30 ℃ (10 h to O/N) until clear zones of inhibition were observed.

3.5.5.2. BioTLC assay for confirmation of inactivation of 6'-*N*-acylated AGs by addition of an acetyl group at position 3

Enzymatic sequential di-acetylation reactions were carried out as described above in MES (50 mM, pH 6.6) by first incubating AAC(6')/APH(2'') (0.5 μM) with NEO (15 nmol) and AcCoA (60 nmol) for 1 h at 37 ℃. TLC was used to monitor the progress of the reaction. After the completion of the first acetylation reaction, AAC(3)-IV (0.5 μM) was added, and the mixture was incubated at rt until the reaction was complete (~1 h) as indicated by TLC. The mixture was treated as described above by using MeOH-NH_4OH

at a 3:1 ratio as the TLC eluent system. Bacteria were added as described above and were grown overnight prior to visualization for zones of inhibition. The position of ring II of GEN compared to that of ring I could explain the residual activity for 3-*N*-acetyl-GEN and 3-*N*-*n*-propionyl-GEN (Fig. 3.6).

3.5.6. UV-Vis spectrophotometric assay for determining sequential modifications

To establish if sequential modifications can be achieved, the assays described below were performed. In all of these sequential assays, the first reaction (100 μL reaction mixture) was followed by addition of the second enzyme in combination with the appropriate indicator and buffer (100 μL) for a total volume of 200 μL. All concentrations reported are the final concentrations in the 200 μL total reaction volume.

3.5.6.1. AACs followed by AACs

AGs (50 μM) were first acetylated at 37 °C using AcCoA (150 μM) and AAC(6')/APH(2") (0.5 μM) in MES buffer (50 mM, pH 6.6). After 45 min of incubation, a mixture of AAC(3)-IV (0.5 μM) and DTDP (2 mM) was added, and the reaction was monitored (324 nm, 25 °C) using a plate reader by taking measurements every 30 s for 30 min. This procedure was also used to monitor the sequential AAC(3)-IV (25 °C) and AAC(6')/APH(2") (37 °C) reactions.

3.5.6.2. APH(2") followed by AACs

AGs (50 μM) were first phosphorylated at 37 °C using GTP (0.75 mM) (GTP was previously reported to be a cosubstrate of APH, and we found that it yielded better experimental data than ATP[33,34]) and APH(2") (1 μM) in HEPES buffer (50 mM, pH 8.0), $MgCl_2$ (5 mM), and KCl (20 mM). After 1 h of incubation, the pH of the solution was lowered to 6.8 by addition of HCl (1.12 μL of a 1 M stock) to accommodate the reactivity of the AAC enzymes. AcCoA (100 μM) was then added, and the acetylation reactions were initiated by addition of a solution containing AAC(3)-IV (0.25 μM) or AAC(6')/APH(2") (0.5 μM) and DTDP (2 mM). The reaction mixtures were incubated at

25 ℃ (AAC(3)-IV) or 37 ℃ (AAC(6')/APH(2")), and measurements were taken at 324 nm every 30 s for 30 min.

3.5.6.3. ANT(4') followed by AACs

AGs (50 μM) were first nucleotidylated at 25 ℃ using ATP (150 μM) and ANT(4') (1 μM) in HEPES buffer (50 mM, pH 7.5). After 16 h, the nucleotidylation reactions were stopped by acidification to pH 6.8 by the addition of HCl (1.12 μL of a 1 M stock). AcCoA (150 μM) was then added, and the acetylation reactions were initiated by the addition of a solution containing AAC(3)-IV (0.5 μM) or AAC(6')/APH(2") (0.5 μM) and DTDP (2 mM). The reactions were monitored at 25 ℃ (AAC(3)-IV) or 37 ℃ (AAC(6')/APH(2")), and measurements were taken at 324 nm every 30 s for 30 min.

3.5.6.4. ANT(4') followed by APH(2")

AGs (50 μM) were first nucleotidylated at 25 ℃ using ATP (150 μM) and ANT(4') (1 μM) in HEPES buffer (50 mM, pH 7.5). After overnight incubation, a mixture of APH(2") (2.5 μM), NADH (0.5 mg/mL), phosphoenolpyruvate (2.5 mM), GTP (1.25 mM), and the pyruvate kinase-lactic dehydrogenase mixture (5 μL) was added to initiate the reaction. The phosphorylation reaction was monitored at 37 ℃, and measurements were taken at 340 nm every 30 s for 30 min.

3.5.6.5. AACs followed by APH(2")

AGs (100 μM) were first acetylated using AcCoA (150 μM) and AAC(6')/APH(2") (0.25 μM) at 37 ℃ or AAC(3)-IV (0.125 μM) at 25 ℃ in HEPES buffer (50 mM, pH 6.8). After 45 min of incubation, the acetylation reactions were stopped by basification to pH 8.0 by addition of KOH (4.2 μL of a 4 M stock). A mixture of APH(2") (2.5 μM), $MgCl_2$ (10 mM), KCl (40 mM), NADH (0.5 mg/mL), phosphoenolpyruvate (2.5 mM), GTP (1.25 mM), and the pyruvate kinase-lactic dehydrogenase mixture (5 μL) was added to initiate the reaction. The phosphorylation reaction was monitored at 37 ℃, and measurements were taken at 340 nm every 30 s for 30 min.

3.5.7. Mass spectrometric analyses

3.5.7.1. AACs followed by AACs

For the first reaction, a 10 μL solution containing AGs (2 mM), AcCoA (3 mM), and AAC(6')/APH(2") (9 μM) (or AAC(3)-IV (22 μM)) in HEPES buffer (50 mM, pH 6.8) was incubated at rt overnight. Then a solution (10 μL) containing acetyl-CoA (3 mM) and AAC(3)-IV (22 μM) (or AAC(6')/APH(2") (9 μM)) in HEPES buffer (50 mM, pH 6.8) was added, and the mixture was incubated at rt overnight. Proteins were precipitated by addition of ice-cold methanol (20 μL) and were kept at -20 ℃ for at least 10 min prior to centrifugation (at 13,000 rpm for 10 min). Seventy microliters of H_2O was added to 10 μL of the supernatant, and at least 20 μL of the diluted sample was loaded onto a Shimadzu LCMS-2010EV mass spectrometer system for mass analysis using H_2O (with 0.1% formic acid) under positive-ionization conditions. The results were in perfect agreement with the spectrophotometric data (Table. 3.3).

3.5.7.2. AACs followed by APH(2")

For the first reaction, a 10 μL solution containing AGs (2 mM), AcCoA (3 mM), and AAC(6')/APH(2") (9 μM) (or AAC(3)-IV (22 μM)) in HEPES buffer (50 mM, pH 6.8) was incubated at rt overnight. The pH of the reaction mixture was adjusted to 8.0 by the addition of KOH (1 μL of a 4 M stock) to accommodate the reactivity of APH(2"). After the first incubation, a solution (10 μL) containing GTP (3 mM) and APH(2") (20 μM) in HEPES buffer (50 mM, pH 8.0) was added, and the mixture was incubated at 37 ℃ overnight. Proteins were precipitated, and samples were analyzed, as described above.

3.5.7.3. APH(2") followed by AACs

For the first reaction, a 10 μL solution containing AGs (2 mM), GTP (3 mM), and APH(2") (20 μM) in HEPES buffer (50 mM, pH 8.0) was incubated at rt overnight. The pH of the reaction mixture was adjusted to 6.8 by the addition of HCl (0.1 μL of a 1 M stock) to accommodate the reactivity of the AAC enzymes. After the first incubation, a solution (10 μL) containing AcCoA (3 mM) and AAC(3)-IV (22 μM) (or AAC(6')/APH(2") (9 μM)) in HEPES buffer (50 mM; pH 6.8) was added, and the

mixture was incubated at rt overnight. Proteins were precipitated, and samples were analyzed, as described above.

3.5.7.4. ANT(4') followed by AACs

For the first reaction, a 10 μL solution containing AGs (2 mM), ATP (3 mM), and ANT(4') (4.5 μM) in HEPES buffer (50 mM, pH 7.5) was incubated at rt overnight. Then a solution (10 μL) containing AcCoA (3 mM) and AAC(3)-IV (22 μM) (or AAC(6')/APH(2") (9 μM)) in HEPES buffer (50 mM, pH 6.8) was added, and the mixture was incubated at rt overnight. Proteins were precipitated, and samples were analyzed, as described above.

3.5.7.5. ANT(4') followed by APH(2")

For the first reaction, a 10 μL solution containing AGs (2 mM), ATP (3 mM), and ANT(4') (4.5 μM) in HEPES buffer (50 mM, pH 7.5) was incubated at rt overnight. Then a solution (10 μL) containing GTP (3 mM) and APH(2") (20 μM) in HEPES buffer (50 mM, pH 8.0) was added, and the mixture was incubated at 37 ℃ overnight. Proteins were precipitated, and samples were analyzed, as described above.

3.5.8. *In vivo* analyses of AG modifications

The procedure used was analogous to a method reported previously.[34] Bacteria containing AAC(3)-Ib/AAC(6')-Ib' (pET82a) were grown (at 37 ℃ O/N) in the presence of GEN (10 μM, which equates to 4.7 μg/mL). The cultures were centrifuged (3,500 rpm, 20 min, 4 ℃), and the spent medium was set aside for analysis. The cell pellets were resuspended in buffer C (150 mM NaCl and 25 mM Tris-HCl pH 8.0) and were boiled for 15 min. The suspension was centrifuged (3,500 rpm, 20 min, 4 ℃) and the lysate collected. The lysate and spent medium were lyophilized separately. The residues were resuspended in MeOH (1 mL) and were centrifuged (3,500 rpm, 20 min, 4 ℃). The solvent was removed by decantation, and the resulting residue was resuspended in a H_2O:EtOAc:MeOH mixture (1:1:1) (1.5 mL). After centrifugation (3,500 rpm, 20 min, 4 ℃) and removal of the supernatant, the residue was dissolved in H_2O (250 μL) and was analyzed by mass spectrometry using H_2O (with 0.1% formic acid) under positive-ionization conditions.

3.6. References

(1) Houghton, J. L.; Green, K. D.; Chen, W.; Garneau-Tsodikova, S. *Chembiochem : a European journal of chemical biology* **2010**, *11*, 880.
(2) Dubois, V.; Poirel, L.; Marie, C.; Arpin, C.; Nordmann, P.; Quentin, C. *Antimicrobial agents and chemotherapy* **2002**, *46*, 638.
(3) Kim, C.; Villegas-Estrada, A.; Hesek, D.; Mobashery, S. *Biochemistry* **2007**, *46*, 5270.
(4) Boehr, D. D.; Daigle, D. M.; Wright, G. D. *Biochemistry* **2004**, *43*, 9846.
(5) Centron, D.; Roy, P. H. *Antimicrobial agents and chemotherapy* **2002**, *46*, 1402.
(6) Kim, C.; Hesek, D.; Zajicek, J.; Vakulenko, S. B.; Mobashery, S. *Biochemistry* **2006**, *45*, 8368.
(7) Zhang, W.; Fisher, J. F.; Mobashery, S. *Current opinion in microbiology* **2009**, *12*, 505.
(8) Green, K. D.; Chen, W.; Houghton, J. L.; Fridman, M.; Garneau-Tsodikova, S. *Chembiochem : a European journal of chemical biology* **2010**, *11*, 119.
(9) Daigle, D. M.; Hughes, D. W.; Wright, G. D. *Chemistry & biology* **1999**, *6*, 99.
(10) Magalhaes, M. L.; Blanchard, J. S. *Biochemistry* **2005**, *44*, 16275.
(11) Shaul, P.; Green, K. D.; Rutenber, R.; Kramer, M.; Berkov-Zrihen, Y.; Breiner-Goldstein, E.; Garneau-Tsodikova, S.; Fridman, M. *Organic & biomolecular chemistry* **2011**.
(12) Porter, V. R.; Green, K. D.; Zolova, O. E.; Houghton, J. L.; Garneau-Tsodikova, S. *Biochem Biophys Res Commun* **2010**, *403*, 85.
(13) Borovinskaya, M. A.; Pai, R. D.; Zhang, W.; Schuwirth, B. S.; Holton, J. M.; Hirokawa, G.; Kaji, H.; Kaji, A.; Cate, J. H. *Nature structural & molecular biology* **2007**, *14*, 727.
(14) Carter, A. P.; Clemons, W. M.; Brodersen, D. E.; Morgan-Warren, R. J.; Wimberly, B. T.; Ramakrishnan, V. *Nature* **2000**, *407*, 340.
(15) Burk, D. L.; Ghuman, N.; Wybenga-Groot, L. E.; Berghuis, A. M. *Protein science : a publication of the Protein Society* **2003**, *12*, 426.
(16) Burk, D. L.; Hon, W. C.; Leung, A. K.; Berghuis, A. M. *Biochemistry* **2001**, *40*, 8756.
(17) Fong, D. H.; Berghuis, A. M. *Antimicrobial agents and chemotherapy* **2009**, *53*, 3049.
(18) Fong, D. H.; Berghuis, A. M. *EMBO J* **2002**, *21*, 2323.
(19) Magalhaes, M. L.; Vetting, M. W.; Gao, F.; Freiburger, L.; Auclair, K.; Blanchard, J. S. *Biochemistry* **2008**, *47*, 579.
(20) Maurice, F.; Broutin, I.; Podglajen, I.; Benas, P.; Collatz, E.; Dardel, F. *EMBO reports* **2008**, *9*, 344.
(21) Nurizzo, D.; Shewry, S. C.; Perlin, M. H.; Brown, S. A.; Dholakia, J. N.; Fuchs, R. L.; Deva, T.; Baker, E. N.; Smith, C. A. *Journal of molecular biology* **2003**, *327*, 491.
(22) Pedersen, L. C.; Benning, M. M.; Holden, H. M. *Biochemistry* **1995**, *34*, 13305.
(23) Stogios, P. J.; Shakya, T.; Evdokimova, E.; Savchenko, A.; Wright, G. D. *The Journal of biological chemistry* **2011**, *286*, 1966.
(24) Toth, M.; Frase, H.; Antunes, N. T.; Smith, C. A.; Vakulenko, S. B. *Protein science : a publication of the Protein Society* **2010**, *19*, 1565.
(25) Vetting, M. W.; Hegde, S. S.; Javid-Majd, F.; Blanchard, J. S.; Roderick, S. L. *Nature structural biology* **2002**, *9*, 653.
(26) Vetting, M. W.; Magnet, S.; Nieves, E.; Roderick, S. L.; Blanchard, J. S. *Chemistry & biology* **2004**, *11*, 565.
(27) Vetting, M. W.; Park, C. H.; Hegde, S. S.; Jacoby, G. A.; Hooper, D. C.; Blanchard, J. S. *Biochemistry* **2008**, *47*, 9825.
(28) Wolf, E.; Vassilev, A.; Makino, Y.; Sali, A.; Nakatani, Y.; Burley, S. K. *Cell* **1998**, *94*, 439.
(29) Wybenga-Groot, L. E.; Draker, K.; Wright, G. D.; Berghuis, A. M. *Structure* **1999**, *7*, 497.
(30) Young, P. G.; Walanj, R.; Lakshmi, V.; Byrnes, L. J.; Metcalf, P.; Baker, E. N.; Vakulenko, S. B.; Smith, C. A. *Journal of bacteriology* **2009**, *191*, 4133.

(31) Azucena, E.; Grapsas, I.; Mobashery, S. *Journal of the American Chemical Society* **1997**, *119*, 2317.
(32) Thompson, P. R.; Hughes, D. W.; Wright, G. D. *Biochemistry* **1996**, *35*, 8686.
(33) DM, D.; DW, H.; GD., W. *Chemistry & biology* **1999**, *6*, 99.
(34) Toth, M.; Chow, J. W.; Mobashery, S.; Vakulenko, S. B. *The Journal of biological chemistry* **2009**, *284*, 6690.

Note:

This chapter is adapted from a published manuscript: Green, K. D.; **Chen, W.**; Garneau-Tsodikova, S. *Antimicrobial agents and chemotherapy* **2011**, *55*, 3207. **Wenjing Chen** did all the LCMS experiments, crystal structure analysis, and some parts of the spectrophotometric assay and bioTLC.

Chapter 4

Unusual regioversatility of acetyltransferase Eis, a cause of drug resistance in XDR-TB

4.1. Abstract

The emergence of multidrug-resistant (MDR) and extensively drug-resistant (XDR) tuberculosis (TB) is a serious global threat. Aminoglycoside (AG) antibiotics are used as a last resort to treat XDR-TB. Resistance to the AG kanamycin (KAN) is a hallmark of XDR-TB. Here, we reveal the function and structure of the mycobacterial protein Eis responsible for resistance to KAN in a significant fraction of KAN-resistant *Mycobacterium tuberculosis* (*Mtb*) clinical isolates. We demonstrate that Eis has an unprecedented ability to acetylate multiple amines of many AGs. Structural and mutagenesis studies of Eis indicate that its acetylation mechanism is enabled by a complex tripartite fold that includes two general control non-derepressible 5 (GCN5)-related *N*-acetyltransferase regions. An intricate negatively charged substrate-binding pocket of Eis is a potential target of new antitubercular drugs expected to overcome AG resistance.

4.2. Introduction

Tuberculosis (TB) is a deadly infectious disease caused by the bacterium *Mtb*. With over 9 million new cases and nearly 2 million deaths each year, TB is one of the most serious health problems worldwide. Continuous use of the same multidrug therapy needed to treat TB and noncompliance have led to emergence of MDR and XDR strains of *Mtb*, an alarming problem due to their global spread. *Mtb* strains are classified as XDR when they are resistant to the two most potent first-line oral antituberculosis drugs, rifampicin and isoniazid, as well as to a fluoroquinolone and to at least one of three second line-injectable antituberculosis drugs KAN, amikacin (AMK), and capreomycin.[1]

KAN and AMK belong to the AG family of antibiotics[2] that inhibit protein synthesis in bacteria by targeting the 16S rRNA of the 30S subunit[3,4] of the ribosome.[5] Recently, mechanisms of clinical resistance of *Mtb* to KAN were elucidated. In one-third of clinical isolates, encompassing a large set of strains from different regions of the world, clinical resistance to KAN was solely due to the up-regulation of the chromosomal *eis* (enhanced intracellular survival) gene bearing mutations in its promoter.[6] In the other two-thirds, the resistance was due to ribosomal mutations. A previous study established that increased expression of the AG acetyltransferase (AAC) Eis, encoded by the *eis* gene harboring such mutations, rendered resistance to KAN in H37Rv, an AG-sensitive strain of *Mtb*.[7] Here, we report the *in vitro* characterization of Eis and show that this resistance enzyme has an unprecedented ability to multi-acetylate many AGs. We also present structural and mutagenesis studies of Eis, which explain its acetylation mechanism.

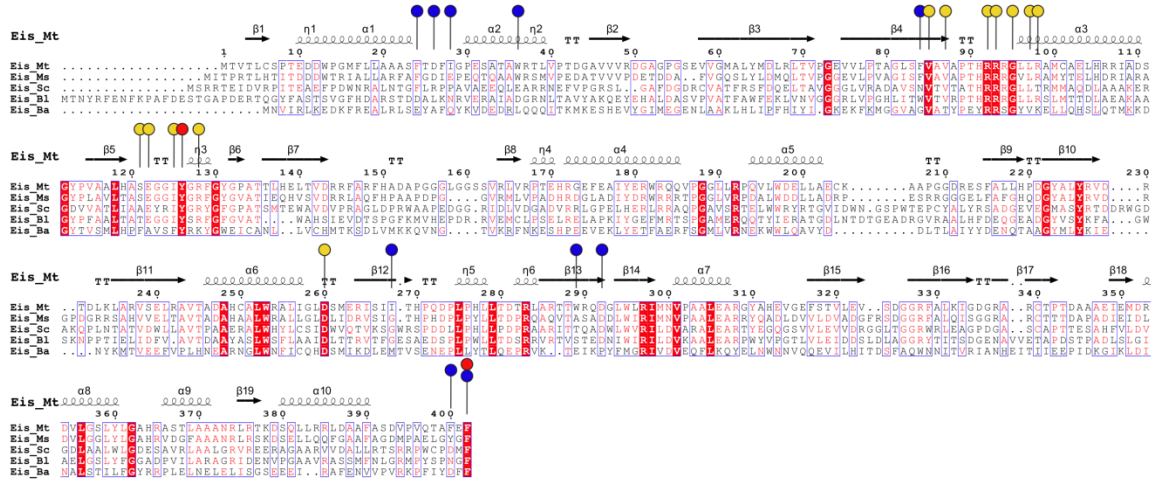

Fig. 4.1. Multiple sequence alignment of Eis homologs. The residues that are directly involved in the acetyl transfer are marked by red circles, those that bind CoA by yellow circles, and those that form the AG binding pocket by blue circles. The abbreviated names of bacterial species correspond to the following: *Mycobacterium tuberculosis* H37Rv (Mt), *Mycobacterium smegmatis* str. MC2 155 (Ms), *Streptomyces coelicolor* A3(2) (Sc), *Brevibacterium linens* BL2 (Bl), and *Bacillus anthracis* str. Sterne (Ba).

4.3. Results and discussion

4.3.1. Unique multi-acetylation of AGs by Eis

Eis is a member of a conserved chromosomally encoded family of proteins present in many pathogens (Fig. 4.1). It is highly divergent from previously characterized AACs. To gain insight into the mechanism of acetylation of AGs by Eis, we first explored its substrate specificity profile by using a wide set of AGs: netilmicin (NET), sisomicin

(SIS), neamine (NEA), ribostamycin (RIB), paromomycin (PAR), neomycin B (NEO), KAN, AMK, tobramycin (TOB), hygromycin (HYG), apramycin (APR), spectinomycin (SPT), and streptomycin (STR). Eis efficiently acetylated a broad variety of AGs (all AGs tested, except APR, SPT, and STR; Fig. 4.2) as observed by spectrophotometric (Fig. 4.3 and Table 4.1) and mass spectrometry (Table 4.2) assays. Remarkably, and to our surprise, Eis catalyzed an unprecedented multi-acetylation (di-, tri-, and even tetra-acetylation) of its AG substrates. Such multiple acetylation has not been documented for any other known AAC. To confirm the uniqueness of multi-acetylation by Eis, we tested six other AACs known to perform mono-acetylation at the 2'-, 3-, or 6'- positions.[8-16] UV-visible (UV-Vis) and mass spectrometry assays of these six AACs with the ten AGs that are multi-acetylated by Eis, showed only mono-acetylation. These reactions were performed under individually optimized conditions with ten equivalents of acetyl coenzyme A (AcCoA). To assess catalytic specificity of Eis, we measured k_{cat} and K_m values in steady-state kinetic assays monitoring net acetylation of a variety of AGs (Table 4.1). Catalytic efficiencies (k_{cat}/K_m) varied in a 40-fold range (from 267 $M^{-1}s^{-1}$ for AMK to 10,042 $M^{-1}s^{-1}$ for NET). Most of this variation was due to differences in k_{cat} (a 24-fold range), whereas K_m only displayed a four-fold variation, suggesting that Eis evolved to bind different AGs with similar affinities.

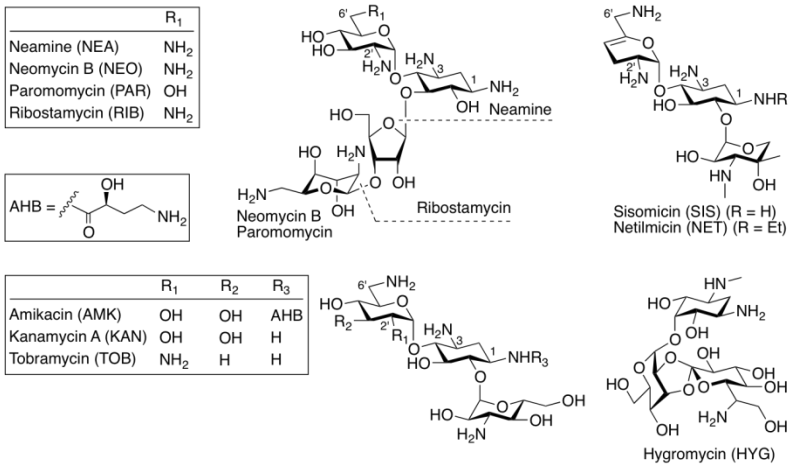

Fig. 4.2. Structures of AGs that are substrates of Eis.

Table 4.1. Kinetic parameters of net acetylation by Eis.

AG	K_m (μM)	k_{cat} (s^{-1})	k_{cat}/K_m ($M^{-1}s^{-1}$)
AMK	75 ± 3	0.020 ± 0.007	267 ± 94
KAN	99 ± 5	0.039 ± 0.004	394 ± 45
NEA	178 ± 2	0.070 ± 0.002	393 ± 12
NEO	98 ± 8	0.130 ± 0.019	1,300 ± 200
NET	48 ± 5	0.482 ± 0.037	10,000 ± 1,300
PAR	82 ± 9	0.058 ± 0.009	700 ± 100
SIS	58 ± 15	0.270 ± 0.024	4,700 ± 1,300
TOB	63 ± 6	0.162 ± 0.004	2,600 ± 250

Table 4.2. Mass analysis of AGs acetylated by the Eis protein and its mutants.

AG[a]	Calculated	$[M + H]^+$	Observed[f] $[M + H]^+$							
			(NHis)	(CHis)	1-399	F24A	F27A	I28A	W36A	F84A
AMK	Mono[b]	628.30					628.25			
	Di[c]	670.31	670.30				670.20			
	Tri[d]	712.32	712.35							
HYG	Mono	570.24	570.25				570.20	570.25		
	Di	612.25	612.25							
KAN	Mono	527.25	527.24						527.25	
	Di	569.26	569.25				569.25	569.20		
NEA	Mono	365.20								
	Di	407.21	407.22				407.15	407.20	407.22	
	Tri	449.22	449.23							
NEO	Mono	657.32								657.32
	Di	699.33					699.35	699.35	699.25	
	Tri	741.34	741.30			741.30	741.35	741.35	741.40	
NET	Mono	518.31	518.35	518.35	518.25	518.35	518.25	518.20	518.35	518.35
	Di	560.32	560.35	560.35	560.35	560.35	560.25	560.30		560.35
PAR	Mono	658.31					658.25			658.31
	Di	700.32	700.35				700.25		700.40	700.35
	Tri	742.33								
RIB	Mono	497.24								
	Di	539.25	539.25				539.25	539.35		
	Tri	581.26	581.15							
SIS	Mono	490.28	490.25	490.25	490.30	490.25	490.30	490.25	490.30	490.25
	Di	532.29	532.30	532.30	532.30	532.25	532.30	532.30		532.30
	Tri	574.30	574.30							
TOB	Mono	510.27				510.28				510.27
	Di	552.28	552.30			552.30	552.20	552.25	552.30	552.30
	Tri	594.29	594.31							
	Tetra[e]	636.30	636.32							

AG[a]	Calculated	$[M + H]^+$	Observed[f] $[M + H]^+$							
			V87A	R93A	H119A	S121A	R128A	R148A	W197A	D292A
AMK	Mono	628.30						628.25		
	Di	670.31						670.20		
	Tri	712.32								
HYG	Mono	570.24				570.25		570.35		
	Di	612.25								
KAN	Mono	527.25				527.24				
	Di	569.26				569.25		569.30		
NEA	Mono	365.20								
	Di	407.21				407.23				
	Tri	449.22				449.23		449.22		
NEO	Mono	657.32			657.30	657.32				
	Di	699.33	699.35		699.30		699.35			
	Tri	741.34						741.35		
NET	Mono	518.31	518.35	518.25	518.25	518.35	518.35		518.35	518.30
	Di	560.32		560.20		560.35	560.20	560.25	560.30	560.30
PAR	Mono	658.31				680.31 (+Na)	658.25	658.25		
	Di	700.32				700.35				
	Tri	742.33				742.34				
RIB	Mono	497.24								
	Di	539.25								
	Tri	581.26								
SIS	Mono	490.28	490.30		490.25	490.25			490.25	490.20
	Di	532.29	532.30			532.32	532.25	532.20	532.25	532.35
	Tri	574.30				574.30	574.30			
TOB	Mono	510.27	510.28							
	Di	552.28	552.25	552.30	552.30	552.30	552.30	552.30		
	Tri	594.29			594.20	594.31				
	Tetra	636.30				636.32				

[a]APR, SPT, and STR were found not to be substrates of Eis. [b]Mono indicates mono-acetylation. [c]Di indicates di-acetylation. [d]Tri indicates tri-acetylation. [e]Tetra indicates tetra-acetylation. [f]Note: The deletion mutants Eis1-311 and Eis292-402 as well as the single point mutants EisY126A and Y310A did not exhibit any activity.

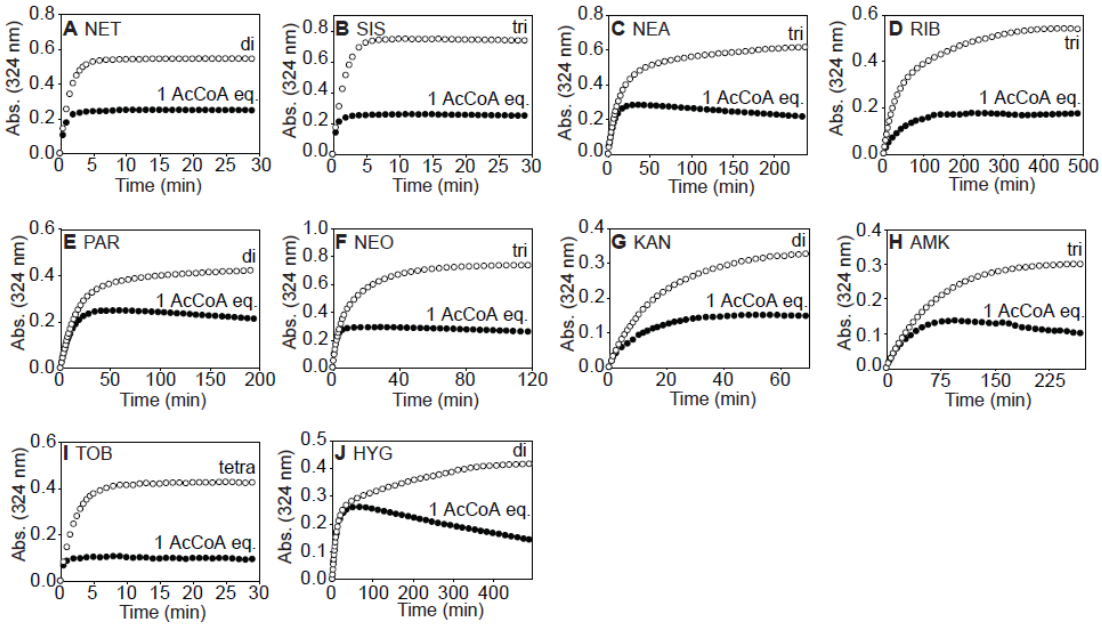

Fig. 4.3. Multi-acetylation of AGs by Eis. Spectrophotometric assay plots monitoring the conversion of various AGs by Eis (black circles) when using 1 equivalent of AcCoA (panels **A**-**J**), and to their di- (panels **A**, **E**, **G**, and **J**), tri- (panels **B**, **C**, **D**, **F**, and **H**), and tetra-acetylated (panel **I**) counterparts (white circles) when using 10 equivalents of AcCoA.

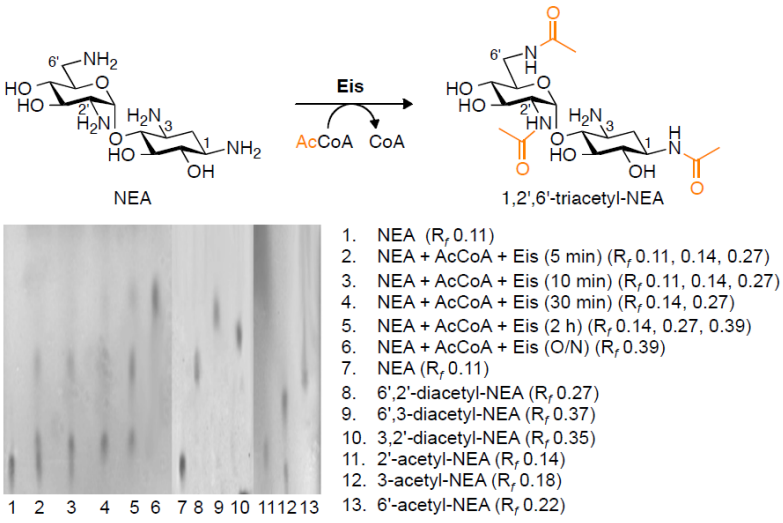

Fig. 4.4. Conversion of NEA to 1,2',6'-tri-acetyl-NEA. TLC time course showing the mono-, di-, and tri-acetylated NEA products generated by Eis using 5 equivalents of AcCoA. Control reactions for mono- and di-acetylation were performed using AAC(2')-Ic, AAC(3)-IV, and AAC(6') individually or sequentially.

4.3.2. Regiospecificity of tri-acetylation of NEA by Eis

To examine the regiospecificity and the potential order of multi-acetylation by Eis, we investigated the tri-acetylation of NEA (Fig. 4.3). NEA contains four primary amines located at positions 1, 2', 3, and 6'. The reaction progress was monitored by thin-layer chromatography (TLC) (Fig. 4.4 and Table 4.3). By comparing the R_f values of the mono-, di-, and tri-acetylated NEA species formed over time by Eis to those of 2'-, 3-, and 6'-acetyl-NEA obtained by using mono-acetylating enzymes, as well as to 6',2'-, 6',3-, and 3,2'-di-acetyl-NEA obtained by

the sequential use of pairs of these enzymes, we demonstrated that Eis tri-acetylates NEA, first at the 2'-, then at the 6'-, and, finally, at the 1-position. At a qualitative level, Fig. 4.4 demonstrates that these acetylations occur at comparable rates.

Table 4.3. R_f values[a] of mono-, di-, and tri-acetylated NEA by the AAC(2')-Ic, AAC(3)-IV, AAC(6'), and Eis proteins.

		Enzymes utilized										
								Eis				
AG		None	(2')[f]	(3)[g]	(6')[h]	(3) then (2')	(6') then (2')	(6') then (3)	5 min	10 min	30 min	2 h	O/N
NEA	Parent	0.11							0.11	0.11			
	Mono		0.14	0.18	0.22				0.14	0.14	0.14	0.14	
	Di					0.35	0.27	0.37	0.27	0.27	0.27	0.27	
	Tri[e]											0.39	0.39

[a]The eluent system used for TLCs was 3:0.8/MeOH:NH_4OH. [b]Parent indicates non-acylated. [c]Mono indicates mono-acetylation. [d]Di indicates di-acetylation. [e]Tri indicates tri-acetylation. [f](2') indicates AAC(2')-Ic. [g](3) indicates AAC(3)-IV. [h](6') indicates AAC(6') of the AAC(6')/APH(2").

Because a purified AAC(1) enzyme was not available, and because no tri-acetylation of NEA was observed by action of AAC(2')-Ic, AAC(3)-IV, and AAC(6') in any order, we could not obtain standards of tri-acetylated NEA. Thus, we scaled-up the enzymatic tri-acetylation reaction of NEA to unambiguously establish the specific positions on the NEA scaffold acetylated by Eis. The structure was determined from 1-D and 2-D ^1H and ^{13}C NMR spectra of the tri-acetylated NEA purified by flash chromatography. Corresponding spectra of the non-acetylated NEA were used for comparison. This analysis confirmed acetylation of NEA at the 1-, 2'-, and 6'-positions by Eis (Figs. 4.5-4.9 and Tables 4.4 and 4.5).

Table 4.4. Proton chemical shifts determined for NEA and 1,2',6'-tri-acetyl-NEA.[a]

Ring	H position	NEA[d]	1,2',6'-tri-acetyl-NEA	Δppm
II	1	3.41-3.36 (m)[b] [3.38][c]	3.89-3.74 (m) [3.84]	**0.46**
	2_{ax}	2.04 (ddd (app. q), $J_{2ax,2eq} = J_{2ax,1} = J_{2ax,3}$ = 12.6 Hz)	1.68 (ddd (app. q), $J_{2ax,2eq} = J_{2ax,1} = J_{2ax,3}$ = 12.8 Hz)	-0.36
	2_{eq}	2.55 (ddd (app. dt), $J_{2eq,2ax}$ = 12.6 Hz, $J_{2eq,1} = J_{2eq,3}$ = 4.1 Hz)	2.32 (ddd (app. dt), $J_{2eq,2ax}$ = 12.8 Hz, $J_{2eq,1} = J_{2eq,3}$ = 4.2 Hz)	-0.23
	3	3.59 (ddd, $J_{3,2ax}$ = 12.6 Hz, $J_{3,4}$ = 10.3 Hz, $J_{3,2eq}$ = 4.1 Hz)	3.51-3.43 (m) [3.50]	-0.09
	4	4.10-4.04 (m) [4.10]	3.89-3.74 (m) [3.73]	-0.37
	5	3.75 (t, J = 9.1 Hz)	3.69-3.64 (m) [3.66]	-0.09
	6	3.66 (t, J = 9.9 Hz)	3.51-3.43 (m) [3.47]	-0.19
I	1'	6.04 (d, $J_{1',2'}$ = 3.9 Hz)	5.48 (d, $J_{1',2'}$ = 3.9 Hz)	-0.56
	2'	3.51-3.48 (m) [3.49]	4.01 (dd, $J_{2',3'}$ = 10.8 Hz, $J_{2',1'}$ = 3.9 Hz)	**0.52**
	3'	4.10-4.04 (m) [4.07]	3.89-3.74 (m) [3.80]	-0.27
	4'	3.51-3.48 (m) [3.50]	3.51-3.43 (m) [3.44]	-0.06
	5'	4.10-4.04 (m) [4.05]	3.89-3.74 (m) [3.82]	-0.23
	$6'_a$	3.27 (dd, $J_{6'a,6'b}$ = 13.5 Hz, $J_{6'a,5'}$ = 8.0 Hz)	3.55 (dd, $J_{6'a,6'b}$ = 14.6 Hz, $J_{6'a,5'}$ = 3.4 Hz)	**0.28**
	$6'_b$	3.54 (dd, $J_{6'b,6'a}$ = 13.5 Hz, $J_{6'b,5'}$ = 3.2 Hz)	3.69-3.64 (m) [3.65]	**0.11**
Acetyl	NH-1	×	8.20 (d, $J_{NH,1}$ = 3.7 Hz)*	
	NH-2'	×	8.21 (d, $J_{NH,2'}$ = 4.6 Hz)*	
	NH-6'	×	8.12 (t, $J_{NH,6'}$ = 5.8 Hz)*	
	$CH_3C=O$	×	2.08 (s)	
	$CH_3C=O$	×	2.07 (s)	
	$CH_3C=O$	×	2.05 (s)	

[a]The chemical shift were established based on ^1H, 2D-TOCSY and 2D-COSY NMR. [b]Multiplicity and J are given in (). [c]The numbers in [] were determined from 2D-COSY. [d]The chemical shifts reported for NEA are in accordance with those previously reported in the literature.[17,18] *Indicates that the values were determined from spectra taken in 9:1/H_2O:D_2O. × Indicates that acetyl moiety is not present in the molecule.

Table 4.5. Carbon chemical shifts determined for NEA and 1,2',6'-tri-acetyl-NEA.[a]

Ring	C position	NEA[b]	1,2',6'-tri-acetyl-NEA	Δppm
II	1	49.7	48.8	**-0.9**
	2	28.1	30.2	2.1
	3	48.4	49.7	1.3
	4	76.7	79.8	3.1
	5	75.2	75.7	0.5
	6	72.4	74.1	1.7
I	1'	95.3	98.2	2.9
	2'	53.5	53.3	**-0.2**
	3'	68.1	69.9	1.8
	4'	71.0	71.3	0.3
	5'	69.1	70.7	1.6
	6'	40.4	39.5	**-0.9**
Acetyl	$CH_3\underline{C}=O$	×	174.9	
	$CH_3\underline{C}=O$	×	174.5	
	$CH_3\underline{C}=O$	×	174.2	
	$\underline{C}H_3C=O$	×	22.0	
	$\underline{C}H_3C=O$	×	21.9	
	$\underline{C}H_3C=O$	×	21.8	

[a]The chemical shift were established based on ^{13}C, DEPT and HETCOR NMR. [b]The chemical shifts reported for NEA are in accordance with those previously reported in the literature.[17,18] × Indicates that the acetyl moiety is not present in the molecule.

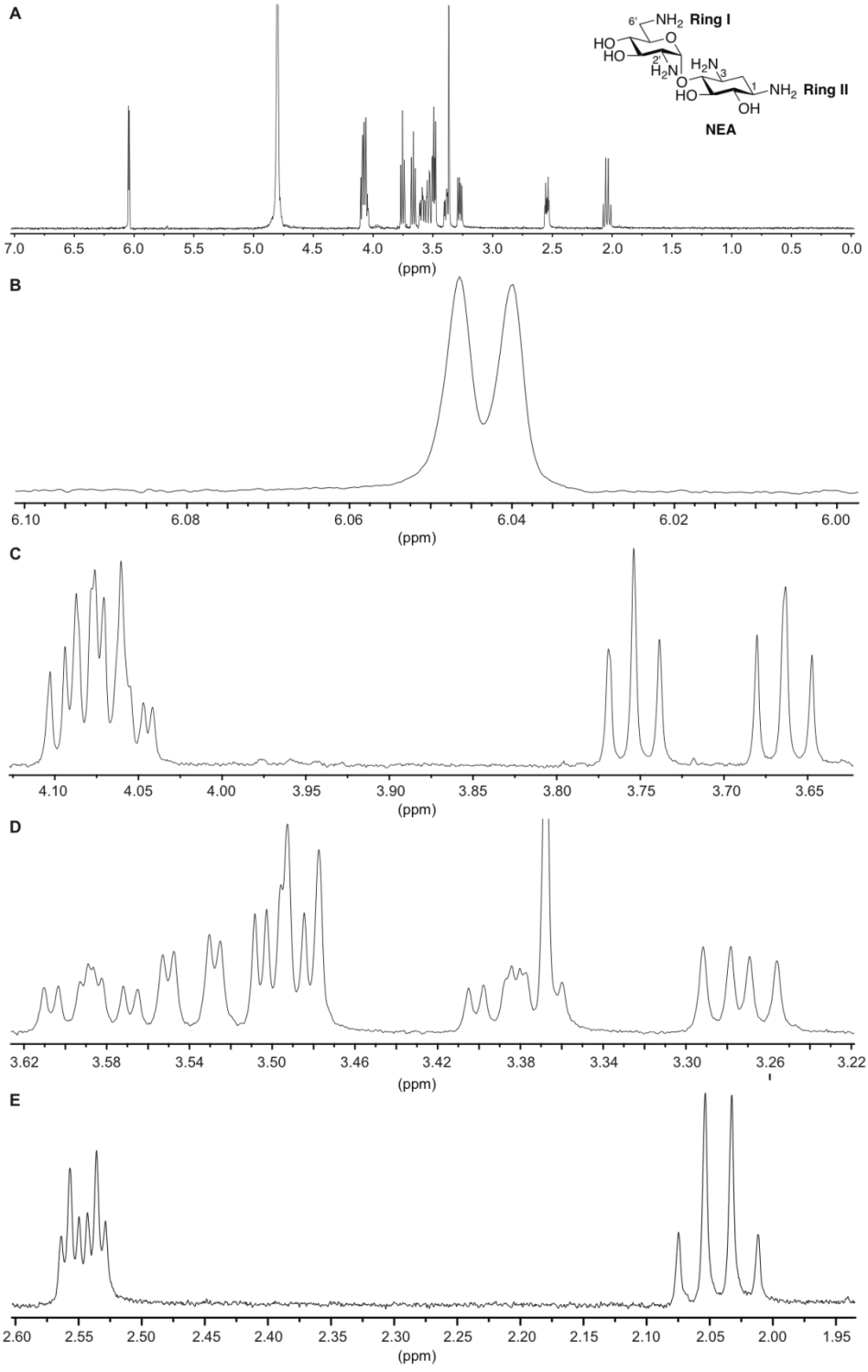

Fig. 4.5. ^{1}H NMR of NEA in D_2O. The full spectrum is shown in panel **A** and the expansions in panels **B-E**.

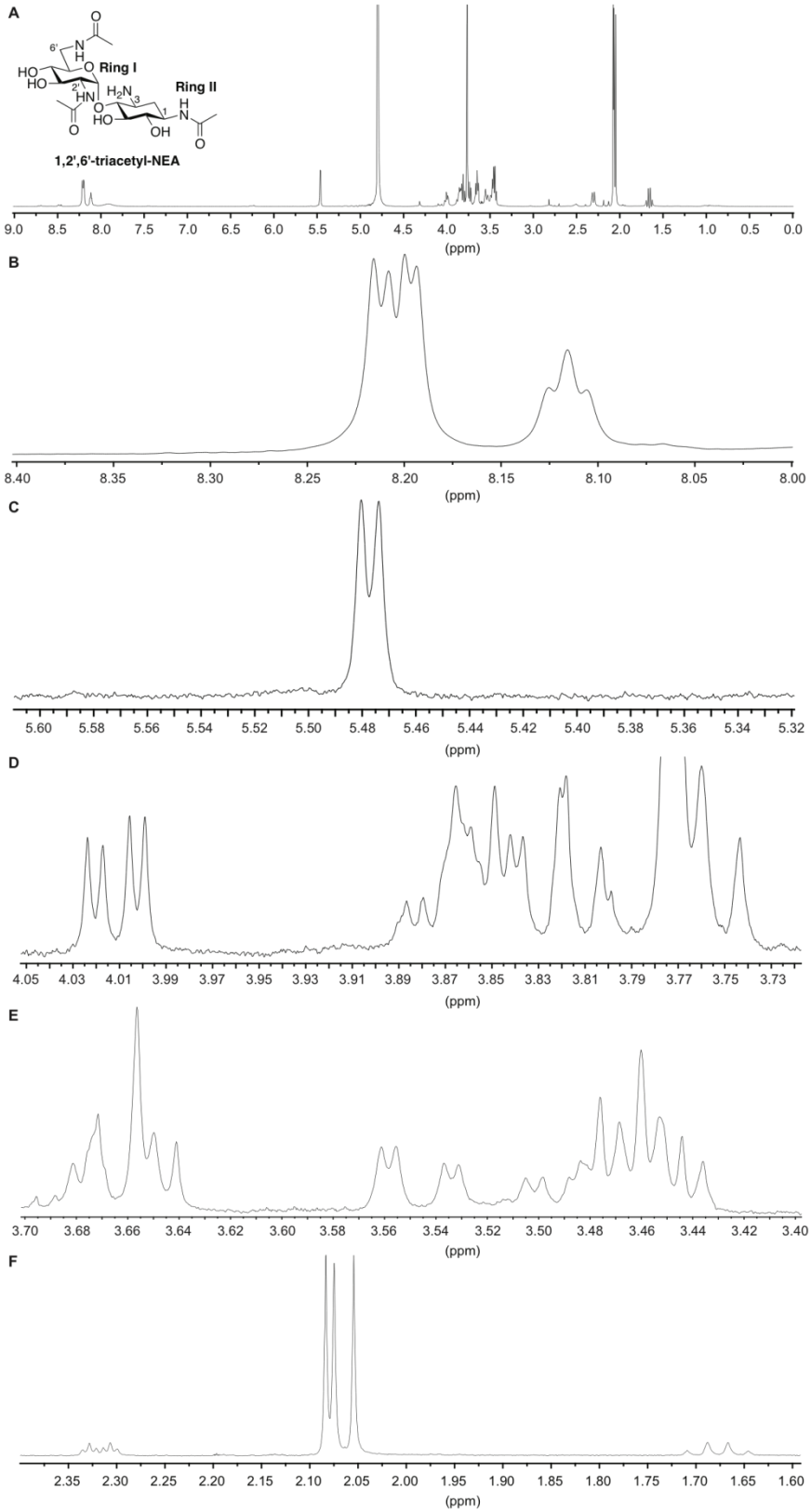

Fig. 4.6. ^{1}H NMR of 1,2',6'-tri-acetyl-NEA in 9:1/H_2O:D_2O (panels **A** and **B** to see the amide Hs) and in D_2O (panels **C-F**). The full spectrum is shown in panel **A** and the expansions in panels **B-F**.

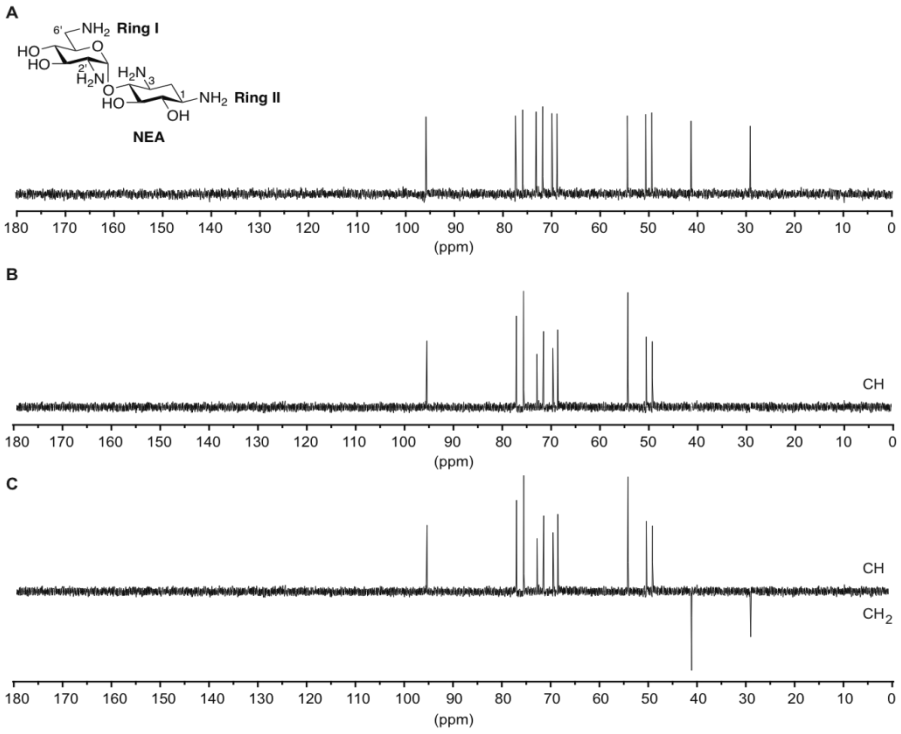

Fig. 4.7. ^{13}C DEPT of NEA in D_2O.

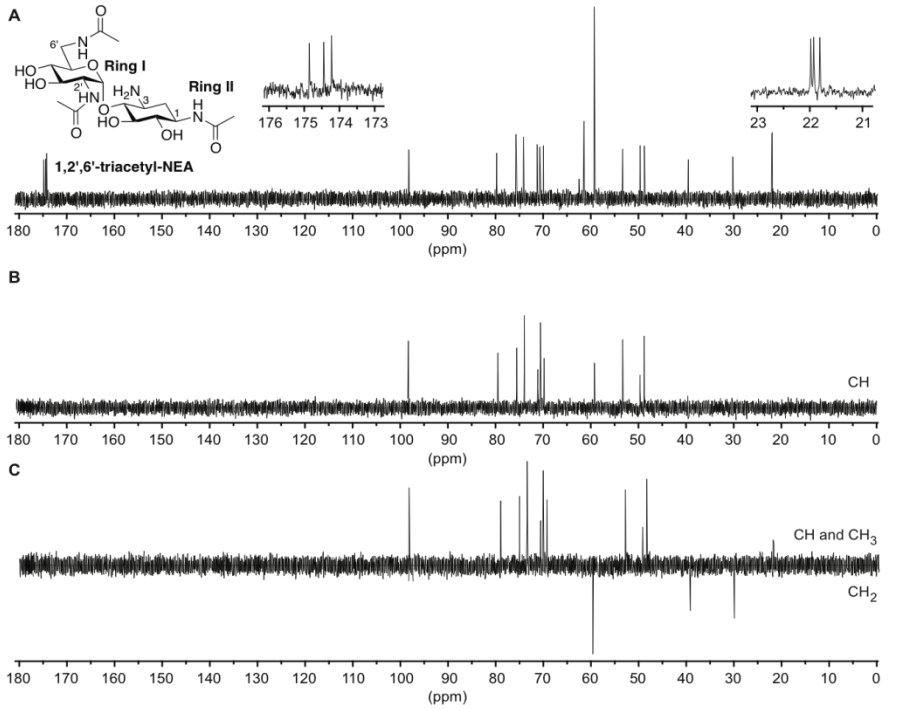

Fig. 4.8. ^{13}C DEPT of 1,2',6'-tri-acetyl-NEA in D_2O.

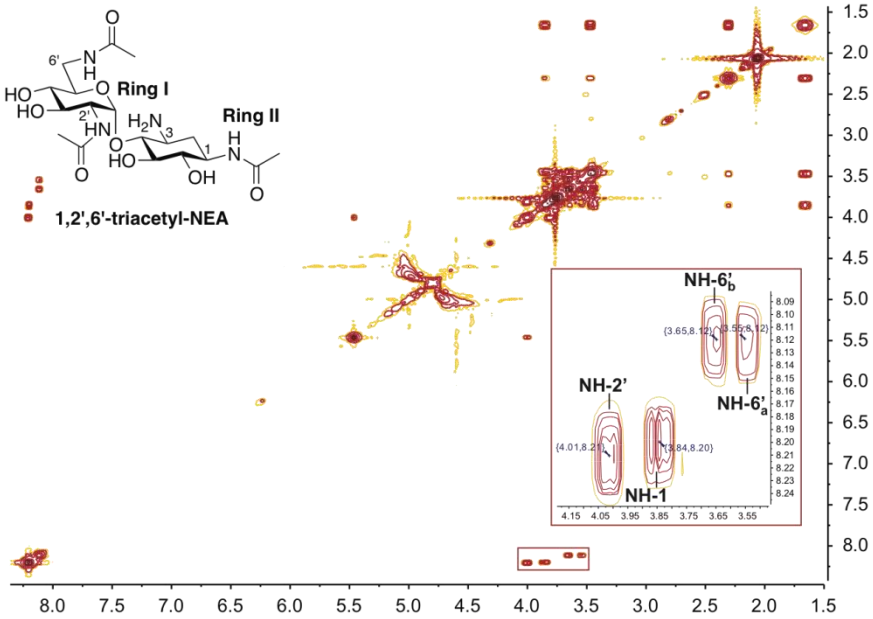

Fig. 4.9. 2D-COSY of 1,2',6'-tri-acetyl-NEA in 9:1/H_2O:D_2O. The insert shows the expansion for the amide protons connected to the protons at positions 1, 2', and 6' (6'$_a$ and 6'$_b$ shown (note: a and b are arbitrarily assigned)).

4.3.3. Crystal structure of Eis

Seeking an understanding of the catalytic mechanism of Eis, we determined a crystal structure of Eis in complex with the reaction products CoA and acetylated HYG, at a resolution of 1.95 Å (Figs. 4.10A-C, 4.11, 4.12 and Table 4.7). Eis forms a tightly packed hexamer, in agreement with its hexameric state in solution (Fig. 4.13). The hexamer resembles a sandwich of two threefold symmetrical trimers (Fig. 4.10A). Overall, 3,800 Å^2 of solvent-accessible surface area of each monomer is buried in the hexameric interface,[19] indicating extensive intimate contacts between the monomers. The Eis monomer consists of three regions that are assembled into a heart-shaped molecule (Fig. 4.10B). This shape is formed by an unusual fusion of two GCN5-related *N*-acetyltransferase (GNAT) regions and a C-terminal region (Fig. 4.11). The GNAT fold is common among *N*-acetyltransferases in all kingdoms of life. A clearly distinguishable CoA and an acetamide moiety of acetylated HYG in the electron density in the N-terminal GNAT region of Eis are positioned analogously to those found in other AACs.[8,20] This observation indicates that this region is involved in catalysis. Despite our efforts of crystallization of Eis with many different AGs under a variety of conditions, we did not observe defined electron density for the rest of the AG molecule, reflecting its

multiple orientations or flexibility when bound in the active site. The central region of Eis, also resembling a GNAT fold, lacks conserved Arg residues that bind CoA phosphates in this superfamily and, therefore, it is unlikely to be catalytically active. The juxtaposition of the N-terminal and the central GNAT regions creates a large and intricate AG binding pocket (Fig. 4.10B,C). The C-terminal region, which consists of a 5-stranded β-sheet flanked by four helices on one side, resembles the fold of the animal sterol carrier protein (SCP).[21,22] However, it lacks the hydrophobic cavity used by SCP to bind lipids. This organization enables the C-terminal peptide of Eis (residues 392-402) to wedge between the two GNAT regions and reach into the active site.

Table 4.6. Primers used for the PCR amplification of the *eis* gene from *Mtb*.

gene (vector)	5' primer	3' primer
eis(NHis) (pET28a)	CCGCGGCATATGCTACAGTCGGATTC	CTAGCAGGATCCTCAGAACTCGAACGCG
eis(CHis) (pET22b)	CCGCGGCATATGCCACAGTCGGATTC	GCACGGAAGCTTGAACTCGAACGCGGTC
eis1-311(NHis) (pET28a)	CCGCGGCATATGCTACAGTCGGATTC	CTCGCCGGATCCTCAAGCGTAACCACGCGCC
eis1-399(NHis) (pET28a)	CCGCGGCATATGCTACAGTCGGATTC	CCTTCAGGATCCTCACGCGGTCTGGACGGG
eis292-402(NHis) (pET28a)	ACCTGGCATATGGACGGCCTGTGGTTGCGC	CTAGCAGGATCCTCAGAACTCGAACGCG
eisF24A(NHis) (pET28a)	GCCGCGGCCAGTgcgACCGATTTCATC	GATGAAATCGGTcgcACTGGCCGCGGC
eisF27A(NHis) (pET28a)	CCAGTTTCACCGATGCGATCGGCCCTG	CAGGGCCGATcgcATCGGTGAAACTGG
eisI28A(NHis) (pET28a)	CACCGATTTCgcgGGCCCTGAATC	GATTCAGGGCCcgcGAAATCGGTG
eisW36A(NHis) (pET28a)	CAGCGACCGCCgcgCGGACCCTGGTGCC	GGCACCAGGGTCCGcgcGGCGGTCGCTG
eisF84A(NHis) (pET28a)	GCCGGTCTCAGTgcgGTCGCGGTGGCG	CGCCACCGCGACcgcACTGAGACCGGC
eisV87A(NHis) (pET28a)	GTTTCGTCGCGgcgGCGCCGACGCATC	GATGCGTCGGCGCcgcCGCGACGAAAC
eisR93A(NHis) (pET28a)	CCGACGCATCGCgcgCGCGGCTTGCTGCGC	GCGCAGCAAGCCGCGcgcGCGATGCGTCGG
eisH119A(NHis) (pET28a)	GTCGCGGCACTGgcgGCTAGCGAGGGCGGC	GCCGCCCTCGCTAGCcgcCAGTGCCGCGAC
eisS121A(NHis) (pET28a)	GCACTGCATGCTgcgGAGGGCGGCATC	GATGCCGCCCTCcgcAGCATGCAGTGC
eisY126A(NHis) (pET28a)	GAGGGCGGCATCgcgGGCCGGTTCGGC	GCCGAACCGGCCcgcGATGCCGCCCTC
eisR128A(NHis) (pET28a)	CGGCATCTACGGCgcgTTCGGCTACGGGC	GCCCGTAGCCGAAcgcGCCGTAGATGCCG
eisR148A(NHis) (pET28a)	CCGACGCTTCGCGgcgTTTCACGCCGACG	CGTCGGCGTGAAAcgcCGCGAAGCGTCGG
eisW197A(NHis) (pET28a)	CCGCAGGTGCTCgcgGACGAGCTGCTG	CAGCAGCTCGTCcgcGAGCACCTGCGG
eisD292A(NHis) (pET28a)	ACCTGGCGCCAGgcgGGCCTGTGGTTG	CAACCACAGGCCcgcCTGGCGCCAGGT
eisY310A(NHis) (pET28a)	GAGGCGCGTGGTgcgGCTCACGAAGTT	AACTTCGTGAGCcgcACCACGCGCCTC

The introduced restriction sites are underlined for each primer. The 5' primers all introduced an *Nde*I restriction site. The 3' primer for *eis*(NHis) (pET28a) and all *eis* mutants introduced a *Bam*HI restriction site, whereas the 3' primer for *eis*(CHis) (pET22b) introduced a *Hind*III restriction site. The mutation site is indicated in lower-case.
The tags added to the Eis proteins are:
NHis (pET28a/*Nde*I) = MGSSHHHHHHSSGLVPRGSHMLQSDS
CHis (pET22b/*Hind*III) = KLAALEHHHHHH

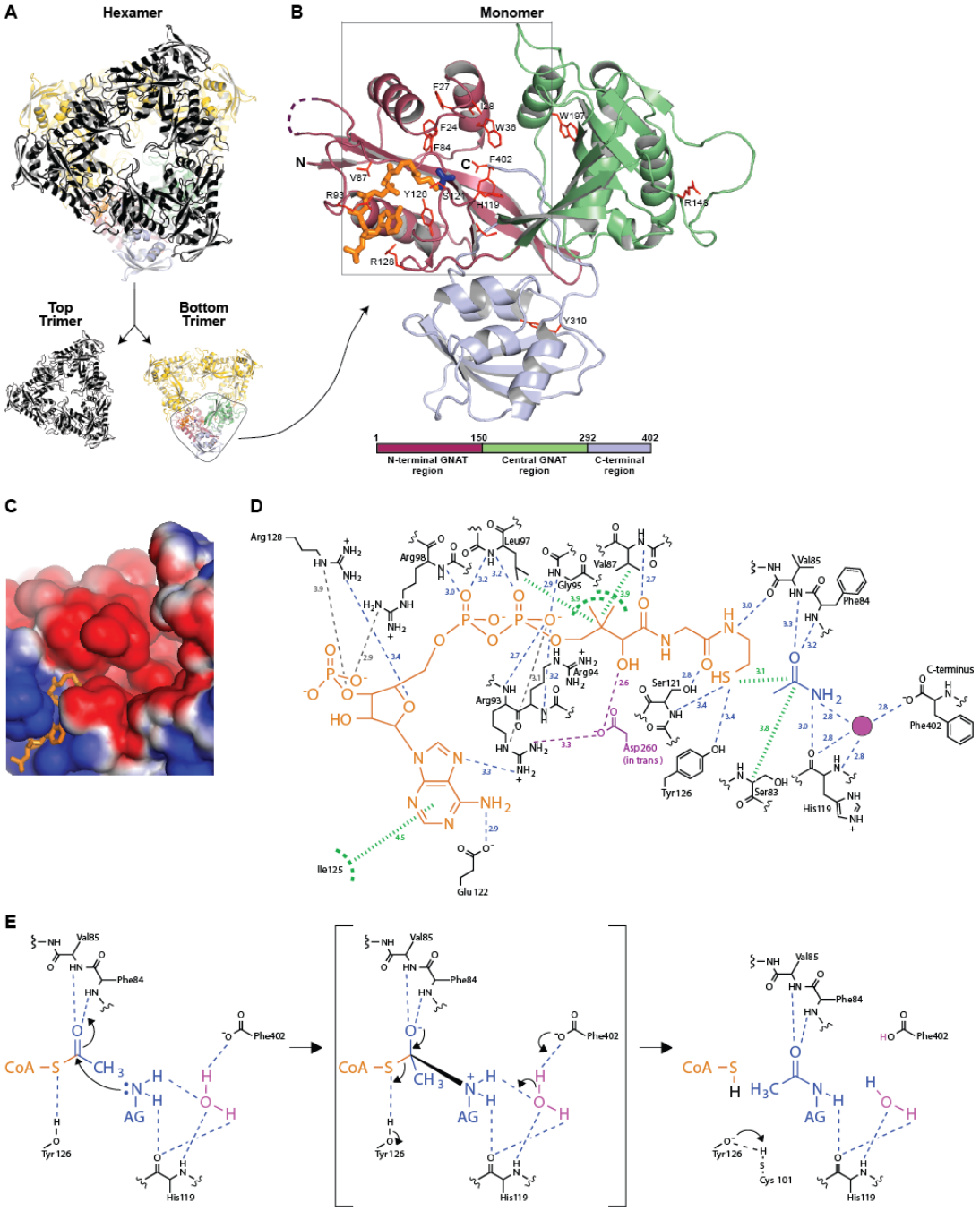

Fig. 4.10. A crystal structure and a proposed mechanism of Eis. **A.** A structure of Eis hexamer composed of two trimeric layers as shown in the bottom of this panel. **B.** The tripartite fold of an Eis monomer bound to CoA (orange sticks) and acetamide (blue sticks). Residues explored in mutagenesis studies are shown as red sticks. **C.** A zoom-in of the Eis active site (as indicated by the rectangle in panel **B**). The electrostatic surface of Eis shows the positive charge (blue), negative charge (red), and hydrophobic patches (white). **D.** Interactions between Eis, CoA, acetamide, and a proposed catalytic water molecule (magenta). Hydrogen bonds, ionic interactions, and hydrophobic contacts are shown by blue, grey, and green dashed lines, respectively. The carboxylate of Asp260 (magenta) from an adjacent monomer in the hexamer makes a hydrogen bond to the Ppant arm of the CoA and forms salt bridges with Arg93 and Arg94 (*in trans*) thereby positioning these Arg residues for binding CoA. **E.** A proposed mechanism of Eis acetylation.

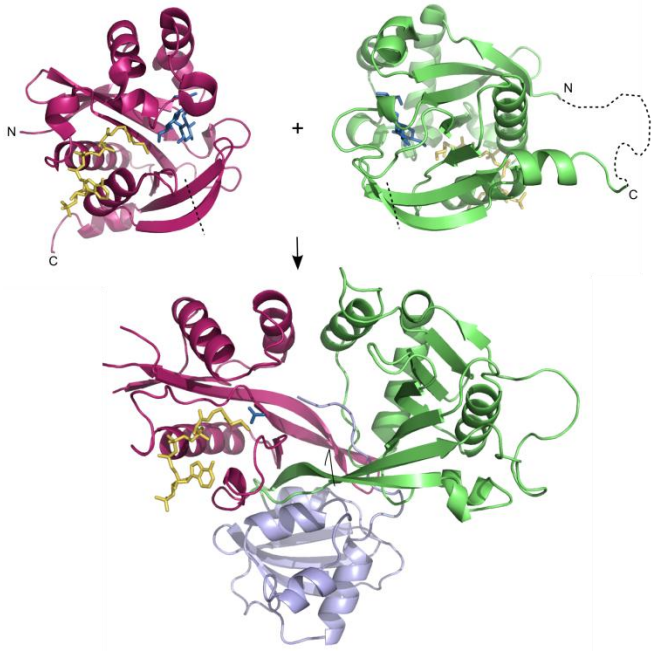

Fig. 4.11. Topology of the assembly of the N-terminal (magenta, bottom panel) and the central (green, bottom panel) GNAT regions of Eis. The N-terminal and the central regions have a GCN5-type fold. The structure of AAC(6')-Ib (PDB code: 2BUE)[23] that has a similar fold is shown in top left and right panels, each oriented and colored to match the respective regions of Eis below. The Eis fold topology can be obtained by breaking the two strands of the β-sheet in the two top structures and adjoining them as well as connecting the N- and the C-terminus of the top right fold (a cyclic permutation of a GNAT fold), as shown by the dashed lines. Therefore, Eis was likely a result of gene duplication and fusion events in which one of the two GNAT folds was cyclically permuted.

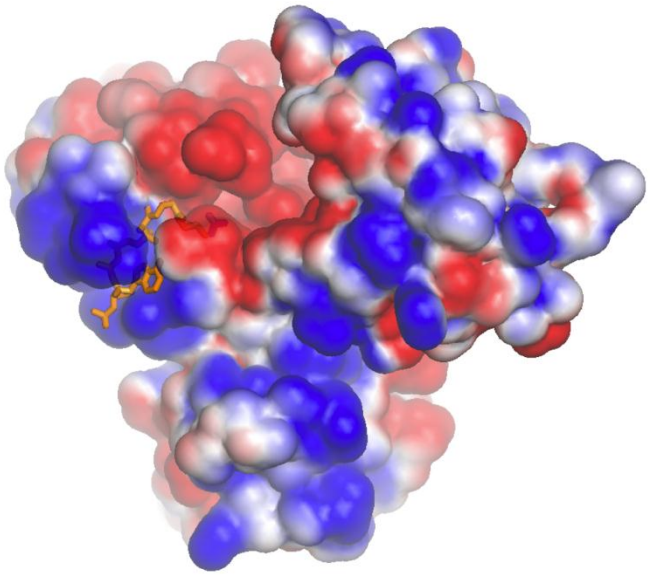

Fig. 4.12. The surface representation of the Eis monomer colored according to its electrostatic potential, positive in blue, negative in red, and hydrophobic in white.

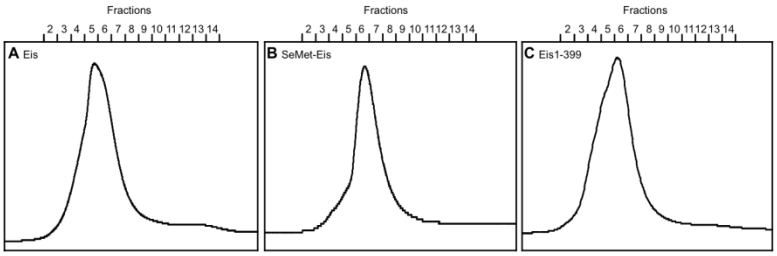

Fig. 4.13. Size-exclusion chromatogram of **A.** Eis, **B.** SeMet-Eis, and **C.** Eis1-399. Panel **C** shows that the C-terminal portion of the Eis tail (amino acid residues 400-402) is not required for hexamerization of Eis.

Table 4.7. Crystallographic data collection and structure refinement statistics of Eis.

Data collection:	***Native Eis in complex with CoA and acetylated HYG***	***SeMet-Eis in complex with CoA, Se peak, wavelength = 0.9794 Å***
Space group	H32	$P4_122$
Monomer per asymmetric unit	1	3
Unit cell dimensions		
a, b, c (Å)	174.9, 174.9, 124.7	109, 109, 142
α, β, γ (°)	90, 90, 120	90, 90, 90
Resolution (Å)	50.00-1.95 (1.98-1.95)[a]	50-2.7 (2.75-2.70)[a]
I/σ	19.8 (2.0)	28.4 (5.1)
Completeness (%)	96.8 (79.2)	99 (100)
Redundancy	5.4 (3.9)	12.4 (12.1)
R_{merge}	0.09 (0.47)	0.12 (0.73)
Number of unique reflections	100,857	59,864
Refinement:		
Resolution (Å)	40.00-1.95 (2.00-1.95)[a]	
R (%)	19.6 (24.8)	
R_{free} (%)	22.4 (34.2)	
Bond length deviation (rmsd) from ideal (Å)	0.013	
Bond angle deviation (rmsd) from ideal (°)	1.54	
Ramachandran plot statistics		
Residues in most favored and additional allowed regions (%)	100	
Residues in generously allowed regions (%)	0	
Residues in disallowed regions	0	

[a]Numbers in parentheses indicate the values in the highest resolution shell.

4.3.4. Mechanism of acetylation by Eis

The bound CoA and the acetamide reveal a network of ionic, hydrophobic, and hydrogen bonding interactions that stabilize the cosubstrate in the Eis active site pocket, and indicate a likely acetylation mechanism (Fig. 4.10D). This mechanism is very similar to that proposed for 2'-*N*-acetylation by AAC(2')-Ic.[8] The AG amino group to be acetylated is ideally positioned by the His119 backbone for a direct nucleophilic attack on the CoA thioester. The tetrahedral transition state is stabilized by polarization of the thioester carbonyl through hydrogen bonding to Phe84 and Val85. As proposed for the *N*-myristoylation mechanism by Nmt1p,[24] the C-terminal carboxylate of Phe402 interacts with the amino group through a bridging water molecule and likely serves as a remote

base. We propose that the universally conserved Tyr126 at a distance of 3.4 Å from the sulfhydryl group of CoA (3.6 Å in the case of the 2'-*N*-acetylation) likely serves as a general acid to protonate the CoA thiolate.

To probe this mechanism in solution, we first investigated the importance of the proposed catalytic residues Phe402 and Tyr126 (Figs. 4.1, 4.14, 4.15 and Table 4.2). Either the addition of a $CHis_6$ tag or the removal of the three C-terminal amino acid residues (Eis1-399) nearly abolished the acetylation activity of Eis on all AGs tested. These observations confirmed the important role of the C-terminal tail and the Phe402 residue in catalysis. A deletion mutant lacking the C-terminal region (Eis1-311) and the C-terminal region alone (Eis292-402) were also inactive, as expected. The presence of the central GNAT region of Eis indicated a formal possibility that Eis contained a second active site in this region, even though AcCoA coordinating residues were not present. The mutant of the proposed catalytic acid Tyr126Ala completely abolished the acetylation activity on all substrates tested, which agreed with its proposed role in the mechanism and ruled out the possibility of the existence of another active site. We next probed the importance of His119 involved in coordination of the proposed catalytic water molecule (Fig. 4.10E). Mutation of this residue to an Ala resulted in a decrease in activity and a change in the number of acetylated sites (mono- vs. di- vs. tri-) of all AGs tested, thereby confirming its key role in Eis action. Complete inactivity of the Tyr310Ala mutant of the hydrophobic core of Eis indicated that structural stability is crucial for catalytic activity of the enzyme. Similarly, mutating either Trp197 in the hydrophobic core or Asp292 partially buried in the interface of the two GNAT folds to an Ala, almost completely eradicated Eis activity. As another control, we generated an Ala mutant of the surface-exposed Arg148 located far away from any important surface or interface. As expected, we found that this mutation had no significant effect on the Eis activity.

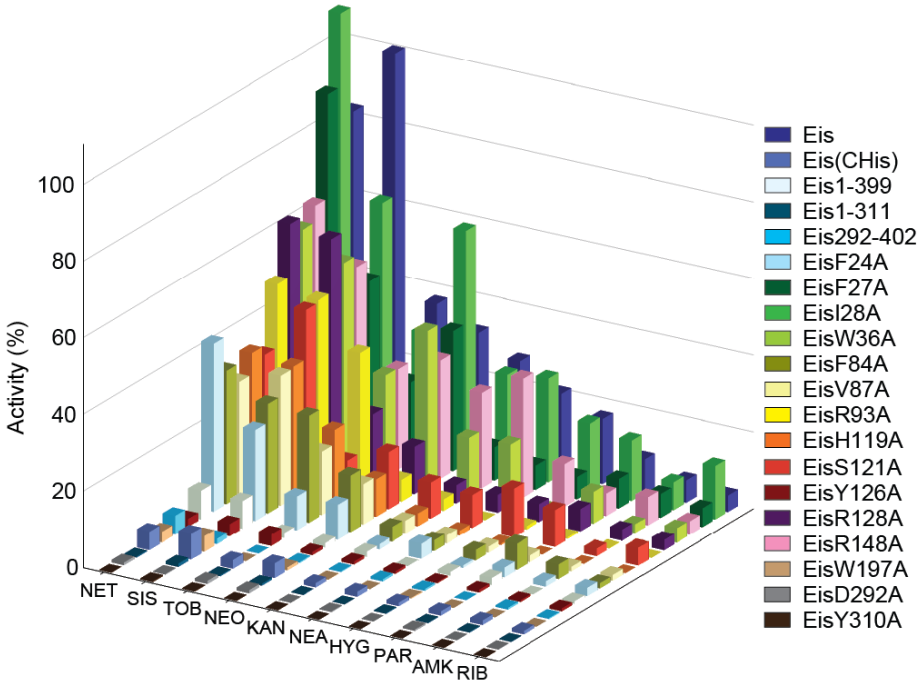

Fig. 4.14. Relative activity of Eis and its mutants towards the ten tested AGs. All activities are normalized against the acetylation of NET by wild-type Eis.

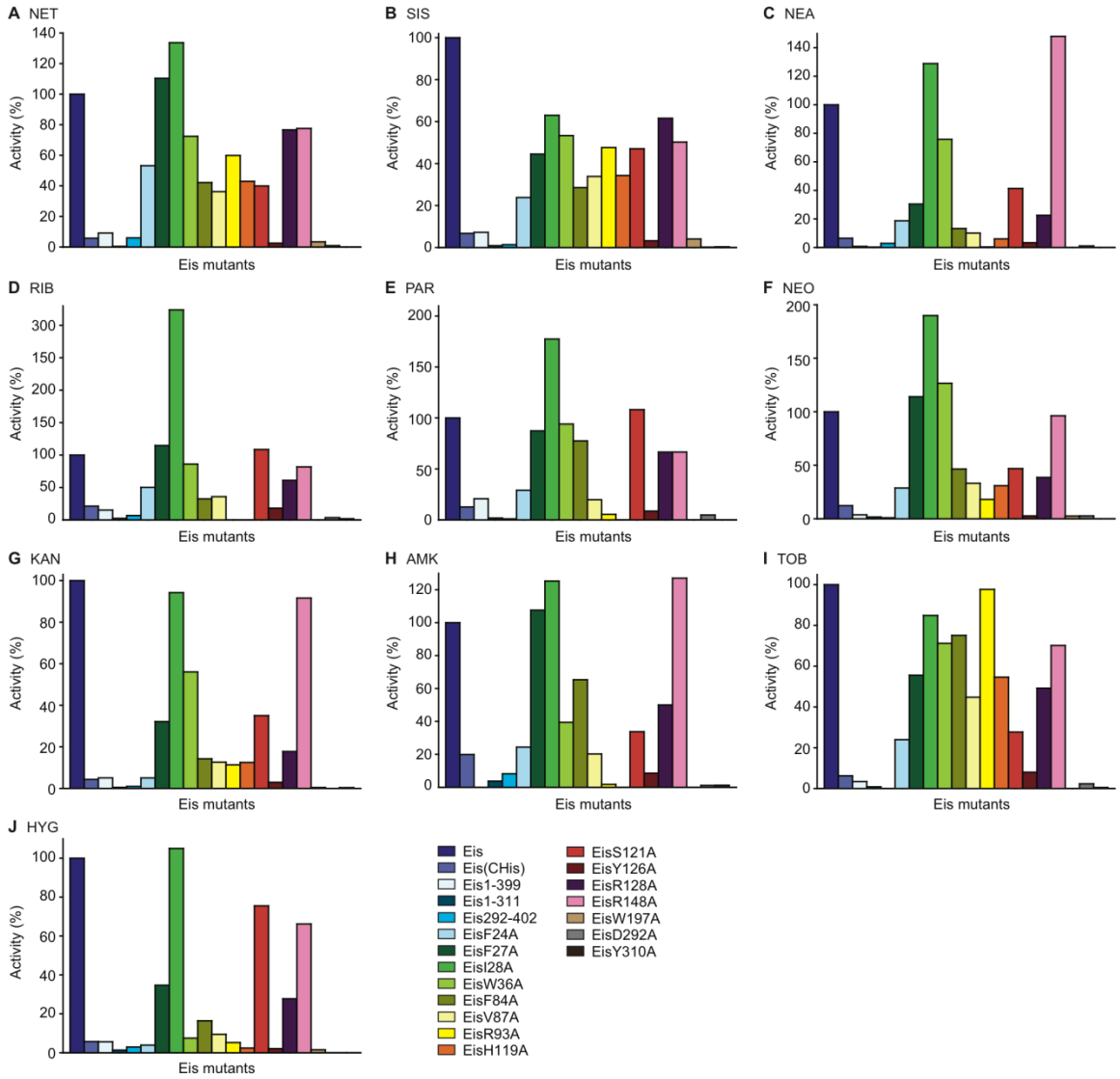

Fig. 4.15. Relative activity towards the ten AGs tested for all Eis proteins and mutants studied. All activities are calculated relative to the activity of the wild-type Eis with the respective AGs.

A close examination of the AG binding pocket reveals that it is formed by the adjoining surfaces of the two GNAT folds (Fig. 4.10C). This deep and bifurcated AG binding pocket must allow for AGs of different sizes and structures to be accommodated. The surface of the binding pocket and its entrances are highly negatively charged with occasional hydrophobic patches, which must ensure electrostatic attraction to amine-rich substrates. The residues that line the binding pocket are marked in Fig. 4.1.

We next inspected the effects of residues lining the AG and AcCoA binding surfaces on the Eis activity by point mutagenesis (Figs. 4.14, 4.15 and Table 4.2). Interestingly,

although the Phe24Ala mutant drastically decreased acetylation activity, mutations of the neighboring Phe27, Ile28, and Trp36 to Ala did not affect the efficiency of the acetylation reactions, but instead resulted in a change in the number of acetylated sites of many of the AGs tested. These observations are in agreement with the proposed role of these residues in AG binding. In addition, we confirmed that Val87, Arg93, Ser121, and Arg128 all play an important role in AcCoA binding as their mutations to Ala led to a general decrease in catalytic activity of Eis. Finally, the Ala mutation of Phe84 whose backbone amide is proposed to stabilize the oxyanion of the acetyl group of AcCoA and whose side chain is buried in the hydrophobic core, resulted in both a large catalytic deficiency and a change in the number of acetylated sites of most AGs studied.

The biological function of Eis in *Mtb* has been the subject of recent interest.[6,7,25-32] The biochemical and structural studies described in this report provide clear evidence for an unprecedented multi-acetylation capability of Eis that inactivates AG antibiotics. Eis homologs are found in a variety of pathogens that have developed resistance to AGs. Up-regulation of *eis* genes in these bacteria may confer resistance to AGs, as observed in *Mtb*, although such studies have not yet been reported. The unique and efficient strategy of deactivation of AGs by multi-acetylation presented herein may be a general, widespread resistance mechanism, and yet another evolutionary hurdle to overcome.

4.4. Materials and methods

4.4.1. Bacterial strains, plasmids, materials, and instrumentations

Restriction endonucleases, T4 DNA ligase, and Phusion DNA polymerase were bought from NEB (Ipswich, MA). DNA primers for PCR were ordered from Integrated DNA Technologies (IDT; Coralville, IA). The pET28a and pET22b vectors were purchased from Novagen (Gibbstown, NJ). The chemically competent bacterial strains *E. coli* TOP10 and BL21 (DE3) were bought from Invitrogen (Carlsbad, CA). The *Mtb* H37Rv genomic DNA was obtained from the Biodefense & Emerging Infections Research Resources Repository (BEI resources, Manassas, VA). DNA sequencing was performed at the University of Michigan DNA Sequencing Core. FPLC was done as the last protein purification step on a Bio-Rad BioLogic DuoFlow (Bio-Rad, Hercules, CA) using a

HighPrep^{TM} 26/60 Sephacryl^{TM} S-200 High Resolution Column (GE Healthcare, Piscataway, NJ). DTDP, AcCoA, and AGs (APR, AMK, HYG, KAN, NEO, SIS, SPT, STR, and RIB) were purchased from Sigma-Aldrich (Milwaukee, WI). NEA, NET, PAR, and TOB were bought from AK Scientific (Mountain View, CA) (Fig. 4.2). Determination of substrate specificity by UV-Vis assays was done on a multimode SpectraMax M5 plate reader using 96-well plates (Fisher Scientific). TLCs (Merck, Silica gel 60 F_{254}) were visualized using a cerium-molybdate stain (5 g CAN, 120 g ammonium molybdate, 80 mL H_2SO_4, 720 mL H_2O). 1,2',6'-tri-acetyl-NEA was purified by SiO_2 flash chromatography (Dynamic Absorbents 32-63). ^{13}C NMR, DEPT, and HETCOR spectra were recorded on a Bruker Avance^{TM} 500 MHz spectrometer. ^{1}H NMR, 2D-COSY, and 2D-TOCSY spectra were recorded on a Bruker Avance III^{TM} 600 MHz spectrometer. All NMR spectra were recorded in D_2O as well as in 9:1/H_2O:D_2O (in order to identify the amide connectivity). LCMS was performed on a Shimadzu LCMS-2019EV equipped with a SPD-20AV UV-Vis detector and a LC-20AD liquid chromatograph. All buffer pH were adjusted at rt.

4.4.2. Cloning, overexpression, and purification of Eis proteins

4.4.2.1. Preparation of pEis-pET28a(NHis), pEis-pET22b(CHis), Eis single point mutant(NHis), and Eis deletion mutant(NHis) overexpression constructs

The primers used for the amplification of *eis* and mutant *eis* genes (gene locus Rv2416c) are listed in Table 4.6. PCRs were performed using *Mtb* H37Rv genomic DNA and Phusion DNA polymerase (NEB, Ipswich, MA) according to the instructions provided by NEB. For the construction of the pEis-pET28a(NHis), pEis1-311-pET28a(NHis), pEis1-399-pET28a(NHis), pEis292-402-pET28a(NHis), and pEis-pET22b(CHis), the amplified *eis* genes were inserted into the linearized pET28a and pET22b vectors via the corresponding *Nde*I/*Bam*HI and *Nde*I/*Hind*III restriction sites, respectively. The single point Eis mutants were constructed using the SOE method.[33] In the first round of PCR, the sequence downstream and upstream of the mutation were separately amplified using the pEis-pET28a(NHis) plasmid as a template in conjunction with the 5' primer of the *mutant* with the 3' primer for *eis(NHis)* and the 5' primer for *eis(NHis)* with the 3' primer for the *mutant*, respectively (Table 4.6). The resulting amplified PCR fragments were gel-

purified and subjected to a second round of PCR using the forward and reverse primers for *eis(NHis)* (Table 4.6). The newly amplified fragments were then digested with *Nde*I and *Bam*HI and subcloned into the linearized pET28a vector via the corresponding *Nde*I/*Bam*HI restriction sites to give the single mutants F24A, F27A, I28A, W36A, F84A, V87A, R93A, H119A, S121A, Y126A, R128A, R148A, W197A, D292A, and Y310A. The plasmids encoding the above proteins were transformed into *E. coli* TOP10 chemically competent cells. The sequences of all expression clones were confirmed at the University of Michigan DNA Sequencing Core.

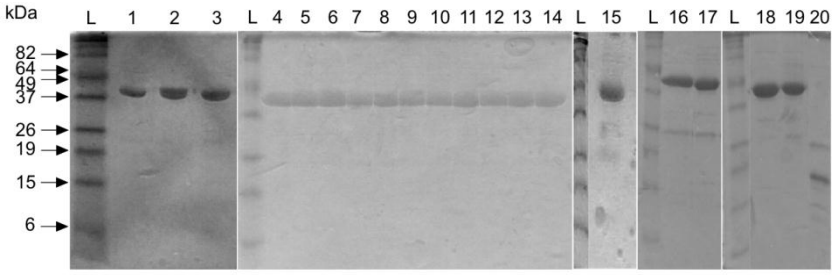

Fig. 4.16. Coomasie blue-stained 15% Tris-HCl SDS-PAGE gel showing the purified Eis proteins: wild-type (46597 Da, lane 1), SeMet (47019 Da, lane2), 1-399 (46173 Da, lane 3), Y310A (46505 Da, lane 4), F84A (46521 Da, lane 5), F24A (46521 Da, lane 6), W36A (46482 Da, lane 7), H119A (46530 Da, lane 8), R128A (46512 Da, lane 9), R93A (46512 Da, lane 10), R148A (46512 Da, lane 11), V87A (46569 Da, lane 12), I28A (46555 Da, lane 13), F27A (46521 Da, lane 14), wild-type (CHis) (45483 Da, lane 15), W197A (46405 Da, lane 16), D292A (46553 Da, lane 17), S121A (46581 Da, lane 18), Y126A (46505 Da, lane 19), and 292-402 (14317 Da, lane 20). L indicates the BenchMark^{TM} pre-stained protein ladder from Invitrogen. 6 μg of each protein were loaded on the gel after boiling the protein samples in loading dye for 5 min.

4.4.2.2. Overproduction and purification of Eis proteins and mutants

All overexpression constructs were transformed into *E. coli* BL21 (DE3) chemically competent cells prior to expression and stored as frozen LB/glycerol stocks at -80 ℃. 1 L of LB medium supplemented with appropriate antibiotics (KAN (50 μg/mL) for the pET28a constructs or ampicillin (100 μg/mL) for the pET22b construct) was inoculated with 10 mL of overnight cultures of each transformant and grown at (37 ℃, 200 rpm) to attenuance of ~0.6 at 600 nm before induction with IPTG (final concentration of 500 μM). The induced cultures were grown for an additional 6 h (28 ℃ (all full length Eis and deletion mutants, and F24A, F84A, Y126A, W197A, D292A), 200 rpm) or overnight (15 ℃ (S121A) or 20 ℃ (F27A, I28A, W36A, V87A, R93A, H119A, R128A, R148A, and Y310A), 200 rpm) after which the cells were harvested by centrifugation (6,000 rpm, 10

min, 4 ℃, Beckman Coulter Aventi JE centrifuge, F10 rotor). The cell pellets were resuspended in lysis buffer (300 mM NaCl, 50 mM Na_2HPO_4 pH 8.0, 10% glycerol) and lysed (1 pass at 10,000-15,000 psi through an Avestin EmulsiFlex-C3 high-pressure homogenizer). The insoluble cell debris were removed by centrifugation (16,000 rpm, 45 min, 4 ℃, Beckman Beckman Coulter Aventi JE centrifuge, JA-17 rotor). Imidazole (final concentration of 2 mM) was added to the clear supernatant and incubated with 2 mL of Ni-NTA agarose resin (Qiagen) (for 2 h with gentle rocking at 4 ℃). The resin was loaded onto a column and washed with 10 mL of lysis buffer containing 5 mM imidazole. The protein was then eluted with lysis buffer in a stepwise imidazole gradient (10 mL fraction of 20 mM (1x), 5 mL fractions of 20 mM (2x), 40 mM (3x), and 250 mM imidazole (3x)). The eluted fractions containing more than 95% pure desired proteins, as determined by SDS-PAGE, were pooled, dialyzed extensively against 50 mM Tris-HCl pH 8.0 at 4 ℃, and concentrated using Amicon® Ultra PL-10 (10,000 MWCO). For structural studies, the proteins were further purified by S-200 size exclusion chromatography in the gel filtration buffer (50 mM Tris-HCl, pH 8.0, flow rate: 1.5 mL/min). Protein concentrations were determined using a Nanodrop spectrometer (Thermo Scientific). Protein yields (in mg/L of culture) were 0.94 (Eis(NHis)), 0.50 (Eis(CHis)), 0.17 (1-311), 0.50 (1-399), 0.21 (292-402), 0.87 (F24A), 0.58 (F27A), 0.66 (I28A), 0.31 (W36A), 0.22 (F84A), 0.31 (V87A), 0.38 (R93A), 0.52 (H119A), 0.45 (S121A), 1.28 (Y126A), 0.52 (R128A), 0.48 (R148A), 0.12 (W197A), 0.28 (D292A), and 0.07 (Y310A) (Fig. 4.16). All proteins were stored at 4 ℃ and found to be stable under these storage conditions for at least 2 months.

4.4.2.3. Expression and purification of SeMet-Eis

Ten colonies of the fresh transformant harboring the pEis-pET28a(NHis) construct were inoculated into 6 mL of LB medium supplemented with KAN (50 μg/mL). The culture was grown at 37 ℃ to an attenuance of 0.34 at 600 nm. This LB culture (100 μL) was then used to inoculate 20 mL of minimal media (MM) (1× M9 salts, 0.4% glucose (10% stock), 1 μg/mL thiamine (10 mg/mL stock), 0.1 mM $CaCl_2$ (500 mM stock), and 2 mM $MgSO_4$ (1 M stock), supplemented with KAN (50 μg/mL)). The culture was grown (200 rpm, 37 ℃) to an attenuance of 0.3 at 600 nm. This 20 mL culture was then used to

inoculate 200 mL of MM, and the cells were grown (200 rpm, 37 ℃) to attenuance of 0.3 at 600 nm. Subsequently, this 200 mL culture was utilized to inoculate 1 L of MM, and the culture was grown (200 rpm, 37 ℃) to an attenuance of 0.4 at 600 nm. At this moment, L-leucine (50 mg/L), L-isoleucine (50 mg/L), L-valine (50 mg/L), L-lysine (100 mg/L), L-threonine (100 mg/L), L-phenylalanine (100 mg/L), and L-SeMet (75 mg/L) were added. All amino acids were prepared by dissolving into 5 mL of distilled H_2O, except for L-phenylalanine, for which 5 μL of 10 M NaOH was added to the solution. The 1 L culture was incubated (200 rpm, 37 ℃) for an additional 33 min before induction with IPTG (final concentration, 500 μM). The induced culture was grown (200 rpm, 28 ℃) for an additional 8 h. The cells were harvested by centrifugation (6,000 rpm, 10 min, 4 ℃). The cell lysis and Ni^{2+}-chelating chromatography steps were carried out as described above. β-mercaptoethanol (0.7 μL) was added to each fraction (5 mL) to prevent oxidation of the SeMet protein. Fractions containing the desired protein (as determined by SDS-PAGE) were combined and further purified by FPLC (1.5 mL/min using 50 mM Tris-HCl, pH 8.0, 2 mM β-mercaptoethanol) (Fig. 4.13). The pure protein was concentrated using Amicon® Ultra PL-10 (10,000 MWCO). Protein concentration was determined using a Nanodrop spectrometer (Thermo Scientific). SeMet-Eis used for crystallization was concentrated to 4.74 mg/mL and stored at 4 ℃. The yield of SeMet-Eis was 0.53 mg/L of culture.

4.4.3. Biochemical characterization of Eis proteins and mutants

4.4.3.1. Determination of AG profile for all Eis proteins and mutants by UV-Vis assay

The acetyltransferase activity of Eis proteins was monitored by a UV-Vis assay in which the free thiol group of CoA, generated by enzyme catalyzed reaction, is coupled to DTDP to produce thiopyridone, which can be monitored by increase in absorbance at 324 nm (ε_{324} = 19 800 $M^{-1}cm^{-1}$).[9] The reaction mixtures (100 μL) containing AcCoA (0.5 mM, 5 eq), AG (0.1 mM, 1 eq), DTDP (2 mM), and Tris-HCl pH 8.0 (50 mM), were initiated by adding protein (0.5 μM) at 25 ℃. Reactions were monitored by taking readings every 30 s for 15 min in 96-well plate format. Using this assay, APR, SPT, and STR were found to not be substrates of Eis(NHis), whereas AMK, HYG, KAN, NEA, NEO, NET, PAR, RIB,

SIS, and TOB were found to be substrates of this enzyme. Therefore, only the last ten AGs were tested with Eis(CHis) and Eis deletion and single point mutants (Figs. 4.14 and 4.15).

4.4.3.2. Determination of number of sites acetylated on each AG by all Eis proteins and mutants by UV-Vis assay and LCMS

As described above, reaction mixtures (100 μL) containing AG (0.1 mM), DTDP (2 mM), Tris-HCl (50 mM, pH 8.0), and AcCoA (0.1 mM, 1 eq or 0.5 mM, 5 eq), were initiated by adding protein (0.5 μM) at 25 ℃. Reactions were monitored at 324 nm by taking readings every 30 s until reaching plateau (Fig. 4.3). To confirm the established number of acetylation sites for each AG substrate by each Eis proteins/mutants, reactions (30 μL) containing AG (0.67 mM, 1 eq), AcCoA (6.7 mM, 10 eq), Tris-HCl (50 mM, pH 8.0), and Eis proteins/mutants (10 μM) were performed overnight at 25 ℃. Ice-cold MeOH (30 μL) was added to the reaction mixture, which was then kept at -20 ℃ for at least 20 min. The precipitated protein was removed by centrifugation (13,000 rpm, rt, 10 min). The masses of the novel acetylated AGs present in each sample were determined by LCMS in positive mode using H_2O (0.1% formic acid) after dilution of the supernatant (10 μL) with H_2O (20 μL) and injection of all 30 μL (Table 4.2). Representative MS of all AGs modified by Eis are provided in Fig. 4.12.

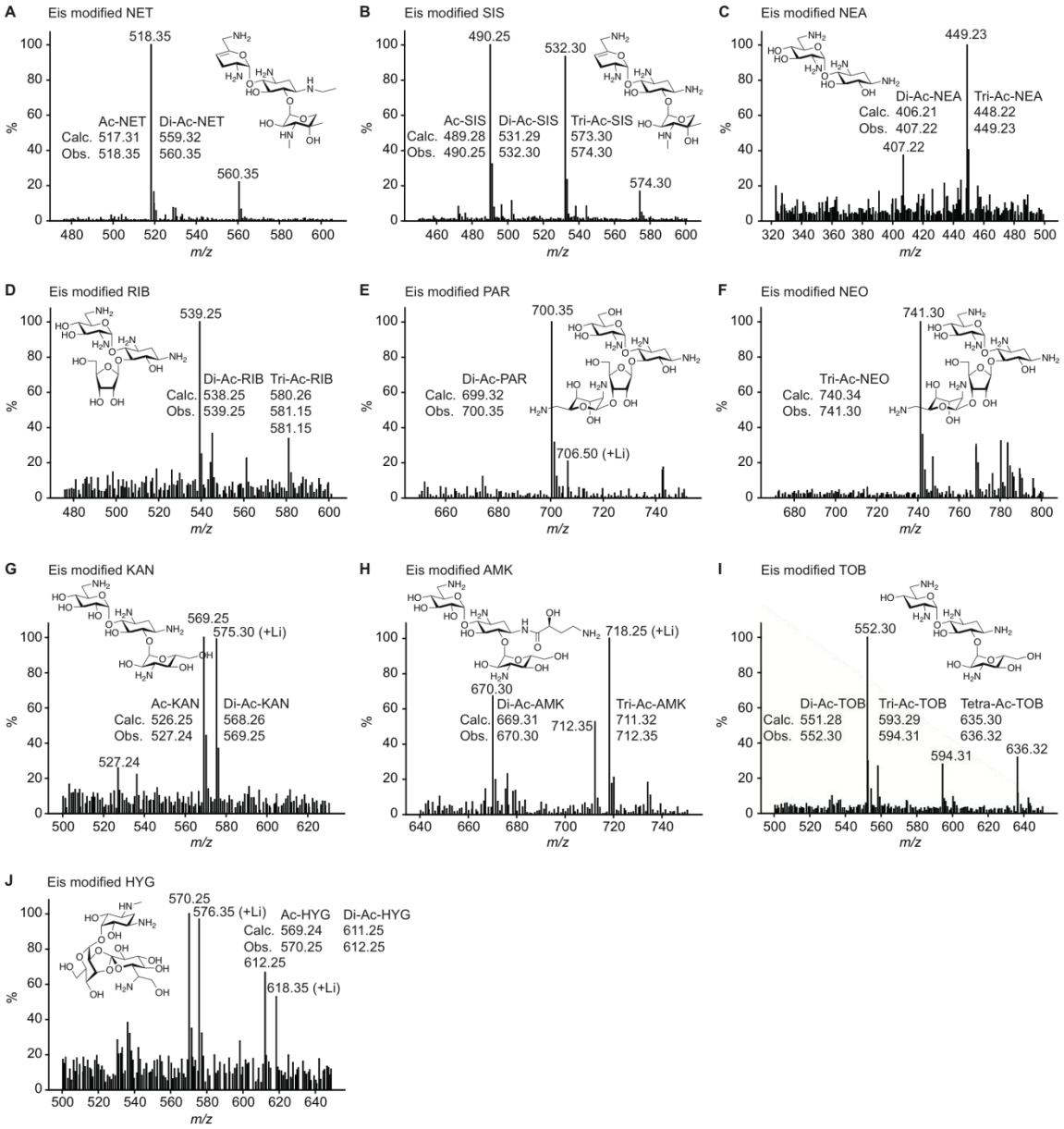

Fig. 4.17. Representative mass spectra of AGs multi-acetylated by Eis.

To confirm the uniqueness of multi-acetylation by Eis, we tested with 10 eq of AcCoA and all 10 AG substrates of Eis the six following AACs: AAC(2')-Ic from *Mtb*,[8,9] AAC(3)-IV from *E. coli*,[16,18] AAC(3)-Ib and AAC(6')-Ib' from the bifunctional AAC(3)-Ib/AAC(6')-Ib' from *Pseudomonas aeruginosa*,[12,13] AAC(6') from the bifunctional AAC(6')/APH(2")-Ia from *S. aureus*,[10,14] and AAC(6')-IId from the bifunctional ANT(3")-Ii/AAC(6')-IId from *Serratia marcescens*.[15,16] We found each of them to only mono-acetylate all AGs tested.

4.4.3.3. Steady-state kinetic measurements of net acetylation of AGs by Eis

The kinetic parameters for Eis acetylation of several AGs (AMK, KAN, NEA, NEO, NET, PAR, SIS, and TOB) were determined at 25 ℃ in reactions (100 μL) containing a fixed concentration of AcCoA (0.1 mM), varied concentrations of AGs (0, 20, 50, 100, 250, 500 μM), DTDP (2 mM), Tris-HCl pH 8.0 (50 mM), and Eis (0.25 μM). Reactions were initiated by the addition of AcCoA and were carried out in duplicate. Net acetylation was monitored by measuring absorbance at 324 nm (as described in Section 4.4.3.1) as a function of time. The kinetic parameters, K_m and k_{cat} (Table 4.1) were determined from the linear parts of these time courses by using Lineweaver-Burk plots.

4.4.3.4. Determination of amine positions acetylated by Eis

In order to establish the amine positions acetylated by Eis, NEA was chosen as the model AG. Control experiments with other AG acetyltransferases (AAC(2')-Ic, AAC(3)-IV, and AAC(6')) known and confirmed by us by UV-Vis assays and LCMS to acetylate only at the 2'-, 3-, and 6'-positions, respectively) of all AG substrates used in this study were performed.

4.4.3.4.1. Preparation of pAAC(2')-Ic-pET28a(NHis) overexpression construct

The gene encoding AAC(2')-Ic was PCR-amplified using *Mtb* H37Rv genomic DNA and Phusion DNA polymerase as described by NEB. The forward and reverse primers used were 5'-ATTCCATATGCACACCCAGGTACACACGG-3' and 5'-GCGGAATTCTTACCAGACGTCGCCCGC-3', respectively (the *Nde*I and *Eco*RI restriction sites are underlined). The amplified gene was inserted into the linearized pET28a vector via the corresponding *Nde*I/*Eco*RI restriction sites. Expression of AAC(2')-Ic-pET28a was done following transformation into *E. coli* TOP10 competent cells. The expression clone was characterized by DNA sequencing (The University of Michigan DNA Sequencing Core) and compared to its corresponding gene sequence (GenBank accession no. U72714).

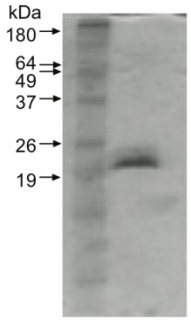

Fig. 4.18. Coomassie blue-stained 15% Tris-HCl SDS-PAGE gel showing the purified AAC(2')-Ic (22332 Da). 6 μg of protein were loaded on the gel.

4.4.3.4.2. Overproduction and purification of AAC(2')-Ic, AAC(3)-IV, and AAC(6')/APH(2")

The AAC(3)-IV and AAC(6')/APH(2") proteins were overexpressed and purified as previously described.[10] As none of the reactions performed in this study contain a nucleotide substrate for the APH(2") domain of the bifunctional AAC(6')/APH(2") protein, for the sake of simplicity we will call this bifunctional enzyme AAC(6') in the text. For the production of AAC(2')-Ic, the protocol described for the purification of Eis protein was used with the following modifications: The cells were grown at 37 ℃ to attenuance of ~1.0 at 600 nm prior to cooling to 20 ℃ for 15 min before induction with IPTG (200 μM final concentration) and additional growth at 20 ℃ for 9 h. The lysis buffer utilized was composed of 25 mM triethanolamine pH 7.8, 50 mM NaCl, 1 mM EDTA, and 10% (v/v) glycerol. The dialysis buffer contained the same components as the lysis buffer with additional 1 mM DTT and 1 mM EDTA. Glycerol (50% final concentration) was added to the pure AAC(2')-Ic protein after dialysis and concentration. 0.3 mg of AAC(2')-Ic was obtain per L of culture (Fig. 4.18). The protein was stored at -20 ℃.

4.4.3.4.3. TLC assays

The eluent system utilized for all TLCs of reactions performed with NEA was 3:0.8/MeOH:NH_4OH. The R_f values observed are reported in Table 4.3. The exact reaction conditions are reported below.

4.4.3.4.3.1. Control TLCs of AGs mono-acetylated at the 2'-, 3-, and 6'-position by AAC(2')-Ic, AAC(3)-IV, and AAC(6'), respectively

Reactions (15 μL) were carried out at rt in MES buffer (50 mM, pH 6.6) (AAC(3)-IV and AAC(6')) or in potassium phosphate buffer (100 mM, pH 7.0) (AAC(2')-Ic) in the presence of AcCoA (0.96 mM, 1.2 eq), AG (0.8 mM, 1 eq), and AAC enzyme (10 μM). After overnight incubation, aliquots (5 μL) of the reaction mixtures were loaded and run onto a TLC plate.

4.4.3.4.3.2. Control TLCs of AGs di-acetylated sequentially by pairwise treatment with AAC(2')-Ic, AAC(3)-IV, and AAC(6')

Reactions (10 μL) were carried out at rt in MES buffer (50 mM, pH 6.6) in the presence of AcCoA (1.92 mM, 2.4 eq), AG (0.8 mM, 1 eq), and AAC enzyme (10 μM). After overnight incubation, the second AAC enzyme (10 μM) was added to the reaction mixture, which was incubated for an additional 16 h. Aliquots (5 μL) of each di-acetylation reaction mixture were loaded and run onto a TLC plate.

4.4.3.4.3.3. TLCs showing time course of tri-acetylation of NEA by Eis

Reactions (30 μL) were carried out at rt in Tris-HCl buffer (50 mM, pH 8.0) in the presence of AcCoA (4 mM, 5 eq), NEA (0.8 mM, 1 eq), and Eis (5 μM). Aliquots (4 μL) were loaded and run onto a TLC plate after 0, 5, 10, 30, and 120 min as well as after overnight incubation (Table 4.6 and Fig. 4.4).

4.4.3.4.4. Tri-acetylation of NEA by Eis and NMR analysis of the 1,2',6'-tri-acetyl-NEA product

In order to establish which 3 positions Eis acetylates on NEA, a large-scale reaction was performed. Briefly, a reaction mixture (5 mL) containing NEA (5 mM, 1 eq), AcCoA (25 mM, 5 eq), and Eis (0.5 mg) in Tris-HCl (50 mM, pH 8.0) was incubated with gentle shaking at rt for 48 h prior to addition of additional portions of AcCoA (5 mM) and Eis (0.1 mg) followed by further incubation for 24 h. The progress of the Eis reaction was monitored by LCMS. After 90% conversion of NEA into tri-acetyl-NEA, the Eis enzyme was removed from the mixture by filtration using an Amicon® Ultra-4 centrifugal filter (3,000 MWCO), and the filtrate was lyophilized prior to further purification. The lyophilized solid was dissolved in H_2O (5 mL) and purified by flash chromatography (SiO_2; 1:1/MeOH:H_2O, R_f 0.39 (3:0.8/MeOH:NH_4OH)) to give 1,2',6'-tri-acetyl-NEA as a white powder after removal of the solvents by concentration under reduced pressure followed by lyophilization. For NMR analyses, 1,2',6'-tri-acetyl-NEA was dissolved in D_2O (3 mL) and the pH was adjusted to ~3.0 by addition of H_2SO_4 (5%) prior to lyophilization and further re-dissolving in D_2O or 9:1/H_2O:D_2O. The positions of acetylation, purity, and structure identification were confirmed by ^{1}H, ^{13}C, 2D-TOCSY,

2D-COSY, DEPT, and HETCOR NMR as well as LCMS. Proton connectivities were assigned using 2D-TOCSY and 2D-COSY spectra. Signals of all carbons were derived by examination of HETCOR and DEPT spectra. Representative spectra for 1,2',6'-tri-acetyl-NEA are provided in Figs. 4.6, 4.8 and 4.9.

To unambiguously establish the 3 acetylated positions on the NEA scaffold, the ^{1}H and ^{13}C NMR were compared to a standard of pure non-acetylated NEA (Tables 4.4 and 4.5). The sample of NEA for NMR was prepared as described for the 1,2',6'-tri-acetyl-NEA NMR sample. Representative spectra for NEA are provided in Figs. 4.5 and 4.7.

4.4.4. Structural characterization of Eis

4.4.4.1. Crystallization, diffraction data collection, and structure determination and refinement of Eis

The initial conditions for growing SeMet-Eis-CoA co-crystals were found using Hampton Research Crystal Screen solutions (Hampton Research, Aliso Viejo, CA). Upon optimization, single crystals of SeMet-Eis-CoA (0.15 μm × 0.15 μm × 0.15 μm in size) were obtained in 2-3 weeks. Crystals were grown by hanging-drop vapor-diffusion technique at 22 ℃. The drops contained 1 μL of a mixture of SeMet-Eis (3.5 mg/mL) in 50 mM Tris-HCl pH 8.0, KAN (10 mM), and CoA (8.8 mM) mixed with 1 μL of the reservoir solution (Tris-HCl pH 8.5 (0.1 M), PEG8000 (10-15% w/v), and $(NH_4)_2SO_4$ (0.1 or 0.4 M)) and were equilibrated against 1 mL of the reservoir solution. The crystals were gradually transferred into a cryoprotectant solution (Tris-HCl pH 8.5 (0.1 M), PEG8000 (10% w/v), $(NH_4)_2SO_4$ (0.1 M), glycerol (15%), and CoA (1 mM)) and flash-frozen in liquid nitrogen. The crystals of the native Eis-CoA-acetylated HYG ternary complex were grown and harvested analogously, but by using a different reservoir solution (Tris-HCl pH 8.5 (0.1 M) and PEG 8000 (8-12% w/v)), except that a mixture of Eis with CoA (1 mM) and KAN (10 mM) was used. The CoA and KAN molecules were soaked out of the crystals by a gradual replacement of the crystallization buffer with the cryoprotectant solution (Tris-HCl pH 8.5 (0.1 M), PEG 8000 (8-12% w/v), and 15% glycerol) that contained AcCoA (1 mM) and 10 mM HYG (10 mM), and subsequent overnight incubation, before flash-freezing in the liquid nitrogen. Other AGs (KAN, NET,

PAR, SIS, and AMK) were also tried in the growth and soaking of the crystals, with similar electron density in the active site. The best-diffracting crystals were obtained with the KAN (during growth) and HYG (during soak) pair.

The diffraction data were collected at beamline 21-ID at the Advanced Photon Source at the Argonne National Laboratories. The data were indexed, integrated and scaled with HKL2000.[34] Initially, we attempted to determine the structure of the SeMet-Eis-CoA by molecular replacement using program PHASER[35] and a structure of a weakly homologs putative acetyltransferase from *Enterococcus faecalis* determined by the Midwest Center for Structural Genomics (PDB code: 2I00), as a search model. This approach yielded a clear solution, however the quality of the electron density map was not sufficiently high for refinement. By using sequence homology between this model and Eis, we obtained putative positions of 21 Se atoms (7 per monomer) in the asymmetric unit and used these heavy atom sites to obtain phases from the Se anomalous signal by the SAD phasing with PHASER.[35] The resulting electron density map was of high quality and was readily interpretable. The structure of SeMet-Eis-CoA (KAN was not found in the difference density) was then built and refined iteratively using programs Coot[36] and REFMAC[37], respectively. This structure was used as a molecular replacement model to obtain the structure of Eis-CoA-acetylated HYG by PHASER. The Eis model was further altered and refined. The data collection and refinement statistics for the structures reported here are given in Table 4.6. In the omit electron density map generated by using with Eis and no ligands or water, strong (>3.0σ) Fo-Fc density in the active site for bound CoA and the acetamide moiety of the acetylated HYG was present that allowed facile building and refinement of these ligands. The density for the rest of the HYG was too weak to allow us to build the rest of the AG molecule. Only the acetamide moiety of the acetylated AG was observed when other AGs were used in the crystal growth or soaking conditions. The Eis-CoA-acetamide structure was deposited in the Protein Data Bank with the PDB accession number 3R1K.

4.4.4.2. The structure of the Eis monomer

The topology of the assembly of the N-terminal (magenta, bottom panel) and the central (green, bottom panel) regions of Eis is presented in Fig. 4.11. The surface representation of the Eis monomer showing a complex and negatively charged substrate-binding cavity is depicted in Fig. 4.12.

4.5. References

(1) Caminero, J. A.; Sotgiu, G.; Zumla, A.; Migliori, G. B. *Lancet Infect Dis* **2010**, *10*, 621.
(2) Houghton, J. L.; Green, K. D.; Chen, W.; Garneau-Tsodikova, S. *Chembiochem : a European journal of chemical biology* **2010**, *11*, 880.
(3) Carter, A. P.; Clemons, W. M.; Brodersen, D. E.; Morgan-Warren, R. J.; Wimberly, B. T.; Ramakrishnan, V. *Nature* **2000**, *407*, 340.
(4) Moazed, D.; Noller, H. F. *Nature* **1987**, *327*, 389.
(5) Steitz, T. A. *Nat Rev Mol Cell Biol* **2008**, *9*, 242.
(6) Campbell, P. J.; Morlock, G. P.; Sikes, R. D.; Dalton, T. L.; Metchock, B.; Starks, A. M.; Hooks, D. P.; Cowan, L. S.; Plikaytis, B. B.; Posey, J. E. *Antimicrobial agents and chemotherapy* **2011**, *55*, 2032.
(7) Zaunbrecher, M. A.; Sikes, R. D., Jr.; Metchock, B.; Shinnick, T. M.; Posey, J. E. *Proceedings of the National Academy of Sciences of the United States of America* **2009**, *106*, 20004.
(8) Vetting, M. W.; Hegde, S. S.; Javid-Majd, F.; Blanchard, J. S.; Roderick, S. L. *Nature structural biology* **2002**, *9*, 653.
(9) Hegde, S. S.; Javid-Majd, F.; Blanchard, J. S. *The Journal of biological chemistry* **2001**, *276*, 45876.
(10) Green, K. D.; Chen, W.; Houghton, J. L.; Fridman, M.; Garneau-Tsodikova, S. *Chembiochem : a European journal of chemical biology* **2010**, *11*, 119.
(11) Magalhaes, M. L.; Blanchard, J. S. *Biochemistry* **2005**, *44*, 16275.
(12) Dubois, V.; Poirel, L.; Marie, C.; Arpin, C.; Nordmann, P.; Quentin, C. *Antimicrobial agents and chemotherapy* **2002**, *46*, 638.
(13) Kim, C.; Villegas-Estrada, A.; Hesek, D.; Mobashery, S. *Biochemistry* **2007**, *46*, 5270.
(14) Boehr, D. D.; Daigle, D. M.; Wright, G. D. *Biochemistry* **2004**, *43*, 9846.
(15) Centron, D.; Roy, P. H. *Antimicrobial agents and chemotherapy* **2002**, *46*, 1402.
(16) Kim, C.; Hesek, D.; Zajicek, J.; Vakulenko, S. B.; Mobashery, S. *Biochemistry* **2006**, *45*, 8368.
(17) Park, W. K. C.; Auer, M.; Jaksche, H.; Wong, C.-H. *J. Am. Chem. Soc.* **1996**, *118*, 10150.
(18) Andac, C. A.; Stringfellow, T. C.; Hornemann, U.; Noyanalpan, N. *Bioorganic chemistry* **2011**, *39*, 28.
(19) Tsodikov, O. V.; Record, M. T., Jr.; Sergeev, Y. V. *J Comput Chem* **2002**, *23*, 600.
(20) Maurice, F.; Broutin, I.; Podglajen, I.; Benas, P.; Collatz, E.; Dardel, F. *EMBO reports* **2008**, *9*, 344.
(21) Choinowski, T.; Hauser, H.; Piontek, K. *Biochemistry* **2000**, *39*, 1897.
(22) Dyer, D. H.; Lovell, S.; Thoden, J. B.; Holden, H. M.; Rayment, I.; Lan, Q. *The Journal of biological chemistry* **2003**, *278*, 39085.
(23) Vetting, M. W.; Park, C. H.; Hegde, S. S.; Jacoby, G. A.; Hooper, D. C.; Blanchard, J. S. *Biochemistry* **2008**, *47*, 9825.
(24) Bhatnagar, R. S.; Futterer, K.; Waksman, G.; Gordon, J. I. *Biochim Biophys Acta* **1999**, *1441*, 162.
(25) Wei, J.; Dahl, J. L.; Moulder, J. W.; Roberts, E. A.; O'Gaora, P.; Young, D. B.; Friedman, R. L. *Journal of bacteriology* **2000**, *182*, 377.
(26) Dahl, J. L.; Wei, J.; Moulder, J. W.; Laal, S.; Friedman, R. L. *Infect Immun* **2001**, *69*, 4295.
(27) Roberts, E. A.; Clark, A.; McBeth, S.; Friedman, R. L. *Journal of bacteriology* **2004**, *186*, 5410.
(28) Dahl, J. L.; Arora, K.; Boshoff, H. I.; Whiteford, D. C.; Pacheco, S. A.; Walsh, O. J.; Lau-Bonilla, D.; Davis, W. B.; Garza, A. G. *Journal of bacteriology* **2005**, *187*, 2439.
(29) Samuel, L. P.; Song, C. H.; Wei, J.; Roberts, E. A.; Dahl, J. L.; Barry, C. E., 3rd; Jo, E. K.; Friedman, R. L. *Microbiology* **2007**, *153*, 529.

(30) Lella, R. K.; Sharma, C. *The Journal of biological chemistry* **2007**, *282*, 18671.
(31) Wu, S.; Barnes, P. F.; Samten, B.; Pang, X.; Rodrigue, S.; Ghanny, S.; Soteropoulos, P.; Gaudreau, L.; Howard, S. T. *Microbiology* **2009**, *155*, 1272.
(32) Shin, D. M.; Jeon, B. Y.; Lee, H. M.; Jin, H. S.; Yuk, J. M.; Song, C. H.; Lee, S. H.; Lee, Z. W.; Cho, S. N.; Kim, J. M.; Friedman, R. L.; Jo, E. K. *PLoS Pathog* **2010**, *6*, e1001230.
(33) Ho, S. N.; Hunt, H. D.; Horton, R. M.; Pullen, J. K.; Pease, L. R. *Gene* **1989**, *77*, 51.
(34) Otwinowski, Z.; Minor, W. In *Methods in Enzymology, Macromolecular Crystallography, part A*; C.W. Carter, J. R. M. S., Eds. , Ed.; Academic Press: New York, 1997; Vol. 276, p 307.
(35) McCoy, A. J.; Grosse-Kunstleve, R. W.; Adams, P. D.; Winn, M. D.; Storoni, L. C.; Read, R. J. *J Appl Crystallogr* **2007**, *40*, 658.
(36) Emsley, P.; Cowtan, K. *Acta crystallographica. Section D, Biological crystallography* **2004**, *60*, 2126.
(37) Murshudov, G. N.; Vagin, A. A.; Dodson, E. J. *Acta crystallographica. Section D, Biological crystallography* **1997**, *53*, 240.

Note:

This chapter is adapted from a published manuscript: **Chen, W.**; Biswas, T.; Porter, V. R.; Tsodikov, O. V.; Garneau-Tsodikova, S. *Proceedings of the National Academy of Sciences of the United States of America* **2011**, *108*, 9804. **Wenjing Chen** did all the biochemical characterizations and grew the protein crystals.

Chapter 5

Identification and characterization of inhibitors of the aminoglycoside resistance acetyltransferase Eis from *Mycobacterium tuberculosis*

5.1. Abstract

The unusually regioversatile acetyltransferase Eis is a cause of resistance to KAN in cases of tuberculosis (TB). En route to new TB treatments, several inhibitors of the Eis enzyme were identified and characterized.

5.2. Introduction

With an anticipated 9.8 million new cases this year,[1] the TB epidemic is one of the most serious health problems worldwide. The continuous emergence and global spread of multidrug-resistant (MDR) and extensively drug-resistant (XDR) strains of *Mycobacterium tuberculosis* (*Mtb*), the causative agent of TB, underscore the pressing clinical need for novel treatments of this deadly infectious disease and for new solutions to alleviate the resistance problem.[2,3]

Aminoglycoside (AG) antibiotics[4] such as kanamycin A (KAN) (**1**) and amikacin (AMK) (**2**) are currently used as a last resort for treatment of XDR-TB (Fig. 5.1A). However, resistance to KAN is constantly rising, and treatment options for patients affected with XDR-TB are becoming fewer.[5] In most bacterial strains, a major mechanism of resistance to AGs is the enzymatic modification of the drugs by AG-modifying enzymes such as AG acetyltransferases (AACs), AG phosphotransferases (APHs), and AG nucleotidyltransferases (ANTs).[6,7] In *Mtb*, resistance to AGs results either from mutations of the ribosome that prevent the drugs from binding to it,[8-10] or from up-regulation of the chromosomal *eis* (enhanced intracellular survival) gene caused by mutations in its promoter.[11,12] Other biological functions of the mycobacterial protein Eis have been the

subject of numerous investigations.[13-20] We recently demonstrated that Eis is a unique AAC that inactivates a broad set of AGs via a multi-acetylation mechanism.[21]

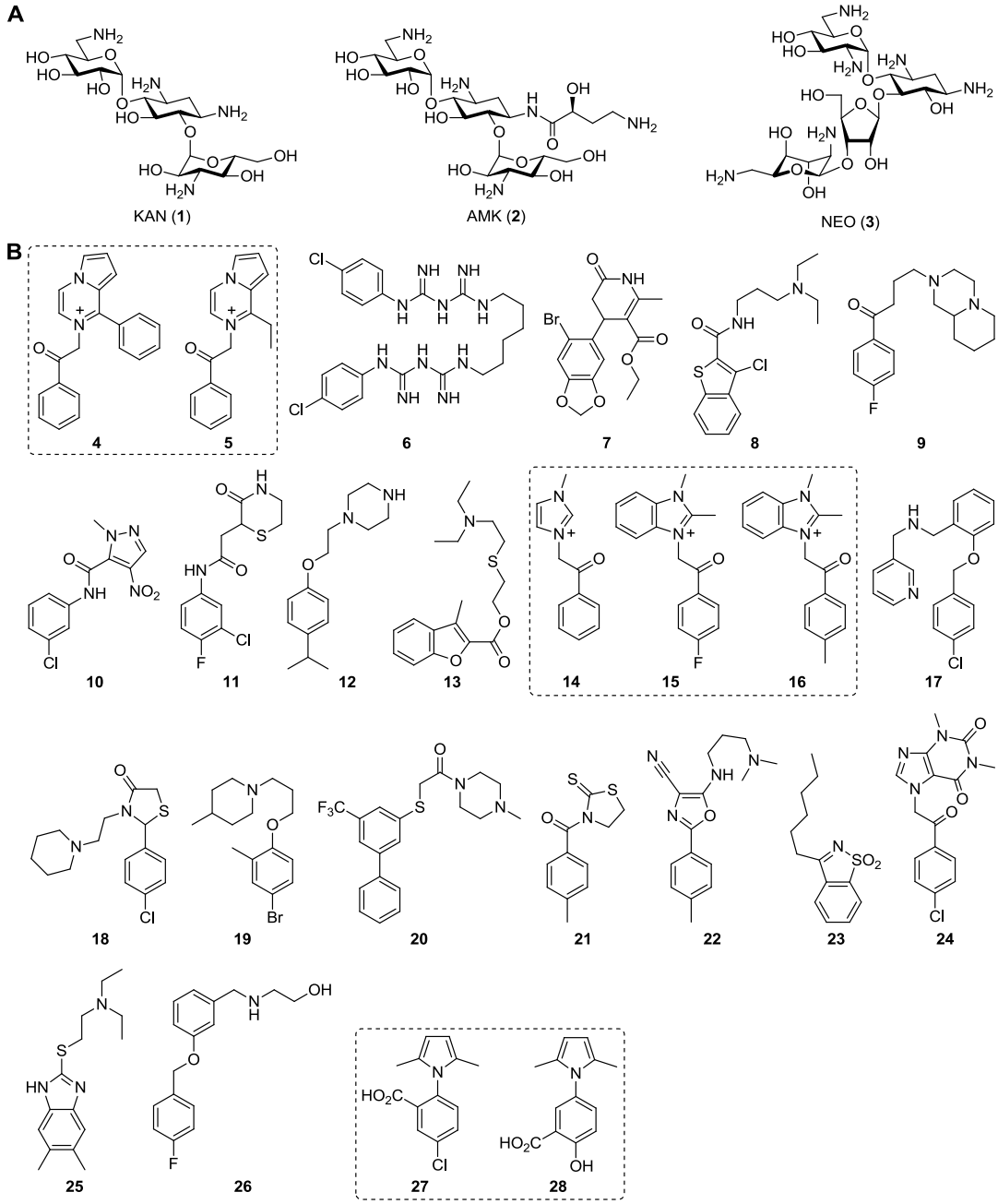

Fig. 5.1. A. Structures of AGs used in this study. **B.** Structures of the 25 inhibitors of Eis identified via high-throughput screening.

Two main strategies to overcome the effect of Eis in *Mtb* can be envisioned: 1) the development of new AGs not susceptible to Eis and 2) the use of Eis inhibitors. We recently reported a chemoenzymatic methodology[22] and a complementary protecting-

group-free chemical strategy[23] for the production of novel AG derivatives. However, as Eis is capable of multi-acetylation of a large variety of AG scaffolds, it is unlikely that novel AGs will provide a viable and/or sustainable solution to the resistance problem in *Mtb*. Blanchard and co-workers previously showed that, when used in conjunction, the β-lactamase inhibitor clavulanate and meropenem are effective against XDR-TB.[24] The AG tobramycin and the macrolide antibiotic clarithromycin have also showed promising synergistic effects in *Mtb* clinical isolates.[25] Wright and colleagues also demonstrated that, in general, combinations of antibiotics and non-antibiotic drugs could result in enhancement of antimicrobial efficacy.[26] Similarly, an inhibitor of the resistance acetyltransferase Eis in combination with the currently used second-line antituberculosis drugs KAN or AMK may provide a potential solution to overcome the problem of XDR-TB. Herein, by using *in vitro* high-throughput screening (HTS), we identified and characterized the first series of potent inhibitors of Eis (Fig. 5.1B).

5.3. Results and discussion

To identify inhibitors of *Mtb* Eis, we used neomycin B (NEO) (**3**) owing to the robust activity of the enzyme with this AG. We screened a total of 23,000 compounds from three small molecule libraries: ChemDiv, BioFocus NCC, and MicroSource MS2000 spectrum. From the 23,000 molecules tested, 300 (1.3%) showed a reasonable degree of inhibition (>3σ from the mean negative control) against Eis, out of which 56 showed dose-dependent inhibition. The 25 compounds discussed herein (Fig. 5.1B) were found to have IC_{50} values in the low-micromolar range (Table 5.1 and Figs. 5.2-5.4). While most of these have not yet been biologically characterized, compounds **7**, **14**, **27**, and **28** have found application as anti-HIV treatments (**27**[27,28] and **28**[27-29]), molecules to prolong eukaryote longevity (**7**),[30] antibacterials (**27** and **28**),[31] anticancer agents (**28**),[32] and hypoglycemia therapeutics (**14**).[33]

At first glance, the 25 identified compounds appear to have vastly different structures. However, upon closer inspection of their scaffolds, two structural features link these 25 Eis inhibitors: the presence of at least one aromatic ring and one amine functional group. In general, we observed that positively or potentially positively charged molecules,

including chlorhexidine (**6**), displayed lower IC_{50} values than preferably negatively charged (**27** and **28**) or neutral compounds. The highly negatively charged AG-binding cavity of the Eis protein (PDB ID: 3R1K)[21] is consistent with this general trend.

Table 5.1. Eis inhibition constants (IC_{50}) of hit compounds **4-28** for NEO acetylation.[a]

Compound[b]	IC_{50} (μM)[c]	Compound[b]	IC_{50} (μM)[c]
4	0.364 ± 0.032	**15**	3.24 ± 0.32
4	0.331 ± 0.082 (AMK)[a]	**16**	3.84 ± 0.55
4	0.585 ± 0.113 (KAN)[a]	**17**	3.39 ± 0.61
5	9.25 ± 1.50	**18**	4.90 ± 0.75
6	0.188 ± 0.030	**19**	5.54 ± 0.63
6	0.321 ± 0.058 (AMK)[a]	**20**	5.68 ± 0.88
6	0.666 ± 0.193 (KAN)[a]	**21**	5.75 ± 0.66
7	1.09 ± 0.14	**22**	6.50 ± 1.32
8	1.24 ± 0.16	**23**	7.64 ± 0.60
9	2.01 ± 0.12	**24**	9.79 ± 1.97
10	2.29 ± 0.52	**25**	11.4 ± 1.6
11	2.37 ± 0.41	**26**	15.9 ± 2.6
12	2.63 ± 0.60	**27**	> 200
13	2.64 ± 0.36	**28**	41 ± 9
14	3.06 ± 0.56		

[a]IC_{50} values were also determined for compounds **4** and **6** using AMK and KAN. [b]See Fig. 5.1B for chemical structures. [c]Determined from at least 3 trials. Best fit values were obtained by using KaleidaGraph 4.1.

Seven of the 25 Eis inhibitors identified were divided into three groups for a preliminary and limited structure-activity relationship (SAR) analysis: 1) compounds **4** and **5**, 2) **14**, **15**, and **16**, as well as 3) **27** and **28** (Fig. 5.1B). Compounds **14**, **15**, and **16** differ in their imidazolium versus benzoimidazolium substitution on one side of the ketone and in their *para* substituents at the phenyl ring on the opposite side of the carbonyl. These differences had no effect on the IC_{50} values, indicating the importance of the imidazolium, but a secondary role of the additional features to the core structure for biological activity. In contrary, the differences in benzyl ring substitutions in compounds **27** and **28** (alternative placement (*ortho* versus *meta*) of the carboxylic acid and replacement of the *para*-chloro group with a *para*-hydroxy group) resulted in a greater than fivefold increase in the inhibition of Eis. Similarly, replacement of the ethyl group of **5** adjacent to the cationic nitrogen with a phenyl moiety in **4** resulted in a 25-fold increase in the inhibitory activity of compound **4**. Further kinetic analysis of compound **4** revealed a mixed mode of inhibition against NEO (Fig.

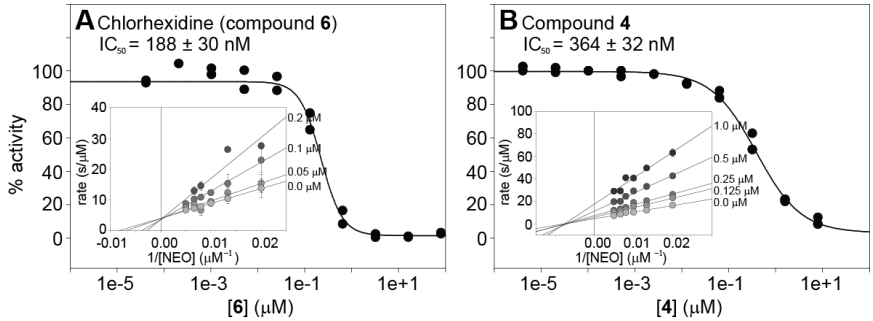

Fig. 5.2. Representative examples of IC_{50} curves for **A.** chlorhexidine (**6**) and **B.** compound **4**. The plots showing the competitive and mixed inhibition with respect to NEO for compounds **6** and **4**, respectively, can be viewed as the inset in each panel.

5.2B). The observed mixed mode of inhibition could be explained by the three substrates (NEO, acetyl-NEO, and di-acetyl-NEO) that are produced during the reaction of NEO with Eis. Here, compound **4**, may be competing differently with each possible substrate.

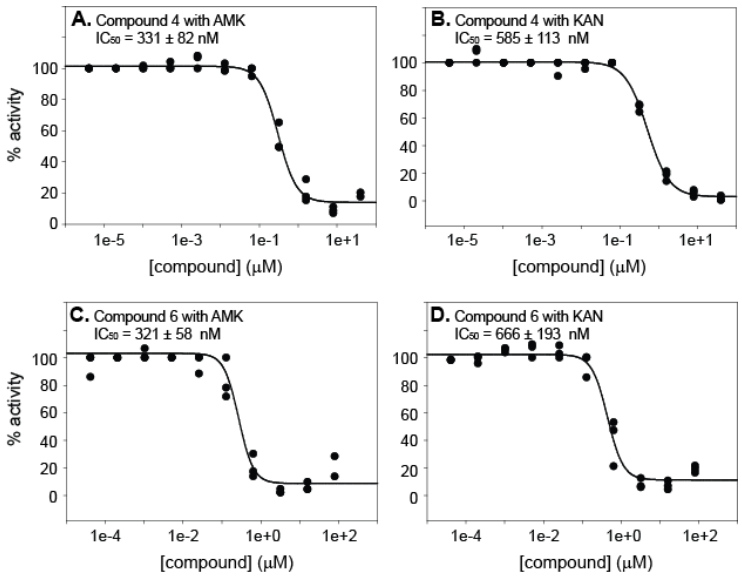

Fig. 5.3. IC_{50} curves for compounds **4** and **6** determined using AMK and KAN.

Interestingly, in contrast to compound **4**, the best inhibitor identified in this study with an IC_{50} value of 188 ± 30 nM, chlorhexidine (**6**), was found to behave as an AG-competitive inhibitor against NEO, KAN, and AMK (Fig. 5.2A). Chlorhexidine is an antibiotic used mainly as a topical antibacterial, as a mouthwash, and as a sterilizing agent for surgical equipment.[34] Because of its toxic effects on pulmonary tissues,[35] chlorhexidine cannot be pursued as a potential TB treatment, but will continue to serve as a positive control for future HTS experiments for the identification of additional Eis inhibitor scaffolds.

With their structurally diverse scaffolds, the remaining compounds cannot be divided into distinct groups for SAR analyses. However, grouping the compounds by their IC_{50} values does reveal some trends. In comparison with compounds **4** and **6**-**8**, the fewer hydrogen bonding sites of compounds **9**-**13** could explain the relatively higher IC_{50} values for these molecules. Likewise, the increased structural rigidity of compounds **17**-**26** could limit the ability of these molecules to adopt an ideal conformation for binding, potentially explaining the higher inhibitory constants observed for these molecules.

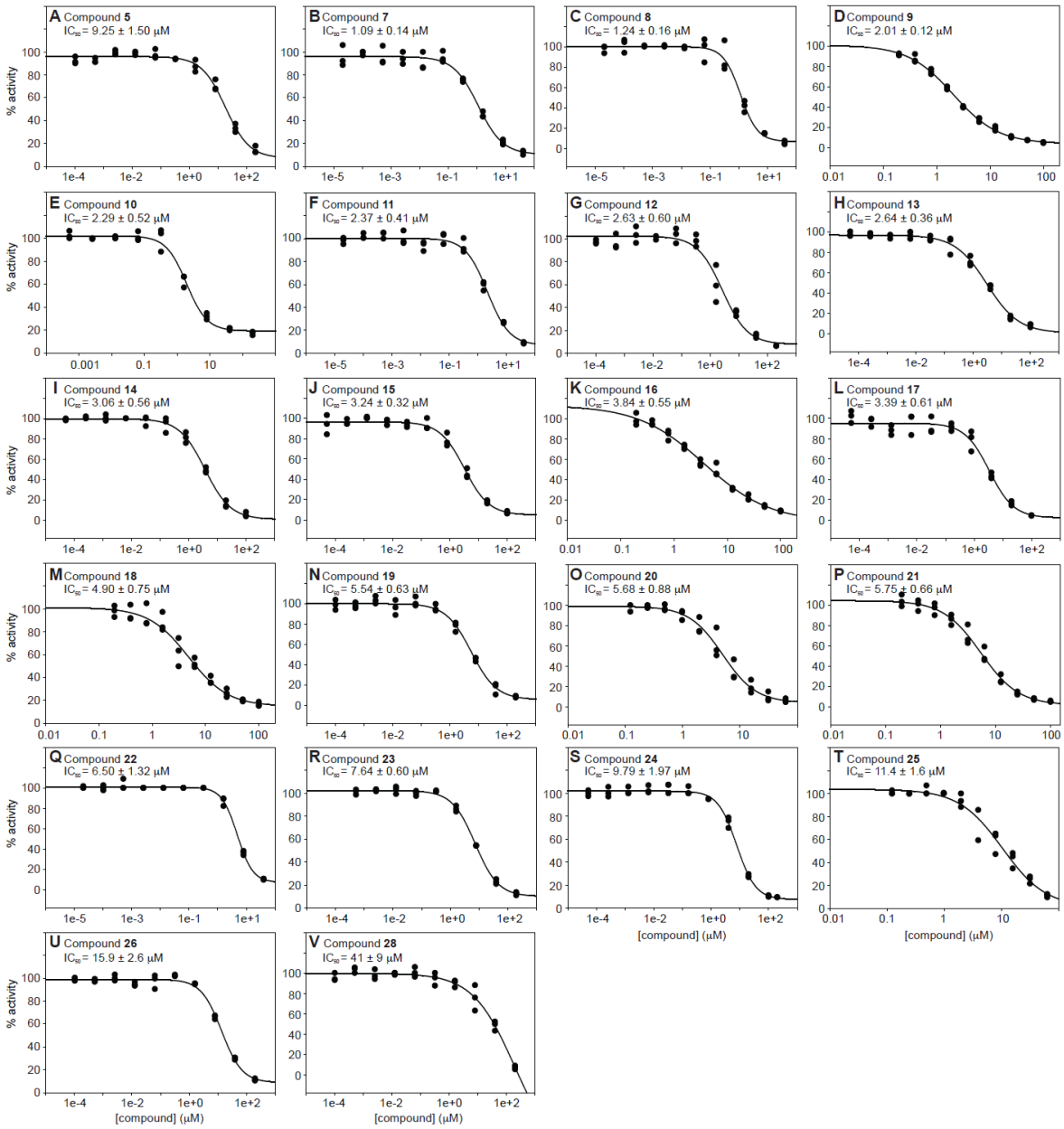

Fig. 5.4. IC_{50} curves for compounds **5**, **7-26**, and **28** determined using NEO. (Note: The IC_{50} value for compound **27** was not determined as value was >200 μM).

Because many AACs have a negatively charged AG-binding site that could be accessible for ligand binding,[36-38] in order to confirm the specificity of the identified inhibitors for Eis, we tested whether the four best compounds (**4**, **6**, **7**, and **8**) inhibit other AAC enzymes with negatively charged AG-binding sites from three different classes: AAC(2')-Ic from *Mtb*, AAC(3)-IV from *E. coli*, and AAC(6')/APH(2") from *S. aureus*. With the exception of compound **4** against AAC(2')-Ic, which displayed an IC_{50} value of 367 ± 129 μM (1000-fold worse than with Eis), no significant inhibition was observed for the

combinations tested. This lack of cross-inhibition indicates that the inhibitors identified display high selectivity toward the Eis AG-binding site. Eis has been shown to multi-acetylate a large number of AGs[21] and is therefore potentially able to accommodate various conformations of structurally diverse and/or similar molecules in contrast to the mono-acetylating AACs (AAC(2'), AAC(3), and AAC(6')) for which substrates can only bind in a single conformation. The unique flexibility of the AG-binding site of Eis could therefore explain the intriguing selectivity of the inhibitors identified for this enzyme. For example, the selectivity of chlorhexidine (**6**) for Eis, normally non-selectively binding to negatively charged sites and therefore expected to inhibit AAC(2'), AAC(3), and AAC(6'), could be justified by the uniqueness of the Eis AG-binding site that could accommodate compound **6** in conformation(s) that the other AACs cannot.

In summary, by using an *in vitro* HTS UV-Vis assay, we have identified 25 inhibitors of Eis from *Mtb* with 21 distinct scaffolds. The compounds display selective and potent inhibitory activity *in vitro* against the purified *Mtb* Eis and different modes of inhibition, with the known antibacterial chlorhexidine (**6**) competing with the AG for binding Eis. These findings provide the foundation for testing whether the Eis inhibitors will overcome KAN resistance in *Mtb* strains in which Eis is up-regulated. This work also lays the groundwork for exploration of scaffold diversification and SAR studies of the identified biologically active compounds to be used in combination therapies with KAN or AMK against TB.

5.4. Materials and methods

5.4.1. Reagents and small molecule libraries

All reagents including DTNB, NEO, KAN, AMK, and AcCoA were purchased from Sigma-Aldrich (St. Louis, MO, USA). Eis was screened against 23,000 compounds from three diverse libraries of small molecules: 1) the BioFocus NCC library, 2) the ChemDiv library (20,000 compounds), and 3) the MicroSource MS2000 library, composed of ~2,000 bioactive compounds (343 molecules with reported biological activities, 629 natural products, 958 known therapeutics, and 70 compounds approved for agricultural use). The activity of promising compounds was confirmed by using repurchased samples

from Sigma-Aldrich (compound **6**) and ChemDiv (San Diego, CA, USA) (compounds **4**, **5**, and **7**-**28**). All buffer pH were adjusted at rt.

5.4.2. Expression and purification of Eis and other AAC proteins

The Eis and AAC(2')-Ic from *Mtb*,[21] as well as the AAC(3)-IV from *E. coli*[22,39] and AAC(6')/APH(2'')-Ia from *S. aureus*[22,40] were overexpressed and purified as previously described.

5.4.3. Eis chemical library screening

The inhibition of Eis activity was determined by a UV-Vis assay monitoring the increase in absorbance at 412 nm (ε_{412} = 13,600 $M^{-1}cm^{-1}$) resulting from the reaction of DTNB with the thio group of CoA released upon acetylation of NEO. The final reaction mixtures (40 μL) contained Eis (0.25 μM), NEO (100 μM), Tris-HCl (50 mM, pH 8.0), AcCoA (40 μM), DTNB (0.5 mM), and the potential inhibitors (20 μM). Positive and negative control experiments were performed using chlorhexidine (**6**) (5 μM) and DMSO (0.5% v/v), respectively, instead of the potential inhibitors. Briefly, a mixture (30 μL) containing Eis (0.33 μM) and NEO (133.33 μM) in Tris-HCl (50 mM, pH 8.0) was added to 384-well non-binding-surface plates (Thermo Fisher Scientific, Waltham, MA, USA) using a Multidrop dispenser (Thermo Fisher Scientific). The potential inhibitors (0.2 μL of a 4 mM stock), chlorhexidine (**6**) (0.2 μL of a 1 mM stock), or DMSO (0.2 μL) were then added to each well by Biomek HDR (Beckman, Fullerton, CA, USA). After 10 min at rt, reactions were initiated by the addition of a mixture (10 μL) containing AcCoA (160 μM), DTNB (2 mM), and Tris-HCl (50 mM, pH 8.0). After an additional 5 min of incubation at rt, the absorbance was measured at 412 nm using a PHERAstar plate reader (BMG Labtech, Cary, NC, USA). The average Z' score for the entire HTS assay was 0.65.

5.4.4. Hit validation

Using the above conditions, all compounds deemed a hit (>3σ as a statistical hit threshold from the mean negative control) were tested in triplicate. Compounds that displayed inhibition at least in two of the three independent assays were then tested for a dose-

response using two-fold dilutions from 20 μM to 78 nM. IC_{50} values were determined for all compounds displaying dose-dependent activity.

5.4.5. Inhibition kinetics

IC_{50} values were determined on a multimode SpectraMax M5 plate reader using 96-well plates (Thermo Fisher Scientific) by monitoring absorbance at 412 nm taking measurements every 30 s for 20 min. Eis inhibitors were dissolved in Tris-HCl (50 mM, pH 8.0 containing 10% v/v DMSO) (100 μL) and a two- or five-fold dilution was performed. To the solution of inhibitors, a mixture (50 μL) containing Eis (1 μM), NEO (400 μM), and Tris-HCl (50 mM, pH 8.0) was added. After 10 min, the reactions were initiated by addition of a mixture (50 μL) containing AcCoA (2 mM), DTNB (2 mM), and Tris-HCl (50 mM, pH 8.0). Overall, inhibitor concentrations ranged from 200 μM to 4 pM. Initial rates (first 2-5 min of reaction) were calculated and normalized to reactions containing DMSO only. All assays were performed at least in triplicate. IC_{50} values were calculated by using a Hill plot fit with KaleidaGraph 4.1 software. The IC_{50} curves are provided in Figs. 5.2 and 5.4. Determination of IC_{50} values of compounds **4** and **6** against AMK and KAN were also performed as described above (Fig. 5.3). All IC_{50} values are listed in Table 5.1.

5.4.6. Mode of inhibition

By using the conditions described for inhibition kinetics with varying concentrations of NEO (50, 75, 100, 125, 150, and 200 μM) and compounds **4** (1, 0.5, 0.25, and 0.125 μM) or **6** (5, 10, 20, and 40 nM), mixed inhibition was determined for compound **4**, and compound **6** was found to be a competitive inhibitor of NEO. Resulting reaction rates were plotted as Lineweaver-Burk plots (Fig. 5.2 inserts of panels A and B). Using the same assay conditions, chlorhexidine (**6**) was also found to be a competitive inhibitor of KAN and AMK.

5.4.7. Inhibitor selectivity for Eis

To determine if the identified inhibitors are selective for Eis, we tested the four best Eis inhibitors (**4**, **6**, **7**, and **8**) with three other AACs: AAC(2')-Ic, AAC(3)-IV, and

AAC(6')/APH(2")-Ia. The conditions described for inhibition kinetics were used with varying concentrations of compounds **4**, **6**, **7**, or **8** (200-0.2 μM, 10-fold serial dilution) and AAC(2')-Ic (0.125 μM), AAC(3)-IV (0.25 μM), or AAC(6')/APH(2")-Ia (0.25 μM) instead of Eis. For AAC(2')-Ic with compound **4**, the concentration of inhibitor ranged from 1 μM to 500 pM and a five-fold serial dilution was used.

5.5. References

(1) Dye, C.; Williams, B. G. *Science* **2010**, *328*, 856.
(2) Koul, A.; Arnoult, E.; Lounis, N.; Guillemont, J.; Andries, K. *Nature* **2011**, *469*, 483.
(3) Barry, C. E., 3rd; Blanchard, J. S. *Current opinion in chemical biology* **2010**, *14*, 456.
(4) Houghton, J. L.; Green, K. D.; Chen, W.; Garneau-Tsodikova, S. *Chembiochem : a European journal of chemical biology* **2010**, *11*, 880.
(5) Yew, W. W.; Lange, C.; Leung, C. C. *The European respiratory journal : official journal of the European Society for Clinical Respiratory Physiology* **2010**, *37*, 441.
(6) Green, K. D.; Chen, W.; Garneau-Tsodikova, S. *Antimicrobial agents and chemotherapy* **2011**, *55*, 3207.
(7) Ramirez, M. S.; Tolmasky, M. E. *Drug resistance updates : reviews and commentaries in antimicrobial and anticancer chemotherapy* **2010**, *13*, 151.
(8) Shcherbakov, D.; Akbergenov, R.; Matt, T.; Sander, P.; Andersson, D. I.; Bottger, E. C. *Molecular microbiology* **2010**.
(9) Jugheli, L.; Bzekalava, N.; de Rijk, P.; Fissette, K.; Portaels, F.; Rigouts, L. *Antimicrobial agents and chemotherapy* **2009**, *53*, 5064.
(10) Zhang, Y.; Yew, W. W. *INT J TUBERC LUNG DIS* **2009**, *13*, 1320.
(11) Campbell, P. J.; Morlock, G. P.; Sikes, R. D.; Dalton, T. L.; Metchock, B.; Starks, A. M.; Hooks, D. P.; Cowan, L. S.; Plikaytis, B. B.; Posey, J. E. *Antimicrobial agents and chemotherapy* **2011**, *55*, 2032.
(12) Zaunbrecher, M. A.; Sikes, R. D., Jr.; Metchock, B.; Shinnick, T. M.; Posey, J. E. *Proceedings of the National Academy of Sciences of the United States of America* **2009**, *106*, 20004.
(13) Shin, D. M.; Jeon, B. Y.; Lee, H. M.; Jin, H. S.; Yuk, J. M.; Song, C. H.; Lee, S. H.; Lee, Z. W.; Cho, S. N.; Kim, J. M.; Friedman, R. L.; Jo, E. K. *PLoS Pathog* **2010**, *6*, e1001230.
(14) Dahl, J. L.; Wei, J.; Moulder, J. W.; Laal, S.; Friedman, R. L. *Infect Immun* **2001**, *69*, 4295.
(15) Dahl, J. L.; Arora, K.; Boshoff, H. I.; Whiteford, D. C.; Pacheco, S. A.; Walsh, O. J.; Lau-Bonilla, D.; Davis, W. B.; Garza, A. G. *Journal of bacteriology* **2005**, *187*, 2439.
(16) Wu, S.; Barnes, P. F.; Samten, B.; Pang, X.; Rodrigue, S.; Ghanny, S.; Soteropoulos, P.; Gaudreau, L.; Howard, S. T. *Microbiology* **2009**, *155*, 1272.
(17) Wei, J.; Dahl, J. L.; Moulder, J. W.; Roberts, E. A.; O'Gaora, P.; Young, D. B.; Friedman, R. L. *Journal of bacteriology* **2000**, *182*, 377.
(18) Lella, R. K.; Sharma, C. *The Journal of biological chemistry* **2007**, *282*, 18671.
(19) Roberts, E. A.; Clark, A.; McBeth, S.; Friedman, R. L. *Journal of bacteriology* **2004**, *186*, 5410.
(20) Samuel, L. P.; Song, C. H.; Wei, J.; Roberts, E. A.; Dahl, J. L.; Barry, C. E., 3rd; Jo, E. K.; Friedman, R. L. *Microbiology* **2007**, *153*, 529.
(21) Chen, W.; Biswas, T.; Porter, V. R.; Tsodikov, O. V.; Garneau-Tsodikova, S. *Proceedings of the National Academy of Sciences of the United States of America* **2011**, *108*, 9804.
(22) Green, K. D.; Chen, W.; Houghton, J. L.; Fridman, M.; Garneau-Tsodikova, S. *Chembiochem : a European journal of chemical biology* **2010**, *11*, 119.
(23) Shaul, P.; Green, K. D.; Rutenberg, R.; Kramer, M.; Berkov-Zrihen, Y.; Breiner-Goldstein, E.; Garneau-Tsodikova, S.; Fridman, M. *Organic & biomolecular chemistry* **2011**, *9*, 4057.
(24) Hugonnet, J. E.; Tremblay, L. W.; Boshoff, H. I.; Barry, C. E., 3rd; Blanchard, J. S. *Science* **2009**, *323*, 1215.
(25) K, S.; H, T.; F, V.; M., F.-D. *Int J Tuberc Lung Dis* **2009**, *13*, 1041.
(26) Ejim, L.; Farha, M. A.; Falconer, S. B.; Wildenhain, J.; Coombes, B. K.; Tyers, M.; Brown, E. D.; Wright, G. D. *Nat Chem Biol* **2011**, *7*, 348.
(27) Liu, K.; Lu, H.; Hou, L.; Qi, Z.; Teixeira, C.; Barbault, F.; Fan, B. T.; Liu, S.; Jiang, S.; Xie, L. *Journal of medicinal chemistry* **2008**, *51*, 7843.

(28) Teixeira, C.; Barbault, F.; Rebehmed, J.; Liu, K.; Xie, L.; Lu, H.; Jiang, S.; Fan, B.; Maurel, F. *Bioorganic & medicinal chemistry* **2008**, *16*, 3039.
(29) Wang, Y.; Lu, H.; Zhu, Q.; Jiang, S.; Liao, Y. *Bioorganic & medicinal chemistry letters* **2010**, *20*, 189.
(30) Goldfarb, D. S.; University of Rochester: U.S.A., 2009, p 57pp.
(31) Schepetkin, I. A.; Khlebnikov, A. I.; Kirpotina, L. N.; Quinn, M. T. *Journal of medicinal chemistry* **2006**, *49*, 5232.
(32) Qin, H.; Shi, J.; Noberini, R.; Pasquale, E. B.; Song, J. *The Journal of biological chemistry* **2008**, *283*, 29473.
(33) Dominianni, S. J.; Yen, T. T. *Journal of medicinal chemistry* **1989**, *32*, 2301.
(34) Saravia, M. E.; Nelson-Filho, P.; Ito, I. Y.; da Silva, L. A.; da Silva, R. A.; Emilson, C. G. *Microbiol Res* **2010**, *166*, 63.
(35) Xue, Y.; Zhang, S.; Yang, Y.; Lu, M.; Wang, Y.; Zhang, T.; Tang, M.; Takeshita, H. *Hum Exp Toxicol* **2011**.
(36) Vetting, M. W.; Hegde, S. S.; Javid-Majd, F.; Blanchard, J. S.; Roderick, S. L. *Nature structural biology* **2002**, *9*, 653.
(37) Wolf, E.; Vassilev, A.; Makino, Y.; Sali, A.; Nakatani, Y.; Burley, S. K. *Cell* **1998**, *94*, 439.
(38) Vetting, M. W.; Park, C. H.; Hegde, S. S.; Jacoby, G. A.; Hooper, D. C.; Blanchard, J. S. *Biochemistry* **2008**, *47*, 9825.
(39) Magalhaes, M. L.; Blanchard, J. S. *Biochemistry* **2005**, *44*, 16275.
(40) Boehr, D. D.; Daigle, D. M.; Wright, G. D. *Biochemistry* **2004**, *43*, 9846.

Note:

This chapter is adapted from a published manuscript: Green, K. D.; **Chen, W.**; Garneau-Tsodikova, S. *ChemMedChem* **2012**, *7*, 73. **Wenjing Chen** did the optimization of HTS assay, helped with HTS, and part of inhibition kinetics.

Chapter 6

Cosubstrate promiscuity of the aminoglycoside resistance enzyme Eis from *Mycobacterium tuberculosis*

6.1. Abstract

The ability of enzymes to accept cosubstrate derivatives has led to the development of useful biochemical probes and a unique understanding of catalytic enzymes. Previously, we demonstrated that aminoglycoside acetyltransferases (AACs), owing to their expanded cosubstrate promiscuity, have the potential to generate a variety of novel *N*-acylated aminoglycosides. The enhanced intracellular survival (Eis) protein of *Mycobacterium tuberculosis* is responsible for the resistance of this pathogen to kanamycin A in a large fraction of clinical isolates. Recently we discovered that Eis is a unique AAC capable of acetylating multiple amine groups on a large pool of aminoglycoside antibiotics, an unprecedented property among AAC enzymes. Here, we report a detailed study of the acyl-CoA cosubstrate profile of Eis. We show that, in contrast to other AACs, Eis efficiently uses only 3 out of 15 tested acyl-CoA derivatives to modify a variety of aminoglycosides. We establish that for almost all acyl-CoAs, the number of sites acylated by Eis is smaller than the number of acetylated sites. We demonstrate that the order of *n*-propionylation of the aminoglycoside neamine by Eis is the same as the order of its acetylation. We also show that the 6'-position is the first to be *n*-propionylated on amikacin and netilmicin. By sequential acylation reactions, we show that aminoglycosides can be acetylated after maximum possible *n*-propionylation of their scaffolds by Eis. The information learned herein will advance our understanding of the potential of using Eis as a target and a tool for future drug development to combat the ever-growing resistance problem.

6.2. Introduction

The tuberculosis (TB) epidemic, caused primarily by *Mycobacterium tuberculosis* (*Mtb*), kills millions of people worldwide each year. Taking into account the 2 billion currently infected and the current rate of infection, nearly 10 million people will become infected in the next year.[1] The widespread overuse of the same anti-TB drugs and the failure to comply with a proper therapeutic regimen have led to the emergence of multidrug-resistant (MDR) *Mtb* strains resistant to the first-line antibiotics isoniazid and rifampicin, as well as extensively drug-resistant (XDR) *Mtb* strains additionally rendering ineffective second-line anti-TB drugs, including the aminoglycosides (AGs) kanamycin A (KAN) and amikacin (AMK).[2,3]

Resistance to the broad-spectrum AG antibiotics is a continuously rising problem for the treatment of many serious bacterial infections.[4] AG resistance results, in great part, from the evolution or acquisition of AG-modifying enzymes (AMEs) that acetylate (AG acetyltransferases; AACs), phosphorylate (AG phosphotransferases; APHs), or nucleotidylate (AG nucleotidyltransferases; ANTs) various positions on the AG scaffolds resulting in their deactivation as antibacterials.[5] To broaden their AG-resistance profile, bacteria have also evolved bi-functional AMEs: AAC(6')-30/AAC(6')-Ib,[6] AAC(6')-Ie/APH(2'')-Ia,[7,8] AAC(3)-Ib/AAC(6')-Ib'[9-11] and ANT(3'')-Ii/AAC(6')-IId.[12,13] For a large fraction of *Mtb* clinical isolates, it was recently shown that up-regulation of the enhanced intracellular survival (Eis) protein confers KAN resistance to the mycobacterium, a hallmark of XDR-TB.[14,15] We recently discovered that Eis is a unique AAC that can modify multiple amine functionalities on a variety of AG scaffolds.[16] This novel enzyme is, to date, the only known mono-functional AME capable of catalyzing multi-acetylation reactions.

Two main directions towards combating the resistance caused by Eis can be proposed: (i) the development of novel AGs that are not Eis substrates,[17-19] and (ii) combination drug therapy[20,21] involving already approved or novel AGs used together with Eis inhibitors. Towards developing new AGs, we reported the preparation of 6'-*N*-acylated AGs[22] and 6''-thioether tobramycin (TOB) derivatives[23] and demonstrated that they can overcome

some, but not all of the Eis activity. By high-throughput screening we also identified inhibitors of Eis.[24] We previously demonstrated that the broad acyl-CoA cosubstrate promiscuity of acetyltransferases is useful for the chemoenzymatic synthesis of novel drug derivatives.[25-27]

Here, to gain insight into the mechanism of multi-acetylation of Eis and to explore the potential of this AAC as a tool for the chemoenzymatic formation of new AG scaffolds for future use as drugs, inhibitors, or probes, we performed an in-depth study of the cosubstrate promiscuity of Eis. Through sequential use of acyl-CoAs, we established the limits of Eis cosubstrate promiscuity. We also investigated the effect that the nature of different acyl-CoA derivatives has on the multiplicity of acylation.

6.3. Results

6.3.1. Acyl-CoA cosubstrate promiscuity of Eis

Table 6.1. CoA analogs kinetic parameters for Eis.

CoA analogs	AG	K_m (μM)	k_{cat} (min^{-1})	k_{cat}/K_m ($M^{-1}s^{-1}$)
AcCoA	AMK	7.88 ±1.35	1.14 ±0.30	2,411 ±757
	HYG	176.62 ±6.42	16.26 ±0.48	1,534 ±72
	KAN	9.44 ±1.20	5.56 ±0.36	9,816 ±1400
	NEA	47.30 ±1.46	4.50 ±0.36	1,586 ±136
	NEO	24.44 ±0.68	6.54 ±0.18	4,460 ±175
	NET	62.95 ±2.44	14.82 ±1.02	3,923 ±310
	PAR	45.50 ±5.52	3.24 ±0.78	1,187 ±320
	RIB	22.18 ±1.72	3.54 ±0.06	2,660 ±211
	SIS	69.41 ±0.80	4.20 ±0.12	1,009 ±31
	TOB	47.04 ±1.31	16.92 ±4.92	5,995 ±1751
ProCoA	AMK	53.14 ±6.18	1.14 ±0.30	358 ±103
	HYG	30.84 ±0.62	1.80 ±0.01	973 ±20
	KAN	55.66 ±13.28	0.48 ±0.06	144 ±39
	NEA	55.53 ±6.08	0.60 ±0.06	180 ±28
	NEO	53.22 ±0.14	1.98 ±0.12	620 ±38
	NET	31.24 ±3.76	3.23 ±0.02	1,723 ±208
	PAR	25.12 ±2.62	0.48 ±0.06	318 ±52
	RIB	66.76 ±3.61	1.32 ±0.30	330 ±77
	SIS	105.79 ±4.79	6.42 ±1.50	1,011 ±241
	TOB	74.49 ±7.78	6.36 ±0.24	1,423 ±158
CroCoA	NEO	88.86 ±7.40	0.33 ±0.04	62 ±9
MalCoA	NEO	81.49 ±5.07	1.51 ±0.02	309 ±20

We previously reported that Eis is an AAC capable of multi-acetylation of a variety of AG scaffolds by using AcCoA as a cosubstrate.[16] Here, in order to determine the cosubstrate profile of Eis, we tested fifteen additional acyl-CoA derivatives with the five Eis AG substrates with the best catalytic transfer efficiency.[16] By UV-Vis assay, we established that only three of the acyl-CoA derivatives tested, CroCoA, MalCoA, and ProCoA, displayed any significant reactivity with an AG in the presence of Eis. To gain a better understanding of the catalytic efficiency of Eis towards its accepted cosubstrates, we first determined the steady-state kinetic parameters for AcCoA and ProCoA with all ten AGs (AMK, HYG, KAN, NEA, NEO, NET, PAR, RIB, SIS, and TOB) (Table 6.1 and Fig. 6.1).

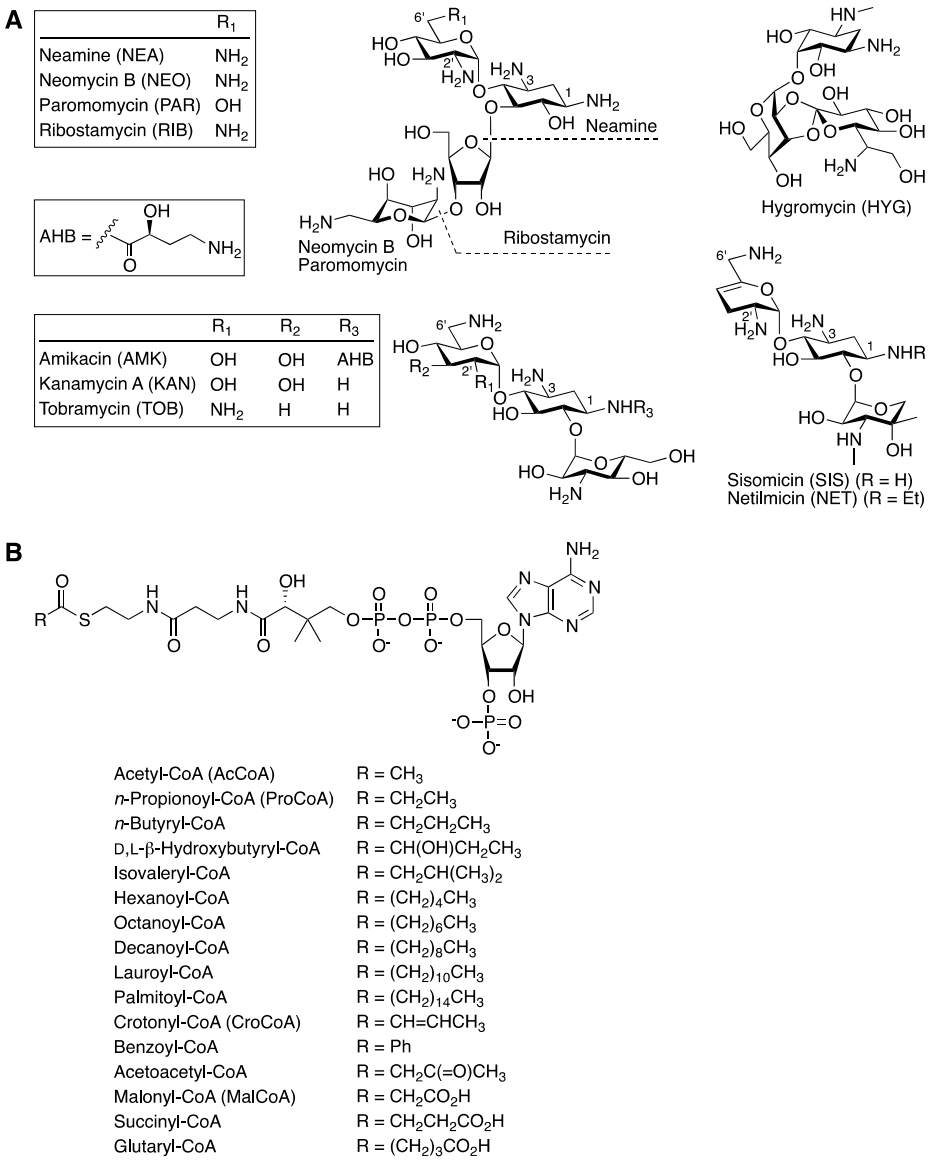

Fig. 6.1. Structures of **A.** aminoglycosides (AGs) and **B.** acyl-CoAs used in this study.

Briefly, for AcCoA the K_m values ranged from 7.88 ± 1.35 μM (AMK) to 176.62 ± 6.42 μM (HYG), representing a 22-fold range. The catalytic turnover constants varied in a 15-fold range with AMK displaying the lowest k_{cat} value (1.14 ± 0.30 min^{-1}) and TOB exhibiting the highest k_{cat} value (16.92 ± 4.92 min^{-1}). Overall, the catalytic efficiencies (k_{cat}/K_m) for AcCoA varied in a 10-fold range with SIS displaying the lowest catalytic efficiency (1,009 ± 31 $M^{-1}s^{-1}$) and KAN the highest (9,816 ± 1,400 $M^{-1}s^{-1}$). For ProCoA, the K_m values ranged from 25.12 ± 2.62 μM (PAR) to 105.79 ± 4.79 μM (SIS), a 4.2-fold range. Interestingly, the higher variability of the K_m values for AcCoA is due solely to the

two AGs that are used against TB in clinic, KAN and AMK, which display significantly lower μM K_m values than do the other AGs with AcCoA, but not with ProCoA. The k_{cat} values varied in a 13-fold range with KAN exhibiting the slowest catalytic turnover (0.48 ± 0.06 min^{-1}) and SIS the fastest (6.42 ± 1.50 min^{-1}). Generally, the catalytic efficiencies for ProCoA spanned a 8.5-fold range with KAN exhibiting the lowest k_{cat}/K_m value (144 ± 39 $M^{-1}s^{-1}$) and NET the highest (1,723 ± 208 $M^{-1}s^{-1}$). The order of AGs ranked by either their K_m or k_{cat} values was different for ProCoA from that of AcCoA. We next determined the steady-state kinetic parameters for MalCoA and CroCoA using NEO as a substrate. MalCoA had a K_m of 81.49 ± 5.07 μM and a k_{cat} of 1.51 ± 0.02 min^{-1}, resulting in a catalytic efficiency of 309 ± 20 $M^{-1}s^{-1}$. CroCoA displayed a K_m of 88.86 ± 7.40 μM and a k_{cat} of 0.33 ± 0.04 min^{-1}, yielding an efficiency of 62 ± 9 $M^{-1}s^{-1}$.

6.3.2. Multiplicity of AG acylation by Eis

Table 6.2. Comparison of the number of acylations for reactions of Eis with various acyl-CoAs and AGs.

AG	Acetyl[a] (CH_3)	*n*-Propionyl (CH_2CH_3)	Crotonyl ($CH{=}CHCH_3$)	Malonyl (CH_2CO_2H)
AMK	Tri[d]	Di[c]	Mono[b]	--[f]
HYG	Di	Mono	--	--
KAN	Di	Di	Mono	--
NEA	Tri	Di	Mono	--
NEO	Tri	Tri	Mono	Mono
NET	Di	Mono	Mono	Di
PAR	Di	Mono	Mono	Mono
RIB	Tri	Di	--	--
SIS	Tri	Mono	Mono	Mono
TOB	Tetra[e]	Di	Mono	--

[a] Data from reference 16.
[b] Mono indicates a single modification.
[c] Di indicates a double modification.
[d] Tri indicates a triple modification.
[e] Tetra indicates a quadruple modification.
[f] -- indicates no modification.

We recently reported that Eis can acetylate between two to four amines on the same AG, depending on its scaffold.[16] To investigate the maximum number of sites that can be *n*-propionylated, crotonylated, and malonylated by Eis, we monitored by mass spectrometry the reactions of ten AGs (AMK, HYG, KAN, NEA, NEO, NET, PAR, RIB, SIS, and TOB) with ProCoA, CroCoA, and MalCoA, respectively (Tables 6.2 and 6.3 as well as Figs. 6.2 to 6.5). When using ProCoA as the cosubstrate, we observed that the ten AGs tested were modified, but the number of acylations was generally different from the number of acetylations. HYG, NET, PAR and SIS were mono-*n*-propionylated, AMK, KAN, NEA, RIB, and TOB became di-*n*-propionylated, and NEO turned out to be tri-*n*-propionylated. When utilizing the CroCoA cosubstrate, we found that Eis transferred a single propenyl group to eight AG scaffolds (AMK, KAN, NEA, NEO, NET, PAR, SIS, and TOB). We determined that

MalCoA modified only four AGs, three of which were mono-malonylated (NEO, PAR, and SIS) and one di-malonylated (NET).

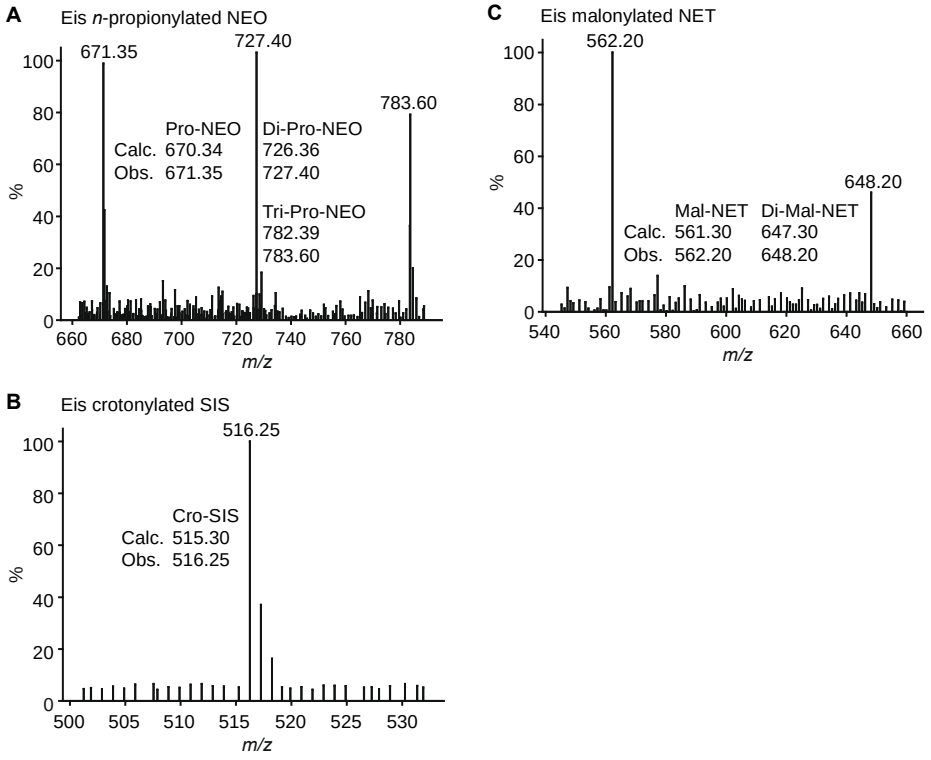

Fig. 6.2. Representative mass spectra of AGs multi-acylated by Eis. **A.** Mono-, di-, and tri-*n*-propionyl-NEO (*m/z* $[M+H]^+$ 671.35, 727.40, and 783.60, respectively) generated by reaction of NEO, Eis, and ProCoA. **B.** Mono-crotonyl-SIS (*m/z* $[M+H]^+$ 516.25) generated by reaction of SIS, Eis, and CroCoA. **C.** Mono- and di-malonyl-NET (*m/z* $[M+H]^+$ 562.20 and 648.20, respectively) generated by reaction of NET, Eis, and MalCoA.

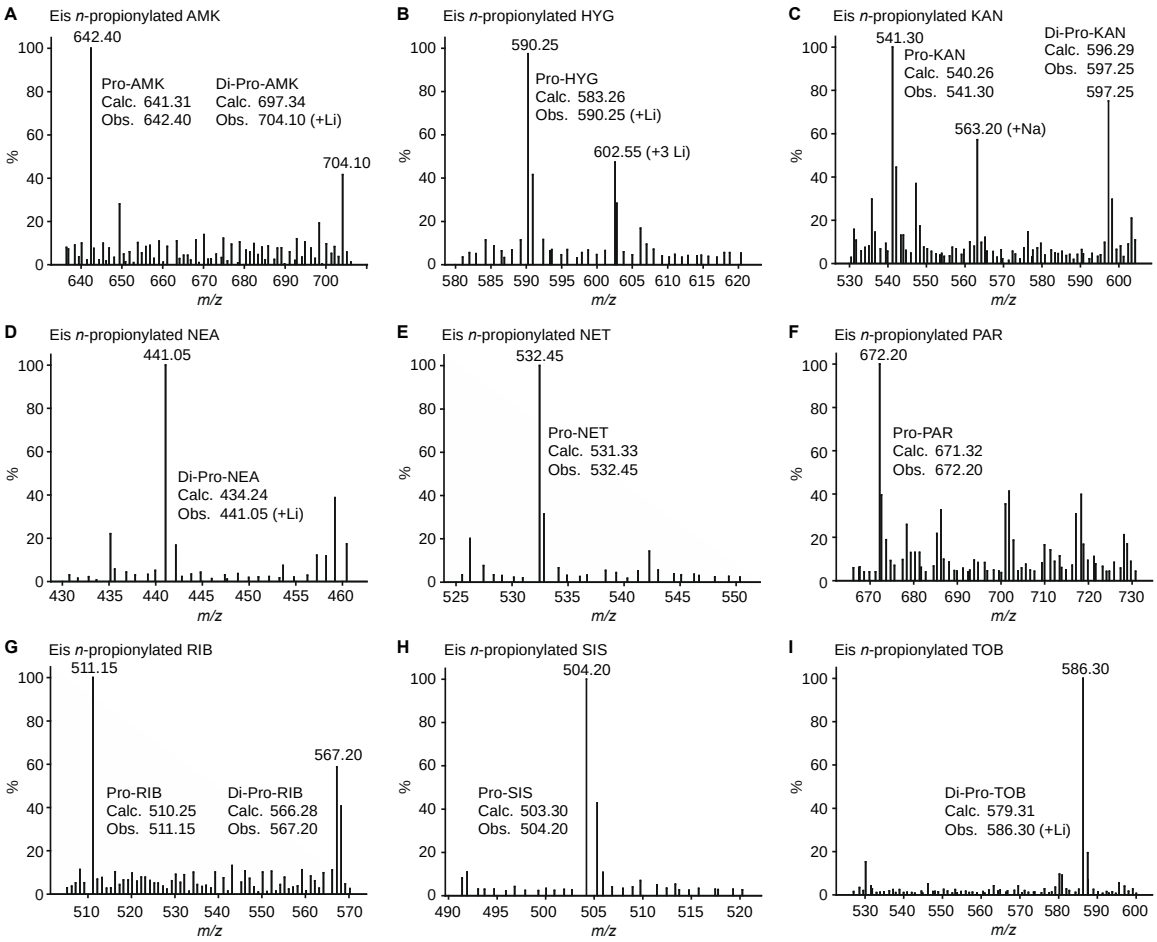

Fig. 6.3. Mass spectra for mono- and di-*n*-propionylation by Eis of various AGs: **A.** AMK (mono and di), **B.** HYG (mono), **C.** KAN (mono and di), **D.** NEA (di), **E.** NET (mono), **F.** PAR (mono), **G.** RIB (mono and di), **H.** SIS (mono), and **I.** TOB (di).

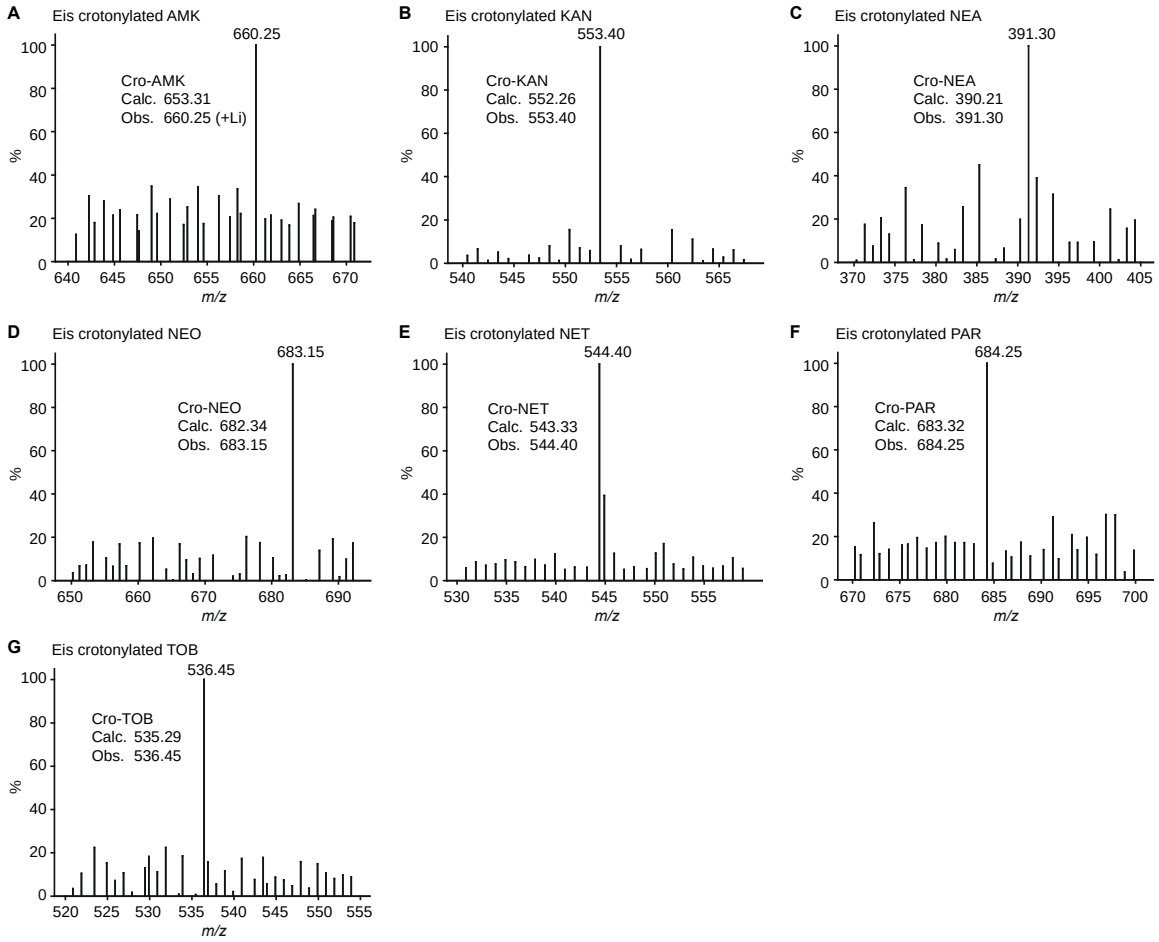

Fig. 6.4. Mass spectra for mono-crotonylation by Eis of various AGs: **A.** AMK, **B.** KAN, **C.** NEA, **D.** NEO, **E.** NET, **F.** PAR, and **G.** TOB.

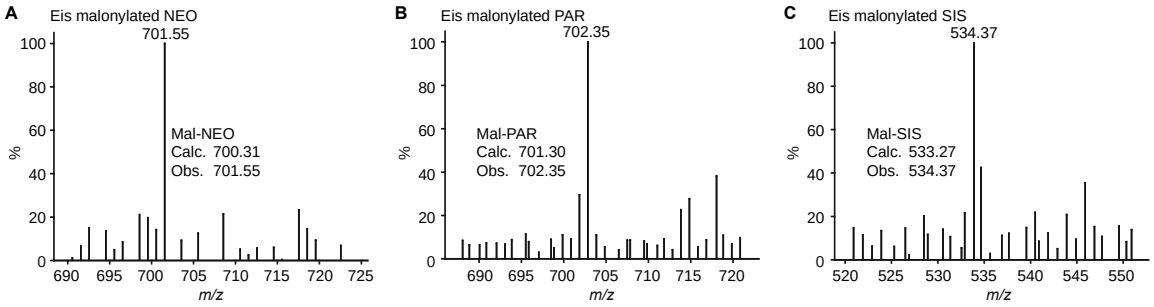

Fig. 6.5. Mass spectra for mono-malonylation by Eis of various AGs: **A.** NEO, **B.** PAR, and **C.** SIS.

Table 6.3. Mass analysis of AGs acylated by Eis.

		n-Propionylation			Crotonylation			Malonylation	
AG		Calc $[M + H]^+$	Obs $[M + H]^+$		Calc	Obs		Calc	Obs
AMK	Mono[a]	642.32	642.40	Mono	654.32	660.25 (+Li)	Mono	672.29	--[d]
	Di[b]	698.35	704.10 (+Li)						
HYG	Mono	584.27	590.25 (+Li)	Mono	569.27	--	Mono	614.24	--
KAN	Mono	541.27	541.30	Mono	553.27	553.40	Mono	571.25	--
	Di	597.30	597.25						
NEA	Mono	379.22	--	Mono	391.22	391.30	Mono	409.19	--
	Di	435.25	441.05 (+Li)						
NEO	Mono	671.35	671.35	Mono	683.35	683.15	Mono	701.32	701.55
	Di	727.37	727.40						
	Tri[c]	783.40	783.60						
NET	Mono	532.33	532.45	Mono	544.33	544.40	Mono	562.31	562.20
							Di	648.31	648.20
PAR	Mono	672.33	672.20	Mono	684.33	684.25	Mono	702.30	702.35
RIB	Mono	511.26	511.15	Mono	523.26	--	Mono	541.24	--
	Di	567.29	567.20						
SIS	Mono	504.30	504.20	Mono	516.30	516.25	Mono	534.28	534.37
TOB	Mono	524.29	--	Mono	536.29	536.45	Mono	554.27	--
	Di	580.32	586.30 (+Li)						

[a]Mono indicates mono-acylation. [b]Di indicates di-acylation. [c]Tri indicates tri-acylation. [d]-- indicates that no mass was observed.

6.3.3. Order of AG *n*-propionylation by Eis

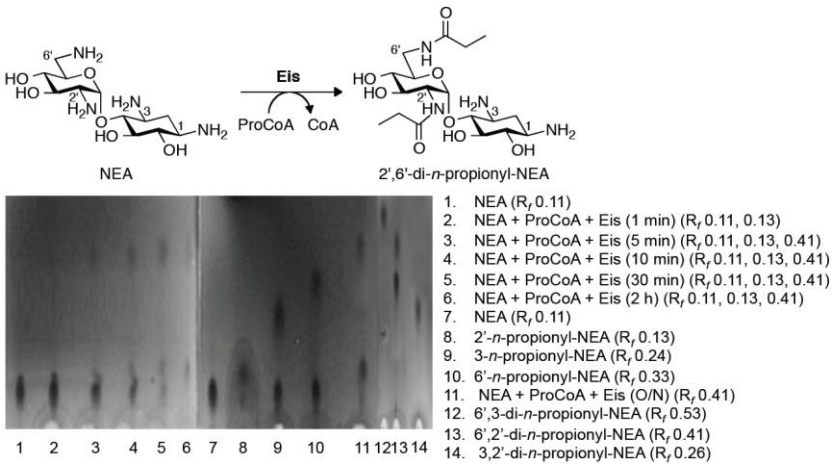

Fig. 6.6. TLC time course showing the 2'-mono- and 2',6'-di-*n*-propionylated NEA products generated by Eis using 5 equivalents of ProCoA. Control reactions for mono- and di-*n*-propionylation were done using AAC(2')-Ic, AAC(3)-IV, and AAC(6') individually or sequentially.

Earlier, we demonstrated that Eis tri-acetylates NEA in a sequential manner by first modifying the 2'-position followed by the 6'- and then 1-positions.[16] Here, we showed that Eis can di-*n*-propionylate NEA. To determine if the order of *n*-propionylation of NEA by Eis is consistent with that of the first two acetylation of this AG scaffold by this enzyme, we explored by TLC assays the regio-specificity and order of NEA *n*-propionylation by Eis (Fig. 6.6). By comparing the R_f values of *n*-propionylated Eis products formed over time to mono- and di-*n*-propionylated NEA standards obtained by using individually or sequentially AAC enzymes that catalyze a single acylation reaction (AAC(6'), AAC(3)-IV, and AAC(2')-Ic), we established that the order of *n*-propionylation of NEA was similar to that of acetylation with the 2'-position

being modified first and the 6'-position second (Table 6.4). Using a similar TLC approach we also performed a preliminary investigation of the order of *n*-propionylation of two other AGs, AMK and NET (Fig. 6.7 and Table 6.4). AMK appeared to be *n*-propionylated at the 6'-position and at a second site that could not be identified by TLC as AMK could not be di-acetylated using AAC(6'), AAC(3)-IV, and AAC(2')-Ic sequentially or simultaneously (Fig. 6.7A). By comparing the retention factor of the product of the reaction of NET with ProCoA and Eis (R_f = 0.36) to a 6'-*n*-propionoyl-NET standard (R_f = 0.36), we determined that 6'-*n*-propionoyl-NET was the product of the enzymatic reaction (Fig. 6.7B). These results indicate that the 6'-position is a common site of acylation of AGs by Eis.

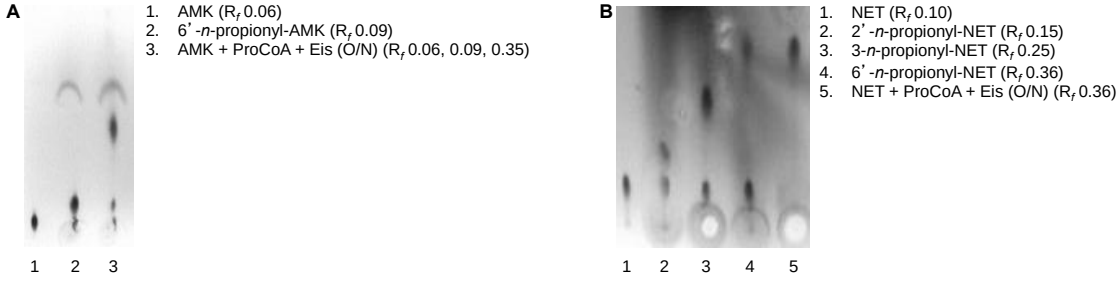

Fig. 6.7. TLC analysis of the *n*-propionylation of **A.** AMK and **B.** NET.

Table 6.4. R_f[a] values of mono- and di-*n*-propionylated AGs by AAC(2')-Ic, AAC(3)-IV, AAC(6') and Eis proteins.

		Enzymes utilized												
		None	(2')[e]	(3)[f]	(6')[g]	(3) then (2')	(6') then (2')	(6') then (3)	Eis					
AG									1 min	5 min	10 min	30 min	2 h	O/N
AMK	Parent	0.06												0.06
	Mono		--[h]	--	0.09									0.09
	Di					--	--	--						0.35
NEA	Parent[b]	0.11							0.11	0.11	0.11	0.11	0.11	
	Mono[c]		0.13	0.24	0.33				0.13	0.13	0.13	0.13	0.13	
	Di[d]					0.26	0.41	0.53		0.41	0.41	0.41	0.41	0.41
NET	Parent	0.10												
	Mono		0.15	0.25	0.36									0.36

[a]The eluent systems used for TLCs were 5:2/MeOH:NH_4OH, 3:0.8/MeOH:NH_4OH, and 12:1/MeOH:NH_4OH for AMK, NEA, and NET, respectively. [b]Parent indicates non-modified AGs. [c]Mono indicates mono-*n*-propionylated AG product. [d]Di indicates di-*n*-propionylated AG product. [e](2') indicates that the AG was *n*-propionylated using AAC(2')-Ic. [f](3) indicates that the AG was *n*-propionylated using AAC(3)-IV. [g](6') indicates that the AG was *n*-propionylated using the AAC(6') of the AAC(6')/APH(2") bifunctional enzyme. [h]-- indicates that the AG cannot be *n*-propionylated at this position.

6.3.4. Sequential modification of AGs by Eis

By close inspection of the data presented in Table 2, we observed that for almost all AGs studied the number of sites of *n*-propionylation was lower than that of acetylation. To examine if the *n*-propionylated AGs could be subsequently acetylated, we first incubated AGs with Eis and an excess of ProCoA, and after completion of the *n*-propionylation

reactions we added an excess of AcCoA. By mass spectrometry analysis, we established that the results of these sequential modification studies could be broken down into three scenarios (Table 6.5 and Fig. 6.8) where after complete *n*-propionylation: (i) some AGs, intriguingly, were further acetylated to reach the number of modifications presented in the column for acetylation reaction in Table 6.2. This was the case for AMK, NEA, PAR, and TOB, whose final products were Mono-Ac-Di-Pro-AMK, Mono-Ac-Di-Pro-NEA, Mono-Ac-Mono-Pro-PAR, and Di-Ac-Di-Pro-TOB, respectively. (ii) Some AGs were not further derivatized, which was observed when the number of *n*-propionylations reached the reported number of acetylations. This was the scenario followed by KAN and NEO where only Di-Pro-KAN and Tri-Pro-NEO were produced, respectively. (iii) The other AGs were not further modified even though the level of acetylation reported was larger than that of *n*-propionylation. This was the case for HYG, NET, RIB, and SIS where Mono-Pro-HYG, Mono-Pro-NET, Di-Pro-RIB, and Mono-Pro-SIS were formed, respectively.

Table 6.5. Mass analysis of ProCoA and AcCoA sequential and competitive reactions with AGs and Eis.

		Pro → Ac[a]			Ac + Pro[b]	
AG		Calc $[M + H]^+$	Obs $[M + H]^+$		Calc	Obs
AMK	Mono[c]-Ac-Di[d]-Pro	740.36	740.30			
				Di-Ac	670.31	670.20
				Tri[e]-Ac	712.32	712.15
HYG	Mono-Pro	584.27	584.35 / 606.35 (+Na)			
				Mono-Ac	570.25	592.35 (+Na)
				Mono-Ac-Mono-Pro	626.28	626.05
KAN	Di-Pro	597.30	597.15			
				Di-Ac	569.27	569.15
NEA	Mono-Ac-Di-Pro	477.26	477.65			
				Tri-Ac	449.22	449.25
				Di-Ac-Mono-Pro	463.24	463.20
NEO	Di-Pro	727.36	727.10			
				Tri-Ac	741.35	741.55
	Tri-Pro	783.40	783.10	Tri-Pro	783.40	783.50
NET	Mono-Pro	532.33	532.25			
				Mono-Ac	518.32	518.25
				Di-Ac	560.33	560.20
PAR	Mono-Ac-Mono-Pro	714.34	714.25			
				Di-Ac	700.32	700.25
RIB	Di-Pro	567.29	567.15			
				Di-Ac	539.26	539.30
SIS	Mono-Pro	504.30	504.20 / 526.10 (+Na)			
				Mono-Ac	490.29	490.05
				Di-Ac	532.30	532.30
				Mono-Ac-Mono-Pro	546.32	546.30
TOB	Mono-Ac-Di-Pro	622.33	622.25			
	Di-Ac-Di-Pro	664.34	664.60			
				Di-Ac	552.29	552.40
				Tri-Ac	594.30	594.25
				Tetra-Ac	636.31	636.45

[a]ProCoA (5 eq) reactions with Eis (5 μM) and AG (1 eq) were followed by incubation with AcCoA (5 eq) and an additional Eis (5 μM). [b]AcCoA (5 eq) and ProCoA (5 eq) were incubated simultaneously with Eis (10 μM) and AG (1 eq). [c]Mono indicates mono-acylation. [d]Di indicates di-acylation. [e]Tri indicates tri-acylation.

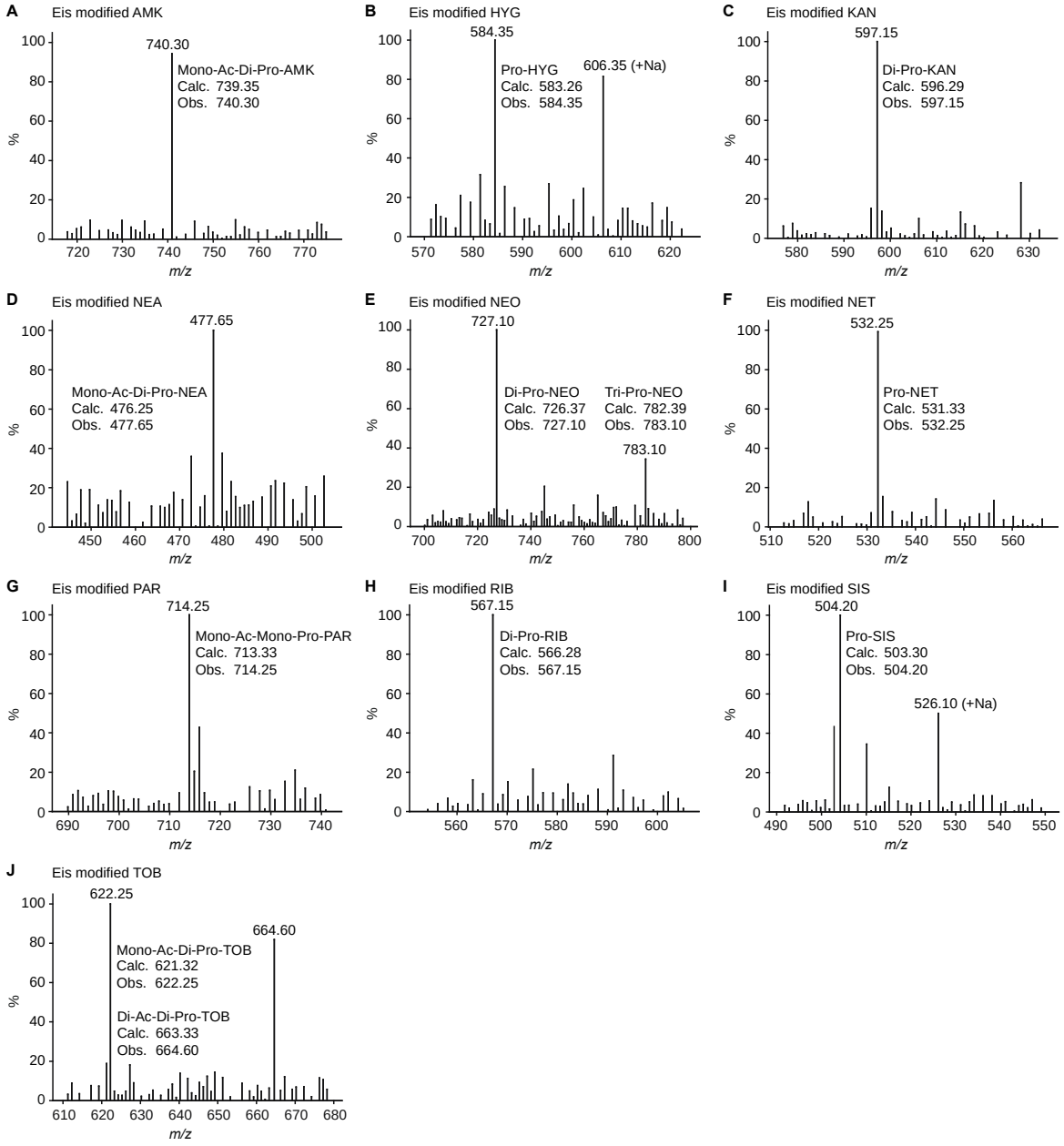

Fig. 6.8. Mass spectra for sequential reactions monitoring *n*-propionylation followed by acetylation by Eis of various AGs: **A.** AMK, **B.** HYG, **C.** KAN, **D.** NEA, **E.** NEO, **F.** NET, **G.** PAR, **H.** RIB, **I.** SIS, and **J.** TOB.

6.3.5. Competition assays using AcCoA and ProCoA simultaneously for AG modifications by Eis

As both AcCoA and ProCoA are found in abundance inside bacterial cells, to corroborate our steady-state kinetic analysis studies, we performed cosubstrate competition assays where AGs were incubated in the presence of Eis and a 1:1 mixture of AcCoA and

ProCoA (Table 6.5 and Fig. 6.9). As expected, in all cases (AMK, KAN, NET, PAR, and RIB) where the catalytic efficiencies for transfer of an acetyl group were far superior to those for transfer of an *n*-propionyl moiety, multi-acetylation occurred almost exclusively. Two exceptions to this pattern were observed with NEA and NEO. For NEA, with k_{cat}/K_m values of 1,586 $\pm$ 136 $M^{-1}s^{-1}$ for AcCoA and 180 $\pm$ 32 $M^{-1}s^{-1}$ for ProCoA, one would have expected multi-acetylation to be almost exclusive. However, Di-Ac-Mono-Pro-NEA was detected by mass spectrometry when NEA was reacted with a 1:1 mixture of AcCoA and ProCoA. For NEO, with k_{cat}/K_m values of 4,460 $\pm$ 39 $M^{-1}s^{-1}$ for AcCoA and 620 $\pm$ 38 $M^{-1}s^{-1}$ for ProCoA, one would have expected multi-acetylation to dominate. However, both Tri-Ac-NEO and Tri-Pro-NEO were detected by mass spectrometry. As predicted for HYG and SIS, which had similar catalytic efficiencies for AcCoA (1,534 $\pm$ 72 $M^{-1}s^{-1}$ for HYG and 1,009 $\pm$ 31 $M^{-1}s^{-1}$ for SIS) and ProCoA (973 $\pm$ 20 $M^{-1}s^{-1}$ for HYG and 1,011 $\pm$ 241 $M^{-1}s^{-1}$ for SIS), Mono-Ac-Mono-Pro-AG were detected by mass spectrometry.

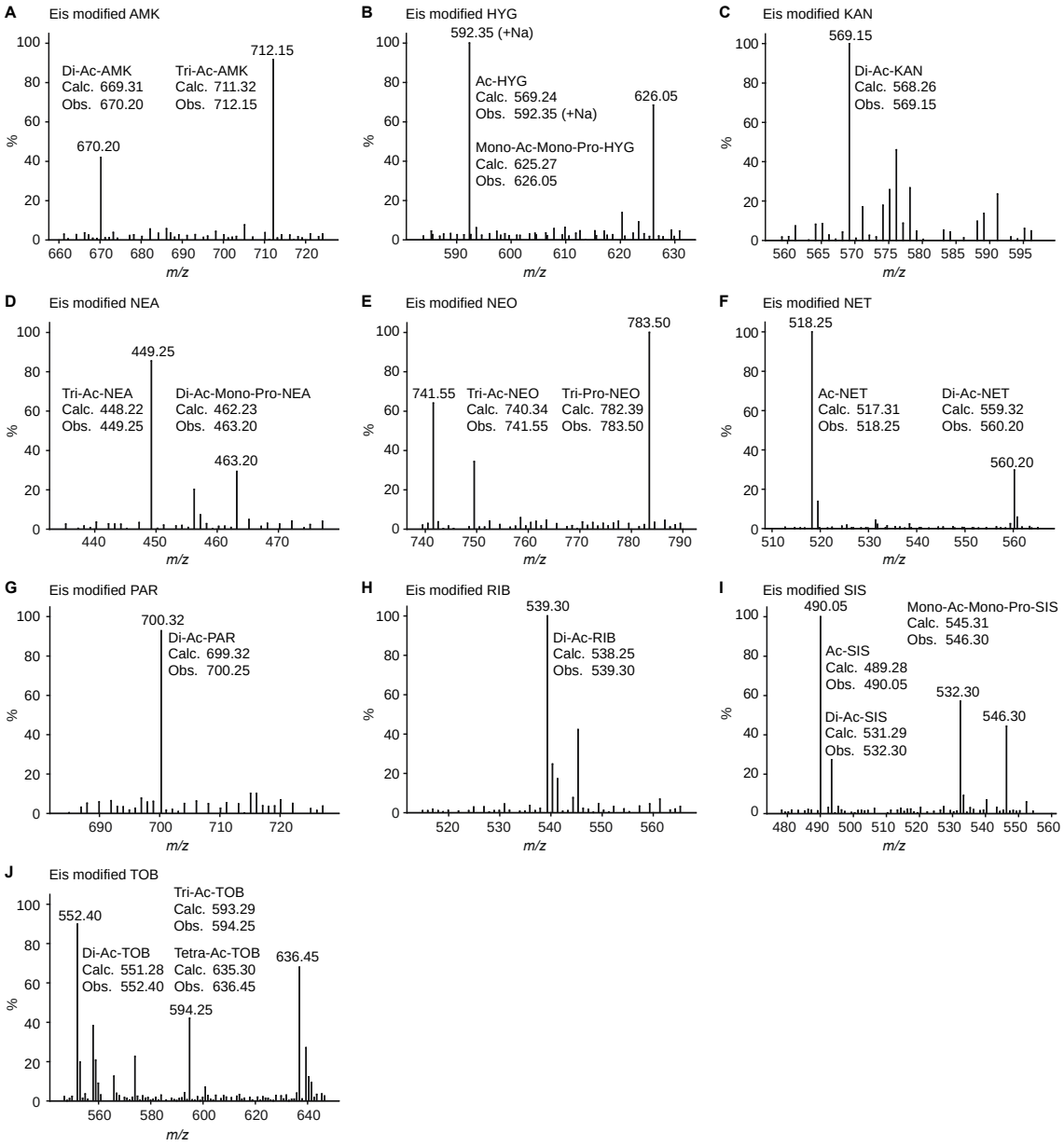

Fig. 6.9. Mass spectra for reactions monitoring the competition between *n*-propionylation and acetylation by Eis of various AGs: **A.** AMK, **B.** HYG, **C.** KAN, **D.** NEA, **E.** NEO, **F.** NET, **G.** PAR, **H.** RIB, **I.** SIS, and **J.** TOB.

6.4. Discussion

Many studies aimed at utilizing the natural and/or engineered substrate and/or cosubstrate promiscuity of enzymes for scaffold diversification or building block preparation towards the development of new drugs have been reported. For example, the catalytically promiscuous hydrolases have been extensively used for non-conventional reactions in organic synthesis.[28] By exploiting the promiscuous aldolase activity of the enzyme

macrophomate synthase, differentially protected 3-deoxysugars, important constituents of complex carbohydrates, were synthesized.[29] By using the natural cosubstrate promiscuity of the acyltransferase CouN7, novel novobiocin analogs were chemoenzymatically generated.[30] By engineering of the macrolide cytochrome P450 monooxygenase PikC, new series of regio-selectively hydroxylated carbocyclic rings linked to a desosamine glycoside were prepared.[31] By using the aldehyde substrate promiscuity of the strictosidine synthase family of enzymes, asymmetric tetrahydro-β-carbolines were biocatalytically formed.[32] By using ketoreductase enzymes capable of stereo-specifically reducing a range of diketide substrates, the potential of these polyketide synthase enzymes as biocatalysts for the chemoenzymatic formation of chiral building blocks was demonstrated.[33] By taking advantage of the cosubstrate promiscuity of AAC(3)-IV, a chemoenzymatic route to diversify AGs enabled the development of a microarray-based method to probe acetyltransferase activity.[34]

We have demonstrated that Eis is an AAC capable of multi-acetylating a large number of AGs.[16] We also previously showed that one could take advantage of the natural AG and acyl-CoA cosubstrate promiscuity of AACs to chemoenzymatically synthesize novel mono-, homo-di-, and hetero-di-*N*-acylated AGs.[26] Here, we performed a detailed study to establish the acyl-CoA cosubstrate promiscuity of Eis in order to gain insight into its multi-acetylation mechanism and to probe its potential as a tool for drug development.

We first examined the cosubstrate profile of Eis using sixteen acyl-CoAs with five AGs. Doing so, we observed that in contrast with AAC(3)-IV and AAC(6')/APH(2") that exhibit broad cosubstrate promiscuity, Eis catalyzed transfer only from a small set of the acyl-CoA derivatives. In addition to the natural cosubstrate AcCoA, only CroCoA, MalCoA, and ProCoA were found to act as cosubstrates of Eis. To rationalize the limited cosubstrate promiscuity of Eis, we closely examined its structure and those of other AACs with bound cosubstrate, including a putative AAC(3) from *B. anthracis*[35] and other AAC(3)s,[36,37] AAC(2')-Ic from *M. tuberculosis*,[38] and AAC(6')s.[39-44] Even though the AG-binding pocket of Eis is larger, the access to it is more limited than in other AACs due to the presence of the central GNAT region, absent in other AACs, whose surface

contributes to the substrate-binding pocket (Fig. 6.10A).[16] For example, in AAC(6')-Ii from *Enterococcus faecium*[44] the AG-binding pocket is open to entry both in the direction orthogonal to the Ppant arm of AcCoA (from the side of the viewer in Fig. 6.10B) and in the direction along the Ppant arm towards the thiol moiety (from the left-hand side in Fig. 6.10B), whereas for Eis access is possible only in the orthogonal direction. Therefore, it is likely that the larger acyl groups of cosubstrates other than those accepted by Eis block the access of the AG to the binding pocket in Eis, but not in other AACs. Interestingly, while Eis could not transfer the acyl moieties of CoA derivatives with bulkier (benzoyl, bromo-thiophene-2-carbonyl, and fluoro-picolinyl) or longer (butyryl and glutaryl) acyl groups that AAC(3)-IV and AAC(6')/APH(2") could transfer to a variety of AGs, Eis was found to readily transfer the crotonyl moiety to eight AGs that the other two AACs could not. With the exception of KAN and NEO for which the number of sites *n*-propionylated and acetylated were identical, we observed that in every other case the number of sites acylated was less than that of sites acetylated (Table 6.2). Not surprisingly, while the smaller and less rigid ProCoA could be transferred to more than one positions on six of the ten AGs tested, the larger malonyl and the less flexible crotonyl moieties generally only got transferred to one amine on some of the AGs tested.

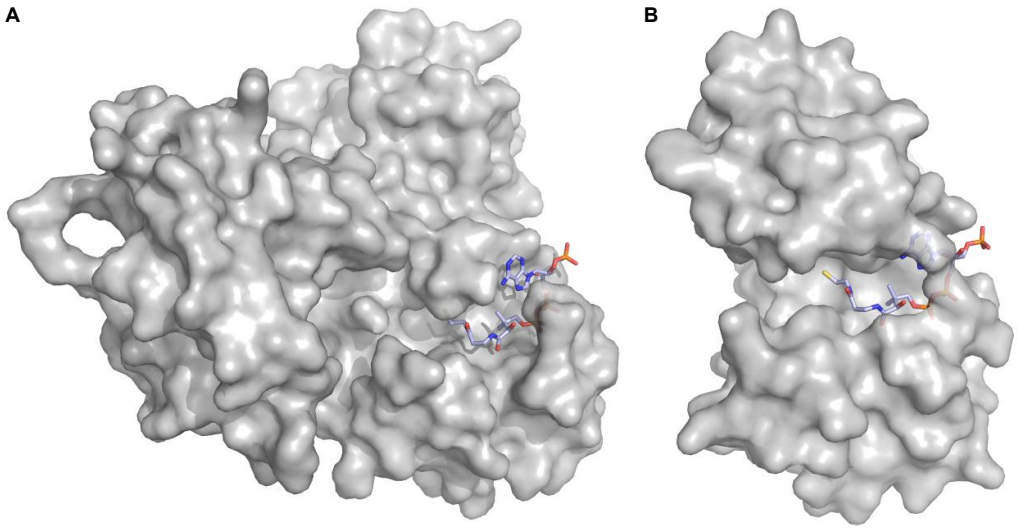

Fig. 6.10. Surface representations of **A.** *M. tuberculosis* Eis (PDB ID: 3R1K) and **B.** *E. faecium* AAC(6')-Ii (PDB ID: 1N71) monomers in complex with CoA (shown as sticks).

We next determined the kinetic parameters (K_m and k_{cat}) for Eis and acyl-CoAs with a variety of AGs and established that for the majority of the AGs tested the binding affinity of ProCoA to Eis was less than that of AcCoA (Table 6.1). We first corroborated our

kinetic data by exploring the sequential modifications of AGs by Eis using first an excess of ProCoA followed by an excess of AcCoA (Table 6.5 and Fig. 6.8). In the cases where the number of *n*-propionylated sites was smaller than that of acetylated sites and where the catalytic efficiency (k_{cat}/K_m) of transfer of the acyl group was much lower for ProCoA than AcCoA, we observed that after maximum *n*-propionylation the AGs were further acetylated to reach the number of modified sites equal to the maximum number of acetylations observed previously. With the exception of RIB that did not get further acetylated after di-*n*-propionylation, this was the case for AMK, NEA, PAR, and TOB. AMK with k_{cat}/K_m values of 2,411 ± 757 $M^{-1}s^{-1}$ and 358 ± 103 $M^{-1}s^{-1}$ for AcCoA and ProCoA, respectively, was transformed into Mono-Ac-Di-Pro-AMK. NEA with k_{cat}/K_m values of 1,586 ± 136 $M^{-1}s^{-1}$ and 180 ± 28 $M^{-1}s^{-1}$ for AcCoA and ProCoA, respectively, was converted into Mono-Ac-Di-Pro-NEA. PAR with k_{cat}/K_m values of 1,187 ± 320 $M^{-1}s^{-1}$ and 318 ± 52 $M^{-1}s^{-1}$ for AcCoA and ProCoA, respectively, was modified into Mono-Ac-Mono-Pro-PAR. TOB with k_{cat}/K_m values of 5,995 ± 1,751 $M^{-1}s^{-1}$ and 1,423 ± 158 $M^{-1}s^{-1}$ for AcCoA and ProCoA, respectively, was transformed into Di-Ac-Di-Pro-TOB. In the cases of HYG, NET, and SIS, where the number of sites *n*-propionylated was lower than that of positions acetylated and the catalytic efficiency (k_{cat}/K_m) of transfer of the acyl group was similar for ProCoA than AcCoA, we observed that the AGs were not further acetylated after complete *n*-propionylation. Finally, as expected, regardless of the catalytic efficiency of acyl transfers, we observed that KAN and NEO were not further acetylated by Eis after di- and tri-*n*-propionylation as the level of number of sites acetylated by the enzyme is equal to that *n*-propionylated. We conclude that modification with large acyl group must, at least in some cases, prevent binding of the acylated AG to allow further acylation or acetylation for steric reasons.

We also corroborated our steady-state kinetic analysis studies and gained valuable knowledge about Eis by investigating the competition between *n*-propionylation and acetylation of AGs by this enzyme (Table 6.5 and Fig. 6.9). In agreement with their much higher k_{cat}/K_m values for AcCoA, we observed that AMK, KAN, NET, PAR, RIB, and TOB were solely acetylated when reacted with a 1:1 mixture of ProCoA and AcCoA. The aforementioned AGs have a higher catalytic efficiency, lower K_m value, higher catalytic

turnover rate, or a combination of these properties, which all can explain the dominating effect of AcCoA in the competition assays. Interestingly in the case of RIB, we observed only di-acetylation of the AG in the presence of a 1:1 mixture of AcCoA and ProCoA, potentially suggesting that the presence of ProCoA inhibits the transfer of the third acetyl group to Di-Ac-RIB and *n*-propionylation cannot occur at the third acylation site of this AG. Interestingly, in the case of NEO where the k_{cat}/K_m values for AcCoA (4,460 ± 175 $M^{-1}s^{-1}$) was much larger than that for ProCoA (620 ± 38 $M^{-1}s^{-1}$), one would have expected multi-acetylation to be dominant. However, both Tri-Ac-NEO and Tri-Pro-NEO were generated when NEO was reacted with a 1:1 mixture of AcCoA and ProCoA. This implies that after the first modification with a particular cosubstrate, only the second and third modifications by a different cosubstrate are strongly disfavored. In addition, the modifications do not follow the same rank order of catalytic efficiency. A plausible model for this effect is that after a NEO molecule is modified once by either AcCoA or ProCoA, the modified AG does not leave the enzyme active site, rather, the second and third modifications occur before the singly-modified AG can dissociate from the binding site resulting in the homogeneity of the modifications of NEO. Finally, as expected, in the case of HYG and SIS where the k_{cat}/K_m values for AcCoA (1,534 ± 72 $M^{-1}s^{-1}$ for HYG and 1,009 ± 31 $M^{-1}s^{-1}$ for SIS) and ProCoA (973 ± 20 $M^{-1}s^{-1}$ for HYG and 1,011 ± 241 $M^{-1}s^{-1}$ for SIS) were very similar, both acetylation and *n*-propionylation occurred. The reaction of a 1:1/AcCoA:ProCoA mixture with HYG in the presence of Eis resulted in Mono-Ac-Mono-Pro-HYG. From our sequential experiments, we established that acetylation of HYG must occur first in order for Mono-Ac-Mono-Pro-HYG to be formed. We also previously reported that HYG can be di-acetylated.[16] Therefore, it can be hypothesized that Mono-Ac-HYG is a better substrate for *n*-propionylation than for a second acetylation. We can also draw a similar conclusion from the results obtained with SIS. The reaction of SIS with a 1:1/AcCoA:ProCoA mixture in the presence of Eis resulted in Mono-Ac-SIS, Di-Ac-SIS, and Mono-Ac-Mono-Pro-SIS. Since we know that mono-*n*-propionylation of SIS results in an unreactive species in our sequential experiments, we can conclude that acetylation must occur before *n*-propionylation in order to generate Mono-Ac-Mono-Pro-SIS. Based on the competition assay (Table 6.5) and the determined kinetic parameters (Table 6.1), we also conclude that Mono-Ac-SIS

has a similar propensity to become acetylated the second time or to become *n*-propionylated.

In summary, we have presented evidence that Eis displays some cosubstrate promiscuity, accepting AcCoA, ProCoA, CroCoA, and MalCoA for the multi-acylation of AGs, albeit more limited than that of AACs of other families. We have established the number of sites acylated these cosubstrates on a variety of AG scaffolds. We have demonstrated that the order of multi-acylation for NEA is identical to that of multi-acetylation. We have shown that after complete *n*-propionylation, further acetylations can be allowed up to the level of multi-acetylation allowed by Eis. Finally, by steady-state kinetic assays and acylation competition assays we have gained insight into the mechanism of multi-acylation of AGs by Eis. In conjunction with our previously reported work on the redesign of cosubstrate specificity of acetyltransferase enzymes,[45] this work sets the stage for future expansion of the cosubstrate promiscuity of Eis for its use as a regio-versatile tool for the production of novel AG derivatives, probes, and inhibitors for potential drug development.

6.5. Materials and methods

6.5.1. Materials and instrumentation

The Eis, AAC(6')-Ie/APH(2'')-Ia, AAC(3)-IV[46] and AAC(2')-Ic[38] enzymes were expressed and purified as previously described.[16,26] AAC(6')-Ie/APH(2'')-Ia was used solely for its AAC(6') activity and is referred as AAC(6') from here on. The acyl-CoAs [acetyl-CoA (AcCoA), acetoacetyl-CoA, benzoyl-CoA, *n*-butyryl-CoA, crotonyl-CoA (CroCoA), glutaryl-CoA, D,L-β-hydroxybutyryl-CoA, isovaleryl-CoA, malonyl-CoA (MalCoA), palmitoyl-CoA, *n*-propionyl-CoA (ProCoA), hexanoyl-CoA, lauroyl-CoA, octanoyl-CoA, succinyl-CoA, and decanoyl-CoA] (Fig. 6.1), 4,4'-dithiodipyridine (DTDP), ammonium molybdate, ammonium cerium nitrate, and the AGs [AMK, hygromycin (HYG), KAN, neomycin B (NEO), paromomycin (PAR), ribostamycin (RIB), sisomicin (SIS), and tobramycin (TOB)] (Fig. 6.1) were purchased from Sigma-Aldrich (Milwaukee, WI). The AGs neamine (NEA) and netilmicin (NET) were purchased from AK Scientific (Mountain View, CA) (Fig. 6.1). 96-Well plates were

bought from Thermo Fisher Scientific (Waltham, MA). UV-Vis assays were monitored on a SpectraMax M5 plate reader. Liquid chromatography mass spectrometry (LCMS) was performed on a Shimadzu LCMS-2019EV equipped with a SPD-20AV UV-Vis detector and a LC-20AD liquid chromatograph. All pHs were adjusted at rt.

6.5.2. Determination of cosubstrate profile for Eis proteins by UV-Vis assays

To determine which CoA derivatives were cosubstrates for Eis, fifteen CoA derivatives (acetoacetyl-CoA, benzoyl-CoA, *n*-butyryl-CoA, CroCoA, glutaryl-CoA, D,L-β-hydroxybutyryl-CoA, isovaleryl-CoA, MalCoA, palmitoyl-CoA, ProCoA, hexanoyl-CoA, lauroyl-CoA, octanoyl-CoA, succinyl-CoA, and decanoyl-CoA) were tested against several AGs (KAN, NEO, NET, SIS, and TOB). Reactions with AcCoA were used as positive controls. The acylation activity of Eis was monitored at 324 nm (ε_{324} = 19,800 $M^{-1}cm^{-1}$) by a UV-Vis assay using DTDP, as previously reported.[26] Reaction mixtures (200 μL) containing a CoA derivative (0.5 mM, 5 eq), AG (0.1 mM, 1 eq), DTDP (2 mM), and Tris-HCl (50 mM, pH 8.0), were initiated by addition of Eis (0.5 μM) at 25 ℃. Reactions were monitored by taking readings every 30 s for 60 min in 96-well plates. In addition to AcCoA, only CroCoA, MalCoA, and ProCoA were found to be cosubstrates of Eis and were further studied with all AGs (AMK, HYG, KAN, NEA, NEO, NET, PAR, RIB, SIS, and TOB) as described below.

6.5.3. Determination of cosubstrate profile for Eis proteins by LCMS

By using LCMS, the results obtained by UV-Vis assays were confirmed and the degree of acylations was determined for all ten AG substrates. Reactions (30 μL) containing AG (0.67 mM, 1 eq), CoA derivatives (3.35 mM, 5 eq), Tris-HCl (50 mM, pH 8.0), and Eis (10 μM) were incubated at rt for 48 h. The Eis protein was then precipitated by addition of ice-cold MeOH (30 μL) to the reaction mixture, which was then kept at -20 ℃ for at least 20 min. The precipitated protein was removed by centrifugation (13,000 rpm, rt, 10 min). The supernatant (10 μL) was diluted with H_2O (20 μL) and loaded onto the LCMS. The masses of the acylated AGs present in each sample were determined in positive

mode using H_2O (0.1% formic acid). MS of all AGs modified by Eis are shown in Figs. 6.2 to 6.5 and Table 6.3.

6.5.4. Steady-state kinetic measurements for CoA derivatives

The kinetic parameters for AcCoA and ProCoA were determined against ten AGs (AMK, KAN, HYG, NEA, NEO, NET, PAR, RIB, SIS, and TOB) in reactions (100 μL) containing a fixed concentration of AG (0.5 mM), varying concentrations of CoA derivatives (0, 20, 50, 100, 250, 500 μM), DTDP (2 mM), Tris-HCl (50 mM, pH 8.0), and Eis (0.25 μM). Using similar reaction conditions, the kinetic parameters for MalCoA and CroCoA were determined in reactions (100 μL) containing a fixed concentration of NEO (1 mM). Reactions were initiated by addition of CoA derivatives and were carried out at least in duplicate at 25 ℃. The reactions were monitored as described above, by taking measurements every 15 s for 15 min. The kinetic parameters K_m and k_{cat} were determined from Lineweaver-Burk plots (Table 6.1).

6.5.5. Thin-layer chromatography (TLC) assays

The eluent system used for AMK reactions was 5:2/MeOH:NH_4OH (~25% in H_2O). The eluent system utilized for NEA reactions was 3:0.8/MeOH:NH_4OH (~25% in H_2O). The eluent system employed for NET reactions was 12:1/MeOH:NH_4OH (~25% in H_2O). AGs were visualized on Silica gel 60 F_{254} TLCs (Merck) by using a cerium-molybdate stain composed of $(NH_4)_2Ce(NO_3)_6$ (5 g), $(NH_4)_6Mo_7O_{24}•4H_2O$ (120 g) in 10% H_2SO_4 (1 L). The observed R_f values are reported in Table 6.4. The exact reaction conditions are reported below.

6.5.5.1. Control TLCs for mono-*n*-propionylated AGs at the 2'-, 3-, or 6'-positions

Reactions (10 μL) were performed at rt in MES buffer (50 mM, pH 6.6 for AAC(3)-IV and AAC(6')) or in potassium phosphate buffer (100 mM, pH 7.0 for AAC(2')-Ic) with ProCoA (0.96 mM, 1.2 eq), AG (0.8 mM, 1 eq), and AAC enzyme (10 μM). After overnight incubation, aliquots (5 μL) of the reaction mixtures were loaded onto a TLC plate and eluted using the solvent system described above.

6.5.5.2. Control TLCs for di-*n*-propionylated NEA by sequential enzymatic reactions

Reactions (10 μL) were performed at rt in MES buffer (50 mM, pH 6.6 adjusted at rt) with ProCoA (1.92 mM, 2.4 eq), NEA (0.8 mM, 1 eq), and AAC(6') or AAC(3)-IV (10 μM). After overnight incubation, the second AAC enzyme (AAC(2')-Ic or AAC(3)-IV) (10 μM) was added to the reaction mixture. After an additional 24 h of incubation, aliquots (5 μL) of each di-*n*-propionylation reaction mixture were loaded onto a TLC plate and eluted using the solvent system described above.

6.5.5.3. TLCs for *n*-propionylation of AMK and NET by Eis

Reactions (20 μL) were performed at rt in Tris-HCl buffer (50 mM, pH 8.0) with ProCoA (2.5 mM, 5 eq), AG (0.5 mM, 1 eq), and Eis (10 μM). After overnight incubation, aliquots (5 μL) of the reaction mixture were loaded onto a TLC plate and eluted using the solvent system described above (Fig. 6.7).

6.5.5.4. TLC time course for *n*-propionylation of NEA by Eis

Reactions (30 μL) were performed at rt in Tris-HCl buffer (50 mM, pH 8.0) with ProCoA (2.5 mM, 5 eq), NEA (0.5 mM, 1 eq), and Eis (5 μM). Aliquots (4 μL) were loaded and run onto a TLC plate after 0, 1, 5, 10, 30, 120 min, and overnight incubation using the solvent system described above (Fig. 6.6).

6.5.6. Monitoring by LCMS of sequential acylations by Eis using ProCoA followed by AcCoA

Reactions (30 μL) containing AG (0.67 mM, 1 eq), ProCoA (3.35 mM, 5 eq), Tris-HCl (50 mM, pH 8.0), and Eis (5 μM) were incubated at rt for 48 h prior to addition of AcCoA (3.35 mM, 5 eq) and an additional portion of Eis (5 μM), which brought the total volume of the reaction to 50 μL. After another 48 h of incubation, the Eis protein was precipitated by addition of ice-cold MeOH (50 μL) to the reaction mixture, which was then kept at -20 ℃ for at least 20 min. The precipitated protein was removed by centrifugation (13,000 rpm, rt, 10 min). An aliquot of the supernatant (20 μL) was

analysed by LCMS in the positive mode by using 0.1% v/v formic acid in H_2O (Fig. 6.8 and Table 6.5).

6.5.7. Monitoring by LCMS of acylation reactions by Eis using ProCoA and AcCoA simultaneously

Reactions (50 μL) containing AG (0.67 mM, 1 eq), AcCoA (3.35 mM, 5 eq), ProCoA (3.35 mM, 5 eq), Tris-HCl (50 mM, pH 8.0), and Eis (10 μM) were incubated at rt for 48 h, after which they were processed and analysed by LCMS as described above for the sequential acylations (Fig. 6.9 and Table 6.5).

6.6. References

(1) Dye, C.; Williams, B. G. *Science* **2010**, *328*, 856.
(2) Caminero, J. A.; Sotgiu, G.; Zumla, A.; Migliori, G. B. *Lancet Infect Dis* **2010**, *10*, 621.
(3) Georghiou, S. B.; Magana, M.; Garfein, R. S.; Catanzaro, D. G.; Catanzaro, A.; Rodwell, T. C. *PLoS One* **2012**, *7*, e33275.
(4) Houghton, J. L.; Green, K. D.; Chen, W.; Garneau-Tsodikova, S. *Chembiochem : a European journal of chemical biology* **2010**, *11*, 880.
(5) Ramirez, M. S.; Tolmasky, M. E. *Drug Resist Updat* **2010**, *13*, 151.
(6) Zhang, W.; Fisher, J. F.; Mobashery, S. *Curr Opin Microbiol* **2009**, *12*, 505.
(7) Boehr, D. D.; Daigle, D. M.; Wright, G. D. *Biochemistry* **2004**, *43*, 9846.
(8) Caldwell, S. J.; Berghuis, A. M. *Antimicrob Agents Chemother* **2012**, *56*, 1899.
(9) Green, K. D.; Chen, W.; Garneau-Tsodikova, S. *Antimicrobial agents and chemotherapy* **2011**, *55*, 3207.
(10) Dubois, V.; Poirel, L.; Marie, C.; Arpin, C.; Nordmann, P.; Quentin, C. *Antimicrobial agents and chemotherapy* **2002**, *46*, 638.
(11) Kim, C.; Villegas-Estrada, A.; Hesek, D.; Mobashery, S. *Biochemistry* **2007**, *46*, 5270.
(12) Centron, D.; Roy, P. H. *Antimicrobial agents and chemotherapy* **2002**, *46*, 1402.
(13) Kim, C.; Hesek, D.; Zajicek, J.; Vakulenko, S. B.; Mobashery, S. *Biochemistry* **2006**, *45*, 8368.
(14) Campbell, P. J.; Morlock, G. P.; Sikes, R. D.; Dalton, T. L.; Metchock, B.; Starks, A. M.; Hooks, D. P.; Cowan, L. S.; Plikaytis, B. B.; Posey, J. E. *Antimicrobial agents and chemotherapy* **2011**, *55*, 2032.
(15) Zaunbrecher, M. A.; Sikes, R. D., Jr.; Metchock, B.; Shinnick, T. M.; Posey, J. E. *Proceedings of the National Academy of Sciences of the United States of America* **2009**, *106*, 20004.
(16) Chen, W.; Biswas, T.; Porter, V. R.; Tsodikov, O. V.; Garneau-Tsodikova, S. *Proceedings of the National Academy of Sciences of the United States of America* **2011**, *108*, 9804.
(17) Aggen, J. B.; Armstrong, E. S.; Goldblum, A. A.; Dozzo, P.; Linsell, M. S.; Gliedt, M. J.; Hildebrandt, D. J.; Feeney, L. A.; Kubo, A.; Matias, R. D.; Lopez, S.; Gomez, M.; Wlasichuk, K. B.; Diokno, R.; Miller, G. H.; Moser, H. E. *Antimicrob Agents Chemother* **2010**, *54*, 4636.
(18) You, X. F.; Li, C. R.; Yang, X. Y.; Yuan, M.; Zhang, W. X.; Lou, R. H.; Wang, Y. M.; Li, G. Q.; Chen, H. Z.; Song, D. Q.; Sun, C. H.; Cen, S.; Yu, L. Y.; Zhao, L. X.; Jiang, J. D. *Antimicrob Agents Chemother* **2009**, *53*, 4525.
(19) Li, J.; Chiang, F. I.; Chen, H. N.; Chang, C. W. *Bioorg Med Chem* **2007**, *15*, 7711.
(20) Ramon-Garcia, S.; Ng, C.; Anderson, H.; Chao, J. D.; Zheng, X.; Pfeifer, T.; Av-Gay, Y.; Roberge, M.; Thompson, C. J. *Antimicrobial agents and chemotherapy* **2011**, *55*, 3861.
(21) Sterling, T. R.; Villarino, M. E.; Borisov, A. S.; Shang, N.; Gordin, F.; Bliven-Sizemore, E.; Hackman, J.; Hamilton, C. D.; Menzies, D.; Kerrigan, A.; Weis, S. E.; Weiner, M.; Wing, D.; Conde, M. B.; Bozeman, L.; Horsburgh, C. R., Jr.; Chaisson, R. E. *N Engl J Med* **2011**, *365*, 2155.
(22) Shaul, P.; Green, K. D.; Rutenberg, R.; Kramer, M.; Berkov-Zrihen, Y.; Breiner-Goldstein, E.; Garneau-Tsodikova, S.; Fridman, M. *Organic & biomolecular chemistry* **2011**, *9*, 4057.
(23) Herzog, I. M.; Green, K. D.; Zrihen-Berkov, Y.; Feldman, M.; Vidavski, R. R.; Eldar-Boock, A.; Stachi-Fainaro, R.; Eldar, A.; Garneau-Tsodikova, S. *Angewandte Chemie Int Ed* **2012**, In press.
(24) Green, K. D.; Chen, W.; Garneau-Tsodikova, S. *ChemMedChem* **2011**.
(25) Porter, V. R.; Green, K. D.; Zolova, O. E.; Houghton, J. L.; Garneau-Tsodikova, S. *Biochem Biophys Res Commun* **2010**, *403*, 85.

(26) Green, K. D.; Chen, W.; Houghton, J. L.; Fridman, M.; Garneau-Tsodikova, S. *Chembiochem : a European journal of chemical biology* **2010**, *11*, 119.
(27) Green, K. D.; Fridman, M.; Garneau-Tsodikova, S. *Chembiochem : a European journal of chemical biology* **2009**, *10*, 2191.
(28) Busto, E.; Gotor-Fernandez, V.; Gotor, V. *Chem Soc Rev* **2010**, *39*, 4504.
(29) Gillingham, D. G.; Stallforth, P.; Adibekian, A.; Seeberger, P. H.; Hilvert, D. *Nat Chem* **2010**, *2*, 102.
(30) Fridman, M.; Balibar, C. J.; Lupoli, T.; Kahne, D.; Walsh, C. T.; Garneau-Tsodikova, S. *Biochemistry* **2007**, *46*, 8462.
(31) Li, S.; Chaulagain, M. R.; Knauff, A. R.; Podust, L. M.; Montgomery, J.; Sherman, D. H. *Proceedings of the National Academy of Sciences of the United States of America* **2009**, *106*, 18463.
(32) Bernhardt, P.; Usera, A. R.; O'Connor, S. E. *Tetrahedron Lett* **2010**, *51*, 4400.
(33) Piasecki, S. K.; Taylor, C. A.; Detelich, J. F.; Liu, J.; Zheng, J.; Komsoukaniants, A.; Siegel, D. R.; Keatinge-Clay, A. T. *Chem Biol* **2011**, *18*, 1331.
(34) Tsitovich, P. B.; Pushechnikov, A.; French, J. M.; Disney, M. D. *Chembiochem : a European journal of chemical biology* **2010**, *11*, 1656.
(35) Klimecka, M. M.; Chruszcz, M.; Font, J.; Skarina, T.; Shumilin, I.; Onopryienko, O.; Porebski, P. J.; Cymborowski, M.; Zimmerman, M. D.; Hasseman, J.; Glomski, I. J.; Lebioda, L.; Savchenko, A.; Edwards, A.; Minor, W. *J Mol Biol* **2011**, *410*, 411.
(36) Hu, X.; Norris, A. L.; Baudry, J.; Serpersu, E. H. *Biochemistry* **2011**, *50*, 10559.
(37) Wolf, E.; Vassilev, A.; Makino, Y.; Sali, A.; Nakatani, Y.; Burley, S. K. *Cell* **1998**, *94*, 439.
(38) Vetting, M. W.; Hegde, S. S.; Javid-Majd, F.; Blanchard, J. S.; Roderick, S. L. *Nat Struct Biol* **2002**, *9*, 653.
(39) Vetting, M. W.; Park, C. H.; Hegde, S. S.; Jacoby, G. A.; Hooper, D. C.; Blanchard, J. S. *Biochemistry* **2008**, *47*, 9825.
(40) Vetting, M. W.; Magnet, S.; Nieves, E.; Roderick, S. L.; Blanchard, J. S. *Chem Biol* **2004**, *11*, 565.
(41) Magalhaes, M. L.; Vetting, M. W.; Gao, F.; Freiburger, L.; Auclair, K.; Blanchard, J. S. *Biochemistry* **2008**, *47*, 579.
(42) Burk, D. L.; Xiong, B.; Breitbach, C.; Berghuis, A. M. *Acta Crystallogr D Biol Crystallogr* **2005**, *61*, 1273.
(43) Wybenga-Groot, L. E.; Draker, K.; Wright, G. D.; Berghuis, A. M. *Structure* **1999**, *7*, 497.
(44) Burk, D. L.; Ghuman, N.; Wybenga-Groot, L. E.; Berghuis, A. M. *Protein Sci* **2003**, *12*, 426.
(45) Green, K. D.; Porter, V. R.; Zhang, Y.; Garneau-Tsodikova, S. *Biochemistry* **2010**, *49*, 6219.
(46) Magalhaes, M. L.; Blanchard, J. S. *Biochemistry* **2005**, *44*, 16275.

Note:

This chapter is adapted from a submitted manuscript: **Chen, W.**; Green, K. D.; & Garneau-Tsodikova, S., titled "Cosubstrate promiscuity of the aminoglycoside resistance enzyme Eis from *Mycobacterium tuberculosis*" **Wenjing Chen** did all the mass spectrometry analysis, TLCs and kinetics.

Chapter 7

The aminoglycoside multi-acetylating activity of the enhanced intracellular survival (Eis) protein from *Mycobacterium smegmatis* and its inhibition

7.1. Abstract

Mycobacterium smegmatis (*Msm*) is used as a model bacterial system for studying mechanisms in other mycobacteria, including the *Mycobacterium tuberculosis* (*Mtb*) pathogen responsible for the tuberculosis epidemic worldwide. The enhanced intracellular survival (Eis) protein was originally found to improve *Msm* survival in macrophages and more recently demonstrated to function as the acetyltransferase responsible for kanamycin A resistance, a marker of extensively drug-resistant (XDR) tuberculosis, in a large number of *Mtb* clinical isolates. We recently demonstrated that Eis from *Mtb* (Eis_*Mtb*) efficiently multi-acetylates a variety of aminoglycoside (AG) antibiotics. We also discovered inhibitors of Eis_*Mtb* as a potential strategy to restore the activity of the AG kanamycin A in XDR-*Mtb* strains. Here, to gain insight into the origin of substrate selectivity of this novel multi-acetylation mechanism of AG deactivation in mycobacteria, we performed a detailed analysis of AG acetylation by Eis_*Msm* and investigated its inhibition by inhibitors of Eis_*Mtb* and compared these functions to those of Eis_*Mtb*. We show that Eis_*Msm* and Eis_*Mtb* differ in their kinetics as well as in the number of sites that they acetylate on some AGs, including the structurally unique apramycin. We propose a structural basis for these differences. We also demonstrate that inhibitors of Eis_*Mtb* can inhibit Eis_*Msm* activity, which suggests that they may be broadly applicable against mycobacterial pathogens.

7.2. Introduction

According to the World Health Organization, over 2 billion people, about one-third of the world's population, are infected with *Mycobacterium tuberculosis* (*Mtb*) bacilli that cause

the highly contagious and life-threatening tuberculosis (TB). With almost 2 million deaths and 9 million new cases each year, the TB epidemic is one of the most devastating health problems worldwide. The rapidly emerging resistance to all of the available anti-TB drugs presents one of the biggest obstacles in treating the disease. Multidrug-resistant (MDR),[1,2] extensively drug-resistant (XDR),[3,4] extremely drug-resistant (XXDR),[5] and more recently totally drug-resistant (TDR)[5] strains of *Mtb* have been identified.

In order to develop novel strategies to fight this notorious human pathogen, a better understanding of the basic biology of *Mtb* and how the bacteria cause the disease is needed. While many laboratories successfully study *Mtb*, faster-dividing and non-pathogenic *Mycobacterium smegmatis* (*Msm*) has been used as a model mycobacterium to gain insight into *Mtb* mechanisms.[6-8] The entire genome of both *Mtb*[9,10] and *Msm* have been sequenced and annotated. *Msm* shares not only more than 2,000 homologs with *Mtb* and most of the *Mtb* virulence genes, but also the same unusual cell wall structure.[7] The hyper-transformable *Msm* str. MC2 155 is now used a convenient tool for mycobacterial genetics.

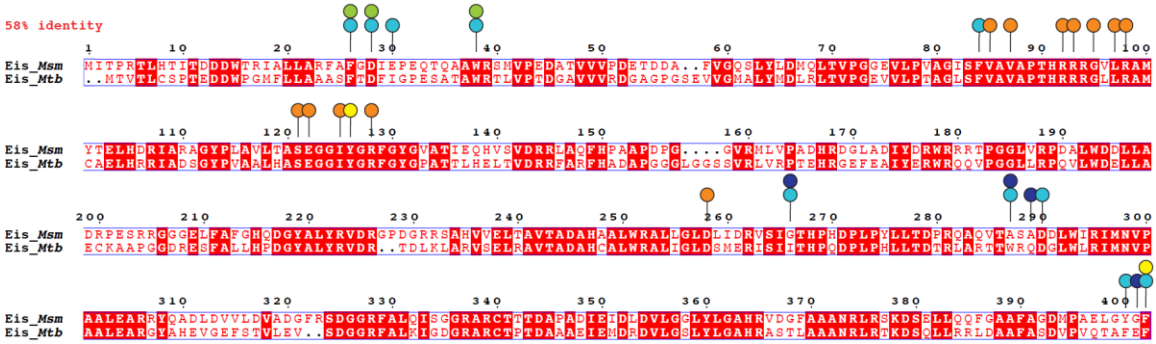

Fig. 7.1. Sequence alignment of Eis_*Msm* from *M. smegmatis* str. MC2 155 and Eis_*Mtb* from *M. tuberculosis* H37Rv. The two Eis homologs exhibit 58% sequence identity. Based on structural and mutagenesis studies of Eis_*Mtb*, the residues proposed to be involved in catalysis, in binding CoA, and in formation of the AG-binding pocket are marked by yellow, orange, and turquoise circles, respectively.[11] Non-conserved residues in the AG-binding pockets of these two proteins are additionally marked by dark blue circles. Conserved residues in the AG-binding pockets of Eis_*Msm* and Eis_*Mtb* are marked by green circles.

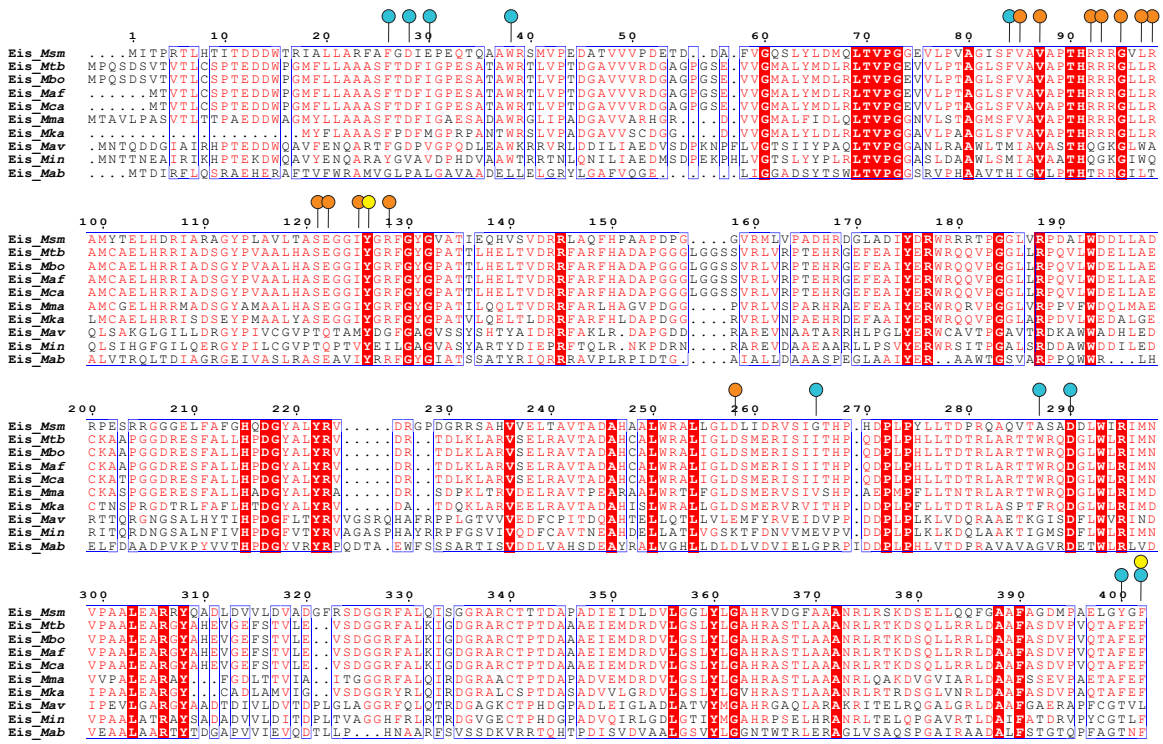

Fig. 7.2. Multiple sequence alignment of Eis homologs from various mycobacteria. Based on structural and mutagenesis studies of Eis_*Mtb*, the residues proposed to be involved in catalysis, to bind CoA, and to form the AG binding pocket are marked by yellow, orange, and turquoise circles, respectively.[11] The abbreviated names of mycobacterial species correspond to the following: *M. smegmatis* str. MC2 155 (*Msm*), *M. tuberculosis* H37Rv (*Mtb*), *M. bovis* BCG str. Pasteur 1173P2 (*Mbo*), *M. africanum* GM041182 (*Maf*), *M. canettii* CIPT 140010059 (*Mca*), *M. marinum* M (*Mma*), *M. kansasii* ATCC12478 (*Mka*), *M. avium* subsp. *avium* ATCC25291 (*Mav*), *M. intracellulare* MOTT-64 (*Min*), and *M. abscessus* 47J26 (*Mab*).

It was previously shown that up-regulation of the *Mtb* enhanced intracellular survival (Eis) protein is responsible for resistance to the aminoglycoside (AG) kanamycin A (KAN), a hallmark of XDR-TB, in a significant fraction of KAN-resistant *Mtb* clinical isolates.[12] Eis homologs have been found in many pathogens and numerous mycobacterial species (Figs. 7.1 and 7.2). When transformed into *Msm*, the *eis_Mtb* gene was found to increase the intracellular survival of *Msm* within the human macrophage-like cell line U-937.[13] Based on both biochemical and structural analyses, we recently demonstrated that Eis_*Mtb* belongs to a novel family of hexameric acetyltransferases, whose tripartite fold is composed of two GCN5 *N*-acetyltransferase regions, only one of which is active, and a sterol carrier protein fold.[11] All three regions contribute to the structure of the active site and the intricate substrate-binding cavity. We showed that Eis_*Mtb* has an unprecedented ability to acetylate multiple amines of many AGs. This

multi-acetylation is regio-specific, however the recognition and specificity rules for the *N*-acetylation remain unclear. Herein, in the hope that functional differences between Eis_*Mtb* and its closely genetically related, but not identical, homolog from *Msm* (Eis_*Msm*) will provide insight into the substrate recognition and *N*-acetylation specificity rules of the Eis family, we performed characterization of Eis_*Msm.* In addition, to probe the active site of Eis_*Msm*, we used AG-competitive acetylation inhibitors of Eis_*Mtb* that we recently discovered.[14]

To gain a better understanding of the evolution of the novel multi-acetylation mechanism of Eis we performed a detailed analysis of AG acetylation by Eis_*Msm* and its inhibition by the Eis_*Mtb* inhibitors and compared these functions to those of Eis_*Mtb*.

7.3. Materials and methods

7.3.1. Bacterial strains, plasmids, materials, and instrumentation

The chemically competent *E. coli* TOP10 and BL21 (DE3) strains were bought from Invitrogen (Carlsbad, CA). The genomic DNA from *M. smegmatis* str. MC2 155 used for PCR was a generous gift from Dr. Sabine Ehrt (Weill Cornell Medical College). The pET28a plasmid was bought from Novagen (Gibbstown, NJ). All restriction enzymes, T4 DNA ligase, and Phusion DNA polymerase were purchased from NEB (Ipswich, MA). PCR primers were purchased from Integrated DNA Technologies (IDT; Coralville, IA). DNA sequencing was performed at the University of Michigan DNA Sequencing Core. Chemical reagents including DTNB, AcCoA, AGs (APR, AMK, HYG, KAN, NEO, SIS, SPT, STR, and RIB) (Fig. 7.7), and chlorhexidine (**1**) were purchased from Sigma-Aldrich (Milwaukee, WI). The rest of the AGs (NEA, NET, PAR, and TOB) (Fig. 7.7) were purchased from AK Scientific (Mountain View, CA). Compound **2** was purchased from ChemDiv Inc. (San Diego, CA). The pH was adjusted at rt. The spectrophotometric assays were performed on a multimode SpectraMax M5 plate reader using 96-well plates (Fisher Scientific; Pittsburg, PA). Silica gel 60 F_{254} plates (Merck) were used for thin-layer chromatography (TLC) analysis. Liquid chromatography mass spectrometry (LCMS) was performed on a Shimadzu LCMS-2019EV equipped with a SPD-20AV UV-Vis detector and a LC-20AD liquid chromatograph.

7.3.2. Preparation of the pEis-pET28a overexpression constructs

The pEis_*Mtb*-pET28a plasmid encoding the Eis_*Mtb* protein was constructed as previously reported.[15] In order to prepare the pEis_*Msm*-pET28a construct, PCR was performed using *M. smegmatis* str. MC2 155 genomic DNA as a template, a forward primer 5'-TCGAGACATATGATCACGCCGCGCACCCTTC-3', a reverse primer 5'-CCCGCGGGATCCTCAGAATCCGTATCCCAGC-3'), and Phusion DNA polymerase. The resulting amplified *eis_Msm* gene PCR fragment was inserted into the linearized pET28a via the corresponding *Nde*I/*Bam*HI restriction sites (underlined above). The plasmid encoding the Eis_*Msm* protein was transformed into *E. coli* TOP10 chemically competent cells. The plasmid that had the correct size *eis_Msm* gene insert was sequenced and showed perfect alignment with the reported gene sequence from *M. smegmatis* str. MC2 155 (locus tag MSMEG_3513).

7.3.3. Overproduction and purification of Eis proteins

The Eis_*Mtb* protein (with a N-terminal His_6 tag) was prepared as previously reported.[15] The overexpression and purification of the Eis_*Msm* protein was performed exactly as reported for Eis_*Mtb*.[15] Both proteins were dialyzed in Tris-HCl buffer (50 mM, pH 8.0) and stored at 4 ℃. After purification, 1.1 mg of the 46,172-Da Eis_*Msm* protein was obtained per L of culture.

7.3.4. Determination of the AG selectivity profile of Eis_*Msm* by a spectrophotometric assay

The acetyltransferase activity of Eis_*Msm* was monitored by a UV-Vis assay in which the free thiol group of CoA, generated by the Eis_*Msm* enzyme catalyzed reaction, is coupled to DTNB to produce the thiolate NTB^{2-}, which can be monitored by increase in absorbance at 412 nm (ε_{412} = 14,150 $M^{-1}cm^{-1}$). The reaction mixtures (100 μL) containing AcCoA (0.5 mM, 5 eq), AG (0.1 mM, 1 eq), DTNB (1 mM), and Tris-HCl (50 mM, pH 8.0), were initiated by adding Eis_*Msm* (0.5 μM) at 25 ℃. Reactions were monitored by taking readings every 30 s for 15 min in 96-well plate format. The data indicated that AMK, APR, HYG, KAN, NEA, NEO, NET, PAR, RIB, SIS, and TOB were substrates of Eis_*Msm*, whereas SPT and STR were not.

7.3.5. Determination and confirmation of number of acetylation sites by the spectrophotometric assay and mass spectrometry

To determine the number of acetylations performed by Eis_*Msm* for a given AG, two reactions were carried out with each AG: a calibration reaction with 1 eq of AG and 1 eq of AcCoA as well as a reaction that ensured complete acetylation with 1 eq of AG and 10 eq of AcCoA. Specifically, reaction mixtures (100 μL) containing AG (0.1 mM), DTNB (1 mM), Tris-HCl (50 mM, pH 8.0), and AcCoA (0.1 mM, 1 eq or 1 mM, 10 eq), were initiated by adding Eis_*Msm* (1 μM) at 25 ℃. Reactions were monitored at 412 nm as described above by taking readings every 30 s until a plateau was reached. Representative plots are shown in Fig. 7.4. To confirm the number of acetylations on each AG substrate established by UV-Vis assays, a third reaction (20 μL) containing AG (0.67 mM, 1 eq), AcCoA (3.35 mM, 5 eq), Tris-HCl (50 mM, pH 8.0), and Eis_*Msm* protein (10 μM) was carried out overnight at 25 ℃. These reactions were terminated by addition of an equal volume of ice-cold MeOH (20 μL), which was then kept at -20 ℃ for at least 20 min. The precipitated protein was removed by centrifugation (13,000 rpm, rt, 10 min). The masses of the acetylated AG products present in each sample were determined by LCMS in positive mode using H_2O (0.1% formic acid) after dilution of the supernatant (10 μL) with H_2O (20 μL) and injection of all 30 μL. Mass spectra of all AGs modified by Eis_*Msm* are provided in Fig. 7.5. A summary of the level of acetylation is presented in Table 7.1.

7.3.6. Kinetic characterization of Eis_*Msm* activity

The steady-state kinetic assays of acetylation of AGs (AMK, KAN, NEA, NEO, NET, PAR, SIS, and TOB) by Eis_*Msm*, were performed in two ways: (i) at a fixed concentration of AcCoA (0.1 mM) and varying concentrations of AGs (0, 31.25, 62.5, 125, 250, and 500 μM), and (ii) at a fixed concentration of each AG (0.5 mM) and varying concentrations of AcCoA (0, 16.625, 31.25, 62.5, 125, and 250 μM). All reactions were carried out in Tris-HCl (50 mM, pH 8.0) and contained AcCoA, AGs, DTNB (1 mM), and Eis_*Msm* (0.25 μM). Both types of reactions were initiated by addition of AcCoA and performed in duplicate at 25 ℃. As described above, the

acetylation reactions were monitored at 412 nm as a function of time and absorbance readings were taken every 15 s. The initial rates were used to calculate the apparent Michaelis-Menten kinetic parameters, $K_{m,AG}^{app}$ and $k_{cat,AG}^{app}$ (for reaction i), $K_{m,AcCoA}^{app}$ and $k_{cat,AcCoA}^{app}$ (for reaction ii), by the Lineweaver-Burk plot analysis. These kinetic parameters are given in Tables 7.2 and 7.3.

In order to convert these apparent kinetic parameters into the mechanistic rate constants, we assumed that Eis acetylation is described by one of the only two mechanisms previously observed for AAC enzymes: 1) the random sequential mechanism observed more commonly, in which either AcCoA or AG can bind to free enzyme followed by binding of the other species,[16-20] and 2) the ordered sequential mechanism, in which AcCoA binds Eis first, followed by AG.[21-23]

The random sequential mechanism is described by the following kinetic steps:

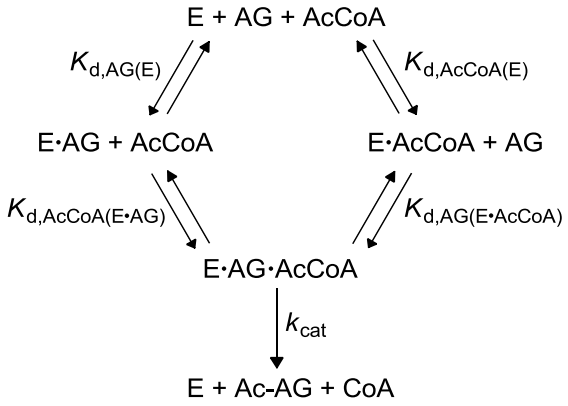

(1)

where E is the enzyme and AG-Ac is the acetylated AG product.

Under the common simplifying assumptions of rapid AcCoA and AG binding equilibrium for this mechanism, one obtains the kinetic parameters observed above in terms of microscopic constants:

$$k_{cat,AG}^{app} = \frac{k_{cat}[AcCoA]}{K_{d,AcCoA(E•AG)} + [AcCoA]} \quad (2)$$

$$K_{m,AG}^{app} = K_{d,AG(E•AcCoA)}\left(\frac{K_{d,AcCoA(E)} + [AcCoA]}{K_{d,AcCoA(E•AG)} + [AcCoA]}\right) \quad (3)$$

$$k_{\text{cat,AcCoA}}^{\text{app}} = \frac{k_{\text{cat}}[\text{AG}]}{K_{\text{d,AG(E•AcCoA)}} + [\text{AG}]} \tag{4}$$

$$K_{\text{m,AcCoA}}^{\text{app}} = K_{\text{d,AcCoA(E•AG)}}\left(\frac{K_{\text{d,AG(E)}} + [\text{AG}]}{K_{\text{d,AG(E•AcCoA)}} + [\text{AG}]}\right), \tag{5}$$

where each subscript of an equilibrium binding constant K_{d} designates the step in Mechanism (1) where the species outside of the parentheses binds to the species in the parentheses and k_{cat} is the microscopic rate constant of the acetylation, *i.e.* the last step in Mechanism (1).

Because the concentration of AGs used in these assays exceeds 2-9 fold the observed $K_{\text{m,AG}}^{\text{app}}$, Eqs. (4) and (5) yield, to a good approximation:

$$k_{\text{cat}} = k_{\text{cat,AcCoA}}^{\text{app}} \tag{6}$$

$$K_{\text{d,AcCoA(E•AG)}} = K_{\text{m,ACCoA}}^{\text{app}} \tag{7}$$

Agreement between $k_{\text{cat,AG}}^{\text{app}}$ calculated from these values by using Eq. (2) and its measurements provides evidence for this mechanism.

In addition, because $K_{\text{d,AcCoA(E)}}$ is independent of AG, the numerator of the expression in the parentheses in Eq. (3) is the same for all AGs and the denominator is known from Eq. (7). Therefore, the ratio of observed $K_{\text{m,AG}}^{\text{app}}$ values for two different aminoglycosides AG1 and AG2 is related to the ratio of their respective microscopic equilibrium binding constants $K_{\text{d,AG(E•AcCoA)}}$ as follows:

$$\frac{K_{\text{d,AG1(E•AcCoA)}}}{K_{\text{d,AG2(E•AcCoA)}}} = \frac{K_{\text{m,AG1}}^{\text{app}}}{K_{\text{m,AG2}}^{\text{app}}}\left(\frac{K_{\text{d,AcCoA(E•AG1)}} + [\text{AcCoA}]}{K_{\text{d,AcCoA(E•AG2)}} + [\text{AcCoA}]}\right) \tag{8}$$

The values of $K_{\text{d,AG(E•AcCoA)}}$ relative to that of NEA reported in Table 7.3 were calculated by using this relationship.

The ordered sequential mechanism, in which AcCoA binds first, is obtained by removing the first line in Mechanism (1). For this mechanism, under the assumption of rapid equilibrium, one obtains:

$$k_{cat,AG}^{app} = k_{cat} \quad (9)$$

$$K_{m,AG,obs} = K_{d,AG}\left(1 + \frac{K_{d,AcCoA}}{[AcCoA]}\right) \quad (10)$$

$$k_{cat,AcCoA}^{app} = \frac{k_{cat}[AG]}{K_{d,AG} + [AG]} \quad (11)$$

$$K_{m,AcCoA,obs} = \frac{K_{d,AcCoA}K_{d,AG}}{K_{d,AG} + [AG]} \quad (12)$$

Eis kinetics do not obey this mechanism, as explained in the Results section.

7.3.7. Determination of positions acetylated on NEA by Eis_*Msm* by TLC

To establish which three positions of the NEA scaffold get acetylated by Eis_*Msm*, reactions (40 μL) were carried out at rt in Tris-HCl buffer (50 mM, pH 8.0) in the presence of AcCoA (4 mM, 5 eq), NEA (0.8 mM, 1 eq), and Eis_*Msm* (5 μM). Aliquots (4 μL) were loaded and run on a TLC plate after 0, 1, 5, 10, 30, and 120 min as well as after overnight incubation (Fig. 7.3C). The eluent system utilized for the TLC was 3:0.8/MeOH:NH_4OH. Visualization was achieved using a cerium-molybdate stain (5 g cerium ammonium nitrate, 120 g ammonium molybdate, 80 mL H_2SO_4, 720 mL H_2O). The R_f values of the Eis_*Msm* modified NEA were compared and found to be in accordance with those obtained for the Eis_*Mtb* reaction with NEA (Fig. 7.3C).[11] Control reactions for mono- and di-acetylation of NEA were performed using individually and sequentially the AG acetyltransferases AAC(2')-Ic from *M. tuberculosis* H37Rv,[11] AAC(3)-IV from *E. coli*,[24] and AAC(6') from the AAC(6')/APH(2'') bifunctional enzyme.[24]

7.3.8. Determination of kinetic parameters and mode of inhibition for inhibitors of Eis_*Msm*

The IC_{50} values of two inhibitors, chlorhexidine (**1**) and compound **2**, were determined as previously described.[14] Briefly, the inhibitors were dissolved in Tris-HCl (50 mM, pH 8.0, containing 10% v/v DMSO) (100 μL) and 5-fold dilution series were performed. To these solutions, a mixture (50 μL) containing Eis (1 μM), NEO (400 μM), and Tris-HCl

(50 mM, pH 8.0) was added and incubated at rt for 10 min. The reactions were initiated by addition of a mixture (50 μL) containing AcCoA (2 mM), DTNB (2 mM), and Tris-HCl (50 mM, pH 8.0). The absorbance change at 412 nm was monitored every 30 s for 15 min at 25 ℃. Initial rates were calculated and the IC_{50} values were determined by using a Hill-plot analysis by using the KaleidaGraph 4.1 software (Synergy software; Reading, PA) (Fig. 7.8).

To determine the mode of inhibition of both compounds tested, varying concentrations of NEO (50, 75, 100, 150, and 200 μM) and chlorhexidine (**1**) (0, 0.5, 1, 2, and 4 μM) or compound **2** (0, 0.0625, 0.125, 0.25, and 0.5 μM) were used. Chlorhexidine (**1**) was found to be a competitive inhibitor of NEO whereas mixed inhibition was observed for compound **2**. Resulting reaction rates were plotted as Lineweaver-Burk plots (Fig. 7.8, insets of panels A and B).

7.4. Results

7.4.1. Substrate specificity and multi-acetylation profiles of Eis proteins

Table 7.1. Comparison of level of acetylation by Eis from *M. smegmatis* and *M. tuberculosis*.

AG	*M. smegmatis*	*M. tuberculosis*[a]
AMK	Tri	Tri
APR	Di	×[b]
HYG	Mono	Di
KAN	Di	Di
NEA	Tri	Tri
NEO	Tri	Tri
NET	Di	Di
PAR	Tri	Di
RIB	Tri	Tri
SIS	Tri	Tri
SPT	×	×
STR	×	×
TOB	Tetra	Tetra

[a]We previously reported these data.[11]
[b] × indicates that no acetylation was observed.

Recently, we reported the structural and biochemical characterization of Eis_*Mtb*, an AG acetyltransferase (AAC) responsible for resistance to KAN in *Mtb* clinical isolates.[15] We discovered Eis to be a novel AAC capable of unprecedented multi-acetylation of a large number of AG scaffolds. In this study, to gain insight into the unique recognition and specificity rules for the *N*-acetylation by Eis proteins, we performed a detailed characterization of AG acetylation by Eis_*Msm*, a close homolog of Eis_*Mtb*, and compared its functional properties to those of Eis_*Mtb*. To ensure the validity of the comparison, we identically cloned and heterologously expressed in *E. coli* the 46,172-Da Eis_*Msm* and the 46,597-kDa Eis_*Mtb* as N-terminally His_6-tagged proteins both. We first investigated the substrate specificity and the multi-acetylation profile of Eis_*Msm* by spectrophotometric assays (Table 7.1, Figs. 7.3A and 7.4) and mass spectrometry (Figs. 7.3B and 7.5). We

found Eis_*Mtb* and Eis_*Msm* to have generally similar AG substrate selectivity and *N*-acetylation profiles with SPT and STR not modified, KAN and NET di-acetylated, AMK, NEA, NEO, RIB, and SIS tri-acetylated, and TOB tetra-acetylated by both Eis proteins. Interestingly, we observed three major differences in the activity of these two Eis proteins: (i) Eis_*Msm* di-acetylated APR, an AG with conformationally restricted and extended cylindrical-like structure (Figs 7.6 and 7.7),[25,26] which Eis_*Mtb* could not chemically modify, (ii) Eis_*Msm* tri-acetylated PAR, which could only be di-acetylated by Eis_*Mtb*, and (iii) Eis_*Msm* mono-acetylated HYG, a structurally unique AG that could be di-acetylated by Eis_*Mtb*. The identity of several non-conserved amino acid residues lining the AG-binding pocket of the two Eis proteins (highlighted in dark blue in Figs. 7.1 and 7.6) is likely responsible for these differences in the number of acetylation sites.

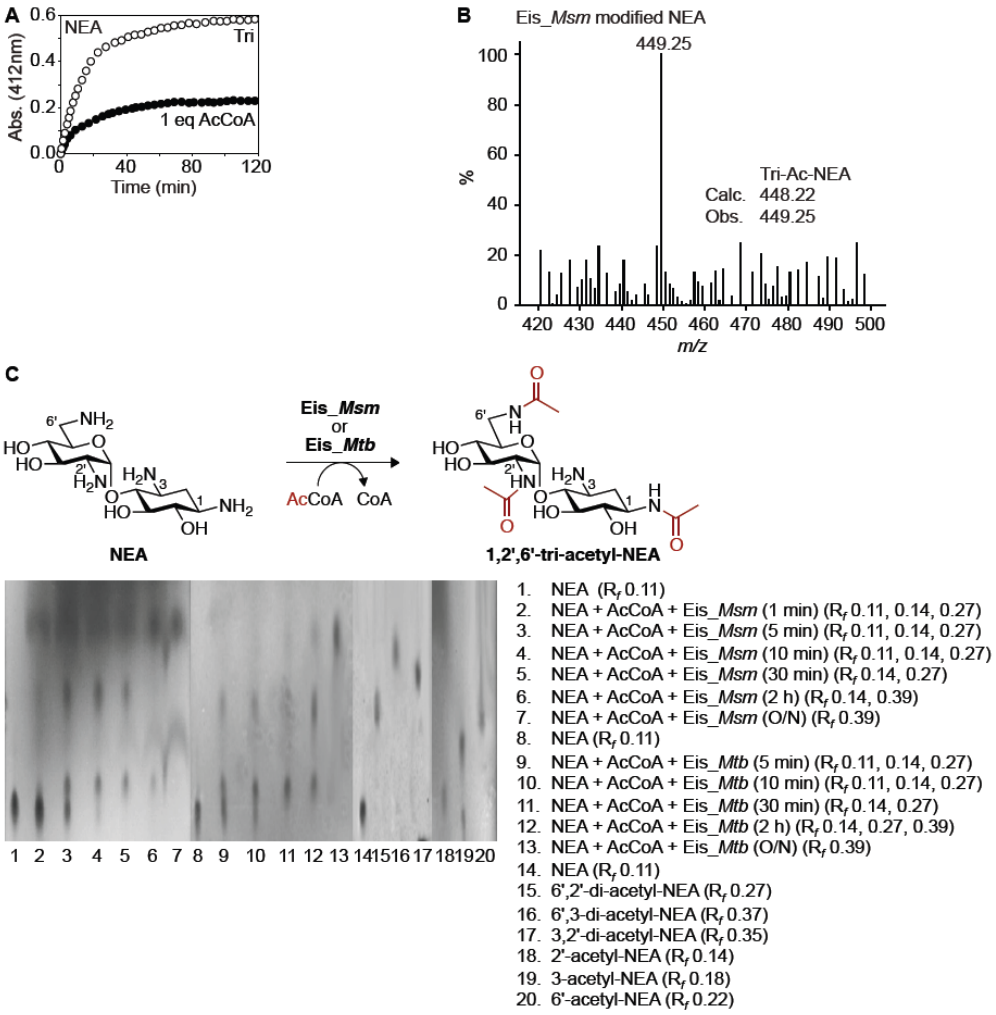

Fig. 7.3. A. UV-Vis assay plot showing the conversion of NEA into its acetylated products using Eis_*Msm* with 1 (black circles) and 10 (white circles) equivalents of AcCoA, respectively. **B.** Mass spectrum confirming the formation of tri-acetyl-NEA by Eis_*Msm*. **C.** Lanes 1-7: TLC time course displaying the mono-, di-, and tri-acetyl-NEA products of the Eis_*Msm* reaction. Lanes 8-13: TLC time course of the NEA reaction with Eis_*Mtb*. Lanes14-20: Controls for di- and mono-acetylation of NEA performed with AAC(2')-Ic, AAC(3)-IV, and AAC(6') sequentially or individually.

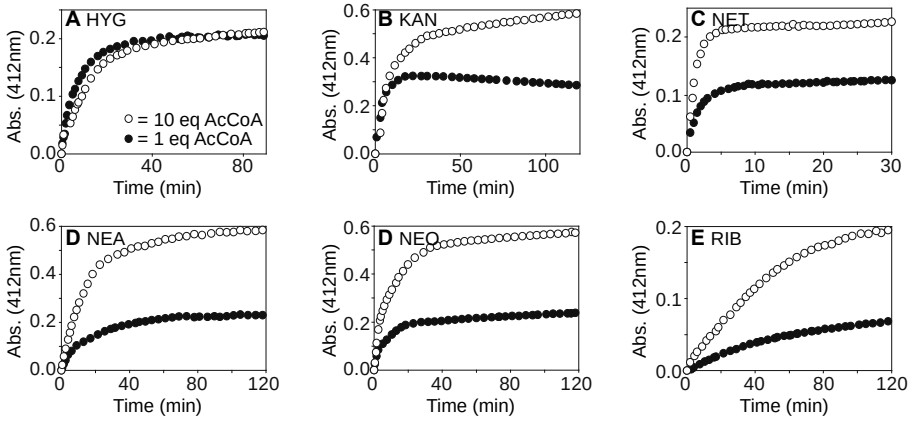

Fig. 7.4. Representative examples of spectrophotometric assay plots monitoring the conversion of a variety of AGs by Eis_*Msm* to their mono- (**A**), di- (**B** and **C**), and tri-acetylated (**D**-**F**) counterparts when using one (black circles) or ten (white circles) equivalents of AcCoA.

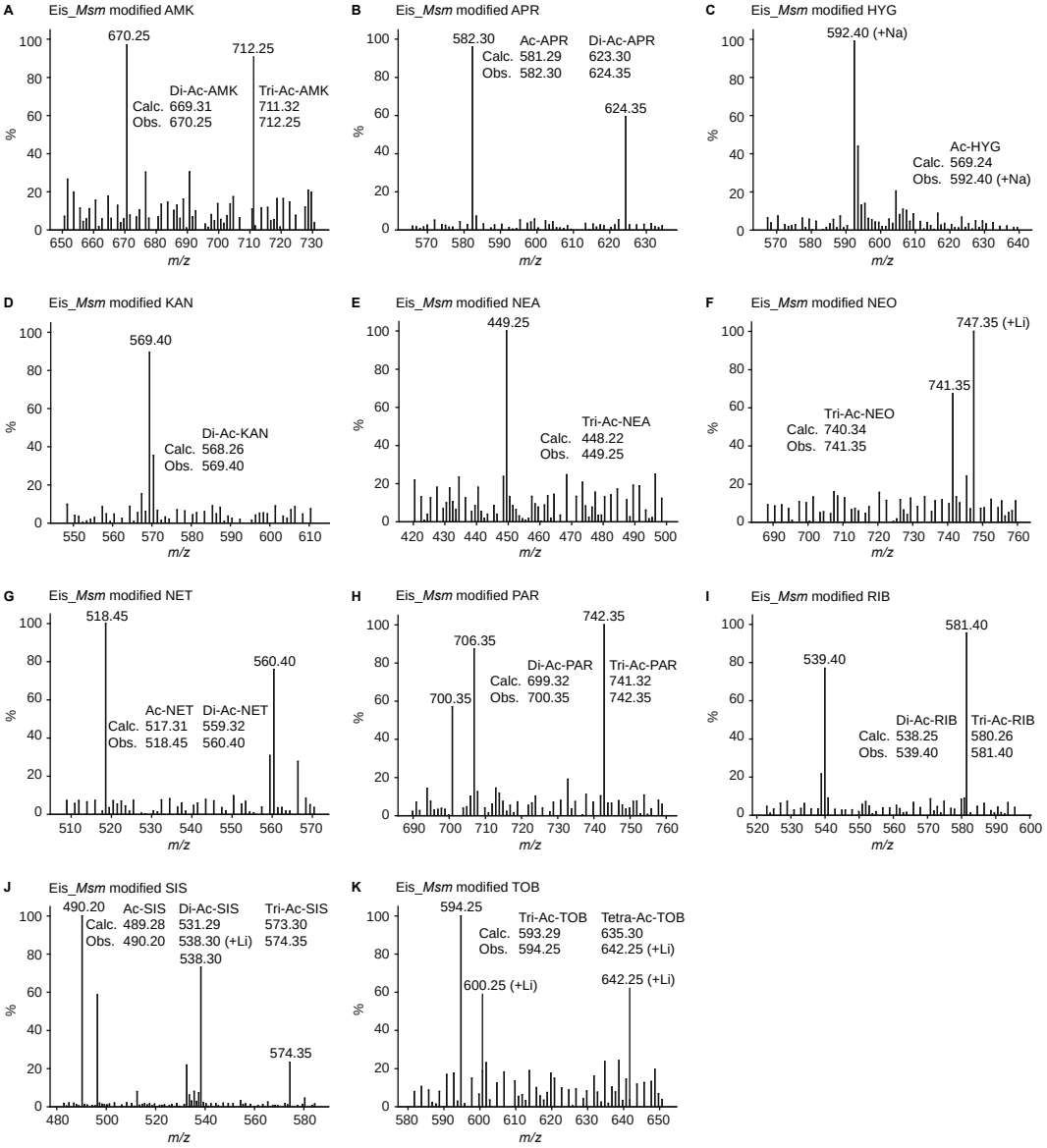

Fig. 7.5. Mass spectra of AGs multi-acetylated by *Eis_Msm.*

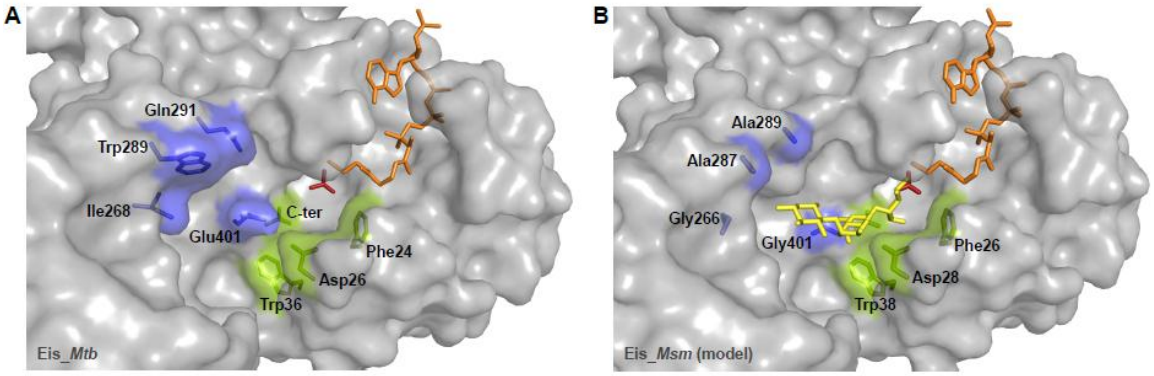

Fig. 7.6. Structural differences between the AG-binding pockets of Eis_*Mtb* and Eis_*Msm*. **A.** The active site and the AG-binding pocket of Eis_*Mtb* bound to CoA and an acetamide, as seen in the recently reported crystal structure (PDB code: 3R1K).[11] In both panels, CoA is shown in orange, acetamide in red, the conserved AG binding pocket residues in green, and the non-conserved residues in blue. The C-terminal carboxyl group is denoted as C-ter. **B.** A model of the active site and the AG-binding pocket of Eis_*Msm*. This model was generated by substituting the non-conserved residues of the AG-binding pocket Eis_*Mtb* with their Eis_*Msm* counterparts (Ile268, Trp289, and Gln291 in Eis_*Mtb* were mutated to Gly266, Ala287, and Ala289 in the Eis_*Msm* numbering, respectively). As a result of these mutations an APR molecule (in yellow) can be accommodated in the pocket in the orientation appropriate for catalysis. The structure of APR was taken from the high-resolution PDB entry 2OE5.[27]

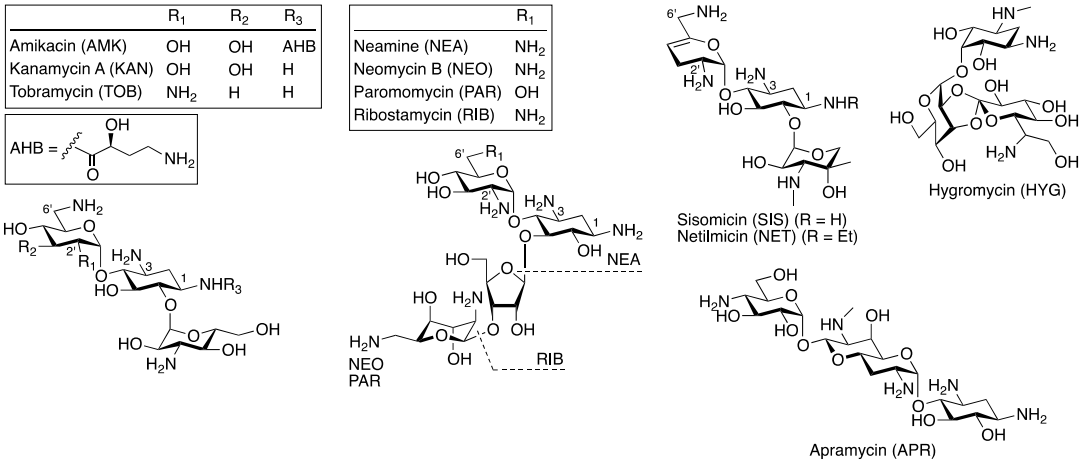

Fig. 7.7. Structures of AG substrates of *Eis_Msm*.

7.4.2. Regio-specificity of tri-acetylation of NEA by Eis proteins

Knowing that the substrate profile for both Eis proteins was generally similar, we sought to compare the regio-specificity of their acetylating activity on an AG scaffold for which the number of sites acetylated was observed to be the same for the two proteins. We recently established by TLC and NMR spectroscopy that Eis_*Mtb* tri-acetylates NEA first at the 2'-, then at the 6'-, and finally at the 1-position.[11] Here, by using TLC and comparing the retention factor (R_f) values of the mono-, di-, and tri-acetylated NEA derivatives produced over time by Eis_*Msm* to the R_f values of their counterparts formed

by Eis_*Mtb* as well as to those of mono- and di-acetylated NEA standards obtained by using individually or sequentially mono-acetylating AAC enzymes, we observed that Eis_*Msm* is also a 2',6',1-NEA-tri-acetylating enzyme (Fig. 7.3C). These results suggest that AG scaffolds with the same number of acetylations by Eis_*Mtb* and Eis_*Msm* are likely modified by these two enzymes at the same positions.

Table 7.2. Observed kinetic parameters[a] for [AG]-dependent acetylation by Eis from *M. smegmatis* and *M. tuberculosis*.

AG	*M. smegmatis*		*M. tuberculosis*[b]	
	$K^{app}_{m,AG}$ (μM)	$k^{app}_{cat,AG}$ (s^{-1})	$K^{app}_{m,AG}$ (μM)	$k^{app}_{cat,AG}$ (s^{-1})
AMK	231 ± 26	0.026 ± 0.002	75 ± 3	0.020 ± 0.007
KAN	149 ± 4	0.047 ± 0.001	99 ± 5	0.039 ± 0.004
NEA	275 ± 32	0.158 ± 0.019	178 ± 2	0.070 ± 0.002
NEO	182 ± 12	0.079 ± 0.013	98 ± 8	0.130 ± 0.019
NET	210 ± 14	0.860 ± 0.078	48 ± 5	0.482 ± 0.037
PAR	286 ± 23	0.050 ± 0.003	82 ± 9	0.058 ± 0.009
SIS	106 ± 5	0.232 ± 0.001	58 ± 15	0.270 ± 0.024
TOB	73 ± 2	0.208 ± 0.004	63 ± 6	0.162 ± 0.004

[a]All parameters are defined in the Materials and Methods section.
[b]We previously reported these data.[11]

7.4.3. Steady-state kinetic analysis of Eis proteins

Seeking a deeper understanding of the subtleties differentiating Eis_*Mtb* and Eis_*Msm*, we determined the observed Michaelis-Menten catalytic parameters of steady-state acetylation for several AGs. We carried out two sets of reactions, one at a fixed concentration of AcCoA and varying concentrations of AGs (Table 7.2), and the other at a fixed concentration of each AG and varying concentrations of AcCoA (Table 7.3). In order to convert the observed kinetic parameters into the mechanistic rate constants, we assumed that Eis acetylation may be described by one of the only two mechanisms previously observed for AAC enzymes: 1) the more common random sequential mechanism, in which either AcCoA or AG can bind to free enzyme followed by binding of the other species,[16-20] and 2) the ordered sequential mechanism, in which AcCoA binds Eis before AG does.[21-23]

Overall, we found $k^{app}_{cat,AG}$ to be smaller than $k^{app}_{cat,AcCoA}$ for Eis proteins (Tables 7.2 and 7.3, respectively). From these observations the ordered sequential mechanism can be ruled out, as for this mechanism $k^{app}_{cat,AG}$ is larger than $k^{app}_{cat,AcCoA}$ (see Eqs. (9) and (11)). In contrast, the observed kinetics generally agree with the random sequential rapid equilibrium mechanism (Mechanism (1)). From the observed kinetic parameters we deduced the microscopic equilibrium constant for binding of AcCoA to the complex of Eis with an AG ($K_{d,AcCoA(E•AG)}$), the catalytic turnover rate constant k_{cat}, and the relative

affinities of different AGs to the complex of Eis with AcCoA (calculated relative to NEA in Table 7.3).

Table 7.3. Observed kinetic parameters[a] for [AcCoA]-dependent acetylation by Eis from *M. smegmatis* and *M. tuberculosis* and microscopic kinetic parameters for the random sequential mechanism.

	M. smegmatis			
AG	$K_{m,AcCoA}^{app}$ (μM) ($\approx K_{d,AcCoA(E•AG)}$)	$k_{cat,AcCoA}^{app}$ (s^{-1}) ($\approx k_{cat}$)	$k_{cat,AcCoA}^{app}/K_{m,AcCoA}^{app}$ ($M^{-1}s^{-1}$)	$\frac{K_{d,AG(E\cdot AcCoA)}}{K_{d,NEA(E\cdot AcCoA)}}$[b]
AMK	55 ± 9	0.130 ± 0.015	2,300 ± 500	0.86 ± 0.14
KAN	95 ± 9	0.603 ± 0.027	6,000 ± 700	1.16 ± 0.05
NEA	45 ± 7	0.137 ± 0.014	3,000 ± 600	1
NEO	197 ± 13	0.867 ± 0.076	4,900 ± 600	0.97 ± 0.07
NET	361 ± 28	1.732 ± 0.141	4,800 ± 500	2.42 ± 0.25
SIS	329 ± 27	1.574 ± 0.179	4,800 ± 700	1.14 ± 0.11
	M. tuberculosis			
AG	$K_{m,AcCoA}^{app}$ (μM) ($\approx K_{d,AcCoA(E•AG)}$)[c]	$k_{cat,AcCoA}^{app}$ (s^{-1}) ($\approx k_{cat}$)[c]	$k_{cat,AcCoA}^{app}/K_{m,AcCoA}^{app}$ ($M^{-1}s^{-1}$)[c]	$\frac{K_{d,AG(E\cdot AcCoA)}}{K_{d,NEA(E\cdot AcCoA)}}$[b]
AMK	8 ± 1	0.019 ± 0.005	2,400 ± 700	0.31 ± 0.04
KAN	9 ± 1	0.093 ± 0.006	10,000 ± 1,000	0.41 ± 0.05
NEA	47 ± 1	0.075 ± 0.006	1,600 ± 100	1
NEO	24 ± 1	0.109 ± 0.003	4,500 ± 200	0.46 ± 0.04
NET	63 ± 2	0.247 ± 0.017	4,000 ± 300	0.30 ± 0.03
SIS	69 ± 1	0.070 ± 0.002	1,000 ± 50	0.37 ± 0.09

[a]All parameters are defined in the Materials and Methods section.
[b]These values were calculated by using Eq. (8) in the Materials and Methods section.
[c]These data for *Mtb* are reported in Chapter 6 and are used here for comparison.

For Eis_*Msm*, the $K_{m,AcCoA}^{app}$ values ranged from 39 ± 1 μM to 361 ± 28 μM, representing a 9-fold range similar to that observed for Eis_*Mtb* ($K_{m,AcCoA}^{app}$ values for Eis_*Mtb* ranged from 8 ± 1 μM to 69 ± 1 μM). For the most part, the $K_{m,AcCoA}^{app}$ values for Eis_*Msm* were several folds higher than those for Eis_*Mtb*, except for NEA and NEO where they were comparable. Interestingly, the strongest affinity was observed for NEO with Eis_*Msm*, whereas it was for AMK with Eis_*Mtb*, whereas the weakest affinity was seen for SIS with both Eis proteins. These data indicate that the nature of the Eis bound AG modulates the binding affinity of AcCoA to the Eis•AG complex. In agreement with this observation, for Eis_*Msm* and with a few exceptions for Eis_*Mtb*, the affinities of AGs to the complex of Eis with AcCoA displayed the same rank order (reported in the right most column of each mycobacterial species in Table 7.3). In general, the k_{cat} values for Eis_*Msm* were several fold higher than those for Eis_*Mtb*, offsetting the lower corresponding $K_{m,AcCoA}^{app}$ values for Eis_*Msm* and resulting in similar catalytic efficiency ratios (with respect to AcCoA) for the two enzymes for all AGs. These ratios varied in a 5-fold range for Eis_*Msm* and in a 10-fold range for Eis_*Mtb*.

7.4.4. Inhibition of Eis proteins

To further probe the differences in the active sites of Eis_*Mtb* and Eis_*Msm*, we next investigated with Eis_*Msm* the activity of the two inhibitors, chlorhexidine (**1**) and

compound **2**, that we recently identified from a high-throughput screening study with Eis_*Mtb* (Fig. 7.8).[14] We previously showed that these two Eis inhibitors display high selectivity towards the Eis_*Mtb* AG-binding site over that of any other types of AAC enzymes. Here, we found both inhibitors of Eis_*Mtb* to be effective against Eis_*Msm*. Interestingly, with an IC_{50} value of 1,848 ± 389 nM, chlorhexidine (**1**) was found to be a 10-fold worse inhibitor of Eis_*Msm* than of Eis_*Mtb* (IC_{50} = 188 ± 30 nM). In contrast, with an IC_{50} value of 108 ± 19 nM, compound **2** was found to be a 3-fold better inhibitor of inhibitor of Eis_*Msm* than of Eis_*Mtb* (IC_{50} = 364 ± 32 nM). As previously reported for Eis_*Mtb*,[14] we observed that compounds **1** and **2** displayed AG-competitive mode and mixed mode of inhibition against NEO, respectively, when tested against Eis_*Msm*. These results demonstrate the potential of inhibitors of Eis_*Mtb* for use against other mycobacterial species.

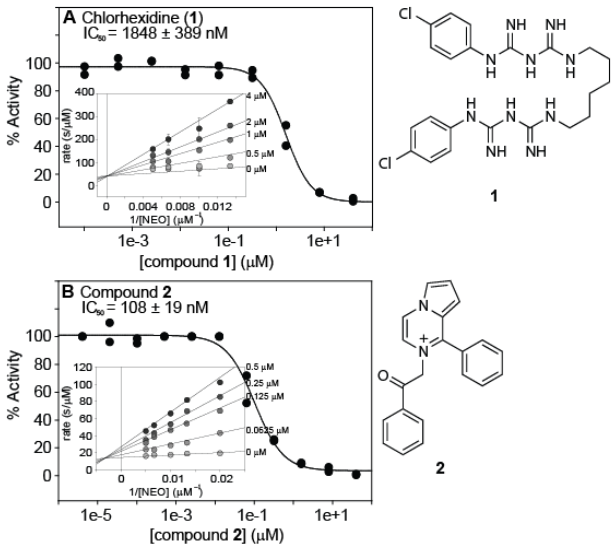

Fig. 7.8. Inhibition of Eis_*Msm*. IC_{50} curves for **A.** chlorhexidine (**1**), and **B.** compound **2**. The insets show the competitive and mixed inhibition modes of compounds **1** and **2**, respectively.

7.5. Discussion

Eis is an *Mtb* protein whose up-regulation leads to KAN resistance, a hallmark of XDR-TB, in a large set of clinical isolates from different regions of the world.[12] With its hexameric structure and its AG multi-acetylating capabilities, Eis_*Mtb* is an AAC that is structurally and functionally highly divergent from all other characterized AACs.[15] Eis homologs are found in a number of pathogenic and non-pathogenic mycobacteria including *Mtb* and *Msm* (Figs. 7.1 and 7.2). The low 10% sequence identity among Eis homologs from ten mycobacteria presented in Fig. 7.2 may prompt one to assume that substrate recognition rules used by Eis_*Mtb* may not apply to other mycobacteria. Upon closer inspection of these sequence alignments, we find that the amino acid residues involved in CoA and AG binding as well as in catalysis

are highly or even strictly conserved. Therefore, we can hypothesize that the discoveries made and information gained for Eis_*Mtb* may find application to other diseases of mycobacterial origin. In fact, the generally minor variation of the putative AG-interacting residues sets up different mycobacteria as good systems for studying the poorly understood AG-recognition rules of Eis.

For several decades, *Msm* has been used as a model system to study mechanisms of *Mtb*. Eis_*Msm* and Eis_*Mtb* share 58% sequence identify (Fig. 7.1). All amino acid residues involved in CoA binding and catalysis are strictly conserved between Eis_*Msm* and Eis_*Mtb*. However, there are four amino acid residues (highlighted in dark blue in Figs 7.1 and 7.6) in the AG-binding pockets of these two proteins that differ.

In this work we have focused on gaining a better understanding of the evolution of the novel multi-acetylation mechanism of Eis and on probing the potential application of novel Eis_*Mtb* inhibitors against other mycobacterial organisms. Our steady-state kinetic measurements indicated that Eis_*Msm*, like Eis_*Mtb*, evolved to efficiently acetylate many AGs. In fact, the binding affinities and the catalytic rate constants differed for the two enzymes, whereas the catalytic efficiencies were very similar. This suggests that the common ancestor of these mycobacteria may have coexisted with a variety of AG-producing bacteria.

Despite this overall similarity between Eis_*Msm* and Eis_*Mtb*, we observed a major variation in the acetylating activity of APR by these two enzymes. Eis_*Msm* di-acetylated APR whereas Eis_*Mtb* did not accept APR as a substrate. APR is a structurally unique AG that contains four rings, with the two middle ones fused (Fig. 7.7). This chemical structure limits the conformational freedom of this molecule and, as a result, APR has an extended cylinder-like conformation, as observed both in a crystalline form[25] and in solution.[26] Furthermore, this extended conformation of APR is essentially unchanged in several crystal structures of APR bound to RNA ligands.[27-29] Therefore, the AG-binding cavity of an enzyme needs to be sufficiently wide and long to accommodate a bound APR molecule for its acetylation. Because Eis_*Mtb* is unable to acetylate APR and

Eis_*Msm* acetylates APR at two positions, the stiff APR scaffold serves as an excellent AG specificity discriminator between the two homologs. In order to explain this major specificity difference, we looked for structural features that could allow Eis_*Msm* to accommodate an APR molecule in the Eis_*Msm*, but not in the Eis_*Mtb* binding site. Because three out of the four primary amines of APR lie on the "terminal" rings, at least one of them is modified, which means that the AG-binding pocket should be wide and long enough to accommodate an APR cylinder with one end of it placed at the active site.

As seen in the crystal structure of Eis_*Mtb* in complex with CoA and an acetamide determined recently by our groups,[15] the AG-binding cavity of Eis_*Mtb* is bifurcated, with Glu401 separating the cavity into two channels (with borders highlighted in green and in blue in Fig. 7.6A). One channel (green) is not straight enough to fit an APR molecule without steric clashes in both Eis_*Mtb* and Eis_*Msm*. Most residues lining this channel are the same in Eis_*Mtb* and Eis_*Msm* (in Eis_*Msm* numbering in Fig. 7.1: Phe26, Asp28, Trp38, and the carboxyl terminus denoted C-ter in Fig. 7.6), In particular, it is not possible to avoid clashes between the APR and the catalytic carboxyl terminus, whose position is likely highly conserved,[15] and with Trp38 (Trp36 in Eis_*Mtb*). The other channel (blue) is fairly shallow in Eis_*Mtb* due to the Glu401. In addition, this channel is capped at the end by Trp289 and Ile268 in Eis_*Mtb* imposing additional steric restrictions on the length of the ligand. As a consequence, a bound APR molecule oriented in this channel would have to be largely exposed to solvent due to its extended conformation. Interestingly, all differences in the AG-binding pockets of Eis_*Mtb* and Eis_*Msm* lie in the residues that line this channel. Moreover, in Eis_*Msm*, the residues in this channel are smaller than those in Eis_*Mtb* thus likely resulting in a longer and wider channel in Eis_*Msm* than in Eis_*Mtb* and creating a cavity large enough to bind an APR molecule in a proper orientation for acetylation (Fig. 7.6B). Specifically, Trp289 in Eis_*Mtb* is changed to an alanine (Ala287 in Eis_*Msm*) and Ile268 and Glu401 in Eis_*Mtb* to glycines (Gly266 and Gly401 in Eis_*Msm*), respectively (Figs. 7.1 and 7.6). In addition, another residue lining this channel, Gln291 in Eis_*Mtb* is replaced by a smaller alanine (Ala289 in Eis_*Msm*) contributing to the channel widening. An APR molecule readily fits into this channel in the model of an Eis_*Msm* structure (Fig. 7.6B).

Even though the structural details of binding of APR to Eis_*Msm* may not all be accurately represented by this model, when taken together our biochemical results and these structural considerations suggest that APR binding occurs in this channel.

Finally, by demonstrating that inhibitors of Eis_*Mtb* can also prevent acetylation of NEO by Eis_*Msm*, we confirmed that the Eis_*Mtb* inhibitory properties of these compounds could potentially be extended to usage against other mycobacteria. As we demonstrated, the inhibitory power of each compound differed between the two mycobacteria, suggesting that these inhibitors would display varying potency among mycobacteria. Further investigations are currently underway in our laboratory to determine appropriate inhibitor-mycobacterium pairs. In the future, testing the activity of these inhibitors against other Eis-containing pathogenic bacteria to evaluate the extent of the application of these molecules will be of interest.

7.6. References

(1) Caminero, J. A. *Int J Tuberc Lung Dis* **2006**, *10*, 829.
(2) Chan, E. D.; Laurel, V.; Strand, M. J.; Chan, J. F.; Huynh, M. L.; Goble, M.; Iseman, M. D. *Am J Respir Crit Care Med* **2004**, *169*, 1103.
(3) Ellner, J. J. *Clin Transl Sci* **2008**, *1*, 249.
(4) Banerjee, R.; Schecter, G. F.; Flood, J.; Porco, T. C. *Expert Rev Anti-Infe* **2008**, *6*, 713.
(5) Udwadia, Z. F.; Amale, R. A.; Ajbani, K. K.; Rodrigues, C. *Clin Infect Dis* **2012**, *54*, 579.
(6) Shiloh, M. U.; DiGiuseppe Champion, P. A. *Current opinion in microbiology* **2010**, *13*, 86.
(7) Reyrat, J. M.; Kahn, D. *Trends Microbiol* **2001**, *9*, 472.
(8) Tyagi, J. S.; Sharma, D. *Trends in microbiology* **2002**, *10*, 68.
(9) Cole, S. T.; Brosch, R.; Parkhill, J.; Garnier, T.; Churcher, C.; Harris, D.; Gordon, S. V.; Eiglmeier, K.; Gas, S.; Barry, C. E., 3rd; Tekaia, F.; Badcock, K.; Basham, D.; Brown, D.; Chillingworth, T.; Connor, R.; Davies, R.; Devlin, K.; Feltwell, T.; Gentles, S.; Hamlin, N.; Holroyd, S.; Hornsby, T.; Jagels, K.; Krogh, A.; McLean, J.; Moule, S.; Murphy, L.; Oliver, K.; Osborne, J.; Quail, M. A.; Rajandream, M. A.; Rogers, J.; Rutter, S.; Seeger, K.; Skelton, J.; Squares, R.; Squares, S.; Sulston, J. E.; Taylor, K.; Whitehead, S.; Barrell, B. G. *Nature* **1998**, *393*, 537.
(10) Fleischmann, R. D.; Alland, D.; Eisen, J. A.; Carpenter, L.; White, O.; Peterson, J.; DeBoy, R.; Dodson, R.; Gwinn, M.; Haft, D.; Hickey, E.; Kolonay, J. F.; Nelson, W. C.; Umayam, L. A.; Ermolaeva, M.; Salzberg, S. L.; Delcher, A.; Utterback, T.; Weidman, J.; Khouri, H.; Gill, J.; Mikula, A.; Bishai, W.; Jacobs Jr, W. R., Jr.; Venter, J. C.; Fraser, C. M. *J Bacteriol* **2002**, *184*, 5479.
(11) Chen, W.; Biswas, T.; Porter, V. R.; Tsodikov, O. V.; Garneau-Tsodikova, S. *Proc Natl Acad Sci U S A* **2011**, *108*, 9804.
(12) Zaunbrecher, M. A.; Sikes, R. D., Jr.; Metchock, B.; Shinnick, T. M.; Posey, J. E. *Proc Natl Acad Sci U S A* **2009**, *106*, 20004.
(13) Wei, J.; Dahl, J. L.; Moulder, J. W.; Roberts, E. A.; O'Gaora, P.; Young, D. B.; Friedman, R. L. *Journal of bacteriology* **2000**, *182*, 377.
(14) Green, K. D.; Chen, W.; Garneau-Tsodikova, S. *ChemMedChem* **2012**, *7*, 73.
(15) Chen, W.; Biswas, T.; Porter, V. R.; Tsodikov, O. V.; Garneau-Tsodikova, S. *Proc Natl Acad Sci U S A* **2011**, *108*, 9804.
(16) Williams, J. W.; Northrop, D. B. *J Biol Chem* **1978**, *253*, 5902.
(17) Magnet, S.; Lambert, T.; Courvalin, P.; Blanchard, J. S. *Biochemistry* **2001**, *40*, 3700.
(18) Magalhaes, M. L.; Blanchard, J. S. *Biochemistry* **2005**, *44*, 16275.
(19) Martel, A.; Masson, M.; Moreau, N.; Le Goffic, F. *Eur J Biochem* **1983**, *133*, 515.
(20) Hegde, S. S.; Javid-Majd, F.; Blanchard, J. S. *J Biol Chem* **2001**, *276*, 45876.
(21) Kim, C.; Villegas-Estrada, A.; Hesek, D.; Mobashery, S. *Biochemistry* **2007**, *46*, 5270.
(22) Kim, C.; Hesek, D.; Zajicek, J.; Vakulenko, S. B.; Mobashery, S. *Biochemistry* **2006**, *45*, 8368.
(23) Draker, K. A.; Northrop, D. B.; Wright, G. D. *Biochemistry* **2003**, *42*, 6565.
(24) Green, K. D.; Chen, W.; Houghton, J. L.; Fridman, M.; Garneau-Tsodikova, S. *Chembiochem* **2010**, *11*, 119.
(25) O'Connor, S.; Lam, L. K. T.; Jones, N. D.; Chaney, M. O. *Journal of Organic Chemistry* **1976**, *41*, 2087.
(26) Szilágyi, L.; Pusztahelyi, Z. S. *Magnetic Resonance in Chemistry* **1992**, *30*, 107.
(27) Hermann, T.; Tereshko, V.; Skripkin, E.; Patel, D. J. *Blood Cells Mol Dis* **2007**, *38*, 193.
(28) Han, Q.; Zhao, Q.; Fish, S.; Simonsen, K. B.; Vourloumis, D.; Froelich, J. M.; Wall, D.; Hermann, T. *Angew Chem Int Ed Engl* **2005**, *44*, 2694.
(29) Kondo, J.; Francois, B.; Urzhumtsev, A.; Westhof, E. *Angew Chem Int Ed Engl* **2006**, *45*, 3310.

Note:

This chapter is adapted from a submitted manuscript: **Chen, W.**; Tsodikov, O. V. & Garneau-Tsodikova, S., titled "The aminoglycoside multi-acetylating activity of the enhanced intracellular survival (Eis) protein from *Mycobacterium smegmatis* and its inhibition" **Wenjing Chen** did all the assays. Dr. Tsodikov did the structural modelling and helped with the kinetic analysis.

Chapter 8

Conclusion and future directions

Despite intensive scientific and technological progress in chemical synthesis, drugs derived from natural products are still a major contribution to drug discovery today. Using natural products for medication purposes has been recognized since ancient times. Such compounds with a tremendous chemical diversity have been found in millions of different species of plants, animals, marine organisms, and microorganisms. Microorganisms such as bacteria are invaluable for drugs and lead compounds discovery since they take the advantage to produce a large selection of antimicrobial agents, which have evolved to kill other competitors in the microbiological world. Aminoglycosides (AGs) are such groups of antibiotics. Streptomycin was the first identified AG from the soil bacteria *Streptomyces griseus.* However, bacteria display an impressive effectiveness to adapt to environmental challenges and to effectively develop resistance mechanisms against antibiotics including AGs. This has been the major obstacles in antibiotic drug use and development. The discovery of novel agents against new bacterial targets is considered to be a risky business endeavor because of the lengthy research and development (R&D) timeline for new drugs. Therefore, the majority of the current antibacterial R&D activities focus on the alteration of existing classes of antibiotics.

Chapters two and three of this dissertation discussed the possibility of a chemoenzymatic methodology to convert existing AGs into novel acylated derivatives for potential antibacterial use. The idea of acylated AGs is based on the fact that several AGs have been identified in which acylation of an amine has led to improved compounds with increased antibacterial potency and lower toxicity in mammals. One such example is butirosin, an AG acylated at the *N*-1 position with an aminohydroxybutyric acid (AHB) moiety that is produced by *Bacillus circulans*. This AHB moiety renders many AGs more

potent, less toxic, and less susceptible to the activity of AG-modifying enzymes. Other examples of AG modifications include *N*-methylation and *N*-glycinylation. Given the success of these modifications, we felt the need to explore the potential of novel AG analogs containing a variety of *N*-acyl groups at different positions on the AG scaffolds. We proposed a chemoenzymatic methodology that utilizes AG acetyltransferases (AACs), which have evolved to regio-selectively modify AGs, to acylate the existing AGs, avoiding the disadvantages of conventional chemical synthesis. We showed that this chemoenzymatic generation of novel compounds, together with the BioTLC assay, might provide us with potentially potent antimicrobial agents for further investigation. This is a demonstration of utilizing the cosubstrate promiscuity of enzymes to re-purpose their use for scaffold diversification towards the development of new drugs.

The majority of AACs are plasmid encoded, which permits the facile exchange of resistance genes among bacteria. However, the evolution and regulation of chromosomally encoded AACs demonstrate the ability of bacteria to adapt to changes in AG use and selective pressure. Eis is such an AAC found in *Mycobacterium tuberculosis* (*Mtb*). Its unprecedented multi-acetylation ability is unique among the AAC family. Being a powerful AG deactivating enzyme, Eis is the cause for a large portion of the kanamycin resistant *Mtb* clinical isolates. Chapters four to seven discussed our initial biochemical and structural characterizations of this enzyme, as well as our effort to identify Eis inhibitors. We hope that understanding the mechanism of this resistance conferring enzyme, will enable us to design better drugs/regimens to fight *Mtb* infection. Some future directions of the Eis project include:

8.1. Regiospecificity of multi-acetylation of AGs by Eis_*Mtb*

In chapter four, we used both NMR and TLC to demonstrate that Eis acetylates NEA at the 1-, 2'-, and 6'-positions. To further examine the regiospecificity, the pattern, and the potential order of multi-acetylation by Eis on other AG substrates, we will start with KAN, AMK, SIS, and NET for scaled-up enzymatic reactions to unambiguously assign the specific positions on each of these AG scaffolds acetylated by Eis. NET has an additional ethyl group on the 1-amine position compared to SIS. Based on the MS and the

spectrophotometric assay results, SIS is modified by Eis at three positions to generate tri-acetyl-SIS, whilst NET is acetylated twice to give di-acetyl-NET. Therefore, we hypothesize that the 1-amine on the SIS scaffold might be acetylated by Eis. Similarly, AMK is thought to be tri-acetylated by Eis and has an additional AHB group compared to KAN, which is converted to di-acetyl-KAN by Eis. Though modification of the AHB group has never been reported, based on our MS data and structures of KAN and AMK, we reason that AHB might potentially serve as an acetylation site for Eis. Both TLC and NMR analysis, which will be done similarly to what we described in chapter four, will be used to test our hypothesis. Ideally, we hope to characterize all products from all ten AG substrates of Eis and identify, if they exist, acetylation patterns utilized by Eis depending on different AG scaffolds. For example, one hypothesized pattern is that Eis will always acetylate the 6'-position if there is an amine group present. These information will help us better understand the reaction mechanism of Eis. Moreover, we will seek to use NMR techniques to monitor the acetylation process in real-time as the enzymatic reaction progresses. We will be able to determine which amine group is modified in each acetylation step by monitoring the appearance of new acetyl peaks and comparing the difference in chemical shifts of each proton on the aminosugar ring. Once the order of multi-acetylation is known, we will be able to determine the kinetic profiles of each acetylation step by feeding the enzyme with the AG product of the previous step. These products may need to be synthesized either chemically or chemoenzymatically. For instance, in the case of NEA, using synthetic 2',6'-di-acetyl-NEA and AcCoA will give us kinetic information for the third acetylation step of Eis reaction which is the acetylation of 1-amine of NEA.

8.2. Crystal structure of the substrate binding site of Eis_*Mtb*

In the crystal structure of Eis reported in chapter four, the density for the rest of HYG molecule is too weak to allow us to reveal the proper positioning of the aminosugar rings expect for the acetamide group. The AG binding site is relatively large and the AG may adapt multiple orientations or flexibility in the active site, making it hard to resolve the AG orientation. The catalytic mechanism would be better understood if a crystal structure of the enzyme•CoA•AG ternary complex, with clear electron density for the substrate

binding pocket, was obtained. We are trying to grow crystals of Eis and Eis mutants with different substrate and CoA combinations under various reservoir solution conditions.

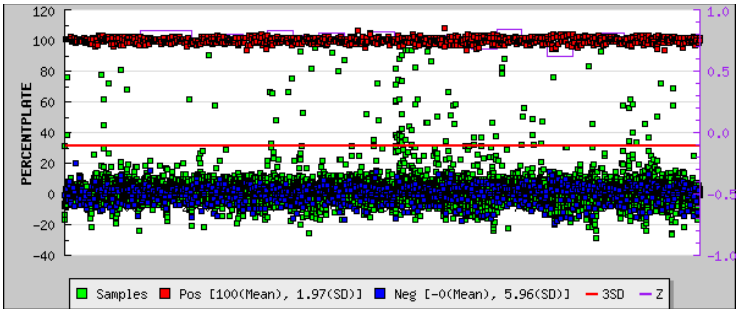

Fig. 8.1. An example of HTS result. Red dots represent the positive control (Eis activity is fully inhibited). Blue dot is the negative control (no inhibitor present). Red line indicates the 3x standard deviation as a statistical hit threshold from the mean negative control.

8.3. Screening for inhibitors of Eis_*Mtb*

We reported the discovery of Eis inhibitors via HTS in chapter five. We are now collaborating with Dr. J. E. Posey (Centers for Disease Control and Prevention, Atlanta, GA) to test the identified inhibitors' activities *in vivo* in various susceptible and drug-resistant *Mtb* strains. The initial results suggested that the MIC value of KAN was decreased significantly in the presence of certain Eis inhibitor compared to no inhibitor present in the drug-resistant *Mtb* strain that has an up-regulated Eis expression level. This promising finding demonstrates that Eis inhibitors and KAN may work synergistically in drug-resistant *Mtb* strains.

Using the same HTS assay described in chapter five, we are screening a much larger set of small molecule library (~100,000) for Eis inhibitors. The *Z'* score is ranging from 0.43 to 0.74. Fig. 8.1 is an example of the assay result, showing that out of 8,000 compounds, 237 hits were found to have inhibitory effect on Eis. We are expecting to have approximately 2% of the total compounds to show a reasonable degree of inhibition (>3σ from the mean negative control) against Eis. From those, hit validation and dose-dependent response assay will be performed to confirm the HTS results. Once new inhibitors will be identified, *in vitro* inhibition kinetics, SAR analysis and *in vivo* testing will follow. We hope that this project will finally lead us to identify potent Eis inhibitor(s) that when used in combination with the currently used second-line anti-TB drugs KAN or AMK, may provide a potential solution to overcome the problem of MDR-TB or XDR-TB.

Table. 8.1. MIC and MBC values of antibiotics

Antitiotics	MIC (μg/mL)		MBC (μg/mL)	
	WT	KO	WT	KO
AMK	1.56	1.56	1.56	1.56
Ampicillin	0.78	0.39	0.78	0.39
chloramphenicol	2.13	2.13	2.13	4.25
Ciprofloxacin	0.08	0.08	0.08	0.08
GEN	0.78	0.78	0.78	0.78
HYG	46.88	46.86	46.88	>187.5
INH	>500	>500	>500	>500
KAN	3.91	7.81	7.81	7.81
NEA	31.25	31.25	125.00	31.25
NEO	7.81	3.91	7.81	3.91
NET	0.781	0.78	0.78	0.78
Norfloxacin	0.20	0.20	0.20	0.20
PAR	3.13	3.13	6.25	12.50
RIB	25.00	12.50	25.00	50.00
SIS	0.78	0.78	0.78	0.78
SPT	62.50	62.50	62.50	62.50
STR	2.44	2.44	2.44	2.44
TOB	1.56	1.56	6.25	1.56

WT = wild-type *Bacillus anthracis* 34F2 Sterne strain; KO = acetyltransferase gene knockout mutant of *Bacillus anthracis* 34F2 Sterne strain.

8.4. Eis homologs in other microorganisms

Besides *Mtb* and *M. smegmatis*, Eis-like proteins are also found in many other bacteria. One example is the GNAT family acetyltransferase from *Bacillus anthracis*. Joachimiak and coworkers (Midwest Center for Structural Genomics) published a 2.75 Å resolution structure of a *B. anthracis* acetyltransferase (pdb ID: 3N7Z) which adapts a tight hexamer structure similar to the Eis_*Mtb* we discussed in chapter four. We cloned and expressed this protein in *E. coli* and tested its activity against a wide panel of AGs with AcCoA as cosubstrate. We find that, like the Eis_*Mtb*, this protein is also capable of acetylating AGs on multiple amines. Based on the structure comparison, these two proteins' active sites are considerably different. This might explain the fact that the *B. anthracis* acetyltransferase does not share the same AG substrates profile with Eis_*Mtb*. For example, apramycin can be mono-acetylated by the *B. anthracis* acetyltransferase but not by Eis_*Mtb*. It might also explain the different number of acetylation sites on each AG substrates between the two enzymes.

In order to better understand the physiological role of Eis protein in *Mtb* or other bacteria, we first decide to knockout the *eis* gene from the bacterial genome and compare how the wild-type and mutant react to AG treatment. We are using *B. anthracis* as the example system to begin with, simply due to the ease of manipulation. With the help of Dr. B. K. Janes (from Professor P. C. Hanna's laboratory, University of Michigan), we successfully removed the gene encoding the aforementioned acetyltransferase from the *B. anthracis* genome using a markerless gene replacement protocol.[1] We then testd the MIC and MBC values of various AGs and several other common antibiotics on both the wild-type and mutant strains (Table 8.1). Data suggest that no significant difference in MIC is observed

between the two strains for most AGs except NEO and RIB. One possible explanation is that, unlike the Eis in *Mtb* H37Rv strain, the *B. anthracis* enzyme has not been evolved yet *in vivo* to target AG. Other experiments need to be designed to elucidate what is the substrate of this enzyme is and how Eis-like acetyltransferase functions *in vivo*. We are in the process of identifying *in vivo* substrate(s) of Eis and/or Eis homologs using various methods such as MS.

In addition, based on protein sequence blast results, we identify several other Eis homologs from pathogens such as *Tsukamurella paurometabola*, *Gordonia bronchialis*, *Kocuria rhizophila*, and *Mycobacterium abscessus*. We are trying to express these proteins and run *in vitro* assays to determine if these proteins also have AG acetyltransferase activity. Also, a 2.0 Å resolution crystal structure (pdb ID: 2OZG) of a GCN5-related *N*-acetyltransferase from cyanobacterium *Anabaena variabilis* displays high structural similarity with Eis_*Mtb*. We think this protein may also function as an AG acetyltransferase *in vitro* and are in the process of cloning it in *E. coli*.

8.5. References

(1) Janes, B. K.; Stibitz, S. *Infect Immun* **2006**, *74*, 1949.